Modulation of DNA strand break induction and repair by tyrosine kinase inhibitors targeted against EGFR and HER2

Jaishree Bhosle

A thesis submitted to the University College London for the degree of Doctor of Philosophy

June 2011

CRUK Drug-DNA Interaction Research Group

UCL Cancer Institute

Paul O'Gorman Building

72 Huntley Street, London, WC1E 6DD, UK

Signed declaration

I, Jaishree Bhosle confirm that the work presented in this thesis is my own. Where information has been derived from other sources, I confirm that this has been indicated in the thesis.

Abstract

Purpose The human epidermal growth factor receptors EGFR (erbB1) and HER2 (erbB2/*neu*) are involved in mediating resistance to chemotherapy and ionising radiation (IR). *In vitro* studies demonstrate that small molecule tyrosine kinase inhibitors (TKIs) which target these receptors can increase the effectiveness of DNA damaging agents. However, these combinations have failed to produce the clinical results anticipated and one potential explanation is that the inhibition of EGFR and HER2 cell signalling pathways by TKIs is short lived, with cells able to switch to alternative mechanisms of signalling through HER3. The purpose of this study was to examine whether the duration of exposure to TKIs modulates the induction and repair of DNA damage produced by chemotherapy or IR and describes attempts to elucidate the role of HER2 in mediating resistance to chemotherapy.

Experimental design Two HER targeting TKIs, lapatinib and gefitinib were investigated. The effect of lapatinib in combination with cisplatin and doxorubicin on the inhibition of cell proliferation and the role of schedule were examined in drug combination assays. The influence of the duration of exposure to TKIs on the induction and repair of DNA lesions induced by cisplatin, IR, doxorubicin, etoposide and m-AMSA were investigated using the alkaline and neutral Comet assays and measurement of γH2AX and RAD51 foci. DNA expression arrays were used to identify the potential mechanisms through which HER2 produces resistance to cisplatin in cells transfected with HER2.

Results Lapatinib is able to synergistically inhibit cell proliferation in combination with cisplatin or doxorubicin in a schedule dependent manner. Duration of exposure to TKIs has no effect on the induction of DNA lesions by cisplatin or IR, but significantly reduces the production of DNA double strand breaks by doxorubicin, etoposide and m-AMSA in part through the down-regulation of the expression of topoisomerase IIα (Topo IIα), increasing resistance to these drugs.

Conclusions These results indicate the scheduling of small molecule TKIs targeted against EGFR and HER2 is important and continuous exposure to these drugs induces resistance to doxorubicin, etoposide and m-AMSA, through reduced expression of their target, Topo IIα. The importance of schedule should be considered when combining TKIs with chemotherapy in clinical practice.

ACKNOWLEDGEMENTS

This work was carried out under the supervision of Professor Daniel Hochhauser, Professor John A Hartley and Dr Andreas Makris and funded by the Breast Cancer Research Trust.

I would like to thank Daniel for his support, guidance and friendship during the last four years, which continues. John for his advice and helping me to stick to the science and Andreas for his enthusiasm, encouragement and coffee. I would also like to thank all three for their advice over the last four years and in the preparation of this manuscript.

I would specifically like to thank Dr J Wu for undertaking the staining, visualisation and counting of the RAD51 and γH2AX foci, Dr P Dhami for undertaking the chromatin immunoprecipitation and Mr J Bingham for performing the RT-PCR.

I am grateful to all my colleagues in the laboratory for putting up with me, as well as teaching and helping me; specifically Giammy, Raisa, Samir, Kostas and Valeria.

Most of all I am grateful for those who believe in me, especially my parents, brother Amit, sister Rajeshree and my best friends, Bianca and Anna, for providing coffee, cakes and gin *PRN*.

COMMUNICATIONS

PRESENTATIONS

July 2009 Interaction of HER Inhibition and Chemotherapy in Breast Cancer. UCL Cancer Institute 2nd Annual Conference, London, UK.

Jaishree Bhosle Jenny Wu, Andreas Makris, John A Hartley and Daniel Hochhauser. Modulation of topoisomerase IIα poison induced DNA damage and repair by tyrosine kinase inhibitors. ***Poster presentation*** *Proceedings of the 100th Annual Meeting of the American Association for Cancer Research; 2009 Apr 18-22. Denver, Colorado, USA AACR 2009; Ab. No. 1829 (Presented by D Hochhauser).*

Jaishree Bhosle, Andreas Makris, John A Hartley and Daniel Hochhauser. Effect of Chronic exposure to tyrosine kinase inhibitors on chemotherapy-induced DNA damage in the SKBr-3 breast cancer cell line. ***Poster Presentation*** *San Antonio Breast Cancer Symposium 10-14 Dec 2008, San Antonio, Texas, USA.*

PUBLICATIONS

Boone JJ, Bhosle J, Tilby MJ, Hartley JA, Hochhauser D (2009)**:**
Involvement of the HER2 pathway in repair of DNA damage produced by chemotherapeutic agents. *Mol Cancer Ther* 8**:** 3015-23.

TABLE OF CONTENTS

INDEX OF FIGURES

INDEX OF TABLES

ABBREVIATIONS

4ICD	HER4 intracellular domain
5-FU	5-Fluorouracil
ABC	ATP binding cassette
ABCC	ATP binding cassette C sub-family
ABCG	ATP binding cassette G sub-family
ADAM	A disintegrin and metalloproteinase
ADCC	Antibody-dependent cellular cytotoxicity
ANOVA	Analysis of variance
ATM	Ataxia telangiectasia mutated homolog protein
ATP	Adenosine triphosphate
ATR	Ataxia telangiectasia and rad3 related protein
BAC	Bacterial artificial chromosome
Bad	Bcl-2-associated death promoter
Bcl-2	B-cell chronic lymphocytic leukaemia/lymphoma 2
BCRP	Breast cancer resistance protein
BER	Base excision repair
BRCA1/2	Breast-cancer susceptibility gene ½
Cbl	Casitas B-lineage lymphoma protein
CCD	Charge-couple device
CDK	Cyclin Dependent kinase
CDKI	Cyclin Dependent kinase inhibitors
CDKN2A	Cyclin kinase dependent inhibitor 2A
cDNA	Complementary DNA
ChIP	Chromatin immunoprecipitation
CI	Confidence Interval
CIX	Combination index
CMF	Cyclophosphamide, methotrexate and 5-FU chemotherapy regimen
COMET	Single-cell gel electrophoresis
COX2	Cyclooxygenase 2
DDB	DNA damage binding protein

DDT	Dichlorodiphenyltrichloroethane
DFS	Disease Free Survival
DMEM	Dulbecco modified eagle's minimal essential medium
DMSO	Dimethyl Sulfoxide
DNA	Deoxyribose nucleic acid
DNA-PK	DNA-activated protein kinase
DNA-PKcs	DNA-activated protein kinase catalytic subunit
EDTA	Ethylenediamine tetraacetic acid
EGF	Epidermal growth factor
EGFR	Epidermal growth factor receptor (erbB1/HER1)
EGFRvIII	Epidermal growth factor receptor variant III
ER	Oestrogen Receptor
ERFFI1	**E**rbB receptor feedback inhibitor
FACS	fluorescence activated cell sorting
FANCA	Fanconi anemia complementation group A
FANCC	Fanconi anemia complementation group C
FANCD	Fanconi anemia complementation group D
FCS	Foetal calf serum
FdUMP	Fluorodeoxyuridine monophosphate
FdUTP	Fluorodeoxyuridine triphosphate
FEC	Fluorouracil, epirubicin, and cyclophosphamide
FEC-D	Fluorouracil, epirubicin, cyclophosphamide and docetaxel
FISH	Fluorescence in situ hybridisation
Gab-1	Grb2 associated binding protein 1
Grb2	Growth factor receptor-bound protein 2
GST	Glutathione-S-transferase
GSTP1	Glutathione-S-transferase P1
H2AX	Histone H2A variant X
HB-EGF	Heparin binding epidermal growth factor
HER2	Epidermal growth factor receptor 2 (erbB2/*neu*)
HER3	HER3, epidermal growth factor receptor 3 (erbB3)
HER4	HER4, epidermal growth factor receptor 4 (erbB4)

HI FCS	Heat inactivated Foetal calf serum
HR	Homologous combination
IC_{50}	Inhibitory concentration producing 50% growth inhibition
IHC	Immunohistochemistry
IF	Immunofluorescence
IGF	Insulin-like growth factor
IGFR1	Insulin-like growth factor receptor 1
iNOS	Inducible nitric oxide synthase
IRS1	Insulin receptor substrate 1
IR	Ionising radiation
JAK	Janus kinase
JNK	Jun terminal kinase
K-RAS	Kristen rat sarcoma
LCIS	Lobular carcinoma *in situ*
mAMSA	N-(4-(acridin-9-ylamino)-3-methoxyphenyl)methanesulfonamide (Amsacrine)
MAPK	Mitogen activated protein kinase
MEK	MAPK/ERK kinase
MET	Hepatocyte growth factor receptor
MDM	Murine double minute
MDR	Multi-drug resistance
MIG6	Mitogen-inducible gene 6 (ERFFI1/RALT)
MMR	Mismatch Repair
MRE11	Meiotic recombination 11
MRN	MRE11/NBS1/RAD51
MRP	Membrane resistance protein
mRNA	Messenger ribonucleic acid
mTOR	Mammalian target of rapamycin
MTT	**T**etrazolium dye3-(4,5-dimethylthiazol-2-yl)-2,5-diphenyltetrazolium bromide
NASBP	National Surgical Breast and Bowel Project
NER	Nucleotide excision repair
NHEJ	Non homologous end-joining
NLS	Nuclear localisation sequence

NPI	Nottingham prognostic index
NSCLC	Non small cell lung cancer
OD	Optical density
OS	Overall survival
p	Level of significance
PAI-1	Plasminogen activator inhibitor-type 1
PBS	Phosphate buffered saline
PCR	Polymerase chain reaction
PDGFR	Platelet-derived growth factor receptor
PDK	Phosphoinositide dependent kinase
PFS	Progression free survival
PI	Propidium iodide
PIK3CA	Phosphoinositide-3-kinase, catalytic alpha polypeptide
PI3K	PhosphatidylInositol-3 kinase
PKC	Protein kinase C
PKC	Protein kinase C
PLC-γ	Phospholipase C-γ
PR	Progesterone receptor
PTEN	Phosphatase and tensin homolog
Ras	Rat sarcoma
Raf	Rapidly accelerated fibrosarcoma
RALT	Receptor-associated late transducer
RB1	Retinoblastoma protein.
ROS	Reactive oxygen species
RPA	Replication protein A
RS	Recurrence score
RT-PCR	Reverse transcriptase polymerase chain reaction
SD	Standard déviation
SEM	Standard error
SGLT	Sodium glucose co-transporter
SH2	Src-Homology 2 protein
siRNA	Small interference Ribonucleic acid

SOS	Son of sevenless protein
SRB	Sulforhodamine B
SSA	Single strand annealing
Src	V-src sarcoma (Schmidt-Ruppin A-2) viral oncogene homolog
STAT	Signal transducer and activator of transcription
TAC	Docetaxel, doxorubicin and cyclophosphamide chemotherapy regimen
TBS	Tris buffered saline
TBST	Tris buffered saline with 0.1% Tween 20
TCR	Transcription coupled repair
TGF	Transforming growth factor
TKI	EGFR and/or HER2 targeted tyrosine kinase inhibitor
TLS	Translesion synthesis
Topo I	Topoisomerase I
Topo IIα	Topoisomerase IIα
Topo IIβ	Topoisomerase IIβ
uPA	Urokinase-type plasminogen activator inhibitor
VEGF	Vascular endothelial growth factor
XPF	Xeroderma pigmentosum group F

REVIEW OF THE LITERATURE

1.1 CANCER

The term 'cancer' is commonly used to describe a group of diseases caused by the uncontrolled growth of cells (due to self-sufficiency in growth signalling, limitless ability to replicate, disregulation of cell metabolism and evasion of growth suppression and cell death), with the potential to spread to other sites (metastasise), evade the immune system and obtain their own blood supply (angiogenesis) (Hanahan and Weinberg, 2000; Hanahan and Weinberg, 2011).

Early in the twentieth century the ability of viruses to induce cancers was recognised with the isolation of a virus from chickens with avian erythroid leukaemia in 1908. This was followed by Peyton Rous in 1911, isolating a virus capable of inducing sarcomas in chickens, the Rous Sarcoma Virus (Rous, 1911). This led to the isolation of other viruses which could cause cancer, including the avian erythroblastic virus which induces erythroid leukaemia and fibrosarcoma in chickens (Beug *et al.*, 1979). Cancer inducing viruses were recognised to transfer genetic material (oncogenes) into infected cells which were responsible for their transformation into cancers. It was also discovered that these same oncogenes were encoded by genes present within avian DNA (Stehelin *et al.*, 1976), and to the understanding that normal cellular genes (proto-oncogenes) could become oncogenes and transform cells into cancers, a hypothesis for which Bishop and Varmus were awarded the Noble Prize in Medicine in 1989. Two oncogenes were isolated from the avian erythroblastic virus and named v-*erbA and v-erbB* (Roussel *et al.*, 1979) with their cellular DNA counterparts denoted as cellular by the 'c' prefix, c-*erbA* and c-*erbB* (Vennstrom and Bishop, 1982).

In the 1960's Stanley Cohen isolated epidermal growth factor (EGF) and demonstrated that it stimulated cell proliferation both *in vitro* and *in vivo* (Cohen, 1964). He went on the isolate the protein to which EGF bound, now known as the epidermal growth factor receptor (EGFR) (Taylor *et al.*, 1974). In 1984 Downward *et al.* identified that the out of 84 amino acids isolated from the EGFR gene, 74 were shared with the *v-erbB* oncogene (Downward *et al.*, 1984). This discovery was closely followed by the identification of *c-erbB2*, a gene similar to, but distinct from EGFR and a human

homolog of the rat oncogene *neu,* responsible for the chemical induction of neuroblastoma and glioblastoma in rats (Schechter *et al.*, 1985; Semba *et al.*, 1985). This led to the recognition of c-*erbB* (c-*erbB1*/EGFR) and c-*erbB2* as oncogenes as demonstrated by their ability to induce transformation and tumour formation in mouse fibroblast cells (Di Fiore *et al.*, 1987; Hudziak *et al.*, 1987; Velu *et al.*, 1987).

Both c-*erbB1* and c-*erbB2*, together with two other receptors, belong to a family of membrane receptor tyrosine kinases known as the human epidermal growth factor receptor (HER) family (Figure 1.1); EGFR (c-*erbB1*/HER1), HER2 (c-*erbB2*/*neu*), HER3 (c-*erbB3*) and HER4 (c-*erbB4*). In the late 1980's Slamon *et al*. demonstrated that the HER2 gene was amplified in 30% of breast cancers and predicted for a disease with a poorer overall survival (OS) and reduced time to relapse (Slamon *et al.*, 1987). This observation led to the development of drugs which target HER2 and their subsequent successful translation into the clinical management of breast cancer.

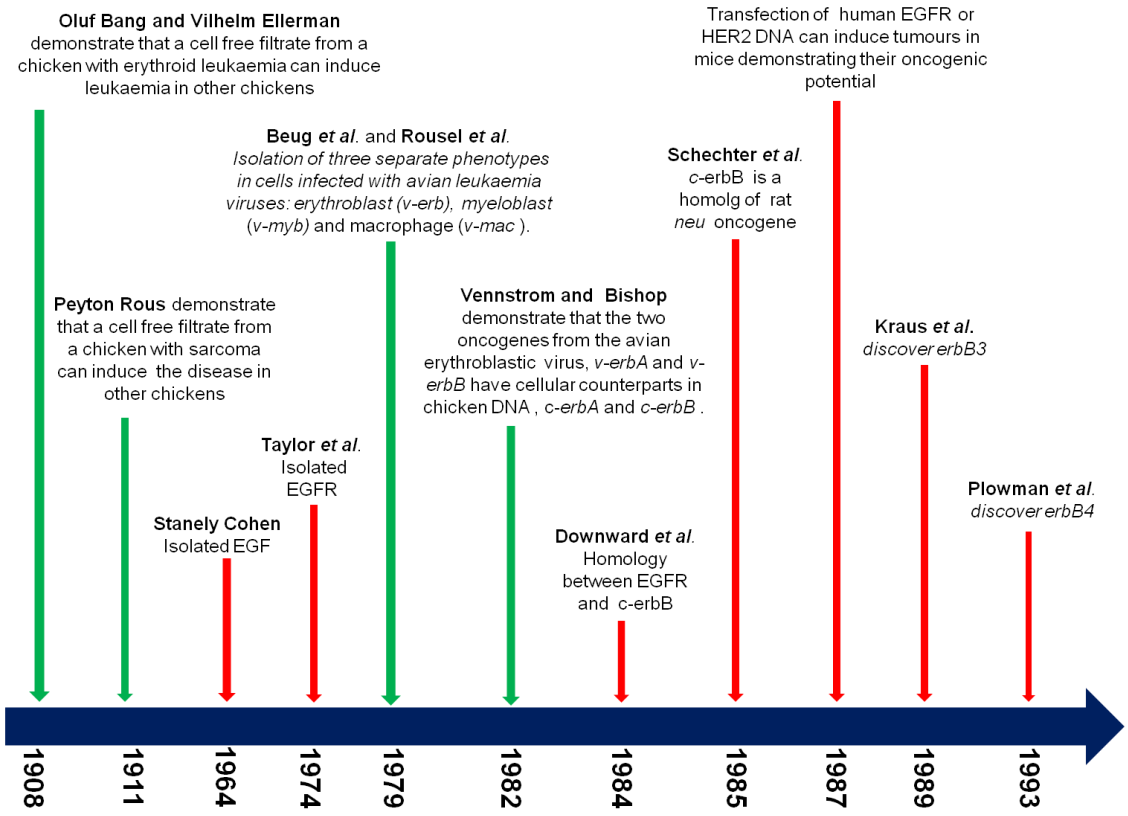

Figure 1.1 Timeline of discovery of the human epidermal growth factor receptor family

1.2 BREAST CANCER

The term 'breast cancer' describes a spectrum of malignancies arising in the breast, including *in situ* carcinomas and invasive tumours. It is the commonest cancer in England, with 39, 681 new cases diagnosed in 2008, accounting for 31% of all new cancer diagnoses with less than 1% of these cases occurring in men (Office for National Statistics, October 2010). Whilst the incidence of breast cancer has been increasing year on year since the 1970's, mortality from the disease has been falling since the late 1980's. This fall is attributed to improvements in both diagnosis and treatment (Quinn *et al.*, 2008). Despite this, metastatic disease cannot be eradicated and only 10% of patients with metastatic breast cancer live for more than 10 years following diagnosis (Statistics and Outlook for Breast Cancer, 2009) causing 10,000 deaths in 2008 (Office for National Statistics, October 2010) .

1.2.1 Presentation of breast cancer

30% of all breast cancers are diagnosed through screening, though this number rises to 50% in those patients aged between 50 and 70 years old and therefore eligible for the breast cancer screening programme (West Midlands Cancer Intelligence Unit, 2009). This means that most patients present with symptomatic breast cancer, usually a self detected breast abnormality, though around 5% of patients have metastatic breast cancer at presentation (Statistics and Outlook for Breast Cancer, 2009) and may present with symptoms such as pain due to bone or liver metastases .

1.2.2 Diagnosis of breast cancer

The standard for diagnosing breast cancer in those with a self or mammogram detected abnormality is triple assessment. This involves clinical examination of the breast, imaging with ultrasound and/or mammogram together with either a fine needle aspiration cytology or core biopsy (National Institute for Health and Clinical Excellence, 2009b).

1.2.2.1 Pathology of breast cancer

Pathological examination of a breast tumour is essential, as in addition to primary breast cancers, other types of cancer occur in breast tissue including lymphomas, neuroendocrine tumours and sarcomas, together with benign breast disease and

lesions associated with an increased risk of developing invasive breast cancer, such as lobular carcinoma *in situ* (LCIS) and ductal carcinoma *in situ* (DCIS). Broadly breast cancers are categorised as non-invasive carcinomas *in situ* (DCIS and LCIS) or invasive breast cancer (Tobias and Hochhauser, 2010).

1.2.2.1.1 Morphological appearance of invasive breast cancer

Invasive breast cancer includes lobular, ductal, tubular, cribriform, mucinous, inflammatory and medullary cancers. Invasive ductal cancers comprise the largest group of invasive breast cancers, account for nearly 70% of breast cancers diagnosed in the UK (West Midlands Cancer Intelligence Unit, 2009). They are defined as having the morphological features of an infiltrating cancer with less than 50% of the characteristic of the other types of invasive breast cancers (Pathology Reporting of Breast Disease, 2005). Invasive lobular cancers are the next most frequent histological type of breast cancer, making up around 10% of breast tumour diagnosed (West Midlands Cancer Intelligence Unit, 2009).

1.2.2.1.2 Histological grade in invasive breast cancer

Invasive breast tumours are graded according to the Bloom Richardson Score. This score grades invasive breast cancers as one, two or three, calculated from a score from three to nine based upon tubule/acinar/glandular formation, nuclear atypia/pleomorphism and frequency of mitoses (Pathology Reporting of Breast Disease, 2005). Grade one tumours (well differentiated tumour with a score of 3-5) have the best prognosis with grade three tumours (poorly differentiated tumours with a score 8-9) having the worst.

1.2.2.1.3 HER2 status in invasive breast cancer

HER2 status is assessed to determine whether therapies targeted against HER2 will be beneficial. Tumours which are defined as being 'HER2 positive' are gene amplified as detected by *fluorescence in situ hybridisation* (FISH) or a score of 3+ as assessed with immunohistochemistry (IHC), with 3+ defined as uniform intense membrane staining of >30% of invasive tumour cells. A score of 2+ requires confirmation by FISH (Wolff *et al.*, 2007). Tumours which do not meet these criteria are classified as 'HER2 negative'.

1.2.2.1.4 Hormone receptor status in invasive breast cancer

Oestrogen receptor (ER) status is assessed in breast tumours in order to determine whether endocrine therapy may be beneficial. This can be done on a core biopsy or surgical specimens using IHC. Tumours are scored for intensity of staining and percentage of nuclear staining using the Allred Score, with a maximum score of eight (scores of 0-5 for percentage of staining and 1-3 for intensity) (Pathology Reporting of Breast Disease, 2005).

1.2.2.2 Staging of invasive breast cancer

Full staging of early breast cancer requires examination of the resected primary breast tumour for size (T) and lymph nodes for involvement with cancer (N). Clinical assessment with radiological investigation as indicated are used to assess for the presence of metastases (M). These features combine to give an overall staging of I-IV, with stage IV identifying the presence of metastatic disease (Edge SB *et al.*, 2010). The tumour should also be assessed for the adequacy of the resection margins and the presence of lymphovascular invasion.

1.2.3 Prognostic features of invasive breast cancer

1.2.3.1 Pathological features and prognosis

Traditionally pathological features useful in predicting survival in early breast cancer are tumour size, number of involved lymph nodes and histological grade as used in the Nottingham Prognostic Index (NPI). The NPI groups tumours into six categories ranging from excellent prognosis with a 10 year survival of 96% to very poor prognosis with a 10 year survival of 38% (Lee and Ellis, 2008). The NPI was originally based on survival figures derived from a prospective study started in 1973, before the introduction of adjuvant therapy. The figures quoted above are derived from data between years 1990-1999, following the introduction of adjuvant therapy and improvements in pathological examination of surgical specimen, including the examination of resection margins (Lee and Ellis, 2008). These figures demonstrate an improvement in survival compared with the original figures and indicates that future attempts to identify prognostic features may be skewed by improvements in diagnosis, staging, surgery and adjuvant treatments.

Other prognostic indicators include urokinase-type plasminogen activator (uPA) and its inhibitor, plasminogen activator inhibitor-type 1 (PAI-1) levels (Annecke *et al.*, 2008), the presence of lymphovascular invasion in node negative breast cancer (Lee *et al.*, 2006a) and HER2 expression (Slamon *et al.*, 1987), with all identifying tumours associated with a poorer prognosis. Other tools being developed include the assessment of the expression of five proteins using IHC; SLC7A5, HTF9C, p53, NDRG1, and CEACAM5 from which a Mammostrat score can be calculated. The test can predict prognosis in early-stage, ER-positive tamoxifen treated breast cancer and potentially in node negative or ER-negative tumours (Bartlett *et al.*, 2010).

1.2.3.2. Genetic profiling in breast cancer

The ability to genetically profile tumours has lead to the identification of gene signatures which can be used to predict the likelihood of recurrence in patients with early breast cancer. These include Onco*type* DX and MammaPrint, which are in clinical use and PAM50, which is still undergoing validation.

Onco*type* DX utilises reverse transcriptase polymerase chain reaction (RT-PCR) on RNA extracted from formalin fixed paraffin embedded tissue for 16 cancer genes (including HER2, ER and PR) and five reference genes. Normalised expression scores are used to calculate a recurrence score (RS) from 0-100, with 100 indicating a higher likelihood of recurrence in patients with hormone receptor positive, node negative breast cancer. The recurrence scores were stratified based on the breast cancer recurrence rates in women with hormone receptor positive, node negative breast cancer who received adjuvant therapy with tamoxifen as part of the National Surgical Breast and Bowel Project (NASBP) 14 trial. Those patients estimated to be of low risk (RS < 18) had a distant recurrence rate of 7% at 10 years compared with the intermediate risk (RS 18–30) of 14% and in the high risk (RS≥31) of 31% (Paik *et al.*, 2004). Onco*type* DX can also be used to identify patients who may not benefit from adjuvant chemotherapy (discussed in section 1.2.4.1.2)

MammaPrint uses the expression profiling of a 70 gene signature, performed on fresh breast cancer tissue. The signature classifies tumours as high or low risk for recurrence

in women under the age of 61 years, with tumours measuring less than 5 cm and node negative disease (Buyse *et al.*, 2006; van de Vijver *et al.*, 2002).

The PAM50 examines 50 genes in RNA extracted from formalin fixed breast tissue. It categorises tumours as luminal A, luminal B, basal-like, HER2-enriched, and normal-like and calculates a risk of recurrence score. In patients with ER positive breast cancer, who received adjuvant tamoxifen therapy alone, it is able to identify a group of women with a low risk of recurrence (Nielsen *et al.*, 2010). In ER positive breast cancer PAM50 has been compared directly with Onco*type* DX. There is significant agreement in the identification of high and low risk of recurrence between both tests; in the those identified as having an intermediate risk of recurrence by Onco*type* DX, nearly 50% were classified as low risk by PAM50 (Bastien *et al.*, 2011). This test is still undergoing validation, but potentially may further stratify the group of patient identified as at intermediate risk of recurrence by Onco*type* DX.

1.2.4 Treatment of invasive breast cancer

The management of patients with breast cancer is multimodal and includes surgery, radiotherapy, chemotherapy, endocrine and targeted therapies together with emotional and psychosocial support. It is recommended that treatment decisions are made by a multi-disciplinary team, guided by features such as tumour size, nodal, hormone and HER2 status, co-morbidities and patient choice (National Institute for Health and Clinical Excellence, 2009b).

1.2.4.1 Treatment of early invasive breast cancer

1.2.4.1.1 Surgery

Surgery remains the key modality in achieving long term disease control in patients presenting with localised breast cancer. It is performed with the key aims of achieving local disease control and to provide staging information from both the primary and ipsilateral axillary nodes. This information guides the use of systemic therapy and enables the prediction of prognosis. Reconstructive surgery is also important for those women who undergo a mastectomy.

Over the last 30 years surgical techniques have evolved and breast conserving surgery followed by radiotherapy in those patients in whom adequate resection margins can be achieved, has become standard. In a 20 year analysis the procedure has been demonstrated to be comparable with a mastectomy in terms of local disease control, progression free survival (PFS) and OS (Fisher *et al.*, 2002). In women with large breast tumours compared to breast size, who would normally require a mastectomy, chemotherapy can be given pre-operatively (neo-adjuvant chemotherapy) (Fisher *et al.*, 1997; van der Hage *et al.*, 2001). The aim of this approach is to increase the breast conservation rate, but also provide an *in vivo* measure of chemosensitivity as response in the primary tumour can be measured clinically, radiologically and pathologically after resection.

Axillary staging increasingly utilises the technique of sentinel lymph node sampling in those patients with clinically negative lymph nodes. This saves those patients without involved sentinel lymph nodes from the morbidity associated with axillary node dissection (Mansel *et al.*, 2006) without compromising local disease control, disease free survival (DFS) or OS (Krag *et al.*, 2010). Patients with clinically involved lymph nodes undergo an ultrasound guided fine needle aspiration. If the cytology is negative patients can undergo sentinel lymph node sampling; those with positive cytology are recommended axillary node dissection.

Breast cancer has long been recognised as systemic disease as borne out by the observation that despite obtaining local disease control, many patients present with metastatic disease years later. The role of adjuvant therapy is important, as only five percent of breast cancer patients present with metastatic disease and therefore the majority of patients dying from the disease, initially presented with localised disease (Statistics and Outlook for Breast Cancer, 2009). The selection of those patients who stand to benefit from adjuvant therapy either with chemotherapy, trastuzumab and/or endocrine therapy is complex and needs to take into account tumour size, nodal status, ER status and pre-existing co-morbidities.

1.2.4.1.2 Adjuvant Chemotherapy

In the adjuvant setting the benefit of combination therapy with cyclophosphamide, methotrexate and 5-Fluorouracil (5-FU) (CMF) following surgery for breast cancer was first reported by Bonadonna *et al*. in 1976, with benefits in terms of PFS and OS (median OS increased from 104 months to 137 months) confirmed after 20 years of follow-up (Bonadonna *et al.*, 1995). By the late 1990's anthracycline based regimens were established and a 15 year meta-analysis demonstrated their benefit over non-anthracycline based regimens (EBCTCG, 2005).

Taxanes are widely used in women with node positive disease, especially if hormone receptor positive, though there is some controversy. The PACS01 trial compared six cycles of fluorouracil, epirubicin, and cyclophosphamide (FEC) with a sequential regimen of three cycles of FEC followed by three cycles of docetaxel (FEC-D) as adjuvant treatment for women with node-positive early breast cancer. Five-year OS rates were 86.7% with FEC and 90.7% with FEC-D, demonstrating a 27% reduction in the relative risk of death (unadjusted P = .014; adjusted P = .017) (Roche *et al.*, 2006). In the BCIRG 001 study, 1491 women with axillary node-positive breast cancer were randomised to six cycles of treatment with docetaxel plus doxorubicin and cyclophosphamide (TAC) or fluorouracil plus doxorubicin and cyclophosphamide (FAC). Treatment with TAC resulted in a 30% reduction in the risk of death (P=0.008) (Martin *et al.*, 2005). However, the TACT study which recruited 4162 women with node-positive or high-risk node-negative operable early breast cancer did not demonstrate any benefit from the addition of docetaxel to standard anthracycline based chemotherapy (Ellis *et al.*, 2009).

Overall patients with node positive breast cancer, ER negative disease and younger patients derive greater benefit from adjuvant chemotherapy (EBCTCG, 2005). In order to help identify specific groups of patients who stand to gain from receiving adjuvant chemotherapy, tools such as the computer programme Adjuvant! Online (Adjuvant! Online), measurement of uPA and PAI-1 (Annecke *et al.*, 2008), the presence of bone marrow micrometastases (Pantel *et al.*, 2009) and the gene signature Onco*type* DX or Mammostrat can be useful.

The 21 gene signature known as Onco*type* DX can be used to identify those patients with node negative, hormone receptor positive breast cancer who are unlikely to derive benefit from adjuvant chemotherapy. These data were derived from the NSABP-20 study in which women were randomised to receive adjuvant, non-anthracycline based chemotherapy or not, in addition to five years of treatment with tamoxifen. Women with tumours with a high RS (≥31) derived the greatest benefit from adjuvant chemotherapy and those with low RS (<18), derived no significant benefit (Paik *et al.*, 2006). The TAILORx study has been designed to examine the addition of chemotherapy to hormonal therapy in ER and/or PR positive, lymph node and HER2 negative, breast cancer. Women with a RS of less than 10 will receive hormonal therapy and those with RS of 26 or greater, hormonal therapy and combination chemotherapy. Patients with RS between 11-25, are randomised between hormonal therapy alone or in combination with chemotherapy (National Cancer Institute, 2011d).

Onco*type* DX may also be useful in patients with node positive, hormone receptor positive breast cancer. Indicating that patients with low RS may not derive benefit from anthracycline based adjuvant chemotherapy, in addition to tamoxifen, despite having a high risk of relapse (Albain *et al.*, 2010).

The Mammostrat Score in the NSABP-20 population was able to stratify patients into high and low risk groups, with the low risk group benefiting from adjuvant chemotherapy by an improvement in 10 year recurrence free interval from 86% to 91% (HR, 0.4 (95% CI, 0.2-0.8); *P* = 0.01). In the high risk group, the absolute benefit was improved by 21%, from 64% to 85% (HR, 0.4 (95% CI, 0.2-0.9); *P* = 0.02) (Ross *et al.*, 2008).

1.2.4.1.3 Adjuvant Endocrine therapy

In 1896 Beatson reported the regression of metastatic breast cancer in two premenopausal women by oophorectomy (Beatson, 1896). Since this time endocrine manipulation has become a key modality in the management of patients whose tumours express ER and/or PR. Endocrine therapies today reduce the stimulation of breast tumours which express these receptors by the hormone oestrogen (Rutqvist *et al.*, 1989). Endocrine therapies include reducing oestrogen production through ovarian

ablation or suppression, the selective oestrogen receptor modulator tamoxifen and aromatase inhibition with, for example, anastrozole or letrozole. Aromatase inhibitors prevent conversion of androgens to oestrogens, through the process of aromatisation within the adrenal gland and adipose tissue (Miller *et al.*, 2008). This means that their use is restricted to post menopausal women, as in pre-menopausal women most oestrogen is produced by the ovaries. Therefore, tamoxifen remains the adjuvant endocrine therapy in pre-menopausal women with hormone receptor positive breast cancer (Burstein *et al.*, 2010).

In post menopausal women, adjuvant treatment with an aromatase inhibitor for five years improves DFS over tamoxifen, though sequential treatment with both tamoxifen and aromatase inhibitor is no different from treatment with an aromatase inhibitor alone for five years in terms of DFS and OS (Burstein *et al.*, 2010).

1.2.4.1.4 Adjuvant trastuzumab therapy

HER2 is recognised to be associated with a more aggressive breast cancer with a shorter time to relapse (Slamon *et al.*, 1987). It can be targeted by the monoclonal antibody trastuzumab and its use for one year following completion of adjuvant chemotherapy is recommended in patients with HER2 positive breast cancer (National Institute for Health and Clinical Excellence, 2009b). Trastuzumab reduces the risk of death with a hazard ratio of 0.66 (95% CI 0.47-0.91; p=0.0115) compared with observation alone with an absolute DFS difference of 6.3% (Piccart-Gebhart *et al.*, 2005; Smith *et al.*, 2007). 52% of patients randomised to the observation arm, opted to receive adjuvant trastuzumab following the publication of the first interim analysis, with treatment beginning at a median time of 22.8 months from randomisation. These patients benefited from adjuvant trastuzumab with fewer DFS events (adjusted HR 0·68; 95% CI 0·51-0·90; p=0·0077) (Gianni *et al.*, 2011). This study (HERA study) scheduled trastuzumab following completion of chemotherapy. The FinHER study examined the use of trastuzumab in combination with docetaxel or vinorelbine. This study randomised 232 women with HER2 and node positive or high risk breast, to receive trastuzumab in combination with docetaxel or vinorelbine for nine weeks followed by three cycles of FEC chemotherapy. Distant DFS was higher in those treated with trastuzumab, docetaxel and FEC compared with docetaxel and FEC or

trastuzumab, vinorelbine and FEC (Joensuu *et al.*, 2009). Therefore, trastuzumab is given sequentially following completion of adjuvant chemotherapy or concurrently with a taxane.

1.2.4.1.5 Adjuvant radiotherapy

Local radiotherapy is important in those women who have undergone breast conserving surgery as higher rates of local recurrence occur in those who do not receive radiotherapy (14.3% vs. 39,2% P<0.001) (Elkhuizen *et al.*, 2000; Fisher *et al.*, 2002). Radiotherapy is also recommended in those patients who have undergone a mastectomy and are high risk for recurrence (large primary tumour, incomplete margins and multiple involved lymph nodes), those with a positive sentinel lymph node who are unable to undergo axillary dissection and those with locally advanced disease with supraclavicular fossa lymphadenopathy (National Institute for Health and Clinical Excellence, 2009a).

1.2.4.2 Treatment of metastatic breast cancer

Patients presenting with metastatic disease require histological confirmation of the type of cancer, HER2 and hormone receptor status to guide treatment. Currently, the reassessment of these features is not recommended in patients presenting with recurrent disease (National Institute for Health and Clinical Excellence, 2009a) but there is evidence that there may be discordance between the primary tumour and metastases (Curigliano *et al.*, 2011; Simmons *et al.*, 2009). The extent of disease is normally assessed using imaging including computed tomography, magnetic resonance imaging, plain radiography and/or bone scintigraphy (National Institute for Health and Clinical Excellence, 2009a).

Surgical resection of the primary breast tumour or local radiotherapy may improve survival in patients with metastatic disease and is considered on an individual patient basis (Ly *et al.*, 2010). Surgery and radiotherapy can also be used to treat symptomatic disease from brain or bone metastases or pathological fractures; bisphosphonates play a role in preventing fracture and improving pain (Rosen *et al.*, 2004). However, the management of metastatic breast cancer is reliant upon systemic therapy to control and delay disease progression.

1.2.4.2.1 Endocrine therapy in metastatic breast cancer

Endocrine therapy is useful in patients with ER positive and/or PR positive metastatic breast cancer. In post menopausal women, treatment with an aromatase inhibitor is more efficacious than tamoxifen (Mouridsen *et al.*, 2001). A further option is the use of the pure ER antagonist, fulvestrant, which is able to achieve response rates of around 7% in patients in whom two endocrine therapies have failed (Chia *et al.*, 2008).

1.2.4.2.2 Chemotherapy and targeted therapies in metastatic breast cancer

Anthracyclines, taxanes, capecitabine, vinorelbine and gemcitabine (Albain *et al.*, 2008; Jones *et al.*, 2005; O'Shaughnessy *et al.*, 2002; Sparano *et al.*, 2009) all demonstrate efficacy in metastatic breast cancer. Patients usually receive sequential therapy with different regimens as tolerated and dependent upon previous chemotherapy exposure. In patients with HER2 positive breast cancer, the addition of trastuzumab to standard chemotherapy regimens, with either anthracyclines or taxanes, was first demonstrated to be beneficial in 2001 (Slamon *et al.*, 2001). The observed higher rates of heart failure in combination with anthracyclines compared with paclitaxel, led to the clinical use of trastuzumab in combination with taxanes over anthracyclines.

In patients whose tumours develop resistance to trastuzumab, further targeting of HER2 with the dual EGFR and HER2 tyrosine kinase inhibitor (TKI), lapatinib, is beneficial in combination with paclitaxel (Di Leo *et al.*, 2008b) or capecitabine (Cameron *et al.*, 2008) over either chemotherapy alone (discussed further in section 1.9.5).

In the HER2 negative patient group, the addition of the anti-vascular endothelial growth factor (VEGF) antibody bevacizumab, to taxane based chemotherapy, increases response and PFS rates but not OS (Gray *et al.*, 2009; Miles *et al.*, 2010).

1.2.5 Future directions in the treatment of breast cancer

The identification of HER2 as a marker of a disease with a poorer prognosis and the ability to target this receptor significantly altered the outlook and management of HER2 positive breast cancer. This has led to the identification of tumours on their

molecular features in addition to their morphological appearance, identifying 'basal like' tumours (ER, PR and HER2 negative, cytokeratin 5/6 positive and/or EGFR positive), HER2 positive ER negative (ER−, PR−, and HER2+), luminal A (ER and/or PR positive and HER2 negative), luminal B (ER and/or PR positive and HER2 positive) and unclassified (negative for all 5 markers) tumours (Carey *et al.*, 2006).

The term 'triple negative breast cancer' refers to a sub-group of breast cancers which are negative for the expression of ER, PR and HER2. Within this group, 60% of tumours express EGFR (Irvin and Carey, 2008). The 'basal like' sub-group of breast cancers are identified through the expression of genes (e.g. cytokeratins 5 and 17, caveolin-1, c-kit and EGFR) usually found in the basal/myoepithelial cells of the normal breast (Rakha *et al.*, 2009). The terms triple negative and basal like breast cancers are often used interchangeably, but studies suggest that there is around 30% discordance between the two groups (Irvin and Carey, 2008; Rakha *et al.*, 2009). Studies are ongoing to evaluate chemotherapy regimens within these specific groups, together with the benefit of targeting EGFR, given the higher rates of expression of this receptor.

1.3 HUMAN EPIDERMAL GROWTH FACTOR RECEPTOR FAMILY

1.3.1 Human epidermal growth factor receptor structure

All receptors share a similar structure with extracellular, membrane spanning and intracellular domains (Figure 1.2). The extracellular domain in made up of four sub-domains, including a ligand binding domain and a dimerisation arm. This domain differs between receptors, which are distinguished by their affinities for different growth factors. This is in contrast to the intracellular domain, which is highly conserved across the HER family and contains an intrinsic tyrosine kinase and a carboxyl tail (Yarden and Sliwkowski, 2001).

1.3.2 Activation of human epidermal growth factor receptors

Receptor activation can be induced by the binding of specific growth factors or through ligand independent mechanisms (discussed below). HER ligands are characterised by an EGF-like motif and 13 ligands have been identified to date, though none bind to HER2 (Table 1.1) (Yarden and Sliwkowski, 2001). Whilst the affinity for

each ligand differs between receptors, it can be altered by the dimerisation partner of a receptor (Karunagaran *et al.*, 1996). For example, both EGF and betacellulin activate cell signalling in the absence of EGFR through HER2/HER3 heterodimers but are not able to activate HER2 or HER3 homodimers (Pinkas-Kramarski *et al.*, 1998).

Ligand	EGFR	HER2	HER3	HER4
EGF	+		+	
TGF-α	+			
HB-EGF	+			+
Amphiregulin	+			
Betacellulin	+			+
Epigen	+			
Epiregulin	+			+
Neuregulin-1			+	+
Neuregulin-2			+	+
Neuregulin-3				+
Neuregulin-4				+

Table 1.1 Human epidermal growth factor receptors ligands
TGF-α – transforming growth factor α
HB-EGF- heparin binding-EGF

1.3.2.1 Ligand-dependent activation

Receptors exist either as monomers or dimers in a 'tethered' autoinhibited conformation or an extended conformation ready to bind ligand (Figure 1.2) (Dawson *et al.*, 2007; Tao and Maruyama, 2008). EGFR has been shown to continually flux between these two states, with dimers requiring ligand binding for signalling (Chung *et al.*). Ligand binding to pre-formed dimers induces a rotational movement within the

transmembrane domain which may be responsible for ligand mediated receptor downstream signalling (Moriki *et al.*, 2001).

Ligand binding to monomeric receptors induces a conformational change exposing the receptors' dimerisation arm, enabling the formation of dimers with other receptors with exposed arms (Figure 1.2) (Schlessinger, 2002). The exception to this is HER2, whose dimerisation arm is permanently exposed, so an activating ligand is not required leading to its continuous ability to form dimers with other receptors (Cho *et al.*, 2003).

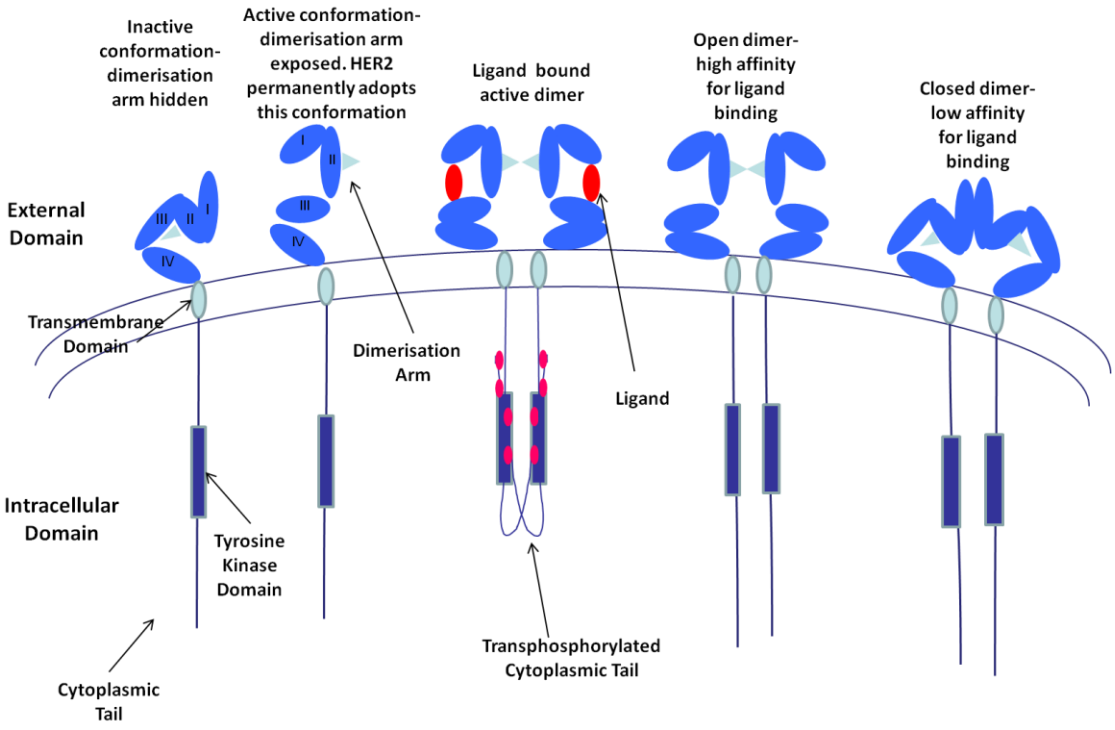

Figure 1.2 Conformation of the human epidermal growth factor receptor
The HER family share a similar structure with an extracellular, membrane spanning and intracellular domains. The extracellular domain is made up of four sub-domains, including dimerisation and ligand binding domains. Receptors can exist in preformed homo or heterodimers in a tethered, closed conformation which is not available for receptor dimerisation, or an extended, open conformation ready for ligand binding. Adapted from Tao & Maruyama, 2008.

1.3.2.2 Ligand-independent activation of HER receptors

In addition to activation by ligand, ligand-independent phosphorylation of EGFR can be induced by ultra-violet radiation (Zwang and Yarden, 2006), ionising radiation (IR) (Rodemann *et al.*, 2007; Schmidt-Ullrich *et al.*, 1997), cytotoxic drugs (Ahsan *et al.*, 2010; Benhar *et al.*, 2002; Van Schaeybroeck *et al.*, 2006), oxidative stress (Khan *et al.*, 2006) and through the direct phosphorylation of EGFR by p38 (Benhar *et al.*, 2002; Winograd-Katz and Levitzki, 2006; Zwang and Yarden, 2006).

1.3.2.3 Human epidermal growth factor receptor dimers

A hierarchy exists within the HER family with HER2 preferentially dimerising with other receptors, over the formation of homodimers (Graus-Porta *et al.*, 1997; Tzahar *et al.*, 1996). HER3 and HER4 preferentially dimerises with HER2 over EGFR, but in the absence of HER2, dimers are formed with EGFR (Graus-Porta *et al.*, 1997). Heterodimers have a number of distinct signalling advantages over homodimers; they have a higher affinity for ligand (Graus-Porta *et al.*, 1997; Sliwkowski *et al.*, 1994; Tzahar *et al.*, 1996), are more potent activators of downstream signalling (Pinkas-Kramarski *et al.*, 1996) and transcription (Kim *et al.*, 2009) and are more likely to be recycled back to the cell membrane after internalisation (Lenferink *et al.*, 1998).

EGFR is also able to dimerise with the platelet derived growth factor receptor (PDGFR) (Habib *et al.*, 1998) and insulin like growth factor receptor (IGFR) (Burgaud and Baserga, 1996); the latter can also dimerise and phosphorylate HER2 (Balana *et al.*, 2001; Nahta *et al.*, 2005). This ability to form multiple dimers with other receptors introduces a high level of redundancy in receptor activation and indicates why alterations in the expression of any one HER receptor can produce marked effects on cell signalling (Yarden and Sliwkowski, 2001).

1.3.3 Downstream signalling of human epidermal growth factor receptors

The dimerisation of ligand bound receptors allows the carboxyl tail of one receptor to be phosphorylated by the other receptor (Figure 1.2). HER3 has been described as ‘kinase dead’ or a ‘pseudokinase’ (Sierke *et al.*, 1997) due to the substitution of amino acids at two sites (Guy *et al.*, 1994) and is reliant upon dimerisation with other receptors for signalling. However, recent reports indicates that HER3 binds ATP in an

inactive conformation (Jura *et al.*, 2009; Shi *et al.*, 2010) and is able to trans-autophosphorylate, though at a lower level than induced by receptor activation and dimerisation (Shi *et al.*, 2010).

Following ligand binding and phosphorylation of the receptor's carboxyl tail, adapter proteins like growth factor receptor-bound 2 (Grb2) and src-homology 2 protein (SH2) are attracted and bind specific regions within the tail. These adapters link into the activation of a number of different downstream signalling pathways including the Ras-Raf-MAPK, phosphatidylinositol-3-kinase-AKT (PI3K/AKT), phospholipase C-γ (PLC-γ) and single transducers and activators of transcription (STAT) pathways (Yarden and Sliwkowski, 2001). In addition activated receptors are internalised, degraded or transported to the nucleus (discussed further below) (Figure 1.3).

1.3.3.1 Phosphatidylinositol 3-kinases signalling

HER3 provides six docking sites for the PI3K regulatory subunit p85 (Hellyer *et al.*, 1998), though p85 can also dock with activated EGFR through the adapter proteins SH2 and Grb2 associated binding protein 1 (Gab-1) (Rodrigues *et al.*, 2000). This enables the p110 subunit of PI3K to phosphorylate, phosphatidyl-(4,5)-bisphosphate to produce phosphatidyl-(3,4,5)-triphosphate which recruits proteins containing a phospholipid binding domains to the plasma membrane including AKT and 3-phosphoinositide-dependent protein kinase 1 (PDK-1). AKT is then phosphorylated by PDK-1 at its threonine 308-residue and/or serine 473 residue to become activated (Cantley, 2002). Phosphorylated AKT is able to activate a number of other cytoplasmic and nuclear proteins including p21 and p27 and murine double minute (MDM2) (Cantley, 2002). MDM2 leads to the degradation of p53, activates the anti-apoptotic protein, nuclear factor kappa β, and inhibits pro-apoptotic proteins like Bcl-2 associated death promoter, forkhead transcription factors and caspase-9. PI3K signalling controls a wide variety of cellular functions including cell growth, survival, apoptosis, metabolism, cell cycle progression, transcription and translation (Marone *et al.*, 2008).

1.3.3.2 Ras-Raf-MAPK pathway

Phosphorylated EGFR and HER2 attracts the adapter protein SH2, which in turn attracts Grb2. Grb2 is bound by the protein son of sevenless (SOS) which recruits and activates Ras-GDP (Bianco *et al.*, 2007). The resulting Ras-GTP triggers a signalling cascade activating B-Raf which activates MEK1&2, which activates the mitogen-activated protein kinases, MAPK1, MAPK2, p38-MAPK and Jun terminal kinases (JNK). MAPK and JNK proteins can also be activated by EGFR through its interaction with PLC-γ which activates protein kinase C (PKC). MAPK translocates to the nucleus upregulating the expression of transcription factors involved in cell proliferation, inhibition of apoptosis and cell migration (Bianco *et al.*, 2007).

1.3.3.3 Signal transducers and activators of transcription

The STAT family is made up of seven proteins, STAT1-5a, 5b and 6, which are activated by tyrosine or src kinases. These proteins are located within the cytoplasm and upon phosphorylation, dimerise and translocate to the nucleus where they bind regulatory elements within the promoters of genes promoting cell proliferation, differentiation and apoptosis (Fox *et al.*, 2008; Yang and Stark, 2008). STAT 3, 5a and 5b are constitutively activated or over-expressed in breast cancer compared with surrounding normal breast tissue, suggesting an oncogenic role (Clevenger, 2004). Overexpression of EGFR and HER2 correlates with ligand induced or constitutive activation of STAT3, STAT5a and STAT5b (Silva and Shupnik, 2007) and EGFR directly controls the activation of STAT proteins (Xia *et al.*, 2002a) or acts through janus kinase (JAK) (Andl *et al.*, 2004). In addition to activating STAT proteins, HER proteins can directly bind to STAT proteins allowing them to interact with genes promoters (discussed below).

1.3.3.4 Receptor internalisation

Inactive EGFR is constantly internalised and recycled back to the cell membrane (Burke and Wiley, 1999). EGFR internalisation can also be induced by the binding of ligand (Opresko *et al.*, 1995) or activation by p38 MAPK in response to cellular stress (Benhar *et al.*, 2002; Zwang and Yarden, 2006). The internalisation of EGFR in response to ligand requires EGFR activation (Johannessen *et al.*, 2006), recruitment of Grb2 and the ubiquitin ligase, Casitas B-lineage lymphoma (Cbl) protein (Jiang *et al.*, 2003; Levkowitz *et al.*, 1999). The recruitment of Cbl leads to the ubiquitination of the cytoplasmic tail

of EGFR, enabling interaction with ubiquitin interaction motifs located within clathrin coated pits (Huang and Sorkin, 2005). These pits pinch off from the cell membrane to form vesicles, delivering the internalised EGFR complex to endosomes where they undergo sorting, either being recycled back to the cell membrane, entering lysosomes to undergo degradation so terminating the EGFR signal, entering the endoplasmic reticulum or Golgi apparatus, or transportation to the nucleus (discussed below) (Madshus and Stang, 2009; Wang *et al.*, 2010).

The internalisation of EGFR in response to phosphorylation by p38 MAPK is less well characterised but the recruitment of Cbl is not required (Adachi *et al.*, 2009) and can occur into clathrin coated pits (Zwang and Yarden, 2006) or caveolae (Dittmann *et al.*, 2008; Khan *et al.*, 2006).

1.3.3.5 Nuclear translocation of human epidermal growth factor receptors

Despite the fact that HER proteins are membrane located receptors, full length nuclear EGFR, HER2 and HER3 and a cleaved C-terminal 80kDa fragment of HER4, known as HER4 intracellular domain (4ICD), can be detected within nuclei using Western blotting, immunofluorescence (IF), confocal or electron microscopy and chromatin immunoprecipitation (ChIP) (Lin *et al.*, 2001; Ni *et al.*, 2001; Offterdinger *et al.*, 2002). Transport of receptors can be induced by ligands (Lin *et al.*, 2001), IR or cisplatin (Dittmann *et al.*, 2005a) and requires the presence of a nuclear localisation sequence (NLS). The NLS is a conserved 13 amino acid sequence located within the juxtamembrane region of all HER receptors (Hsu and Hung, 2007), though HER3 has an additional NLS located within its C-terminal domain (Lin *et al.*, 2001).

Nuclear HER proteins are able to activate the transcription of specific genes (Wang *et al.*, 2010). As they lack a DNA binding domain, they interact with DNA through the binding to transcription factors like STAT3, STAT5a and E2F1 located on gene promoters, allowing the receptor to utilise its transactivational ability to activate transcription (Lo and Hung, 2007; Wang *et al.*, 2010). Examples include the binding of EGFR to STAT3 to regulate the transcription of cytokine inducible nitric oxide synthase (iNOS) and cyclooxygenase 2 (COX-2), to E2F1 to activate the transcription of β-Myb, and STAT5 to activated the Aurora-A promoter as well as regulating the transcription

of cyclin D1 directly (Hanada *et al.*, 2006; Hung *et al.*, 2008; Lin *et al.*, 2001; Lo *et al.*, 2006; Lo and Hung, 2007). HER2 is also able to transactivate the transcription of cyclooxygenase 2 (COX2) (Wang *et al.*, 2004) and thymidylate synthase (Kim *et al.*, 2009).

1.3.3.6 Glucose transport

There is evidence that EGFR stabilises the active sodium glucose co-transporter (SGLT) in a mechanism independent of its kinase activity, increasing the transport of glucose into cells and preventing cell death through autophagy (Weihua *et al.*, 2008).

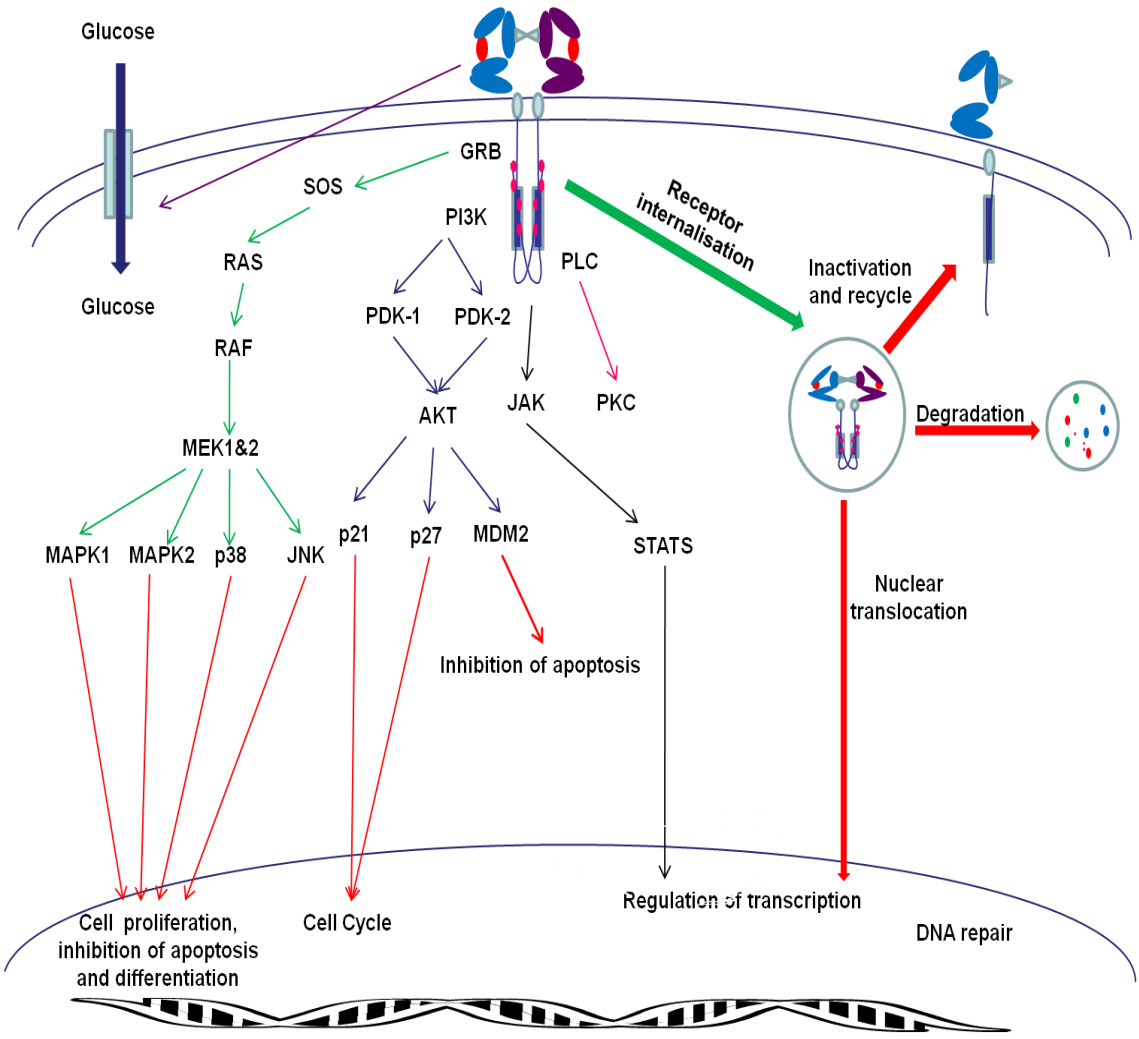

Figure 1.3 Human epidermal growth factor receptor signalling
The HER family signals into a number of downstream pathways including the PI3K/AKT, MAPK and STAT pathways.

1.4 HUMAN EPIDERMAL RECEPTOR EXPRESSION AND CANCER

The HER family of proteins are expressed in variety of normal tissues but gain an oncogenic role through overexpression, gene amplification, constitutive activation, increased ligand stimulation or down-regulation of mitogen-inducible gene 6 (MIG6) also known as negative regulator erbB receptor feedback inhibitor (ERFFI1) and receptor-associated late transducer (RALT).

1.4.1 Overexpression of human epidermal receptors

Overexpression of HER proteins in tumours compared with normal tissue has been demonstrated in breast (Bieche *et al.*, 2003), ovarian (Steffensen *et al.*, 2008) and colorectal cancers (Ciardiello *et al.*, 1991). The clearest link between a member of the HER family and cancer prognosis established so far occurs in breast cancer (Slamon *et al.*, 1987).

1.4.1.1 EGFR overexpression

EGFR is a 170 kDA protein encoded on chromosome 7p12 and is detected in a wide variety of cancers, including head and neck, breast, oesophageal, non small cell lung cancers (NSCLC) and colorectal cancers. The oncogenic role of EGFR is demonstrated by the increase in EGFR expression between normal, hyperplastic, dysplastic and neoplastic tissue in squamous cancers of the head and neck. Increases in EGFR expression are also observed in the normal epithelium surrounding tumours, compared with non-cancerous controls, with a further increases in EGFR expression occurring between dysplastic tissue and carcinomas (Shin *et al.*, 1994).

In patients, EGFR expression rather than gene amplification appears to be a driver of tumours, with gene amplification only detected in 2% gastric cancers (Kim *et al.*, 2008c), 1.6% of triple negative breast tumours (Gumuskaya *et al.*, 2010) and 8-12% of non small cell lung cancers (NSCLC) (Bell *et al.*, 2005; Kim *et al.*, 2008a).

1.4.1.2 HER2 overexpression

HER2 is a 185 kDa protein encoded on chromosome 17q21 and is expressed in normal breast tissue and detected in most breast tumours, with less than 5% of tumours reported as under-expressing HER2 compared with normal breast tissue (Bieche *et al.*,

2003). In the 20-30% of tumours which overexpress HER2 as detected by IHC (Slamon *et al.*, 1987; Toikkanen *et al.*, 1992) all are HER2 amplified at a gene level (Willmore *et al.*, 2005). In other cancers the link between expression and gene amplification is less clear cut; 10-34% of gastric tumours overexpress HER2 as detected by IHC with gene amplification detected in 39-84% of these (Allgayer *et al.*, 2000; Bang *et al.*, 2010; Tsugawa *et al.*, 1993; Yan *et al.*, 2010) and 10-30% of pancreatic adenocarcinoma (Komoto *et al.*, 2009a; Stoecklein *et al.*, 2004) with gene amplification detected in 40% of these but in 24% of all pancreatic tumours analysed (Stoecklein *et al.*, 2004).

1.4.1.3 HER3 overexpression

HER3 is a 185 kDA protein encoded on chromosome 12p13 and overexpression occurs in 20-46% of invasive breast cancers and is associated with a poorer OS (Bieche *et al.*, 2003). A single study has reported HER3 overexpression in 58% of gastric tumours with a correlation with a poorer OS (Hayashi *et al.*, 2008). HER3 gene amplification is less well investigated with a single report of occurrence in 27% of NSCLC (Cappuzzo *et al.*, 2005).

1.4.1.4 HER4 overexpression

HER4 is a 180 kDa protein encoded on chromosome 2q33 and its expression may actually be protective, with reduced expression noted in 40-80% of adenocarcinoma and up to 100% of squamous carcinoma (Srinivasan *et al.*, 1998). In breast cancer the reported expression of HER4 varies widely, with underexpression reported in 20-30% of breast cancer and overexpression in up to 30%. In breast cancer overexpression of HER4 has been shown to be linked with longer DFS (Aubele *et al.*, 2007; Pawlowski V *et al.*, 2000; Sassen *et al.*, 2008). This is not the case in colorectal cancer where HER4 expression has been demonstrated to correlate with lymph node positivity (Kountourakis *et al.*, 2006).

1.4.2 Increase in the secretion of human epidermal growth factor receptor ligands

HER ligands are type I transmembrane proteins, expressed on the cell surface. They are cleaved by cell surface proteases in a process of ectodomain shedding, forming soluble ligands (Higashiyama *et al.*, 2008). The main proteases involved in the shedding of

these ligands are the a disintegrin and metalloproteinase (ADAM) family of enzymes (Singh *et al.*, 2009; Xu and Derynck, 2010).

Higher levels of amphiregulin are detected in colorectal tumours compared with normal tissue (Ciardiello *et al.*, 1991), with increased levels of both amphiregulin and TGF-α in breast cancers compared with normal breast tissue (Panico *et al.*, 1996). ADAM17 expression is increased in 90% of colorectal cancers compared with normal mucosa (Blanchot-Jossic *et al.*, 2005) and its transfection into breast cancer cell lines increases the secretion of the EGFR ligand, TGFα, promoting EGFR signalling, cell proliferation, invasion and angiogenesis (Zheng *et al.*, 2009). These data indicate that increases in ligand production can increase HER signalling.

1.4.3 Constitutive activating mutations

Activating mutations within EGFR were first recognised in glioblastoma, produced by an in-frame deletion in exons 2-7, deleting 267 amino acids from the receptor's extracellular domain (Wong *et al.*, 1992). This deletion produces a truncated EGFR, EGFR variant III (EGFR vIII), which is constitutively active and independent of EGF (Nishikawa *et al.*, 1994). EGFR vIII is expressed in 20-30% of unselected glioblastoma (Gan *et al.*, 2009), 5% of squamous cancers of the lung (Ji *et al.*, 2006), 42% of head and neck squamous carcinomas (Sok *et al.*, 2006) and 4% of breast cancers (Nieto *et al.*, 2007).

Whilst EGFR vIII is not detected in adenocarcinoma of the lung (Ji *et al.*, 2006), in-frame deletions, in-frame insertions and mis-sense substitutions (Shigematsu *et al.*, 2005) in exons 18-21 can be detected in 5-30%, with a higher incidence in female never smokers from East Asia (Riely *et al.*, 2006; Shigematsu *et al.*, 2005). In-frame deletions in exon 19 account for 45% of mutations and a further 45% are due to mis-sense substitutions in exon 21, with the commonest substitution, leucine for arginine at codon 858 (EGFR L858R) (Shigematsu *et al.*, 2005). These mutations cluster around the ATP binding pocket of EGFR, prolonging EGF-induced signalling for up to three hours compared with 15 minutes in wild type receptors (Lynch *et al.*, 2004) and are collectively known as EGFR activating mutations.

The type of EGFR mutation varies between tumours, with mutations in the tyrosine kinase domain of EGFR rare in glioblastoma (Marie *et al.*, 2005), not detected in breast cancer (Bhargava *et al.*, 2005), but more common in lung cancer. Mutations affecting the external EGFR domain occur more frequently in glioblastoma with 14% due to mis-sense mutations (Lee *et al.*, 2006b) and 20-30% due to the expression of EGFR vIII (Gan *et al.*, 2009).

Together this evidence demonstrates the importance of HER signalling within cancer cells and that the HER family can drive tumour growth through the increased receptor activity due to mutations resulting in constitutive activation of the affected receptor, increases in ligand expression driving receptor signalling or receptor overexpression. Therefore the ability to target specific receptors has been a major development in both enhancing our understanding of HER signalling and in the treatment of cancers.

1.4.4 Regulation of human epidermal growth factor receptors by MIG6

MIG6 is a transcriptionally induced negative feedback inhibitor of EGFR and HER2, inhibiting receptor activity and downstream signalling (Fiorentino *et al.*, 2000; Xu *et al.*, 2005) through binding to the erbB-binding region of the receptors' kinase domain (Anastasi *et al.*, 2003). Research has focussed on the interaction between MIG6 and EGFR which results in the inhibition of receptor activity, endocytosis and delivery into lysosomes, leading to degradation thereby reducing receptor expression (Frosi *et al.*, 2010; Ying *et al.*, 2010). The erbB-binding region is conserved across the HER family and MIG6 binds to all four receptors *in vitro* indicating a role in the regulation of all receptors (Anastasi *et al.*, 2003).

1.5 ANTI-HUMAN EPIDERMAL RECEPTOR TARGETED THERAPIES

HER targeted therapies are classified into two groups; the small molecule receptor TKIs (e.g. gefitinib, erlotinib and lapatinib) and the monoclonal antibodies (e.g. trastuzumab, cetuximab, panitumumab and pertuzumab). These drugs bind to different domains of the HER proteins, with TKIs binding the intracellular tyrosine kinase containing domain and monoclonal antibodies to the extracellular domain. In addition to those anti-HER therapies that are in clinical use, there are a number agents undergoing evaluation in early phase clinical trials (Table 1.2) plus small molecule TKIs

research compounds e.g. the EGFR targeted TKI A1478 and the HER2 targeted TKI AG825.

Drug	Target	Type
Pertuzumab (Baselga and Swain, 2010)	HER2 dimerisation arm	Humanised mAb
Canertinib (Rixe *et al.*, 2009)	HER1-4	Irreversible TKI
BMS-599626	EGFR, HER2 & HER4	TKI
Neratinib (HKI-272) (Sequist *et al.*, 2010)	HER2	Irreversible TKI
ARRY-334543	EGFR & HER2	Reversible TKI
Afatinib (BIBW-2992) (Yap *et al.*, 2010)	EGFR & HER2	Irreversible TKI

Table 1.2 Anti-HER targeted drugs undergoing evaluation in clinical trials
Information obtained from http://clinicaltrials.gov/ct2/home

1.5.1 Clinical HER targeted monoclonal antibodies

1.5.1.1 Cetuximab (C225/Erbitux®)

Cetuximab is a mouse chimeric monoclonal antibody with high affinity for EGFR, preventing ligand-induced phosphorylation and inhibiting tumour growth (Goldstein *et al.*, 1995). In colorectal cancer cetuximab increases response rates and PFS in combination with chemotherapy in patients whose tumours express wild type K-ras (Bokemeyer *et al.*, 2009; Van Cutsem *et al.*, 2009) or as single agents in patients with irinotecan refractory colorectal cancer (Cunningham *et al.*, 2004). In squamous cell cancer of the head and neck, cetuximab in combination with radiotherapy increases OS in patients with unresectable disease (Bonner *et al.*, 2010), response rates in patients with metastatic disease in combination with cisplatin (Burtness *et al.*, 2005) and OS in patients with recurrent or metastatic disease in combination with platinum and 5FU based chemotherapy regimens (Vermorken *et al.*, 2008). In NSCLC, the addition of cetuximab to standard chemotherapy with cisplatin and vinorelbine increases median OS (Pirker *et al.*, 2009)

Cetuximab binds to EGFR, occluding its ligand binding domain and preventing the receptor from adopting the extended conformation required for dimerisation (Brehmer *et al.*, 2005), inhibiting the formation of EGFR homodimers and EGFR-HER2 heterodimers (Patel *et al.*, 2009). The binding of cetuximab to EGFR can induce receptor phosphorylation (Liao and Carpenter, 2009; Yoshida *et al.*, 2008b) and internalisation, with both increased transport to the nucleus (Liao and Carpenter, 2009) and inhibition, with accumulation in the cytoplasm demonstrated (Dittmann *et al.*, 2005b). Despite the induction of EGFR phosphorylation, downstream signalling by AKT or MAPK is not stimulated (Yoshida *et al.*, 2008b).

1.5.1.2 Panitumumab (ABX-EGF/Vectibix®)

Panitumumab is a fully humanised monoclonal antibody which binds to the external domain of EGFR. As a single agent it increases PFS in patients with chemorefractory metastatic colorectal cancer (Van Cutsem *et al.*, 2007) and in combination with oxaliplatin or irinotecan based chemotherapy regimens in the first line setting (Douillard *et al.*, 2010; Peeters *et al.*, 2010).

1.5.1.3 Trastuzumab (Herceptin®)

Trastuzumab has been shown to effective in patients with HER2 positive breast cancer in both the adjuvant and metastatic setting (discussed in sections 1.2.4.1.4 and 1.2.4.2.2). The addition of trastuzumab to standard cisplatin and 5-FU based chemotherapy is also beneficial in advanced gastric cancer, increasing median OS (Bang *et al.*, 2010).

Trastuzumab binds to the juxtamembrane of HER2 (Cho *et al.*, 2003), inhibiting the formation of HER2-HER3 dimers (Junttila *et al.*, 2009) and inducing the phosphorylation of HER2 (Diermeier *et al.*, 2005; Scaltriti *et al.*, 2009) leading to receptor internalisation, ubiquitination and degradation (Scaltriti *et al.*, 2009). Other actions include the Inhibition of PI3K/AKT signalling (Dubska *et al.*, 2005; Junttila *et al.*, 2009) and the induction of a G0/G1 cell cycle arrest (D'Alessio *et al.*, 2009).

1.5.2 Clinical HER targeted small molecule tyrosine kinase inhibitors

1.5.2.1 Gefitinib (ZD 1839/Iressa®)

Gefitinib is an oral low molecular weight quinazoline which is a potent selective and reversible competitive-ATP inhibitor for EGFR. In patients with NSCLC with activating EGFR mutations, gefitinib significantly increases PFS compared with chemotherapy with carboplatin and paclitaxel in the first line setting (Mok *et al.*, 2009a). As discussed in section 1.4.3, activating EGFR mutations occur within the ATP-binding pocket, resulting in a constitutively active receptor (Lynch *et al.*, 2004; Paez *et al.*, 2004; Pao *et al.*, 2004). In patients with NSCLC, who have received first line treatment with a platinum based chemotherapy regimen, gefitinib demonstrates non-inferiority to docetaxel chemotherapy, regardless of EGFR mutation status (Kim *et al.*, 2008a).

In vitro data indicates that gefitinib binds to EGFR when it is in an open conformation (Johnson, 2009), promoting the formation of EGFR homodimers and binding to EGF (Lichtner *et al.*, 2001) whilst inhibiting EGFR, HER2 and HER3 receptor phosphorylation (Chun *et al.*, 2006; Morgan *et al.*, 2008; Sergina *et al.*, 2007), reducing FOXM1 (McGovern *et al.*, 2009) and FOXO3a expression (Krol *et al.*, 2007) inducing a G0/G1 cell cycle arrest (D'Alessio *et al.*, 2009; Krol *et al.*, 2007). Gefitinib also inhibits the formation of HER2 and HER3 dimers through direct interaction with HER2 (Hirata *et al.*, 2005).

1.5.2.2 Erlotinib (OSI-774/Tarceva®)

Erlotinib is an oral reversible inhibitor of EGFR and is able to directly inhibit HER2 (Schaefer *et al.*, 2007). Erlotinib increases both PFS and OS in patients with NSCLC refractory to at least one chemotherapy regimen (Shepherd *et al.*, 2005) and increases PFS in combination with gemcitabine in patients with pancreatic cancer over gemcitabine alone (Moore *et al.*, 2007).

Clinically, as with gefitinib, increased sensitivity is observed in patients with NSCLC expressing an activating EGFR mutation (Pao *et al.*, 2004). Erlotinib has a similar mechanism of action to gefitinib, inhibiting EGFR and HER2 activation, therefore inhibiting PI3K/AKT and Ras-Raf-MAPK signalling (Schaefer *et al.*, 2007). Erlotinib also inhibits the transcription of thymidylate synthase and its activity (a target of the active

metabolites of 5-FU) (Giovannetti *et al.*, 2008) and increases the expression of the enzyme thymidine phosphorylase, which is required for the conversion of 5-FU into its active metabolites (Ouchi *et al.*, 2006) (see section 1.8.4).

1.5.2.3 Lapatinib (Tykerb®)

Lapatinib is an oral quinazoline derived competitive reversible ATP-inhibitor, binding to the ATP binding site of both EGFR and HER2; the drug binds to the closed conformation of EGFR (Johnson, 2009). It increases time to progression and overall response rates in combination with chemotherapy is patients with HER2 positive breast cancer refractory to anthracyclines, taxanes and trastuzumab treatment (discussed in sections 1.2.4.2.2 and 1.9.5).

In vitro lapatinib inhibits the phosphorylation of HER2 but not the formation of dimers with other receptors (Scaltriti *et al.*, 2009), including EGFR (Xia *et al.*, 2002b). In turn it inhibits the activation of downstream signalling including the PI3K/AKT and Ras-Raf-MAPK pathways (Konecny *et al.*, 2006; Xia *et al.*, 2002b), induces G0/G1 cell cycle arrest (Kim *et al.*, 2008b), prevents the nuclear translocation of both EGFR and HER2 (Kim *et al.*, 2009) and reduces the expression of FOXM1 (McGovern *et al.*, 2009) and thymidylate synthase (Kim *et al.*, 2009).

1.5.3 Differences between monoclonal antibodies and small molecule tyrosine kinase inhibitors on HER inhibition

There are obvious differences between antibodies and TKIs including their size (monoclonal antibodies are around 150kDa and EGFR TKI 500Da which prevents them crossing the blood brain barrier), administration (intravenous versus orally) and half life (monoclonal antibodies have a half life measured in days, so can be given weekly and TKIs around 36-48 hours so are given daily) (Imai and Takaoka, 2006). Whilst TKIs bind to their target receptor with high affinity they are not specific, binding to other HER members and have a number of off target effects as they are able to enter cells and inhibit their targets regardless of location (Brehmer *et al.*, 2005). In contrast, monoclonal antibodies are specific to their receptor target and require it to be located on the cell membrane. However, this may confer an advantage over TKIs, in that they can trigger complement and antibody-dependent cellular cytotoxicity which may

actually be enhanced by the chimeric nature of some monoclonal antibodies (Imai and Takaoka, 2006).

The inhibition of HER signalling by monoclonal antibodies and TKIs is not the same *in vitro,* a fact which may explain clinical differences. This is demonstrated by the fact that the EGFR targeted antibody cetuximab and the anti-EGFR TKIs gefitinib or erlotinib produce a greater inhibition of the growth of cancer cell lines and xenografts in combination than either drug alone (Huang *et al.*, 2004; Matar *et al.*, 2004). Gefitinib is also able to inhibit the cell growth of cetuximab resistant cell lines (Huang *et al.*, 2004), and in combination with cetuximab, induces greater inhibition of EGFR, AKT and MAPK activation (Matar *et al.*, 2004).

Differences in the targeting of HER2 with trastuzumab or lapatinib are also apparent. Firstly lapatinib is able to inhibit cell proliferation in cell lines resistant to trastuzumab (Konecny *et al.*, 2006) and the combination of both drugs together produces a greater effect than either drug on its own in both breast and gastric cancer cell lines (Wainberg *et al.*, 2010; Xia *et al.*, 2005). This may be explained by the observed differences in the actions of each drug, as lapatinib inhibits the phosphorylation of HER2 homo or heterodimers and hence their internalisation increasing the accumulation of inactive HER2 on the cell membrane. This increases the availability of HER2 which can be bound by trastuzumab, leading to increased levels of immune mediated cytotoxicity (Scaltriti *et al.*, 2009).

1.6 DNA DAMAGING AGENTS IN ANTI-CANCER THERAPY

The systemic treatment of cancer utilises a single or combination of cytotoxic drugs in the neo-adjuvant, adjuvant and palliative settings with drugs that damage DNA forming the base of a number of standard chemotherapy regimens. Nitrogen mustard was the first systemic anti-cancer agent introduced into clinical practice in the 1940's (Goodman *et al.*, 1984) and since its use in the treatment of lymphoma, many more drugs have been developed and are now in routine clinical use, including platinum (e.g. cisplatin, carboplatin and oxaliplatin), taxane (e.g. docetaxel and paclitaxel), epipodophyllotoxin (e.g. etoposide) and anthracycline (e.g. doxorubicin, epirubicin and idarubicin) drugs. Whilst DNA damaging agents such as IR and platinum drugs inflict a

variety of insults on cells, the importance of their ability to damage DNA in order to producing cell death is illustrated by the fact that cells with defects in specific DNA repair pathways are more sensitive to these agents (Hoeijmakers, 2009).

1.6.1 Cisplatin

Upon entry into a cell, the cisplatin molecule loses its chloride ions due to the lower intracellular low chloride concentration. These ions are replaced by water molecules which can readily be substituted for the N7 of guanine or adenine bases in DNA (Kartalou and Essigmann, 2001), thus forming monoadducts (Figure 1.4). Monoadducts can link with other nearby DNA monoadducts on the same strand of DNA forming intrastrand crosslinks, the complementary DNA strand forming interstrand crosslinks or proteins forming DNA-protein adducts (Figure 1.4) (Wang and Lippard, 2005). Intrastrand crosslinks account for 90% of cisplatin-induced DNA lesions, with interstrand crosslinks accounting for 5-8% (Dronkert and Kanaar, 2001). The latter lesion is reported to be the cause of the cytotoxicity of cisplatin by preventing DNA unwinding and separation required for DNA replication and transcription (Dronkert and Kanaar, 2001).

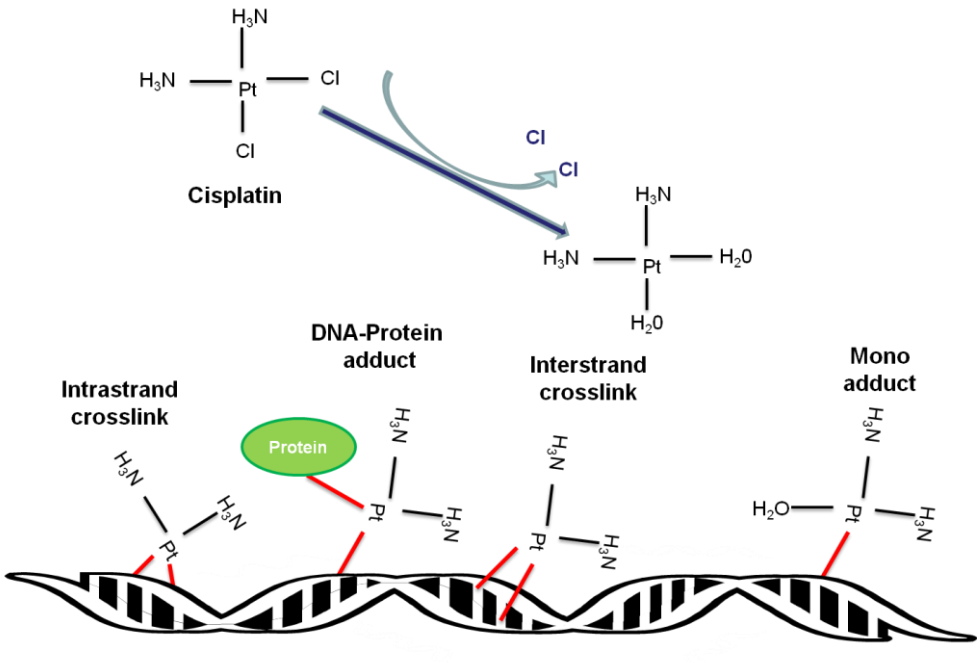

Figure 1.4 Induction of DNA lesions by cisplatin
On entry into a cell, cisplatin loses its two chloride ions through a series of spontaneous aquation reactions. The water molecules can be readily substituted for N7 sites of purine bases forming DNA protein adducts, mono adduct and intrastrand or interstrand crosslinks.

1.6.2 Topoisomerase II poisons

The enzyme topoisomerase II (Topo II) is a target of both anthracyclines and epipodophyllotoxins, enabling these drugs to produce DNA double strand breaks (DSBs).

1.6.2.1 Isoforms of the Topoisomerase II enzyme

Two isoforms of Topo II enzyme exist in mammalian cells, topoisomerase IIα (Topo IIα and topoisomerase IIβ (Topo IIβ). These two isoforms demonstrate 72% similarity with the main differences occurring in the N and C terminals (Jenkins *et al.*, 1992). Topo IIα expression alters with cell cycle phase with expression peaking during G2/M, in contrast with Topo IIβ, which is constantly expressed at the same level regardless of the cell cycle (Woessner *et al.*, 1991).

1.6.2.2 Topoisomerase II function

Topo II plays an essential role in removing knots, supercoils and catenanes from DNA allowing the double helix to be unwound for replication and transcription (Pommier *et al.*, 2010). Topo II acts as a homodimer with each molecule binding a strand of DNA, known as the G segment. Upon binding ATP, Topo II dimerises and undergoes a conformational change, forming a closed clamp cleaving the phosphodiester backbone of the DNA strand to form a DNA DSB (Figure 1.5) (Oestergaard *et al.*, 2004).

The free ends of DNA remain bound at their 5' ends by Topo II, so that they can be rejoined. This complex is known as the cleavable complex and is transient in nature. The break in the DNA strand allows the passage of another section of DNA, known as the T segment, through the break, so resolving catenanes and knots. Following strand passage, the two free DNA stands within the cleavable complex are religated, with ATP hydrolysis releasing Topo II from the DNA (Pommier *et al.*, 2010).

In addition to enabling the replication and transcription of DNA, Topo II is required to separate intertwined sister chromatids before chromosome segregation can occur in mitosis (Holm *et al.*, 1989b).

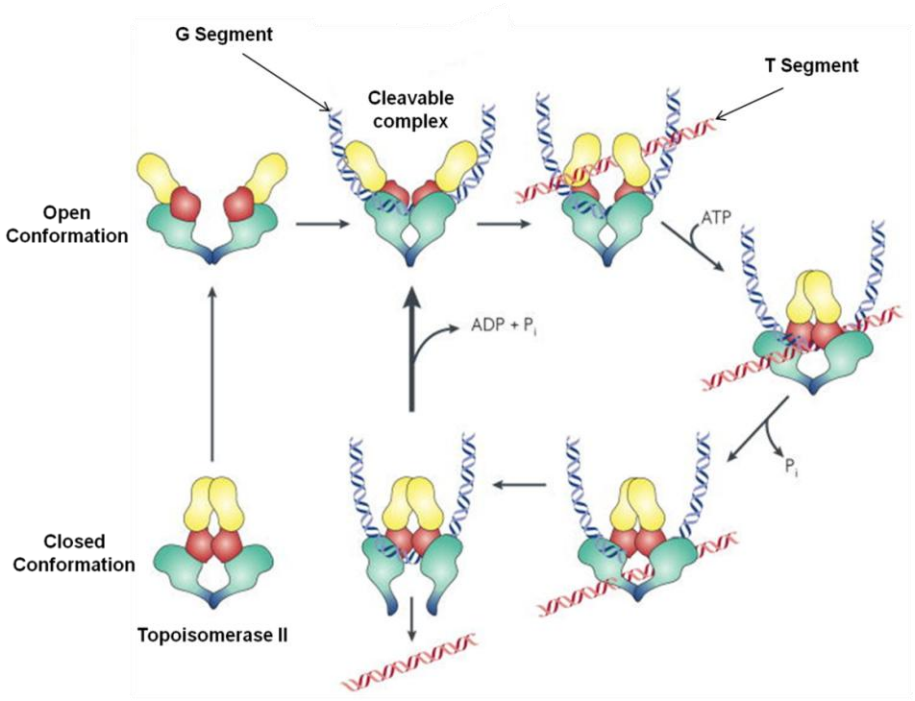

Figure 1.5 Mechanism of action of topoisomerase IIα poisons
Topo II forms a homodimer and binds to a segment of the DNA helix, known as the G segment. It then introduces a DNA DSB within the G segment to form a cleavable complex, made up of the two free ends of DNA, bound by a molecule of Topo IIα. The DNA DSB allows a segment of the DNA double helix, the T segment, to pass through DNA double helix, following which the DNA break is religated and Topo IIα released from the G segment. Reprinted by permission from Macmillan Publishers Ltd: Nature Reviews Molecular Cancer, Nitiss 2009b, 9:338-350; ©2009; http://www.nature.com/nrc/index.html

1.6.2.3 Topoisomerase structure

The full crystal structure of human Topo II has not been defined, but three functional regions have been identified, the N and C terminal regions and a catalytic core. These domains are conserved across eukaryotic Topo II (Nitiss, 2009a). The N-terminal region contains an ATP-binding site and is able to hydrolyse ATP, a process required for the passage of one strand of DNA through the Topo II produced DSB (Oestergaard *et al.*, 2004). The C-terminal domain is phosphorylated at serine and threonine residues with 14 sites characterised to date (Grozav *et al.*, 2009). These control the function and location of the enzyme, though are not required for catalytic activity *in vitro* (Oestergaard *et al.*, 2004). The catalytic core of the enzyme is responsible for DNA cleavage and religation (Oestergaard *et al.*, 2004) and is connected to the ATP-binding domain by the transducer domain (Oestergaard *et al.*, 2004). The transducer domain is important for communication between the ATP-binding region of Topo II and the catalytic core, with mutations within this domain preventing DNA strand passage

despite not interfering with the binding of ATP or DNA cleavage (Oestergaard *et al.*, 2004).

1.6.2.4 Targeting Topoisomerase II

Topo II is targeted by two distinct types of drugs, poisons and inhibitors. Topo II poisons differ from inhibitors in that they require a functioning enzyme to form cleavable complexes. The poisons act either by preventing the religation of DNA within the cleavable complex, forming DNA single and double strand breaks, or by promoting the formation of cleavable complexes (Nitiss, 2009a). In contrast, Topo II inhibitors inhibit activity of Topo II, for example by preventing the enzyme from binding to DNA, therefore inhibiting its normal cellular action. This is thought to be the mechanism through which they produces cytotoxicity (Pommier *et al.*, 2010). This explains the antagonism between Topo II poisons and inhibitors (Jensen *et al.*, 1991), why sensitivity to Topo II poisons increases with increasing Topo II expression (Fry *et al.*, 1991) whereas sensitivity to Topo II inhibitors increases with falling Topo II expression (Davies *et al.*, 1997). Drugs which poison Topo II in clinical use include etoposide, doxorubicin, m-AMSA, idarubicin and epirubicin. All of these drugs act as Topo II poisons by preventing DNA religation by Topo II within the cleavable complex (Nitiss, 2009b).

1.6.2.4.1 Etoposide

Etoposide is a Topo II poison which targets both isoforms of Topo II, though most research has concentrated on investigating its effect on Topo IIα (Ross *et al.*, 1984; Willmore *et al.*, 1998). Drug sensitivity correlates with the expression and activity of Topo II (Kasahara *et al.*, 1992). Etoposide is an ATP-dependent Topo II poison, with ATP-depletion conferring resistance to the drug (Sorensen *et al.*, 1999). Two binding sites for the drug have been isolated, one in the catalytic core of Topo II and the other, a lower affinity site, in the N-terminal ATP-binding pocket (Vilain *et al.*, 2003). Etoposide binds to a complex made up of DNA, Topo II and ATP, stabilising one half of the cleavable complex, forming a single strand break (Osheroff, 1989). Whether Topo II needs to be bound to DNA in order to be targeted by etoposide *in vivo* is unclear, but it can be targeted in the absence of DNA *in vitro* (Leroy *et al.*, 2001). The formation of a DSB requires one etoposide molecule to bind to each of the two Topo II molecules

which makes up a cleavable complex (Bromberg *et al.*, 2003). DNA replication or transcription are important in the induction of cell death by etoposide (D'Arpa *et al.*, 1990; Holm *et al.*, 1989a). This observation may be explained by the fact that Topo II rapidly religates DNA DSBs following removal of etoposide, as per its normal function and etoposide cytotoxicity relies upon the removal of Topo II from the DSB, which occurs during replication and transcription, converting the DSB into a permanent lesion (Nitiss, 2009b).

1.6.2.4.2 Doxorubicin

In vitro studies demonstrate that doxorubicin can induce a number of cytotoxic processes including intercalation with DNA, free radical formation leading to DNA damage, lipid peroxidation, DNA alkylation and the poisoning or inhibition of Topo II, leading to cell cycle arrest and apoptosis (Gewirtz, 1999). Its effects are dose dependent, with DNA intercalation and Topo II inhibition occurring at concentrations of 10 µM and greater. *In vivo* the main mechanisms of doxorubicin-induced cytotoxicity are mediated through the poisoning of Topo II, free radical and DNA-adduct formation (Gewirtz, 1999). Like etoposide, doxorubicin is dependent upon ATP to poison Topo II (Sorensen *et al.*, 1999) and though the precise site at which doxorubicin targets Topo II is unresolved, the binding to DNA to form a tertiary structure is thought to be essential (Moro *et al.*, 2004).

1.6.3 Ionising Radiation

IR describes types of radiation that have enough energy to detach electrons from atoms or molecules (ionising), producing ionised atoms and free electrons, examples include x-rays, γ-rays and ultra-violet radiation. IR induces DNA damage through the direct and indirect ionisation of DNA, producing single and double DNA strand breaks and modifying DNA bases. Approximately 1000 single strand breaks and 25-40 DSBs are produced per gray of IR in a single diploid cell, though this number can be altered by hypoxia and cellular levels of glutathione (Olive, 1998). 30% of DNA strand breaks are produced directly by IR, with indirect DNA damage due to the production of reactive oxygen species (ROS) and free radicals, accounting for the remaining 70% of damage (Wallace, 1998). These reactive species can also produce DNA single and

double strand breaks, DNA-protein crosslinks, alterations to DNA bases and DNA base loss (Wallace, 1998).

1.7 RESISTANCE TO DNA DAMAGING AGENTS

Resistance to DNA damaging agents arises through a number of different mechanisms, including evasion of the DNA damaging effects of drugs, the repair of DNA damage or the ability to tolerate the damage inflicted.

1.7.1 Reduced intracellular drug concentration

Reduction in the intracellular concentration of cytotoxic agents can lead to drug resistance. This arises due to a variety of factors which can alter the amount of drug reaching an individual cell, reduce uptake or increase efflux of the drug out of the cell. Water soluble drugs enter cells through membrane located transporters which are involved in the uptake of nutrients and resistance to a number of chemotherapy agents including cisplatin, methotrexate and 5-FU can be mediated through reduced transport of drugs into cells (Gottesman *et al.*, 2002).

The efflux of drugs out of cells confers resistance to a variety of drugs including anthracyclines, vinca alkaloids, taxanes and etoposide resulting in phenotype known as multi-drug resistance (Gottesman *et al.*, 2002). The best characterised transporter protein is P-glycoprotein, which is expressed in a variety of tumours including breast cancer (Clarke *et al.*, 2005; Gottesman *et al.*, 2002). P-glycoprotein is encoded by the multi-drug resistance (MDR1) gene (Ueda *et al.*, 1987) and is a member of the ATP binding cassette (ABC) family (Gottesman *et al.*, 2002). This family has a number of sub-families including the seven members of the ABCC sub-family, known as membrane resistance proteins (MRP 1-7), and the breast cancer resistance protein (BCRP), a member of the ABCG sub-family (Gottesman *et al.*, 2002). These proteins function as membrane located pumps which efflux drugs from cells, reducing intracellular drug concentration, so reducing their cellular effects (Gottesman *et al.*, 2002).

1.7.2 Conjugation to glutathione

Glutathione-S-transferases (GST) are a group of enzymes which detoxify a variety of toxins through their conjugation with glutathione. Expression of glutathione-S-transferase P1 (GSTP1) is linked to resistance to both doxorubicin and cisplatin (Huang *et al.*, 2007). The conjugation of drugs with glutathione only explains a small fraction of this mechanism of resistance (Peklak-Scott *et al.*, 2008) and GSTP1 activation in response to stress activates other key signalling pathway involved in cell survival including upregulation of MAPK p38, MAPK and nuclear factor kappa β signalling (Fiorentino *et al.*, 2000).

1.7.3 Modulation of drug targets

Drugs which target specific enzymes to induce their DNA damaging effects include 5-FU, Topo I and II poisons. Resistance to these drugs can be mediated by the modulation of their drug targets. As discussed in section 1.6.2.4, Topo II poisons like doxorubicin or etoposide, target Topo II preventing the religation of DNA strand breaks produced as part of the normal function of the enzyme. Therefore, their effectiveness is dependent upon the expression and activity of Topo II (Burgess *et al.*, 2008) (discussed below). This is in contrast to 5-FU, which inhibits the enzyme thymidylate synthase and resistance to the drug can be mediated by the increased expression of the enzyme (Longley *et al.*, 2001; Wong *et al.*, 2001).

1.7.3.1 Resistance to topoisomerase II poisons by reduction in the expression of topoisomerase II

Topo IIα expression alters with the cell cycle with levels falling during G0/G1, unlike Topo IIβ which is constantly expressed (Pommier *et al.*, 2010). Topo II poisons have activity against both Topo II isoforms, though the relative contributions of each isoform varies between drugs, with doxorubicin having little activity against Topo IIβ where as the Topo II poison, m-AMSA targets both equally (Errington *et al.*, 2004; Willmore *et al.*, 1998). Correlation between Topo IIα expression and sensitivity to Topo II poisons has been demonstrated by some clinical studies and *in vitro* (Burgess *et al.*, 2008; Di Leo *et al.*, 2008a). However, both Topo IIα gene amplification and deletion have been shown to be associated with sensitivity to anthracyclines, an observation which is contradictory (Di Leo *et al.*, 2008a) but may be explained by the regulation of

Topo II transcription and translation (Di Leo *et al.*, 2008a). The transcription and translation of Topo IIα is highly regulated and linked to cell proliferation, with gene amplified cells expressing high levels of the proliferation marker Ki-67, expressing higher levels of Topo IIα protein than those with low levels of Ki-67, despite Topo IIα gene amplification (Di Leo *et al.*, 2008a).

1.7.3.2 Resistance to topoisomerase II poisons by alteration in the location of topoisomerase II

Topo II can be detected in both cell nuclei and cytoplasm in cancer cell lines (Engel *et al.*, 2004). *In vitro*, cells are able to traffic Topo IIα out of the nucleus through the nuclear envelope protein CRM1 (exportin-1), an act that results in resistance to etoposide (Engel *et al.*, 2004) and doxorubicin (Turner *et al.*, 2009). Resistance is due to the fact that cytoplasmic Topo II is no longer in contact with DNA and therefore unable to produce cleavable complexes, additionally cytoplasmic Topo IIα may bind Topo II poisons reducing the concentration reaching the nucleus.

1.7.3.3 Resistance to topoisomerase II poisons by alteration in topoisomerase II activity

Topo II undergoes a number of post translational modifications including phosphorylation (Heck *et al.*, 1989), sumoylation (Lee and Bachant, 2009) and ubiquitination (Shinagawa *et al.*, 2008). Topo II is phosphorylated in a cell cycle dependent manner (Wells and Hickson, 1995) and a number of specific sites have been characterised within Topo IIα enzyme including serine 1524 (Wells *et al.*, 1994), threonine 1342 (Ishida *et al.*, 1996) and serine 1106 (Chikamori *et al.*, 2003). Four specific site of phosphorylation have been isolated within Topo IIβ, serine 1395, threonine 1426, serine 1545 and tyrosine 656 which is important for the catalytic activity of the enzyme (Grozav *et al.*, 2011). Alterations in both the phosphorylation of the Topo II catalytic domain and binding of ATP have been demonstrated to modulate the effects of Topo II poisons.

1.7.3.3.1 Alterations in ATP binding to topoisomerase II and resistance to topoisomerase II poisons

The process of decatenation and unknotting of DNA by Topo II occurs in an ATP dependent process (Nitiss, 2009a). Some Topo II poisons have been identified as only being active when Topo II is bound to ATP, with ATP depletion conferring resistance leading to classification into two groups- ATP-dependent and independent poisons (Sorensen *et al.*, 1999). Etoposide, doxorubicin, teniposide and daunorubicin are classed as ATP-dependent poisons (Sorensen *et al.*, 1999) with amonafide, bactracyclin and menadione as ATP-independent (Wang *et al.*, 2001). The evidence of the effects of ATP on the ability of m-AMSA to poison Topo II is contradictory with both ATP-dependence and independence demonstrated (Sorensen *et al.*, 1999; Wang *et al.*, 2001).

1.7.3.3.2 Alterations in topoisomerase II phosphorylation and resistance to topoisomerase II poisons

Another mechanism of resistance to Topo II poisons is through the alteration of the phosphorylation of the enzyme. Phosphorylation at serine-1106 in the catalytic domain of Topo IIα is demonstrated to regulate both its activity and sensitivity to Topo II poisons, with dephosphorylation at this site rendering cells resistant to etoposide or m-AMSA- induced DNA cleavage (Chikamori *et al.*, 2003; Grozav *et al.*, 2009).

1.7.4 Cell cycle

The cell cycle is able to modulate the infliction of DNA damage by chemotherapy drugs, its detection and the cellular response to the damage (discussed below). Cell cycle modulates the infliction of DNA damage by drugs which target cellular activities which only occur in a certain phase of the cell cycle. Examples include the Topo II poisons (discussed in section 1.7.3.1), taxanes and pyrimidine analogues such as 5-FU, cytarabine and gemcitabine.

Taxanes act as microtubule inhibitors, stabilising GDP-bound tubulin, therefore preventing chromatid separation and mitosis (Hennequin *et al.*, 1995). Pyrimidine analogues act by becoming incorporated into DNA in place of the pyrimidine bases thymidine and cytosine, preventing the DNA replication. 5-FU also prevents the *de*

novo production of thymidine through the inhibition of thymidylate synthase (discussed in section 1.8.4) (Longley *et al.*, 2003). Therefore, the arrest of cells in G0/G1 protects cells from the effects of taxanes and 5-FU as the processes of mitosis and DNA replication are not active (Hennequin *et al.*, 1995; Shah and Schwartz, 2001) and from Topo II poisons due to reduce expression of Topo IIα.

1.7.5 DNA Repair

Aside from the therapeutic use of DNA damaging agents, an individual cell is estimated to receive 20, 000 DNA damaging lesions every day. These arise from either normal cellular functions, such as the production of oxygen free radicals at sites of inflammation, during DNA replication or from the environment such as cigarette smoke, chemical dyes and ultra-violet radiation. To cope with this level of DNA damage cells have evolved a variety of mechanisms for detecting and repairing DNA damage, or triggering apoptosis when repair is not possible (Hoeijmakers, 2009). These same processes are involved in the repair of DNA damage induced by cancer treatments.

The response to DNA damage is triggered by the recognition of the presence of DNA damage by the cell and the arrest of the cell cycle to allow its repair. Where damage cannot be repaired, cells should undergo apoptosis. This response is complex and requires the coordinated functioning a large number of proteins and pathways. DNA damage results in the activation of the ataxia–telangiectasia mutated (ATM) protein, ataxia–telangiectasia and rad3-related (ATR) and the checkpoint kinases CHK1 and CHK2. This results in increased levels of the cyclin dependent kinase inhibitor (CDKI), p21 or inhibition of CDK activators such as the Cdc25 phosphatases. Cyclin dependent kinases control the cell cycle and their inhibition by p21 leads to activation of the DNA damage check points at G1/S or G2/M transition points, arresting the cell cycle. Cells then undergo DNA repair, apoptosis or enter the senescence (Al-Ejeh *et al.*, 2010; Malumbres and Barbacid, 2009).

The exact processes involved in the repair of DNA damage inflicted by anti-cancer therapies are dependent upon the type of lesion produced, often utilising components of more than one repair pathway (Table 1.3). DNA repair pathways include Nucleotide Excision Repair (NER), Base Excision Repair (BER), Mismatch Repair (MMR),

Homologous Recombination (HR), Non-Homologous End Joining (NHEJ) and Single Strand annealing (SSA).

DNA DSBs are recognised by a protein complex made up of MRE11, RAD50 and NBS1 (MRN complex) which binds to the free DNA strands within a DSB. This complex plays a key role in the processing the free ends of DNA, keeping the ends in close proximity and signalling the presence of a DSB (Scott and Pandita, 2006). NHEJ, HR and SSA are all involved with the repair of DNA DSBs following the recognition of the free DNA ends by a the MRN complex. DNA DSB repair by HR is confined to the S/G2M phase of the cell cycle, due to the requirement of an identical sister chromatid, making it an error free mechanism of DNA repair (Scott and Pandita, 2006).

DNA damaging agent	Type of DNA lesion induced	DNA repair pathway					
		NHEJ	HR	NER	BER	TLS	SSA
Cisplatin	Mono adducts DNA-protein adduct Interstrand Crosslink Intrastrand crosslink	✓	✓	✓ ✓ ✓ ✓		✓	
Topoisomerase II poisons	Double strand break Single strand break	✓	✓				✓ ✓
Ionising radiation	Single strand break Double strand break Altered DNA bases	✓		✓ ✓	✓ ✓		✓ ✓

Table 1.3 Summary of types of DNA repair pathways involved in the repair of DNA damage
NHEJ- non-homologous end joining, HR-homologous recombination, NER-nucleotide excision repair, BER-base excision repair, TLS-translesion synthesis, SSA-single strand annealing.

Briefly, following recognition of the DSB by the MRN complex, HR involves a three step process, presynapsis, synapsis and postsynapsis. Presynapsis involves the processing of free single stranded DNA ends to 3'-OH ends, the formation of a presynaptic filament through binding of replication protein A (RPA), which has a high affinity for single stranded DNA. This allows the loading of RAD51 onto the single stranded DNA, forming a presynaptic filament which invades the DNA of the sister chromatid and searches for the specific DNA sequence it requires. This process requires a number of proteins known as RAD51 paralogs, XRCC2, XRCC3, RAD51C, RAD51D, plus BRCA1, BRCA2,

RAD52 and RAD54 (Scott and Pandita, 2006; Wyman *et al.*, 2004). Once the correct section of DNA is identified, DNA synthesis occurs to fill in the missing DNA using the sister chromatid as a template. Post synapsis involves the two DNA molecules disengaging from each other and ligating to form an intact DNA strand.

In contrast to HR, NHEJ can occur during all phases of the cell cycle, though is more error prone. NHEJ relies on the binding of the DNA-activated protein kinase (DNA-PK) subunits Ku70 and Ku80, to the free DNA ends of a DSB. This in turn recruits the DNA-PK catalytic subunit (DNA-PKcs), forming DNA-PK, which once activated recruits artemis, XRCC4, ligase 4 and DNA polymerase μ. Artemis processes the DNA ends to make them suitable for ligation by ligase 4. DNA polymerase μ then fills in the missing DNA nucleotides (Hoeijmakers, 2009; Scott and Pandita, 2006).

SSA is an error prone mechanism of repair DNA DSB, as a section of DNA is deleted, and utilises components of both HR and NHEJ (Valerie and Povirk, 2003). It involves the generation of single stranded DNA overhangs, the search for homology within the DNA strand, annealing at the site of homology and the trimming of the unwanted DNA, resulting in the loss of DNA sequences.

1.7.5.1 Repair of cisplatin-induced DNA damage

The repair of cisplatin-induced DNA damage is complex and requires processes to remove intrastrand and interstrand DNA crosslinks, DNA-protein adducts and DNA DSBs. The presence of a cisplatin adduct is signalled by the significant distortion it produces in the DNA double helix. These lesions are primarily repaired by NER which has two branches, each with different triggers, but both feed into the same repair pathway (Wang and Lippard, 2005). Transcription coupled repair (TCR) is activated by stalled RNA polymerases whilst transcribing DNA and hence are focused on repairing transcription blocking lesions. The other branch, known as global genomic repair (GGR), is activated by damaged DNA binding protein (DDB), XPC or XPE protein complexes and repairs the untranscribed portion of genes. Following detection of an adduct, DNA around the site is unwound by transcription factor IIH and helicase XPD and XPB, the resulting intermediate is stabilised by replication protein A (RPA) and XPA which orientate the two endonucleases ERCC1/XPF and XPG. They make 5' and 3'

excisions respectively, removing the damaged nucleotides. DNA is then synthesised across the gap, using the opposite DNA strand as a template (Muniandy *et al.*, 2010).

Interstrand crosslinks can be recognised and repaired by the process described above or through the stalling of an RNA polymerase or replication fork (Muniandy *et al.*, 2010). The current proposed mechanism of repair of interstrand crosslinks involves the attraction of proteins belonging to the Fanconi anaemia pathway to stalled replication forks, with repair involving NER, HR and the process of translesion DNA synthesis (TLS). Following recognition of an interstrand crosslink, the crosslink is 'unhooked' from one section of DNA through the action of ERCC1 and XPF, resulting in the formation of a DSB and an adduct attached to a single DNA strand only. The DSB is repaired by HR and the adduct removed by NER, with the gap left filled by TLS (Muniandy *et al.*, 2010).

The role of HR in modulating sensitivity to cisplatin has been recognised for nearly 20 years (Caldecott and Jeggo, 1991) with breast tumours carrying BRCA1 mutations and hence defective HR, more sensitive to cisplatin than non-BRCA1 mutated breast tumours (Byrski *et al.*, 2010). The NHEJ protein DNA-PK appears to be involved in modulating resistance to cisplatin in conjunction with EGFR (Dittmann *et al.*, 2005a; Friedmann *et al.*, 2006) (discussed below). However, in general the role of NHEJ in the repair of cisplatin-induced damage is less clear, with NHEJ deficient cell lines not demonstrating increased sensitivity to cisplatin (Helleday, 2010).

1.7.5.2 Repair of ionising radiation induced DNA damage

The repair of IR-induced DNA DSBs is thought to rely on the process of NHEJ, with damaged bases and single stand breaks repaired by BER and NER (Hoeijmakers, 2009). Increasingly there is evidence that these pathways contain proteins which interact with each other and may act in a coordinated manner to repair DNA damage (Mahaney *et al.*, 2009). For example DNA-PK, a main component of NHEJ, is targeted by the BER protein XRCC1 in response to IR, which is involved in the repair IR-induced single strand breaks and altered bases (Mahaney *et al.*, 2009).

1.7.5.3 Repair of Topo II poison induced DNA-damage

Topo II poisons induce both single and double DNA strand breaks though investigation into their repair has focused on the DNA DSB contained within the Topo II bound cleavable complex. This DSB can normally be religated as part of the normal function of the Topo II enzyme (see Figure 1.5). Doxorubicin and etoposide prevent this religation step through the poisoning of Topo II, so the repair of the DNA DSB is dependent upon other cellular mechanisms of DNA repair. Additionally, cleavable complexes can be turned into permanent DSBs if they block replication or transcription (Fan *et al.*, 2008). The first step in processing and repair involves the removal of the Topo II protein from the free DNA strands, allowing the signaling of the presence of a DSB through the formation of γH2AX foci and recruitment of repair proteins. This can be achieved through one of two pathways; transcription or replication dependent (Nitiss, 2009b). The transcription-dependent pathway degrades the Topo II-DNA covalent complex through proteolysis, with proteasome inhibition reducing the formation of γH2AX foci (Zhang *et al.*, 2006). The replication-dependent pathway uses nucleolytic digestion to remove the protein covalently bound to DNA. A nucleolytic step is also required following proteolysis of the cleavable complex, as some residual amino acids are left attached to DNA (Nitiss, 2009b).

The DNA DSB contained within the cleavable complex can be repaired by NHEJ, HR or SSA. NHEJ appears to be the main pathway involved in repair with increased sensitivity to Topo II poisons demonstrated following the silencing of ligase 4 (Toyoda *et al.*, 2008) and in NHEJ deficient cells (de Campos-Nebel *et al.*, 2010). Additionally, DNA-PK_{cs} inhibitors delay the repair of Topo II poison-induced DNA DSBs (Toyoda *et al.*, 2008). The role of HR is more contentious with the knockdown of Rad54 not increasing sensitivity to etoposide or doxorubicin (Toyoda *et al.*, 2008), though HR deficient cells are more sensitive to the Topo II poisons etoposide and idarubicin (de Campos-Nebel *et al.*, 2010; Treszezamsky *et al.*, 2007). Overall the process of NHEJ is able to repair Topo II-induced DNA DSB throughout the cell cycle, with HR active in the S and S/G2-phases (de Campos-Nebel *et al.*, 2010).

1.8 MECHANISMS OF ENHANCEMENT OF CYTOTOXICITY BY SMALL MOLECULE TYROSINE KINASE INHIBITORS

There is a clear rationale for the combination of HER targeted therapies and cytotoxic agents based upon the correlation between EGFR expression and resistance to chemotherapy (Ang *et al.*, 2004; Buchholz *et al.*, 2005; Kumar *et al.*, 2008; Scambia *et al.*, 1995), radiotherapy (Giralt *et al.*, 2005) and chemoradiotherapy (Kumar *et al.*, 2008; Noordhuis *et al.*, 2009). In addition EGFR phosphorylation is induced in response to IR and chemotherapy drugs including cisplatin, doxorubicin, gemcitabine, irinotecan and paclitaxel (Bianco *et al.*, 2002; Chinnaiyan *et al.*, 2005; Kishida *et al.*, 2005; Morgan *et al.*, 2008; Schmidt-Ullrich *et al.*, 1997; Van Schaeybroeck *et al.*, 2006; Winograd-Katz and Levitzki, 2006; Yoshida *et al.*, 2008a) and the transfection of EGFR into cancer cell lines confers resistance to cytotoxic therapies (Dickstein *et al.*, 1995). These observations suggest that EGFR is involved in mediating resistance to cytotoxic agents and that the addition of anti-EGFR therapies may enhance cell killing. This has been demonstrated extensively *in vitro* with the combination of EGFR TKIs with cytotoxic drugs (Ciardiello *et al.*, 2000; Friedmann *et al.*, 2004; Ren *et al.*, 2008; Sirotnak *et al.*, 2000) or radiation (Bianco *et al.*, 2002; Chinnaiyan *et al.*, 2005; Toulany *et al.*, 2010; Zhou *et al.*, 2004) and in xenograft models (Chun *et al.*, 2006; Morgan *et al.*, 2008; Ouchi *et al.*, 2006).

Unlike EGFR, the expression of HER2 and resistance to chemotherapy is mixed. The amplification of HER2 is associated with sensitivity to anthracyclines (Yamauchi *et al.*, 2001) and resistance to cisplatin (Calikusu *et al.*, 2009). However, these observations are not explained by HER2 alone as the transfection of HER2 into cancer cells lines or xenografts is only able to modulate sensitivity to chemotherapy drugs in a cell line dependent manner (Pegram *et al.*, 1997).

The precise mechanisms through which EGFR targeting TKIs are able to enhance the effects of traditional anti-cancer therapies are being uncovered and include the modulation of a variety of cellular processes, which are discussed below.

1.8.1 Inhibition of EGFR activation by tyrosine kinase inhibition

The phosphorylation of EGFR in response to chemotherapy or IR is mediated by the shedding of EGFR ligands through the activation of ADAM enzymes (Kim *et al.*, 2005; Singh *et al.*, 2009; Xu and Derynck, 2010). This process is dependent upon p38 MAPK (Xu and Derynck, 2010) and Src (Poghosyan *et al.*, 2002) resulting in the shedding of the EGFR ligands amphiregulin, HB-EGF, TGF-α and heregulin, chiefly by ADAM 17 (Kishida *et al.*, 2005; Kyula *et al.*, 2010; Xu and Derynck, 2010; Yoshida *et al.*, 2008a). Irinotecan induced EGFR phosphorylation can be prevented by the inhibition of ADAM17, demonstrating the role of this pathway in activating EGFR in response to cytotoxic agents (Kishida *et al.*, 2005).

In addition to the release of EGFR ligands, the production of ROS by cytotoxic agents inhibits protein-tyrosine phosphatases preventing EGFR dephosphorylation, increasing EGFR signalling (Dittmann *et al.*, 2009; Szumiel, 2006).

Gefitinib, erlotinib and lapatinib inhibit the induction of EGFR phosphorylation by IR and chemotherapy (Bianco *et al.*, 2002; Chinnaiyan *et al.*, 2005; Chun *et al.*, 2006; Morgan *et al.*, 2008; Munk *et al.*, 2007; Ren *et al.*, 2008; Tanaka *et al.*, 2008) and gefitinib is also able to reduce the transcription of amphiregulin and HB-EGF (Kishida *et al.*, 2005). Therefore TKIs are able to prevent the phosphorylation of EGFR by EGFR ligands secreted in response to IR and a variety of chemotherapy drugs together with downregulating the transcription of some EGFR ligands.

1.8.2 Inhibition of multi-drug resistance transporters by tyrosine kinase inhibitors

TKIs reduce resistance to cytotoxic drugs in cells expressing ABC transporter proteins, including P-glycoprotein (Leggas *et al.*, 2006; Yang *et al.*, 2005), BRCP (Lopez *et al.*, 2007; Nakamura *et al.*, 2005; Perry *et al.*, 2010; Yanase *et al.*, 2004), MRP-7 (Kuang *et al.*, 2010), ABCB1 and ABCG2 (Dai *et al.*, 2008). This is mediated through the direct binding of the TKI to the transporter, resulting in hydrolysis of ATP and accumulation of transporter substrate within the cell (Kitazaki *et al.*, 2005; Shi *et al.*, 2007). The transport of drugs by ATP-binding cassette member proteins is an active process using ATP (Gottesman *et al.*, 2002). The stimulation of hydrolysis of ATP by both gefitinib and erlotinib indicates that these drugs are substrates for ABC transporters and therefore

reduce the efflux of other substrates including cytotoxic drugs (Shi *et al.*, 2007). These data demonstrate that TKIs can increase the cytotoxicity of chemotherapy drugs by preventing their export via multi-drug resistance transporters leading to higher concentrations within cells.

1.8.3 Inhibition of conjugation to glutathione by tyrosine kinase inhibitors

EGF increases the level of intracellular glutathione which in turns protects cells from the effects of IR (Wollman *et al.*, 1994) and EGFR can activate the enzyme GSTP1, increasing the conjugation of cisplatin with glutathione, neutralising its cytotoxic effects (Okamura *et al.*, 2009). In cell lines, the TKI lapatinib inhibits EGF-induced activation of GSTP1 sensitising cells to cisplatin (Okamura *et al.*, 2009) and the EGFR TKI AG1478 reduces intracellular glutathione content. Therefore, TKIs may increase cytotoxicity of chemotherapy drugs by reducing glutathione levels and inhibiting the phosphorylation of GSTP1, thereby reducing the ability of cells to detoxify these agents.

1.8.4 Increasing sensitivity to 5-fluorouracil by tyrosine kinase inhibitors

5-FU is a pyrimidine analogue which requires conversion into active metabolites including fluorodeoxyuridine monophosphate (FdUMP) and fluorodeoxyuridine triphosphate (FdUTP). The enzyme thymidine phosphorylase converts 5-FU into fluorodeoxyuridine, which is then converted into FdUMP and FdUTP. These metabolites affect a number of cellular processes, for example FdUMP inhibits the enzyme thymidylate synthase, preventing the *de novo* formation of thymidine required for DNA synthesis (Longley *et al.*, 2003).

TKIs can potentiate the cytotoxic effects of 5-FU through their action on multi-drug resistance transporters (discussed above), the reduced expression of thymidylate synthase (Giovannetti *et al.*, 2008; Magne *et al.*, 2003; Ouchi *et al.*, 2006) and increased expression of the enzyme thymidine phosphorylase (Magne *et al.*, 2003; Ouchi *et al.*, 2006). The downregulation of thymidylate synthase expression is mediated by the inhibition the transcription factor E2F-1 (Giovannetti *et al.*, 2008) and the inhibition of nuclear transport of both EGFR and HER2, which prevents activation of the thymidylate synthase gene promoter (Kim *et al.*, 2009). In addition, increased

expression of thymidine phosphorylase enhances the production of the 5-FU metabolites, FdUMP and FdUTP.

1.8.5 Inhibition of DNA repair by tyrosine kinase inhibitors

TKIs have been demonstrated to reduce DNA repair following IR (Chinnaiyan *et al.*, 2005; Li *et al.*, 2008; Tanaka *et al.*, 2008) or chemotherapy (Friedmann *et al.*, 2004). The inhibition of DNA repair by TKIs may be due to the inhibition of the PI3K/AKT pathway, inhibition of nuclear transport of receptors and modulation of the activity of DNA-PK.

1.8.5.1 Inhibition of PI3K/AKT pathway by tyrosine kinase inhibitors

The phosphorylation of AKT is induced by IR (Tanaka *et al.*, 2008; Toulany *et al.*, 2010) and some chemotherapy drugs (Li *et al.*, 2007) and appears to be a key requirement for successful combination of TKIs with cytotoxic agents. Lapatinib inhibits cell growth in pancreatic cancer cell lines but only induces radiosensitivity when AKT phosphorylation is inhibited. In resistant cells, lapatinib does not inhibit AKT phosphorylation, but the addition of an AKT inhibitor can induce radiosensitivity (Kimple *et al.*, 2010). Gefitinib induced inhibition of AKT is also crucial in drug combinations, with gefitinib following gemcitabine inhibiting AKT phosphorylation and increasing cell death, but when given prior to gemcitabine, no inhibition of AKT is observed and cells are resistant to gemcitabine (Chun *et al.*, 2006). Studies which have examined cytotoxic agents in combination with TKIs on AKT activation, have demonstrated inhibition of AKT phosphorylation in successful combinations (Bianco *et al.*, 2002; Li *et al.*, 2007; Morgan *et al.*, 2008).

AKT is involved in DNA repair by NHEJ (Golding *et al.*, 2009), activating DNA-PK (discussed below), up-regulating the expression of MRE11, a protein involved in the recognition of DNA DSBs (Deng *et al.*, 2011) and controlling the expression of the HR protein RAD51 (Ko *et al.*, 2009). This indicates that the inhibition of AKT signalling by TKIs could inhibit DNA repair through the modulation of both the recognition of DNA damage and the process of repair through NHEJ and/or HR.

1.8.5.2 Inhibition of nuclear translocation of EGFR and HER2 and inhibition of DNA repair

The nuclear translocation of EGFR has been demonstrated in cell lines in response to both IR and cisplatin (Dittmann *et al.*, 2005a; Hsu *et al.*, 2009; Liccardi *et al.*, 2011). Deletion of the NLS sequence from EGFR thereby reducing nuclear translocation, sensitises cells to the cytotoxic effects of cisplatin and reduces DNA end joining activity (Hsu *et al.*, 2009). HER2 transfected into the MDA-MB-468 breast cancer cell line also translocates into the nucleus following exposure to cisplatin, a process that is blocked by the deletion of the NLS sequence (Boone *et al.*, 2009). Lapatinib is able to inhibit the translocation of both EGFR and HER2 into the nucleus and this may be a potential mechanism through which TKIs inhibit DNA repair (Kim *et al.*, 2009). Whilst the inhibition of chemotherapy-induced nuclear translocation of EGFR or HER2 by TKI has not been reported in the literature, this has been demonstrated in our laboratory using gefitinib.

1.8.5.3 Modulation of DNA-activity and location

Immunoprecipitation experiments have demonstrated the nuclear translocation EGFR, binding to DNA-PK_{cs} and increase in its activity in response to IR and cisplatin (Dittmann *et al.*, 2005a; Liccardi *et al.*, 2011). DNA-PK_{cs} plays a key role in the repair of DNA DSBs by NHEJ and its expression and activity is inhibited by erlotinib (Toulany *et al.*, 2010) and gefitinib (Friedmann *et al.*, 2006). Gefitinib treatment only inhibits the repair of cisplatin-induced interstrand crosslinks when EGFR is able to translocate to the nucleus, failing to inhibit repair in cells transfected with a mutated EGFR which does not translocate on exposure to cisplatin (Liccardi *et al.*, 2011). This suggests that gefitinib inhibits cisplatin-induced nuclear translocation of EGFR, resulting in a reduction in nuclear DNA-PK activity, which inhibits DNA repair.

1.9 COMBINATIONS OF ANTI-HER TYROSINE KINASE INHIBITORS WITH CHEMOTHERAPY

1.9.1 Breast Cancer

The addition of gefitinib to epirubicin, paclitaxel and docetaxel has been studied in a number of phase II studies. However, the objective clinical responses reported by

these studies are not significantly higher than those observed with chemotherapy alone (Ciardiello *et al.*, 2006; Dennison *et al.*, 2007; Fountzilas *et al.*, 2005; Gasparini *et al.*, 2005) (Table 1.4). Similar findings have been reported by a phase II study of erlotinib in combination with gemcitabine in patients with pre-treated metastatic breast cancer, where the response rates were lower than historical controls for single agent gemcitabine (Graham DL *et al.*, 2005).

Two phase III trials have examined the addition of lapatinib to chemotherapy in patients with metastatic breast cancer. The combination of lapatinib and capecitabine was granted FDA approval on the basis of a multicentre open label trial comparing capecitabine alone with lapatinib plus capecitabine in women with HER2 amplified breast cancer whose disease had progressed following treatment with trastuzumab, anthracyclines and taxanes (Cameron *et al.*, 2008; Geyer *et al.*, 2006). This study was stopped following an interim analysis of 324 enrolled patients. At this point, time to progression was reported as 27.1 weeks for lapatinib plus capecitabine versus 18.6 weeks for capecitabine alone (hazard ratio, 0.57; p = .00013) (Geyer *et al.*, 2006). The second phase III studied compared lapatinib plus paclitaxel against single agent paclitaxel as first line in the metastatic setting. Women were permitted to have received neo-adjuvant and adjuvant chemotherapy. HER2 status was assessed retrospectively and results for HER2-negative and HER2-positive groups analysed. In the HER2-negative group, there was no statistical significant difference in time to progression or overall response rates between chemotherapy alone or in combination with lapatinib. In contrast, the HER2-positive group demonstrated that combination treatment was superior with overall response rates of 63.3% vs. 37.8% (p 0.023), and delayed time to progression of 11 weeks (36.4 vs. 25.1 weeks (p0.005)) (Di Leo *et al.*, 2008b). Therefore lapatinib is able to produce increased clinical benefits in combination with capecitabine or paclitaxel.

Authors	Phase	Trial Drug Regimen	Prior Therapy	HER Status	Response			
					CR	PR	SD	PD
Geyer, 2006 Cameron, 2008	III	Lapatinib+ capecitabine vs. capecitabine alone	At least 2 regimens + trastuzumab	Pos	<1 vs. 0	23 vs. 14	38 vs. 29	13 vs. 23
Ciardiello, 2006	II	Gefitinib +docetaxel	Adjuvant therapy	Mixed	12	42	14	32
Dennison, 2007	II	Gefitinib + docetaxel	Adjuvant therapy	Mixed	3	36	12	48
Di Leo, 2008	III	Lapatinib+ paclitaxel vs. paclitaxel	Chemotherapy	Pos	10 vs. 3	53 vs. 35	18 vs. 30	14 vs. 22
				Neg	3 vs. 2	27 vs. 21	34 vs. 46	25 vs. 25
Fountzilas, *2005*	II	Paclitaxel+ carboplatin+ gefitinib	Adjuvant chemotherapy	Mixed	13	44	31	4.4
Gasparini, 2005	I	Weekly epirubicin + gefitinib	Adjuvant or taxane or doxorubicin	Mixed		14	50	38
Twelves, 2008	Ib	Dose escalation of erlotinib + docetaxel and capecitabine	Chemotherapy No previous anti-HER2 therapy	Mixed	8	50	21	8

Table 1.4 Clinical trials of tyrosine kinase inhibitors and chemotherapy in breast cancer

1.9.2 Pancreatic Cancer

The benefit of the addition of erlotinib to standard chemotherapy with gemcitabine in patients with advanced pancreatic cancer has been demonstrated in a randomised placebo controlled phase III trial in 559 patients (Moore *et al.*, 2007). 17% of patients treated with gemcitabine alone lived for one year compared with 23% in patients treated with gemcitabine in combination with erlotinib (p 0.023).

1.9.3 Lung Cancer

Clinical trials in non small cell lung cancer provide the largest data set from randomised phase III trials comparing standard chemotherapy with the addition of a TKI or placebo, in over 4000 patients. INTACT 1 examined the combination of gefitinib 250 mg or 500 mg daily or placebo with gemcitabine and cisplatin, in 1093 patients and found no benefit for the addition of gefitinib in terms of median survival, median time

to progression or response rates (Giaccone *et al.*, 2004). INTACT 2 was a similar designed study examining the combination of gefitinib 250 mg or 500mg daily or placebo with paclitaxel and carboplatin. It also reported no significant difference in overall survival, time to progression or response rates (Herbst *et al.*, 2004). TRIBUTE investigated erlotinib or placebo in combination with paclitaxel and carboplatin in 1059 patients, also finding no benefit of the addition of erlotinib in median survival, objective response or time to progression (Herbst *et al.*, 2005). The combination of erlotinib or placebo with gemcitabine and cisplatin in 1172 patients also failed to demonstrate any benefit of the addition of erlotinib in terms of response rates, overall survival or time to progression (Gatzemeier *et al.*, 2007).

1.9.4 Head and Neck Cancer

Erlotinib has been safely combined with cisplatin (Siu *et al.*, 2007) and gefitinib in combination with cisplatin or 5-FU chemoradiotherapy with additional benefits over historical controls demonstrated (Chen *et al.*, 2007; Cohen *et al.*, 2010). However efficacy may be dependent upon the chemotherapy agent used, as gefitinib did not add any additional benefit in combination with paclitaxel and radiotherapy (Van Waes *et al.*, 2010). Lapatinib has also been safety combined with cisplatin based chemoradiotherapy in a phase I study (Harrington *et al.*, 2009).

1.9.5 Colorectal Cancer

Early phase studies have also examined the addition of gefitinib or erlotinib to standard chemotherapy regimens in colorectal cancer. Safety and additional activity over historical data has been demonstrated by the combination oxaliplatin and 5-FU based chemotherapy with erlotinib (Hanauske *et al.*, 2007; Meyerhardt *et al.*, 2006; Van Cutsem *et al.*, 2008) and gefitinib (Fisher *et al.*, 2008). Combination of irinotecan, folinic acid and 5-FU (FOLFIRI) with either erlotinib or gefitinib is associated with significant toxicity (Messersmith *et al.*, 2004; Veronese *et al.*, 2005) and a randomised phase IIb study of the addition of gefitinib to FOLFIRI in 100 patients failed to demonstrate any additional benefit from gefitinib (Santoro *et al.*, 2008).

1.9.6 Ongoing Phase III studies combining lapatinib with chemotherapy

There are a number of phase III clinical trials examining lapatinib in combination with chemotherapy in different tumours (Table 1.5).

Trial	Setting	Chemotherapy regimen	Primary outcome
EGF104383 Phase III	First line HER2 +ve metastatic breast cancer	Paclitaxel+trastuzumab+lapatinib vs. paclitaxel+trastuzumab+placebo	TTP
EGF108919 Phase III	Stage IV disease with HER-2 +ve breast cancer	Taxane+lapatinib vs. taxane+trastuzumab	PFS
LPT109096 Phase II	Neo-adjuvant HER2 +ve breast cancer	Trastuzumab+FEC then paclitaxel vs. lapatinib+FEC then paclitaxel vs. trastuzumab+lapatinib+FEC then paclitaxel	pCR
EGF111438 Phase III	Metastatic HER2+ve breast cancer following taxane or anthracycline	Lapatinib+capecitabine vs. Trastuzumab+capecitabine	CNS metastasis as first relapse
EGF104578 Phase III	HER2 amplified advanced gastric cancer. Second line	Weekly paclitaxel vs. weekly paclitaxel+lapatinib	OS
EGF110656 Phase III	HER2 +ve advanced adenocarcinoma of oesophagus or stomach	Oxaliplatin+capecitabine vs. oxaliplatin+capecitabine+lapatinib	PFS
EGF102988	High risk resected squamous carcinoma of the head and neck	Adjuvant chemoradiotherapy vs. chemoradiotherapy +lapatinib	DFS

Table 1.5 Ongoing clinical trials with lapatinib in combination with chemotherapy

1.10 REASONS FOR FAILURE OF TYROSINE KINASE INHIBITORS IN COMBINATION WITH DNA DAMAGING AGENTS

Despite a clear rationale for the combination of TKIs with cytotoxic agents and *in vitro* support, such combinations have generally failed to produce clinical benefits. The evidence indicates this may be due to the failure to abrogate HER signalling through the PI3K/AKT pathways and highlights the importance of drug scheduling.

1.10.1 Failure to inhibit human epidermal growth factor signalling

TKIs may not always inhibit HER signalling or activation of their downstream pathways. This can be due to EGFR mutations resulting in resistance to TKIs, mutations in key signalling regulators downstream of the membrane receptors (e.g. K-Ras or phosphatase and tensin homolog (PTEN)), or through continued HER signalling, either due to incomplete inhibition of receptors or through dimerisation with other, non-inhibited receptors. This failure to prevent PI3K/AKT signalling may explain why TKIs in combination with DNA damaging agents have not translated into the clinical setting.

1.10.1.1 EGFR mutations and resistance to tyrosine kinase inhibitors

Secondary resistance to TKIs occurs in patients with NSCLC whose tumours initially expressed EGFR with an activating mutation. The commonest mechanism of resistance identified occurs through the acquisition of a mutation in which methionine is substituted for threonine at amino acid position 790 (T790M) in exon 20. The acquisition of this mutation accounts for around 50-60% of acquired resistance to EGFR targeted TKIs (Kobayashi *et al.*, 2005; Oxnard *et al.*, 2011; Pao *et al.*, 2005). This mutation increases affinity of EGFR for ATP over gefitinib or erlotinib (Yun *et al.*, 2008). The gain of other EGFR mutations, as reported in case reports, can also result in secondary resistance to TKIs (Balak *et al.*, 2006; Bean *et al.*, 2008) and the amplification of the hepatocyte growth factor receptor MET, is detected in around 20% of NSCLC with acquired resistance to TKIs. MET is able to phosphorylate HER3 and activate the PI3K/AKT pathways, potentially producing resistance to EGFR targeted TKIs (Engelman *et al.*, 2007).

Whilst the presence of an activating EGFR mutation in NSCLC predicts for an increased response to an EGFR targeted TKI in the first line setting, response rates are around 50-70% (Mok *et al.*, 2009a; Rosell *et al.*, 2009; Sequist *et al.*, 2008) and not all EGFR mutations confer sensitivity to EGFR targeted TKIs. There are case reports of patients with tumours which express the EGFR sensitising mutation L858R, together with the T790M mutation associated with resistance, prior to commencing TKI therapy and as a result are resistant to TKIs (Sequist *et al.*, 2008; Shih *et al.*, 2005). However the commonest EGFR mutation associated with primary resistance to EGFR targeted TKIs is an insertion mutation in exon 20 (Greulich *et al.*, 2005; Sasaki *et al.*, 2007). Though,

this mutation is only detected in around 2% of lung cancer (Sasaki *et al.*, 2007; Shigematsu *et al.*, 2005) and therefore is unlikely to account for the failure of TKIs in combination with chemotherapy.

1.10.1.2 Mutant K-Ras and resistance to tyrosine kinase inhibition

K-Ras is an important mediator in the Ras-Raf-MAPK pathway and links the activation of HER receptors to the activation of MAPK. Mutations in K-Ras produce a constitutively active protein resulting in the escape of the Ras-Raf-MAPK pathway from the control of membrane receptors (Jancik *et al.*, 2010). Mutated K-Ras is a strong predictor of failure of EGFR monoclonal antibodies in colorectal cancer (Amado *et al.*, 2008; Karapetis *et al.*, 2008). The exception to this, is a codon 13 mutation (G13D) in which glycine is substituted for aspartate, as colon tumours with this mutation respond to cetuximab therapy (De Roock *et al.*, 2010).

Data on the influence of K-Ras mutations in TKI therapy is less clear cut, confused by the fact that the data for monoclonal antibodies is derived from clinical trials in colorectal cancer in contrast to TKI data, which is derived from trials in NSCLC. A recent meta-analysis of 22 trials in NSCLC concludes that K-Ras status is not able to predict for response to EGFR TKIs (Mao *et al.*, 2010). This observation does not appear to be due to differences between TKI and antibodies, as mutant K-Ras does not predict for treatment failure of cetuximab in combination with chemotherapy in NSCLC (Khambata-Ford *et al.*, 2010). Whether this observation is due to tumour type has yet to be ascertained, as currently no data on K-Ras status and response to TKI in tumours other than NSCLC, has been published. However, data looking at K-Ras status and response to cetuximab in non-colorectal cancers supports tumour specificity with no predictive value observed in oesophageal (Gold *et al.*, 2010) or gastric cancer (Park *et al.*, 2010). Therefore, mutations in K-Ras are unlikely to explain why TKIs in combination with DNA damaging agents have failed to translate into the clinic.

1.10.1.3 Phosphatase and Tensin homolog

In vitro studies have indicated that the expression of PTEN is an important mediator of sensitivity to gefitinib (She *et al.*, 2003). PTEN is a negative regulator of AKT activation through the dephosphorylation of phosphatidylInositol (3,4,5)-trisphosphate, with

PTEN loss resulting in increased AKT signalling (Sansal and Sellers, 2004); PTEN null cells are resistant to the effects of gefitinib (She *et al.*, 2003). The relevance of PTEN loss and gefitinib resistance has been demonstrated in glioblastoma (Mellinghoff *et al.*, 2005), and lung cancer (Endoh *et al.*, 2006), but both studies are small and confirmation from larger studies is still required. In contrast to gefitinib, the activity of lapatinib is not affected by PTEN status (Xia *et al.*, 2007).

1.10.1.4 Failure to inhibit the PI3K/AKT signalling pathway

The PI3K/AKT pathway is involved in modulating the response of cells to DNA damage through the control of apoptosis and modulation of key proteins involved in DNA repair (discussed in section 1.8.5.1) HER3 is a potent activator of the PI3K/AKT signalling pathway through dimerisation with either EGFR or HER2 and the inhibition of either or both these receptors by TKIs inhibits HER3 and PI3K/AKTs signalling (Kong *et al.*, 2008; Sergina *et al.*, 2007). However, this inhibition is short lived, with phosphorylated HER3 and AKT detectable in cells within 48 hours despite continued EGFR and HER2 inhibition (Kong *et al.*, 2008; Sergina *et al.*, 2007). These data suggest that at least two different mechanisms produce this effect. Firstly, inhibition of AKT signalling upregulates the expression of a number of receptor tyrosine kinases including HER3, IGFR1 and the insulin receptor (Chandarlapaty *et al.*, 2011). The second separate mechanism, controls receptor phosphorylation.

In HER2 amplified cells, receptor phosphorylation is dependent on HER2 activity. AKT inhibition alone induces the expression and phosphorylation of HER3, IGFR1 and the insulin receptor, but in combination with lapatinib (1 μM) receptor phosphorylation is inhibited but not increases in receptor expression (Chandarlapaty *et al.*, 2011), indicating that the inhibition of HER2 alters receptor phosphorylation but not their expression.

Under conditions where only partial or no HER2 inhibition occurs (e.g. ≤1μM gefitinib), EGFR inhibition induces the proteolytic cleavage of HER4 (Kong *et al.*, 2008). This stimulates the autocrine release of the HER3 and HER4 ligands, betacellulin and heregulin, stimulating the production of HER2/HER3 and HER3/HER4 dimers, thus negating the effect of EGFR inhibition (Kong *et al.*, 2008). Under conditions where

HER2 is inhibited in addition to EGFR, (e.g. ≥5μM gefitinib) a forward shift in the dephosphorylation-phosphorylation equilibrium of HER3 is produced, resulting in an increase in the steady state phosphorylation of HER3 and activation of the PI3K/AKT signalling pathway (Sergina *et al.*, 2007).

1.10.2 Why scheduling may be important?

In vitro studies provide evidence that the schedule of TKI and chemotherapy is important with the schedule of TKI followed by chemotherapy being the least efficacious schedule in most studies (Chun *et al.*, 2006; Giovannetti *et al.*, 2008; Li *et al.*, 2007; Morelli *et al.*, 2005; Xu *et al.*, 2003) though these finding are dependent upon the type of cytotoxic agent used (McHugh *et al.*, 2007; Solit *et al.*, 2005). The importance of scheduling is alluded to in a clinical trial of 154 patients with NSCLC. Patients were treated with gemcitabine and cisplatin plus erlotinib or placebo from days 15-28. Significant improvements in response rates and progression free survival were observed in the group treated with erlotinib (Mok *et al.*, 2009b). Given that the large randomised trial of gemcitabine and cisplatin in combination with gefitinib or placebo, INTACT 1 failed to demonstrate any benefit from the addition of gefitinib, the schedule of erlotinib from days 15-28 may be more beneficial than continuous TKI use.

1.10.2.1 Cell cycle arrest

The DNA damaging and cytotoxic effects of some chemotherapy drugs are influenced by cell cycle phase as discussed in section 1.7.4. Pyrimidine analogues exert their effects during S-phase when DNA replication is occurring, paclitaxel in G2M-phase (Shah and Schwartz, 2001) with Topo II poisons inducing the greatest DNA damage during G2/M- phase of the cell cycle when Topo IIα expression is highest (Potter *et al.*, 2002; Potter and Rabinovitch, 2005).

TKIs induce a G1 phase cell cycle arrest in cancer cell lines (Kim *et al.*, 2008b; Krol *et al.*, 2007; Li *et al.*, 2007), which may render cells resistant to the effects of some cytotoxic agents. This has been demonstrated with EGFR inhibition and IR, with the irradiation of cells in G1-phase demonstrating EGFR phosphorylation, transition into S-phase and cell death (Ahsan *et al.*, 2009). Inhibition of EGFR phosphorylation by erlotinib, prevents IR-induced EGFR phosphorylation with cells remaining in G1 and resistant to the cytotoxic

effects of IR (Ahsan *et al.*, 2009). Similar results have been obtained with the pre-treatment of cells with erlotinib or gefitinib which induces a G1 cell cycle arrest, with no alteration in cell cycle and less cytotoxicity induced by pemetrexed or gemcitabine compared with either continuous treatment with TKI and chemotherapy or chemotherapy followed by TKI (Chun *et al.*, 2006; Li *et al.*, 2007; Morgan *et al.*, 2008)

1.10.2.2 EGFR Internalisation and degradation

The phosphorylation of EGFR in response to IR or chemotherapy leads to its internalisation in a p38 dependent process (Zwang and Yarden, 2006). This is followed by the ubiquitination and degradation of EGFR which correlates with sensitivity to cisplatin (Ahsan *et al.*, 2010) and gemcitabine (Feng *et al.*, 2007). In these studies, the inhibition of EGFR phosphorylation by the use of TKI prior to chemotherapy results in resistance to cell death, by preventing EGFR degradation (Ahsan *et al.*, 2010; Feng *et al.*, 2007). The need for EGFR to be degraded rather than just inactivated maybe explained by its' non-kinase dependent role in glucose uptake (Weihua *et al.*, 2008). This explains the observation that cells transfected with EGFR lacking an intrinsic kinase are able to survive (Ewald *et al.*, 2003) and that knockdown of EGFR with siRNA produces a greater level of cell death than kinase inhibition alone (Weihua *et al.*, 2008).

1.11 RATIONALE FOR THE INVESTIGATION OF THE MODULATION OF DNA DAMAGE INDUCTION AND REPAIR BY DURATION OF EXPOSURE TYROSINE KINASE INHIBITOR IN BREAST CANCER

The HER family plays a key role in driving and controlling tumour growth and mediating resistance to traditional cytotoxic agents. Despite *in vitro* data indicating that TKIs in combination with cytotoxic agents produce greater benefits over cytotoxic agents alone, on the whole these have failed to translate into the clinical setting. The reasons for this appear to be multiple and include primary resistance to the effects of TKIs (K-Ras or PTEN), alterations in signalling pathways (EGFR degradation vs. nuclear transport in response to cellular stressors), or the ability to continue HER signalling despite continued exposure to a TKI.

Further work is required to understand the reasons why these combinations have failed to translate into the clinic if the potential benefits of TKIs are to be harnessed. Whilst lapatinib has an established role in the management of metastatic breast cancer, the use of gefitinib and erlotinib in breast cancer is still under investigation focussed on breast tumours identified as 'triple negative'. These tumours do not overexpress HER2 and are negative for ER and PR, though over 50% express EGFR (Burness *et al.*, 2010).

Breast cancer cell lines provide an ideal model in which to investigate the effects of duration of dual EGFR and HER2 inhibition on DNA damage and repair as the pivotal studies demonstrating continued HER3 signalling have also been demonstrated in these cell lines. In addition the management of metastatic breast cancer utilises the DNA damaging effects of both anthracyclines and IR.

1.12 HYPOTHESIS AND OBJECTIVES

Hypothesis: Exposure to tyrosine kinase inhibitors for 48 hours fails to inhibit the repair of DNA damage by cytotoxic agents, explaining why schedule is important when combining these inhibitors with cytotoxic agents.

Objectives:

1. Chapter three examines the ability of lapatinib to synergise with cisplatin and doxorubicin and the effect of schedule.
2. Chapter four examines the modulation of induction of DNA strand breaks by cisplatin, IR, etoposide and doxorubicin by short and long exposure to gefitinib or lapatinib.
3. Chapter five examine the modulation of topoisomerase IIα by gefitinib.
4. Chapter six examines the role of HER2 in mediating resistance to cisplatin

MATERIALS AND METHODS

MATERIALS

2.1 CELL LINES AND CULTURE CONDITIONS

2.1.1 Breast cancer cell lines

MCF-7 and MDA-MB-468 cells (CRUK London Research Institute, London, UK) were grown in Dulbecco's Modified Eagle Medium (DMEM, Autogen Bioclear, UK), supplemented with 10% heat inactivated foetal calf serum (HI FCS) (Autogen Bioclear, UK), 2 mM L-glutamine (Autogen Bioclear, UK), 100U/ml penicillin and 100U/ml streptomycin (Sigma-Aldrich, UK).

SK-Br-3 cells (CRUK, London Research Institute, London, UK) grown in McCoy's SA Medium Modified (Sigma-Aldrich, UK) supplemented with 10% HI FCS, 2 mM L-glutamine, 100 U/ml penicillin and 100U/ml streptomycin.

2.1.2 HTETOP Cells

The HTETOP cell line is a human fibrosarcoma HT1080 cell line in which Topo IIα expression can be depleted by the addition of tetracycline, a gift from Dr A Porter (Imperial College Faculty of Medicine, UK). The creation of this cell line has been described by Carpenter and Porter (Carpenter and Porter, 2004). Briefly, these cells were created by transfecting the HT1080 cell line with a tetracycline transactivator. One of the resulting clones (HTET) was then stably transfected with a plasmid (pUHC13.3hygTOP) in which Topo IIα cDNA is linked to a tetracycline transactivator-responsive promoter. Clones which express the pUHC13.3hygTOP-encoded Topo IIα transcripts (HTETOPwt) were then identified. The endogenous Topo IIα genes in clone HTETOPwt were then disrupted by gene targeting and confirmed using Southern analysis used to confirm disruption of both Topo IIα alleles.

Cells were maintained in DMEM, FCS 10%, sodium pyruvate 100 mM (Sigma-Aldrich, UK), L-glutamine, 20 ml MEM amino acid solution (Gibco, USA) and G418 200 μg/ml (Sigma-Aldrich, UK).

2.1.3 MDA-MB-468 HER2 transfected cells

The MDA-MB-468 cell line was transfected with either full length HER2 or a HER2 from which the 13 amino acid NLS sequence (676-KRRQQHIRKYTMRR-689) has been deleted (HER2-NLS), both obtained from Prof. Hung (MD Anderson Cancer Center, USA) and described previously (Giri *et al.*, 2005). The plasmids contain a green fluorescence and kanamycin resistance gene to assist selection after transformation and selective pressure was maintained using G418 to created stably transfected cell lines. Three cells lines were created named MDA-MB-468-Vector, MDA-MB-468-HER2 (transfected with full length HER2) and MDA-MB-468-NLS (transfected with HER2 from which the NLS sequence has been deleted). The continued presence of the transfected plasmid was checked using fluorescence microscopy to confirm the fluorescence of the green fluorescence protein and using Western blotting to confirm the presence of HER2. The stably transfected cell lines were grown as documented in section 2.1.1, with the addition of G418 1g/ml.

2.1.4 Cell line maintenance

All cell lines were grown in flasks (BD Falcon, UK), in humidity-saturated (95%) incubators (Binder, Germany), at 37^{o}C with 5% CO_2. Procedures were carried out in Class II biological safety cabinet (ESCO, Singapore) using aseptic techniques. Cells were routinely sub-cultured when they reached 80% confluence. Medium was removed and 2-10ml of trypsin-EDTA (Autogen Bioclear, UK) added, depending on flask size. Trypsin was left until cells had detached (a maximum of five minutes) and media containing HI FCS added to stop the action of the trypsin (volume equal to the amount of trypsin used). Cells were then pelleted by centrifugation at 1500 rpm, the supernatant discarded and the cell pellet resuspended in fresh media before reseeding into culture flasks. Cells were passaged to a maximum of 25 times, before being discarded and new stocks grown. Mycoplasma testing was undertaken on all cell lines.

2.1.5 Storage and retrieval from liquid nitrogen

Frozen cell stocks were prepared for long term storage. Cells were grown in 175cm^2 flasks (T175) to 80% confluence, trypsinised and resuspended to a concentration of 1x10^{6}cells/ml in freezing media (FCS containing 10% dimethyl sulfoxide, (DMSO) Sigma-Aldrich, UK). The cell suspension was aliquoted in 1 ml cryotubes and frozen at -

80^{o}C for 24-72 hours, prior to long-term storage in liquid nitrogen. In order to grow cells from frozen stocks, the cell suspension was thawed rapidly by holding the cryotube in a 37^{o}C water bath until partially defrosted, and then mixed with warm media to complete the thawing process. Cells were pelleted and the supernatant containing the freezing mix discarded and the cell pellet resuspended in 10 ml of media, seeded into a 25cm^{2} flask (T25), and incubated until they reached 80% confluence. Cells were passaged at least twice before being used in experiments.

2.1.6 Cell count

Cells were counted using a haemocytometer. Following collection as documented above, cell pellets were resuspended in media and mixed thoroughly by repeated pipetting to produce a single cell suspension. 50 µl of cell suspension was mixed 1:2 with 50 µl of 0.4% trypan blue stain (Sigma-Aldrich, UK) for one to two minutes to identify of dead cells which retain the blue stain due to disruption of the cell membrane. 20 µl of the cell/trypan blue suspension was then transferred to a chamber of the haemocytometer by papillary action. The number of cells in four large 1mm^{2} corner squares in a single chamber were counted, and then averaged to give the number cells per 1 mm^{2} square. Each 1 mm^{2} square holds a volume of 0.1 µl therefore the total number of cells obtained is multiplied by 1x10^{4} and then by the dilution factor giving the number of cells per ml of cell suspension.

2.2 CHEMOTHERAPEUTIC DRUGS AND OTHER REAGENTS

Clinical grade gefitinib (Iressa/ZD1839 AstraZeneca (Macclesfield, UK)) and lapatinib (Tykerb/GW752016, kindly provided by GSK (Stevenage, UK)). Etoposide, doxorubicin, paclitaxel, menadione and m-AMSA (Sigma-Aldrich, UK) were diluted in DMSO, except for menadione which was diluted in sterile water. Cisplatin (DBL, UK) was also diluted in sterile water to a stock concentration 3.3 mM. Stock solutions were either prepared in advance or fresh prior to experiments according to stability of each compound.

Compounds	Structure	Dilution solvent	Stock Concentration	Supplier
Cisplatin	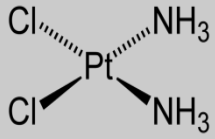	Sterile water	3.3 mM	DBL, UK
Etoposide	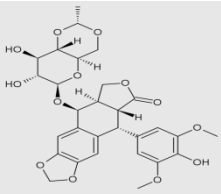	DMSO	10 mM	Sigma-Aldrich, UK
Doxorubicin	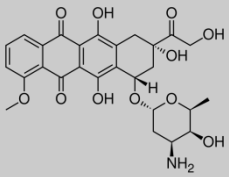	DMSO	1 mM	Sigma-Aldrich, UK
Gefitinib	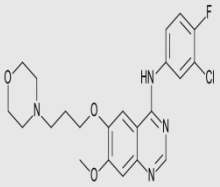	DMSO	10 mM	Astra Zeneca, UK
Lapatinib	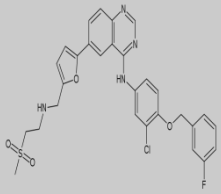	DMSO	10 mM	GSK, UK
m-AMSA (amsacrine)	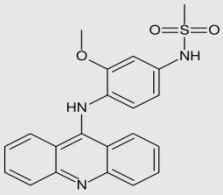	10mM	10 mM	Sigma-Aldrich, UK
Trastuzumab	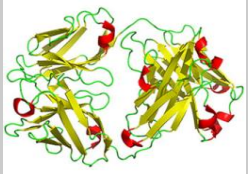 www.3dchem.com	Sterile Water	21 mg/ml	Roche, UK

Table 2.1 Drug compounds

METHODS

2.3 SULFORHODAMINE B ASSAY

Experiments were conducted in 96 well plates, seeded with 2000-4000 cells per well. The number of the cells plated was determined by the rate of proliferation of the individual cell lines. Plates were left to adhere overnight, for a minimum time of 18 hours in a humid box at 37^{o}C in 5% CO_2.

2.3.1 Determination of IC_{50} for single drugs

Varying concentrations of drug were made up in the appropriate complete media. Media from the cells was replaced with 200 μL of media containing the appropriate drug concentration. Each drug concentration was repeated in triplicate per experiment, with a control lane containing only the solvent used to dilute the drug. Plates were left to incubate for 96 hours.

2.3.2 Drug combination assays

To determine synergy a fixed dose of lapatinib was used at a sub-toxic concentration (concentration producing 10-20% inhibition of proliferation) and combined with a range of concentrations of different chemotherapy agents. For combination assays three schedules of drug dosing were used. In the first, both lapatinib and the chemotherapy drug were added at the same time and incubated continuously for 96 hours. In the second, lapatinib was added for 60 minutes, followed by lapatinib plus chemotherapy for two hours and in the third, chemotherapy was given first. After the two hour incubation, the media was removed and replaced by drug free media (DFM) or media containing lapatinib only. Plates were then allowed to incubate for 96 hours in a humid box at 37^{o}C in 5% CO_2.

After the incubation period, cells were fixed by adding 100 μl of cold 10% (w/v) trichloroacetic acid (Sigma-Aldrich, UK) to each well and left for 30 minutes at 4^{o}C. The acid was removed by flicking the inverted plates, followed by washing four times with water. The plates were then air dried overnight. Once the plates were dried, 100 μl of 0.4% (w/v) sulforhodamine B (SRB) (Sigma-Aldrich, UK) in 1% (*v/v*) acetic acid (Sigma-Aldrich, UK) was added to each well. Plates were left for 20 minutes at room

temperature. The SRB stain was removed as described above and then washed with 1% acetic acid to remove the remaining unbound SRB stain. Plates were washed a minimum of three times or until no further SRB could be removed. Plates were left to air dry overnight.

2.3.3 Plate reading

Before plate reading SRB was resolubilised by adding 100 μl of a solution of 10 mM trizma base and 1 mM EDTA (Sigma-Aldrich, UK) to each well. Plates were left for 20 minutes at room temperature and then shaken gently. Mean absorbance of each well was read at 540 nm using a Spectrafluor Plus plate reader (Tecan, UK). Percentage growth was calculated by averaging the absorbance for the three wells treated with the same drug conditions and expressing this as a percentage of the average of the control wells.

$$\% \text{ proliferation} = \frac{\text{OD treated}}{\text{OD control}} \times 100$$

Data obtained are expressed as the average of three or more independent experiments. The IC_{50} being the drug concentration required to produce 50% growth inhibition, was calculated using the four parameter logistic regression model to curve fit. Data are presented on a semi-logarithmic scale of the mean±SD.

2.3.4 Analysis of drug combinations

2.3.4.1 Median effect analysis

Median effect analysis was performed using the CalcuSyn Software (Biosoft, USA) as described by Chou (Chou, 2006). Combination index values were calculated for a non-fixed ratio designed combination experiments as described above.

2.3.4.2 Isobologram construction

The isobologram method was used to assess the effects of the drug combinations. An isobologram graphically depicts a line of additivity by connecting two equally effective doses of the two drugs being investigated. For this analysis the IC_{50} of both investigational drugs was used. A normalised isobologram was constructed to account

for the alteration in ratio of the two drugs (fixed concentration of lapatinib with a range of chemotherapy concentration). A classic isobologram plots the IC_{50} of the individual drugs on the x and y axis which can be used to analyse the effects of two drugs combined at fixed ratio (e.g. both drugs at $IC_{20,}$ IC_{30} etc). A normalised isobologram accounts for the fact in these experiments a fixed $IC_{10\text{-}20}$ of lapatinib was used in combination with the second drug at IC varying from 0 to 100%.

2.4 WESTERN BLOTTING ANALYSIS

2.4.1 Drug treatment

Cells were grown in T25 or T75 flasks seeded at a concentration of 5-15X10^4 cells and left overnight to adhere. For analysis of HER expression as documented in Chapter Three, cells were allowed to grow until 80% confluence. For TKI experiments, the following day the media was replaced with fresh media +/- TKI, with drug replacement every 24 hours if required. In the MDA-MB-468 HER2 transfected cell lines, following overnight adherence cisplatin +/- trastuzumab added to the culture media. Following one hour incubation with cisplatin, the media was replaced with fresh media +/- trastuzumab and cells left to incubate for a further 24 hours at 37^{o}C 5% CO_2.

2.4.2 Total protein extraction

Media was poured off the cells, followed by washing twice with phosphate buffered saline (PBS), pH 7.3 (Sigma-Aldrich UK). 100-300 µL of celLytic (Sigma Aldrich, UK) containing phosphatase and protease inhibitor cocktail (Roche, UK) was pipetted over the adherent surface of the flask and left for five minutes. Cells scrapers (VWR, UK) were used to detach cells from the flask, collected into an collection tube and centrifuged for 20 minutes at 4^{o}C 13,000 rpm, to clear insoluble material. The cell lysate was removed leaving behind the pellet of insoluble material, and placed in a fresh collection tube and stored at -80°C.

2.4.3 Protein quantification and preparation

Once extracted, proteins were quantified using the RC DC protein assay (Bio-Rad Laboratories, USA). 2 µl of each lysate was mixed with 18 µl of distilled water to which 100 µl of a mixture of reagent A and S (20 µl of reagent S with 1 ml of reagent A) was added, followed by 800 µl of reagent B and left to incubated for 15 minutes at room

temperature. Absorbance (OD) was measured, against a control containing only distilled water at 750 nm on a Philips spectrophotometer (Beam PU8620 Series UV/Vis single). The total protein concentration was determined using the formula:

$$\text{Concentration } (\mu g/\mu l) = OD*25.$$

Immunoblotting was performed using 20-50 µg protein, to which a volume of loading dye (5X stock -250mM Tris HCl, pH 6.8, 500 mM DTT, 10% SDS, 0.5% bromophenol blue, 50% glycerol and distilled water) to make a final concentration of 1X was added. Samples were boiled at 100°C for five minutes to denature the proteins, allowed to cool, and centrifuged briefly to ensure mixing.

2.4.4 Immunoblotting

Pre-cast 3-8% or 7% Tris acetate gels (Novex pre-cast gels, Invitrogen, UK), were used depending upon the size of proteins being examined. The XCell SureLock™ Mini-Cell module (Invitrogen, UK) was used to run the gels, with tri-acetate SDS running buffer (100mM Tris Base, 100mM Tricine, 70mM SDS). Gels were electrophoresed at 150V at room temperature until the proteins has been fully separated. Proteins were transferred using the XCell II Blot module (Invitrogen, UK). Briefly immobilon P membranes (Sigma-Aldrich, UK) were activated by immersion in 100% MeOH for 30 seconds, followed by washing in distilled water and then transfer buffer (20% (v/v) MeOH, 25 mM Tris Base, 200 mM Glycine pH 8.3), for 10 minutes each. The tris-acetate gels were released from their plastic casing, the top and bottom part of the gel cut away and an activated immobilon membrane placed on top of the gel, followed by a piece of pre-cut filter paper, a further piece of filter paper was placed on the reverse side of the gel. The resulting gel, membrane, filter paper sandwich was rolled with a glass pipette to ensure all air bubbles were removed. The gel sandwiched was then placed in the blot module on top of two sponges, pre-soaked in transfer buffer, with a further two sponges placed on top of the gel. The blot module was placed back into Surelock tanks and filled with transfer buffer. The outside section of the tank was filled with distilled water and the entire module placed into a $4^{o}C$ cold cabinet and transferred at 38V overnight. Following transfer, membranes were washed for five minutes in tris-buffered saline (TBS-20 mM Tris Base, 0.5 M NaCl, pH 7.5 in distilled

water). Unbound sites on membranes were blocked using blocking buffer: 5% Marvel milk in Tris-Buffered Saline with 0.1% Tween 20 (TBST Sigma-Aldrich, UK) when probing for non-phosphorylated proteins and 5% Bovine Serum Albumin (BSA) (Sigma-Aldrich, UK) in TBST for phosphorylated proteins. Proteins were incubated using the appropriate antibody (Table 2.2), followed by incubation with the appropriate HRP-conjugated polyclonal secondary antibodies.

Antibodies	Dilutions	Dilution buffer	Supplier
Anti-EGFR	1/1000	5% BSA	Cell Signaling Technology, USA
Anti-phospho EGFR (PY1148)	1/1000	5% BSA	Cell Signaling Technology, USA
Anti-HER2	1/1000	5% BSA	Cell Signaling Technology, USA
Anti-phosphoHER2 (PY1221/122)	1/1000	5% BSA	Cell Signaling Technology, USA
Anti-HER3	1/1000	5% BSA	Cell Signaling Technology, USA
Anti-IRS1	1 µg/ml	5% Milk	Milipore, USA
Anti-phosphoHER3 (PY1289)	1/1000	5% BSA	Cell Signaling Technology, USA
Anti-Topo IIα	1/1000	5% Milk	Gift from Prof Ian Hickson
Anti-Topo IIβ	1/1000	5% Milk	BD Bioscience, USA
Anti-Akt	1/1000	5% BSA	Cell Signaling Technology, USA
Anti-phospho Akt (S473)	1/1000	5% BSA	Cell Signaling Technology, USA
Anti-MAPK (p42/44)	1/1000	5% BSA	Cell Signaling Technology, USA
Anti-phospho MAPK	1/1000	5% BSA	Cell Signaling Technology, USA
Anti-Mouse (ab6728)	1/2000	5% milk	Cell Signaling Technology, USA
Anti-Rabbit (ab6721)	1/2000	5% milk	Cell Signaling Technology, USA
Anti- a-tubulin (Clone B-5-1-2)	1/4000	5% milk	Sigma-Aldrich, UK

Table 2.2 List of antibodies used in Western Blotting

2.4.5 Protein visualisation

Chemiluminescence detection (ECL system, Amersham Biosciences, UK) was used to visualise antibody binding. Blots were dried and incubated one minute with ECL reagents before covering them with cling film and exposing them to Kodak X-OMAT™LS film for various times (two seconds to 10 minutes). Films were processed using a film processor (Konica Minolta, UK).

Re-probing of membranes using different antibodies was performed after stripping the original bound antibody from the membranes. This was achieved by reactivating dried membrane in methanol followed by washing in TBST, and incubation stripping buffer (Thermo Scientific, Sweden). Membranes were washed twice 10 minutes in TBST, before blocking and re-probing as previously described.

2.4.6 Quantitation

Quantitation of Western blots was conducted by measurement of pixel density using Adobe Photoshop software version 8.0 (Adobe, USA). Values were expressed as a fraction of the control value which was assigned the value 1.0.

2.5 SINGLE CELL GEL ELECTROPHORESIS (COMET) ASSAY

The comet assay was first developed as a method to measure both single strand and double strand DNA breaks at a single cell level. However, a modification of this assay has been shown to achieve sensitive detection of interstrand crosslinks (Hartley *et al.*, 1999).

2.5.1 Drug treatment

Cells were plated at a concentration of $20x10^4$cells per well of a six well plate and left overnight to adhere at 37^oC in 5% CO_2. Media from the cells was removed and replaced with 2 ml of media +/- TKI. Cells were treated for the required time, with media +/- drug replaced every 24 hours and one hour prior to exposure to the DNA damaging agent under investigation. DNA damaging drugs were added to the media containing TKI and left in contact with the cells for one to two hours, depending on the drug under investigation. After exposure to DNA damaging agent cells were then collected by trypsinisation, pelleted and stored in 1 ml of freezing mixture at $–80^oC$.

2.5.2 Study of DNA repair

Cells were treated as above, but after exposure to the DNA damaging agent the media was replaced with fresh media +/- TKI, and cells left to incubate for the required time to allow DNA damage to repair. Cells were collected as above.

For IR experiments, cells were trypsinised following incubation with media +/- TKI and resuspended at a concentration of $5x10^4$ cells/ml in media +/- TKI. 1 ml of the cell suspension was placed into a 1.5 ml collection tube and cells irradiated on wet ice using an ionising radiation source (AGO, UK). Following irradiation, cells were placed into the incubator and collected at the required time points, as documented above.

2.5.3 Assay methodology

2.5.3.1 Modified Alkaline Comet assay

To study DNA damage caused by the crosslinking agent cisplatin, cells were thawed and resuspended in ice cold media to a concentration of $2.5x10^4$cells/ml. The cell suspension was divided into two aliquots of 2 ml for each time point. One aliquot was irradiated (12.5 Gy) on wet ice to deliver a fixed number of random DNA strand breaks, immediately before analysis. The Comet assay was run with irradiated and unirradiated controls for each time point as per the alkaline Comet assay protocol below.

2.5.3.2 Alkaline and neutral Comet assays

For strand breaking agents (IR, doxorubicin, etoposide and m-AMSA), cells were thawed, counted and diluted in ice cold media to a concentration of $2.5x10^4$cells/ml and stored on wet ice. Following sample preparation as documented above, 0.5 ml of cell suspension was mixed with 1 ml 1% type VII agarose (Sigma-Aldrich, UK). 1 ml of this mixture was pipetted onto a glass microscope slide pre-coated with 1% type 1A agarose (Sigma-Aldrich, UK), covered with a glass coverslip, and left to set on ice. Once set the coverslip was removed and the slides stored in a plastic tray on ice. Two slides were prepared for each sample examined.

2.5.3.3 Alkaline Comet assay

Cells were lysed in the dark on ice for one hour in ice cold lysis buffer (100mM disodium EDTA, 2.5 M NaCl, 10 mM Tris-HCl pH 10.5) containing 1% Triton X-100 (Sigma-Aldrich, UK) added fresh. Slides were subsequently washed in ice cold distilled water for 15 minutes, four times. Slides were then placed in a electrophoresis tank, and were then incubated in ice cold alkali buffer (50 mM NaOH, 1 mM disodium EDTA, pH 12.5), in the dark for 45 minutes, followed by electrophoresis in the same buffer for 25 minutes at 18 V (0.6V/cm), 250 mA. The slides were removed and placed onto a drying tray, rinsed with 1 ml of neutralising buffer (0.5 M Tris-HCl, pH 7.5) and left for 10 minutes, followed by washing with PBS and left to dry overnight. Slides were then re-hydrated for 30 minutes with distilled water and stained with propidium iodide (2.5µg/ml) for 20 minutes in the dark, washed in distilled water and left to dry in a drying oven and stored in the dark.

2.5.3.4 Neutral Comet assay

Cells were lysed in the dark on ice, for one hour in ice cold lysis buffer (100mM EDTA, 2.5 M NaCl, 10 mM Tris-HCl pH 8.0) containing 0.5% Triton X-100 (Sigma-Aldrich, UK), 1% N-lauroylsarcosine (Sigma-Aldrich, UK), 3% DMSO (Sigma-Aldrich, UK) added fresh and pH adjusted to 9.5. Slides were then washed in ice cold distilled water for 10 minutes twice, followed by 400 µl of proteinase K solution 1m/ml (Roche, UK), pipetted onto each slide and incubated for two hours at 37^{o}C. Slides were then washed with ice cold electrophoresis buffer (300 mM sodium acetate, 100 mM Tris-HCL, pH 8.3) containing 1% DMSO added freshly) for 10 minutes, twice. Slides were covered with neutral electrophoresis buffer, incubated in the dark on ice for one hour, then placed in an electrophoresis tank, covered in two litres of fresh electrophoresis buffer and electrophoresed for 60 minutes at 30 V. Following electrophoresis the slides were removed and placed onto a drying tray, rinsed with 1 ml of neutralising buffer (0.5 M Tris-HCl, pH 7.5) and left for 10 minutes, followed by washing with PBS and left to dry overnight. The following day the slides were re-hydrated for 30 minutes with distilled water and stained with propidium iodide (2.5µg/ml) for 20 minutes in the dark, washed in distilled water and left to dry in a drying oven and stored in the dark.

2.5.3.5 Data analysis

Images were visualised using a NIKON inverted microscope with high-pressure mercury light source, 510-560nm excitation filter and 590nm barrier filter at x20 magnification. Images were captured using an on-line charge-couple device (CCD) camera and analysed using Komet Analysis software (Kinetic Imaging, Liverpool, UK). For each duplicate slide 25 individual cells were analysed in the alkaline assay and 50 cells in the neutral assay. The Olive tail moment for each cell was calculated using the Komet Analysis software as the product of the percentage DNA in the comet tail and the distance between the means of the head and tail distributions, based on the definition of Olive *et al.*(Olive, 2002).

For DNA strand breaking agents, the olive tail is representative of the number strand breaks. For cross linking agents results were expressed as percentage decrease in tail moment compared to untreated controls calculated by the following formula:

$$\% \text{ decrease in tail moment} = \left[1 - \left(\frac{TMdi - TMcu}{TMci - TMcu} \right) \right] \times 100$$

TMdi = tail moment of drug-treated irradiated sample
TMcu = tail moment of untreated, unirradiated control
TMci = tail moment of untreated, irradiated control

2.6 MEASUREMENT OF γH2AX FOCI AND RAD51 FOCI

2.6.1 Drug treatment

SK-Br-3 cells were seeded at a concentration of 4×10^4 cells per well of a four well LAB-TEK® II chamber slides™ (Nalge Nunc International, UK) and incubated overnight at 37°C 5% CO_2. The following day the media was removed and replaced with 500 µl of media +/- TKI with replacement every 24 hours and one hour prior to exposure to the DNA damaging agent under investigation. DNA damaging drugs or controls treated with 1 µl of DMSO were added to the media +/- TKI and left in contact with the cells for one to two hours, depending on the drug under investigation. Following drug incubation, the media was replaced with fresh media +/- TKI. For cells exposed to IR, following incubation with TKI cells were irradiated for the required time whilst on ice and then placed back into the incubator for the required duration. Time points were

removed straight after exposure to the DNA damaging agent under investigation and at various time points following exposure. Controls of untreated cells and cell treated with TKI alone were also investigated at each time point.

2.6.2 Cell fixation

Following incubation for the required time, the chamber slides were removed from the incubator and placed on ice. Cells were then fixed by the addition of 0.5 ml of ice cold 50% methanol:acetone (*v*/*v*) for eight minutes at 4 °C. This solution was then removed by aspiration and cells washed with ice cold PBS three times. Permeabilisation was then undertaken by the addition of 0.5 ml of permeabilisation solution (0.5% Triton X-100 (Sigma, UK) in PBS) to each well for five minutes at room temperature. Cells were then washed twice and 0.5 ml of blocking buffer added per well (0.1% Triton X-100, 0.2% skimmed dry milk in PBS) and incubated overnight at 4 °C in a humidified box.

2.6.3 Staining for γH2AX

This procedure was conducted by Dr Jenny Wu**.** Blocked cells were incubated with 200 µl per well of mouse monoclonal anti-γH2AX (Upstate, Hampshire, UK) diluted to 1:10,000 in blocking buffer for one hour at room temperature. After washing three times with wash buffer (0.1% Triton X-100 in PBS), cells were incubated with Alexa Fluor 488 goat anti-mouse secondary antibody (Invitrogen, UK) at a dilution of 1:2000 in blocking buffer for 1 h at 4 °C in the dark. Cells were washed with PBS and counterstained with 0.5 ml per well of propidium iodide (2 µg/ml) for three minutes. Stained cells were washed with cold PBS three times.

2.6.4 Staining for RAD51

This procedure was conducted by Dr Jenny Wu**.** Blocked cells were incubated with 200 µL per well rabbit monoclonal anti-RAD51 (Santa Cruz Biotechnology, USA) diluted 1:50 dilution in blocking buffer for one hour at room temperature. After washing three times with wash buffer (0.1% Triton X-100 in PBS), cells were incubated with Alexa Fluor 488 goat anti-rabbit secondary antibody (Invitrogen, UK) at a dilution of 1:2000 in blocking buffer for 1 h at 4 °C in the dark. Cells were washed with PBS, counterstained with 0.5 ml per well of propidium iodide (2 µg/ml) for three minutes then washed with cold PBS three times.

2.6.5 Visualisation of foci

This procedure was conducted by Dr Jenny Wu. Slides were mounted with Vectashield® (Vector Laboratories, Peterborough, UK), a cover slip added (25 × 80 mm, No. 1 Thickness, VWR International, Leicestershire, UK) and edges sealed with clear nail polish. Images were visualised with a Zeiss LSM510 fluorescence microscope (100× oil immersion objective), equipped with a cooled CCD camera and two detector channels with 488 nm Argon ion and 543 nm HeNe excitation lasers. Foci were counted in 50 cells per time point and results are expressed as mean number of foci per cell (±mean standard error) from three independent experiments.

2.7 CELL CYCLE ANALYSIS

Effect of drug treatment on cell cycle was studied using fluorescence activated cell sorting (FACS).

2.7.1 Drug treatment

$100x10^4$ cells were plated in T25 flasks and incubated at 37^oC in 5%CO_2 overnight. The following day media was replaced with new media or media plus drug, which was replaced every 24 hours as required by the experiment.

2.7.2 Cell fixation and staining

Cells were trypsinised and pelleted as documented previously, the supernatant removed and resuspended in PBS and spun at 1500 rpm for five minutes at 4^oC. Supernatant was discarded and cells fixed with 2.5 ml of cold 70% ethanol overnight at $–20^oC$. Samples were kept for up to a week at -20^oC before staining. For staining, cells were pelleted by centrifugation at 1, 500 rpm or five minutes at 4^oC. The supernatant was discarded and cells re-suspended in 500µl of PI staining solution (50 µg/ml PI, 0.1mg/ml RNAse A, 0.05% triton X-100 and PBS). Samples were incubated for 40 minutes at 37^OC in the dark. Following incubation, 3 ml of PBS was added and cells pelleted again, followed by re-suspension in 500 µl PBS for analysis.

2.7.3 Fluorescence activated cell sorting

Red fluorescence from PI staining was analysed using Becton Dickinson FACscan (UK) on the channel FL2. Gates were drawn in order to only observe individual cells and eliminate clumped cells.

2.7.4 Data analysis

Data were analysed using Summit v4.3 software (Dako, USA) in order to quantify the number of cells in each phase of the cell cycle.

2.8 ANNEXIN V APOPTOSIS ASSAY

2.8.1 Drug Treatment

Cells were plated and treated as described in section 2.5.1, together with an untreated control and cells treated with etoposide 150 µM for 24 hours to act as an apoptosis control. After exposure to DNA damaging agent for the required time, media was replaced with fresh drug free media or media containing TKI and incubated for 24 hours.

2.8.2 Cell staining

After incubation, media was removed and cells washed is ice cold PBS and detached using cell disassociation fluid (Sigma-Aldrich, UK). Cells were then pelleted by centrifugation at 1500 rpm for five minutes at 4^{o}C. Cells were resuspended in 500 µl of binding buffer (BioVision, USA) to which 5 µl annexin-V-PE solution (BioVison, USA) and 1 µl Sytox red dead cell stain was added. Untreated and treated (150 µl etoposide for 24 hours) controls were unstained or stained with annexin-V-PE and Sytox Red dye only. Cells were gently mixed and kept in the dark.

2.8.3 Fluorescence activated cell sorting

Cells fluorescence was detected using Becton Dickinson FACscan (UK) immediately after staining. Control gates were set using an untreated unstained control, an apoptosis control stained with annexin-V-PE only or Sytox Red only**.**

2.8.4 Data analysis

Data were analysed using Summit v4.3 software (Dako, USA) in order to quantify the number of cells in each phase of the cell cycle.

2.9 MEASUREMENT OF INTRACELLULAR DOXORUBICIN

Doxorubicin is naturally fluorescent which can be measured using FACS.

2.9.1 Drug treatment

Cells were plated at a concentration of $20x10^4$cells per well of a six well plate and left overnight to adhere at 37^oC in 5% CO_2 as described in section 2.5.1. Media was removed and replaced with 2 ml of media +/- TKI. Drug was replaced every 24 hours for the 48 hours experiments, and one hour before treatment with doxorubicin 5 μM. Cells were incubated with doxorubicin for two hours and then collected by trypsinisation, pelleted, frozen at $–80^oC$ in FCS +10% DMSO.

2.9.2 Fluorescence activated cell sorting

Prior to analysis cells were defrosted slowly on ice, pelleted and then washed twice in PBS, to remove free doxorubicin. Cells were then resuspended in PBS ready for analysis. As for the cell cycle analysis, cells were analysed with the FL2 channel, with boundaries identified using untreated control cells.

2.9.3 Data Analysis

Data were analysed using Summit v4.3 software (Dako, USA) to assess the frequency of events detected at each channel. Data were expressed as the mean fluorescence intensity (MFI) for each TKI treatment and controlled by subtracting the MFI for doxorubicin untreated, TKI treated samples.

2.10 TOPOISOMERASE II ACTIVITY ASSAY

Topo II activity was assayed using the Topo II assay kit from Topogen (Florida, USA). This assay examines the ability of extracted Topo II to decatenate, exogenous catenated DNA.

2.10.1 Drug treatment

Cells were grown in T75 flasks seeded at a concentration of $25X10^4$ cells and left overnight to adhere. The following day the media was replaced with fresh media +/- TKI, with drug replacement at 23 hours and 47 hours for cells exposed to TKI for 48 hours. Following incubation, flasks were removed from the incubator and placed on ice.

2.10.2 Nuclear extraction

All the steps of this procedure were carried out on ice as Topo II is inactivated readily *in vitro* and easily proteolysed. Cells were gently scraped in media and pelleted in a pre-chilled 15 ml falcon tube, at 800 g for three minutes at 4^oC. The supernatant was discarded and cells were resuspended in 4 ml of ice cold TEMP buffer (10mM Tris-HCl, pH 7.5, 1mM EDTA, 4mM MgCl2, 0.5mM PMSF) by pipetting. Cells were centrifuged as before and resuspended in 3 ml of TEMP. Samples were incubated on ice for 10 minutes and dounced in tight fitting homogeniser with eight strokes. Nuclei were pelleted at 1500 g for 10 minutes at 4^oC and subsequently resuspended in 1 ml of ice cold TEMP buffer. Suspensions were transferred in a collection tube and centrifuge at 4,000 rpm for two minutes at 4^oC. The supernatant was completely removed and pellets were resuspended in a small volume (no more than four pellet volumes) of TEP buffer (same as TEMP but lacking $MgCl_2$). An equal volume of 1 M NaCl was added and solutions were vortexed for five seconds and incubated on ice for 45 minutes. Finally, suspensions were centrifuge at 15,000 g for 15 minutes at 4^oC. The supernatant contains both topoisomerase I and II protein but the kit used is specific of Topo II activity.

2.10.3 Assessment of decatenation activity

1 µl of each sample was mixed with 10 times complete assay buffer (Topogen, Florida, USA), 2 µl of kinetoplast DNA (kDNA) and distilled water to 20 µl. Solutions were incubated for 45 minutes at 37^oC. Since the extract contains high salt (0.5 M) care was taken not to poison the reaction with excessive amounts of the extract (different volumes of extract were used to define the least toxic volume giving the best results). Reactions were stopped by adding 4 µl of loading dye (5% sarkosyl, 0.125% bromophenol blue and 25% glycerol) and loaded, along with decatenated kDNA

control and linearised kDNA control, onto a 1% agarose ethidium bromide gel (using 1xTAE – 2.5mM EDTA, 40mM Tris Base and 0.1% acetic acid). The gel was electrophoresed at 100V and photographed using a dual intensity ultraviolet transilluminator coupled with camera (UVP, UK).

2.10.4 Quantitation

Quantitation of Topo II activity was conducted by measurement of pixel density of the resulting DNA bands using Adobe Photoshop software version 8.0 (Adobe, USA). Values were expressed as a fraction of the control value which was assigned the value 1.0.

2.11 SMALL INTERFERING RNA (siRNA) TRANSFECTION

SiRNA against HER2 was used to knockout the expression of HER2 in the MDA-MB-468-HER2 cell line. SiRNA against four target sequences of HER2 (siGenome smart pool, Thermo Scientific, USA) and scrabbled siRNA pool 2 (siGenome smart pool 2, Thermo Scientific, USA) were used, as per the manufactures' protocol. SiRNA was resuspended in 50 µl of RNAase free water (Sigma-Aldrich, UK), the solution mixed by pipetting and then placed on an orbital shaker for 30 minutes at room temperature. The RNA concentration was quantified using UV spectrophotometry at 260 nm (NanoDrop, Thermoscientific, USA). This stock solution was separated into aliquots at stored at -80^{o}C. An initial experiment was undertaken to determine which transfection agent and concentration to use. This experiment ascertained that 2 µl DharmaFect 1 transfection agent (Thermoscientific, USA) yield significant knockdown of HER2 with acceptable levels of cell death.

2.11.1 Preparation of siRNA

20x10^{4} cells were plated per well of a six well plate and left to adhere overnight. From the stock RNA solution a solution of RNA with a concentration of 2 µM was made in 1xsiRNA buffer (Thermoscientific, USA). A solution of 1 ml siRNA was mixed with 1 ml of serum free media and a separated solution of 20 µl DharmaFect transfection agent 1 plus 1.980 ml serum free media and incubated for five minutes at room temperature. The two solutions were then mixed by pipetting and incubated at room temperature

for 20 minutes. The siRNA solution was then made up to a total of 20 ml by the addition of 16 ml of DMEM, containing 10% HI FCS and 1% L-glutamine without antibiotics. In total two RNA solutions were prepared, one with siRNA against HER2 and the second containing a control scrambled siRNA.

2.11.2 Transfection with siRNA

Cells were washed in sterile PBS at 37^{O}C to remove any trace of HI FCS. 2 ml of media containing siRNA was then added to each well and cell incubated for 24 hours at 37^{o}C in 5% $CO_{2.}$ Following incubation for 24 hours, the media was replaced with fresh media and cells left for a further 24 hours. At this point cells were either collected to assess HER2 protein expression by Western blotting as described in section 2.4 or treated with cisplatin 100 μM for one hour and collected for analysis using the alkaline Comet assay as described in section 2.5.

2.12 CHROMATIN IMMUNOPRECIPITATION

These experiments were undertaken in the MDA-MB-468 cell line transfected with HER2, using a vector transfected cell line as a control. Approximately 1X10^{8} cells were grown in multiple T150 flasks and cells processed when they reached 80% confluence. This procedure was conducted by Dr Pawan Dhami.

2.12.1 DNA-protein crosslinking

On the day of immunoprecipitation, the media was removed and replaced with 50 ml of serum free media. DNA-protein and protein-protein interactions are cross-linked by adding formaldehyde (37%, BDH AnalaR); 1355 μL formaldehyde is added drop-wise to a final concentration of 1% to fix transcription factors. The flask was then placed on a flat shaker at room temperature, with constant but gentle stirring for 15 minutes. 3.425 ml of ice-cold 2 M glycine was added to make a final concentration of 0.125 M with constant but gentle stirring for five minutes at room temperature to stop the cross-linking reaction. Cells were scraped and transferred to 50 ml centrifuge tubes and kept on ice whenever possible. The cells were pelleted by centrifuging at 259 g for six to eight minutes at 4°C, washed with 1.5 ml of ice-cold PBS and pelleted at 720 g at 4°C for five minutes and the supernatant removed.

2.12.2 Cell lysis

Cells were lysed by adding 1.5 x pellet volumes of ice-cold cell lysis buffer (CLB-10 mM Tris-HCl pH 8.0, 10 mM NaCl, 0.2% Igepal, 10 mM Sodium butyrate, 50 µg/ml PMSF, 1 µg/ml leupeptin). The cell pellets were gently resuspended and incubated on ice for 10 minutes. The nuclei were then recovered by centrifuging the samples at 1125 g for five minutes at 4°C. The supernatant removed and the nuclei lysed by resuspending the pellet in 1.2 ml of nuclei lysis buffer (NLB-50 mM Tris-HCl pH 8.1, 10 mM EDTA, 1% SDS, 10 mM Sodium butyrate, 50 µg/ml PMSF, 1 µg/ml leupeptin) and incubated on ice for 10 minutes.

2.12.3 Sonication

720 µL of IP dilution buffer (IPDB-20 mM Tris-HCl pH 8.1, 150 mM NaCl, 2 mM EDTA, 1% Triton X-100, 0.01% SDS, 10 mM Sodium butyrate, 50 µg/ml PMSF, 1 µg/ml leupeptin) was added and the samples were transferred to 5 ml glass tubes. The chromatin was sonicated to reduce the DNA length to an average size of 600 bp using the Sanyo/MES Soniprep sonicator.

The samples were allowed to cool on ice for one minute between each pulse (5 µl of the sheared chromatin was run on an agarose gel to check sonication). The sonicated chromatin was transferred to 2 ml microfuge tubes and spun down at 18000 g for 10 minutes at 4^{o}C .

2.12.4 Immunoprecipitation

The supernatant was transferred to a 15 ml falcon tube and 4.1 ml of IP dilution buffer added. Chromatin was precleared by adding 100 µL of normal rabbit IgG (Upstate Biotechnology). Samples were incubated for one hour at 4°C on a rotating wheel. 200 µL of homogeneous protein G-agarose suspension (Roche, UK) was added to the precleared chromatin and the samples were incubated for three to five hours at 4°C on a rotating wheel. The samples were then centrifuged at 1620 g for two minutes at 4°C to pellet the protein G-agarose beads and the supernatant was used to set up various immunoprecipitation conditions in 2 ml microfuge tubes. An aliquot of 270 µL of chromatin was stored at -20°C to be used as input sample for array hybridisations and

real-time PCR. An NLB:IPDB buffer at the ratio of 1:4 was prepared to set-up IP conditions as follows:

- No chromatin – 1350 µL NLB:IPDB buffer
- No antibody – 675 µL chromatin + 675 µL NLB:IPDB buffer
- Normal Rabbit IgG – 675 µL chromatin + 675 µL NLB:IPDB buffer + 10 µL rabbit IgG (Upstate Biotechnology)
- Test IP conditions – 675 µL chromatin + 675 µL NLB:IPDB buffer + 5-20 µg* of test antibody

The samples were incubated at 4°C overnight on a rotating wheel. The next day the samples were centrifuged at 18000 g for five minutes at 4ºC and the lysate/antibody samples were transferred to fresh 2 ml microfuge tubes. 100 µL of homogeneous protein G-agarose suspension was added to each sample and the samples were incubated at 4°C for at least three hours on a rotating wheel. The samples were then centrifuged at 6800 g for 30 seconds at 4°C to pellet the protein G-agarose beads. The supernatant was removed and the protein G-agarose beads were carefully washed. For each wash, the wash buffer was added, the samples were vortexed briefly, were centrifuged at 6800 g for two minutes at 4°C and left to stand on ice for one minute before removing the supernatant. The washes were carried out in the following sequence:

a) The beads were washed twice with 750 µL of cold IP wash buffer 1. The beads were transferred to a 1.5 ml microfuge tube after the first wash.
b) The beads were washed once with 750 µL of cold IP wash buffer 2.
c) The beads were washed twice with 750 µL of cold TE pH 8.0.

2.12.5 Elution

DNA-protein-antibody complexes were eluted from the protein G-agarose beads by adding 225 µL of IP elution buffer (100 mM $NaHCO_3$, 1% SDS). The bead pellets were resuspended in IP elution buffer, briefly vortexed then centrifuged at 6800 g for two minutes at room temperature. The supernatant was collected in fresh 1.5 ml microfuge tubes. The bead pellets in the original tubes were resuspended in 225 µL of

IPEB again, briefly vortexed and centrifuged at 6800 g for two minutes. Both the elutions were combined in the same tube.

2.12.6 Reversal of cross-links

The reversal of cross-links step was carried out on the Input sample which was stored at -20°C previously. 0.1 µL of RNase A (10 mg/ml, 50, 000 units, ICN Biochemicals) and 16.2 µL of 5 M NaCl (to the final concentration of 0.3 M) was added to the Input DNA sample. Similarly, 0.2 µL of RNase A (10 mg/ml, 50, 000 units) and 27 µL of 5M NaCl (to a final concentration of 0.3 M) was added to each of the IP test samples. All the samples including the input DNA sample were incubated at 65ºC for six hours to reverse the cross-links. 9 µL of proteinase K (10 mg/ml, 20 U/mg, GibcoBRL) was added to each sample and incubated at 45ºC overnight.

2.12.7 Extraction of DNA

2 µL of yeast tRNA (5 mg/ml, Invitrogen) was added to each sample just before adding 250 µL of phenol (Sigma) and 250 µL of chloroform. The samples were vortexed and centrifuged at 18000 g for five minutes at room temperature. The aqueous layer (top layer) was collected in fresh 1.5 ml microfuge tubes and 500 µL of chloroform was added to each sample. The samples were vortexed and centrifuged at 18000 g for five minutes at room temperature. The aqueous layer was transferred to a fresh 2.0 ml microfuge tubes 5 µg of glycogen (5 mg/ml, Roche), 1 µL of yeast tRNA (5 mg/ml, Invitrogen) and 50 µL of 3 M NaAc (pH 5.2) was added to each sample and mixed well. The DNA was precipitated with 1375 µL of 100% ethanol and incubating at –70^{o}C for 30 minutes (or -20°C overnight). The samples were centrifuged at 20800 g for 20 minutes at 4ºC. The DNA pellets were washed with 500 µL of ice-cold 70% ethanol and air-dried for 10-15 minutes. The DNA pellets of the IP samples were resuspended in 50 µL of sterile filtered HPLC water and 100 µL for the Input DNA samples. 5 µL of each sample was run on a 1% agarose 1XTBE gel and visualised with ethidium bromide to check DNA size. Samples were stored at –20°C.

2.12.8 Sample labelling and hybridisation to bacterial artificial chromosomes

The ChIP DNA samples were labelled with Cy3 and genomic DNA with Cy5. Initially bacterial artificial chromosome (BAC) arrays were used to confirm the binding of ErbB2

to DNA clones. Each array contains 32,436 BAC clones, with an average size of 170 kbp, with 892 clones not mapping to genomic DNA. The labelled DNA was transferred to the MAUI Hyb (Biomicrosystems, USA) together with the BAC array and left to hybridise overnight.

2.12.9 Quantitation

ProScanArray express (Perkin Elmer, UK) was used to quantitate the fluorescence of each array spot. Mean signal intensity ratios (spot intensity minus background intensity) were calculated and data sets normalised to intensities achieved from the control rabbit IgG. The MDA-MB-468-Vector data set was set as the baseline level of 1 and the mean ration and SD for the MDA-MB-468-HER data set calculated. The significance threshold was set at three standard deviations above the mean background level.

2.13 GENE EXPRESSION ARRAYS AND REAL TIME PCR

2.13.1 Cell treatment

MDA-MB-468-Vector, MDA-MB-468-HER2 and MDA-MB-468-NLS cells were grown in T75 flasks plated at a concentration of $15x10^4$ cells. Two DNA expression arrays were conducted, the first in cells treated with cisplatin under the same conditions as used to established differences in the ability to repair cisplatin-induced interstrand crosslinks as described (Boone *et al.*, 2009). The second in untreated cells allowed to proliferate until they reached 80% confluence prior to RNA extraction.

2.13.1.1 Drug treatment

Cells were plated at a concentration of $25x10^4$ cells in T75 flasks and left to adhere overnight. The following day the media was removed and replaced with fresh media +/- cisplatin 50 μM for one hour. Following incubation the media was replaced with fresh DFM and incubated at 37^oC 5% CO_2 for 24 hours. At this point cells were processed to extract RNA.

2.13.2 RNA extraction and quantification

Following incubation for the required time, cells were collected by trypsinisation, pelleted and washed is ice cold PBS and re-pelleted as described in section 2.1.4. The

RNeasy minikit (Qiagen, UK) was used to extract RNA using the method as described by the manufacturer. Briefly 600 µL of buffer RLT containing β-mercaptoethanol was used to resuspend the cell pellet. The cells were then homogenised using a manual homogeniser and 600µl of 70% ethanol added to the homogenised cells. The solution was transferred to a RNeasy mini-column and filtered by centrifugation for 15 seconds at 13,000 rpm, with the filtrate discarded. 700 µL of RWI buffer was then added to the column which was centrifuged at 15 seconds at 13,000 rpm and the filtrate discarded. The columns were washed twice with 500 µL of buffer RPE. To extract the RNA, 40 µl of RNase-free water was added onto the membrane of the column and RNA eluted by centrifugation for one minute at 13,000 rpm. The RNA was quantified by measuring the absorbance at 260nm (NanoDrop, Thermoscientific, USA).

2.13.3 Gene expression arrays

This process was conducted by the scientific support service at UCL Cancer Institute (London, UK) using the Affymetrix GeneChip Human Exon 1.0 ST arrays. Each gene is represented by around 40 probes, with each exon covered by approximately four probes, with a total of 5.5 million probes on each array (Affymetrix, 2005). Full details of this process can be found at https://www.affymetrix.com/support/downloads/manuals/expression_s2_manual.pdf

Following assessment of the RNA for both quality and quantity the RNA was processed as follows:

2.13.3.1 Total RNA labeling protocol

Poly-A control stock, 2 µl was diluted with 38 µl poly-A control buffer. 2 µl of this solution was then added to 98 µl of poly-A control buffer to make a 1:50 dilution. This step was repeated to make a 2nd 1:50 dilution. 2 µl of this solution was then mixed with 1 µg of RNA

This step utilises the GeneChip WT cDNA synthesis kit (Affymetrix). A working solution of 500 ng/µl of T7-$(N)_6$ Primer was made by dilution in RNase-free water. This was kept on ice and 2 µl mixed with the 2 µl of the diluted RNA, together with 16 µl of RNase-free water, controls were also made 100 ng RNA, 2 µl of the T7-$(N)_6$ primer solution

and 5 µl of RNase-free water. This sample was incubated at 70°C for five minutes, then cooled at 4°C for a further two2 minutes, then spun and kept on ice.

2.13.3.2 First cycle, first strand synthesis

5 µl of first-cycle, first strand master mix (2 µl of 5x1st Strand buffer, 1 µl 0.1M DTT, 0.5 µl dNTP mix, 10 mM, 0.5 µl RNase inhibitor, 1 µl SuperScript II) was mixed with RNA T7-$(N)_6$ Primer mix. This was spun and incubated at 25^{o}C for 10 minutes, then 42^{o}C for 60 minutes, then 70^{o}C for 10 minutes. The sample was then cooled for at least two minutes. 10 µl of the first cycle second strand master mix (4.8 µl RNase-free water, 4 µl 17.5 mM $MgCl_2$ 0.4 µl dNTP mix 10 mM, 0.6 µl DNA Polymerase I and 0.2 µl RNase H) was then added and incubated in a thermal cycler at 16^{o}C for 120 minutes then 75^{o}C for 10 minutes. The sample was then cooled for two minutes at 4^{o}C.

The sample was then mixed with 30 µl of the IVT master mix (5 µl 10xIVT master mix, 20 µl NTP mix, 5 µl enzyme mix) and the reaction incubated for 16 hours at 37^{o}C.

50 µl RNase-free water was added to the IVT reaction to make a final volume 100 µl and vortexed. Then 350 µl IVT cRNA binding buffer was added, vortexed again and 250 µl ethanol added and mixed with by pipetting. This mix was applied to the cRNA cleanup column placed in a collection tube and centrifuged for 15 seconds at ≥ 8000g. The column membrane was washed with 500 µl IVT cRNA wash buffer, then spun for 15 seconds at ≥ 8000g. The column was transferred to a new collection tube, 500 µl 80% (*v/v*) ethanol was then added and spun for 15 seconds at ≥ 8000g. The cap of the column was then opened and the column spun at maximum speed for five minutes. The column was then transferred to a new collection tube, 15 µl of RNase-free water was applied to the spin column membrane and centrifuged for one minute at maximum speed to elute cRNA. This step was repeated with using the elute, which was incubated for five minutes at room temperature and then centrifuges for one minute at maximum speed. The concentration and quality of cRNA was evaluated using a using NanoDrop (Thermoscientific, UK).

2.13.3.3 Second cycle, first strand synthesis, cleanup and quantification of cRNA

The cRNA was then mixed with 8 µl of random primer solution (1.5 µl random primers 3µg/µl and RNase-free water). The mixture was incubated for five minutes at 70^{o}C followed by five minutes at 25^{o}C and the sample cooled at 4^{o}C for two minutes. This was them mixed with the second cycle, first strand mastermix (4 µl of 5x1st Strand buffer, 2 µl 0.1M DTT, 1.25 µl dNTP+dUTP mix 10 mM, 4.75 µl SuperScript II) and incubated at 25^{o}C for 10 minutes, then 42^{o}C for 60 minutes, then 70^{o}C for 10 minutes. The sample was then cooled sample cooled at 4^{o}C for two minutes.

1 µl of RNase H was then added to the sample and incubated at 37^{o}C for 45 minutes, then 95^{o}C for five minutes, then 4^{o}C for two minutes. Cleanup and RNA quality analysis was then undertaken as outline above.

2.13.3.4 Fragmentation of cRNA

5.5 µg of cRNA was mixed with up to 31.2 µl of RNase-free water and was added to 16 µl fragmentation buffer (10 µl RNase-free water, 10x cDNA fragmentation buffer, 1 µl UDG, 1 µl APE1 10,000 U/µl). This was incubated at 37°C for 60 minutes, 93^{o}C for two minutes then 4^{o}C for two minutes. The fragmentation product was then run on a 2% agarose gel at 120V for 30 minutes for confirmation of fragmentation.

2.13.3.5 Hybridisation

A hybridization mix was prepared from 60 µl fragmented cRNA, 3.7 µl 3 nM control oligonucleotide B2, 11 µl 20x eukaryotic hybridisation controls, 110 µl 2x hybridisation buffer, 15.4 µl DMSO and nuclease free water to a total volume of 220 µl. This was then heated to 99°C for five minutes, then cooled to 45^{o}C for five minutes and centrifuged for one minute as maximum speed. The Exon ST array was allowed to equilibrate to room temperature. 200 µl of the hybridization mix was then injected into the array, the array places in a hybridization oven at 45^{o}C at 60 rpm and incubated for 17 hours.

2.13.3.6 Washing and Staining

SAPE stain solution was made by mixing 600 µl 2x stain buffer, 48 µl 50mg/ml BSA, 12 µl 1mg/ml SAPE and 540 µl ddH2O making a final volume of 1200 µl. Antibody solution

was made by mixing 300 µl 2x stain buffer, 24 µl 50mg/ml BSA, 6 µl 10mg/ml Goat IgG stock (Sigma-Aldrich), 3.6 µl 0.5mg/ml biotinylated antibody and 266.4 µl distilled water. The arrays are washed and stained using the automated Affymetrix wash station using the protocol EukGE_w52v5.450.

2.13.3.7 Scanning

This was performed using the Agilent SureScan (Agilent, USA). Partek Genomic suite (Partek, USA) was used to obtain DAT image files which were then converted to CEL files containing information about the expression levels of the individual probes.

2.13.4 Gene expression analysis

Data were analysed using by the Bioinformatics department at the UCL Cancer Institute. Initial analysis examined whether the arrays had been successful by performing boxplot and principle component analysis. Cluster dendrograms were produced to demonstrate hierarchical clustering between the samples analysed. Differences in gene expression were identified by using analysis of variance (ANOVA) and gene list created based upon a false discovery rate of 0.05. For the second microarray investigation performed on proliferating cells, around a 1000 genes were differentially expressed between the cell lines. These genes were explored for those involved in DNA repair (see appendix one).

2.13.5 Gene Ontology Analysis

Functional pathway analysis was performed using Partek software, to identify potential pathway differences between the MDA-MB-468-Vector and MDA-MB-468-HER2 cell lines. Pathways involved in DNA repair, cell proliferation and transcription and translation were investigated.

2.13.6 Real time PCR

This work was undertaken by Mr John Bingham. Briefly cDNA was synthesised from the RNA using the RNA samples from the MDA-MB-468-Vector, MDA-MB-468-HER2 and MDA-MB-468-NLS cell lines used to perform gene expression arrays. This was performed using a high capacity cDNA reverse transcription kit (Applied Biosystems, UK). Pre-designed FAM™-labelled primers for FANCC and IRS1 were used (TaqMan

Gene Expression, Applied Biosystems, UK). Briefly, 1 µl of TaqMan gene expression solution was mixed with 5 µl cDNA and 10 µl 2x TaqMan gene expression mastermix (Applied Biosystems, UK). 20 µl of the mixture was transferred to a single well of a 48 well plate. Control samples were also prepared without primers and β-actin (TaqMan Gene Expression, Applied Biosystems, UK). The plate was covered, centrifuged and loaded into the 7500 real time PCR system for amplification (Applied Biosystems, UK). Amplification is measured by increasing intensity of the reporter FAM™ dye. Data were analysed using SDS v1.3.1 (Applied Biosystems, UK).

2.14 STATISTICAL ANALYSIS

Observations are presented as mean±SEM, unless stated otherwise. Comparison of means was performed using a one way ANOVA, followed by post analysis Tukey's test, or a two way ANOVA followed by post hoc analysis Bonferroni test. All statistical analysis was performed using GraphPad Prism Software (USA).

Investigation into the effects of lapatinib in combination with chemotherapy on cell proliferation

3.1 INTRODUCTION

The dual EGFR and HER2 TKI lapatinib, inhibits cell proliferation in cancer cell lines with sensitivity correlating with the expression of HER2 (Konecny *et al.*, 2006; Zhang *et al.*, 2008). In combination with cytotoxic drugs, lapatinib produces synergistic effects in breast, endometrial, gastric, pancreatic and ovarian cancer cell lines (Kim *et al.*, 2008b; Komoto *et al.*, 2009b; LaBonte *et al.*, 2009; McHugh *et al.*, 2007). This has translated into the clinical setting in combinations of lapatinib with capecitabine (Geyer *et al.*, 2006) or paclitaxel (Di Leo *et al.*, 2008b) in patients with metastatic breast cancer. The precise mechanisms through which lapatinib produces synergy are still under investigation but include the inhibition of the PI3K/AKT and Ras-Raf-MAPK pathways promoting cell cycle arrest, growth inhibition and apoptosis (Konecny *et al.*, 2006; Wainberg *et al.*, 2010). Lapatinib also inhibits the nuclear translocation of EGFR and HER2, down regulating the transcription of thymidylate synthase, a target of capecitabine (Kim *et al.*, 2009).

3.1.1 Combining tyrosine kinase inhibitors and DNA damaging agents

As discussed in Chapter One, section 1.8 the inhibition of HER signalling can increase sensitivity to cytotoxic agents through a number of mechanisms, including the inhibition of DNA repair. This suggests that the combination of agents which induce DNA strand breaks with HER inhibitors, should produce additional cell death over either agent alone. In the clinical setting, the addition of gefitinib or erlotinib to standard platinum based chemotherapy has been investigated in three separate trials in patients with NSCLC as discussed in section 1.9.3. Together these trials recruited nearly 4000 patients and failed to demonstrate any benefit from the addition of gefitinib or erlotinib over standard doublet chemotherapy alone (Gatzemeier *et al.*, 2007; Giaccone *et al.*, 2004; Herbst *et al.*, 2004; Herbst *et al.*, 2005). Whilst there are a number of potential reasons for this, *in vitro* data suggests that the scheduling of gefitinib may be important. This has been demonstrated in colorectal and oesophageal cancer cell lines where the addition of gefitinib after exposure to chemotherapy drugs

produces at least additive effects and can produce synergy, an observation not seen in cells pre-treated with gefitinib prior to chemotherapy exposure (Chun *et al.*, 2006; Morelli *et al.*, 2005; Xu *et al.*, 2003).

3.1.2 Combining lapatinib with DNA damaging chemotherapy

Unlike gefitinib, lapatinib has successfully translated into the clinical setting in combination with capecitabine or paclitaxel. In order to investigate if lapatinib might act by modulating the cellular response to DNA damaging agents, the inhibition of cell proliferation by doxorubicin or cisplatin in combination with lapatinib was investigated using the SRB assay in three breast cancer cell lines.

Doxorubicin is used in the systemic management of breast cancer in the neo-adjuvant, adjuvant and metastatic settings. It induces cell death through the formation of oxygen free radicals, intercalating with DNA and RNA and poisoning Topo II resulting in the production of DNA DSBs (Takimoto and Calvo, 2008). Cisplatin induces DNA damage through the formation of intra and interstrand crosslinks, which can result in the formation of DSBs as discussed in section 1.6.1. Cisplatin is not routinely used in the management of breast cancer but there is evidence that it may be useful in patients with 'triple negative breast cancer' (Silver *et al.*, 2010). These tumours do not express ER, PR and are not HER2 gene amplified, hence their identification as 'triple negative'; around 60% express EGFR (Nielsen *et al.*, 2004). Therefore in this group, combinations of EGFR inhibitors and cisplatin may be beneficial.

3.2 AIMS

This chapter describes experiments to investigate the interaction between lapatinib and either cisplatin or doxorubicin with the following aims:

1. Does lapatinib interact with the inhibition of cell proliferation by cisplatin or doxorubicin?
2. What is the character of the interaction between lapatinib with either cisplatin or doxorubicin?
3. Is the interaction between lapatinib and cisplatin or doxorubicin schedule dependent?

3.3 HUMAN EPIDERMAL GROWTH FACTOR RECEPTOR EXPRESSION

To investigate the effect of lapatinib in combination with DNA damaging agents three breast cancer cell lines, MCF-7, MDA-MB- 468 and SK-Br-3 were used. These cell lines were chosen as they express different levels of HER proteins. The characteristics of these cell lines as documented in the literature are outlined in Table 3.1; none carry mutations in the BRCA genes (Kenny *et al.*, 2007; Lacroix and Leclercq, 2004).

	MCF-7*	MDA-MB-468	SK-Br-3
Source	Invasive ductal carcinoma from a pleural effusion	Adenocarcinoma from a pleural effusion	Invasive ductal carcinoma from a pleural effusion
EGFR	Low	High	Low
HER2	Low/deleted	Low/deleted	High
ER	Expressed	Negative	Negative
PR	Expressed	Negative	Negative
PTEN	Expressed	Negative	Expressed
Other gene mutations	CDKN2A, PIK3CA	p53, MADH4 and RB1	Not reported

Table 3.1 Characteristics of the MCF-7, MDA-MB-468 and SK-Br-3 cell lines Data taken from review by Lacroix and Leclercq, 2004 and Kenny *et al.,* 2007. CDKN2A-cyclin kinase dependent inhibitor 2A, PIK3CA- phosphoinositide-3-kinase, catalytic alpha polypeptide, RB1- retinoblastoma protein. *The reported characteristics of the MCF-7 cell line have been reported to vary

EGFR, HER2, HER3 and HER4 expression were assessed by Western blotting (Figure 3.1) in the three cell lines.

- The SK-Br-3 cell line expresses high levels of HER2, in addition to EGFR, HER3 and HER4.
- The MDA-MB-468 cell line expresses high levels of EGFR, with no HER2 detected and low levels of HER3 and HER4.
- The MCF-7 cell line expresses high levels of HER4 and low levels of HER3. EGFR and HER2 expression are not detected in normal proliferating cells by Western blotting (Figure 3.1).

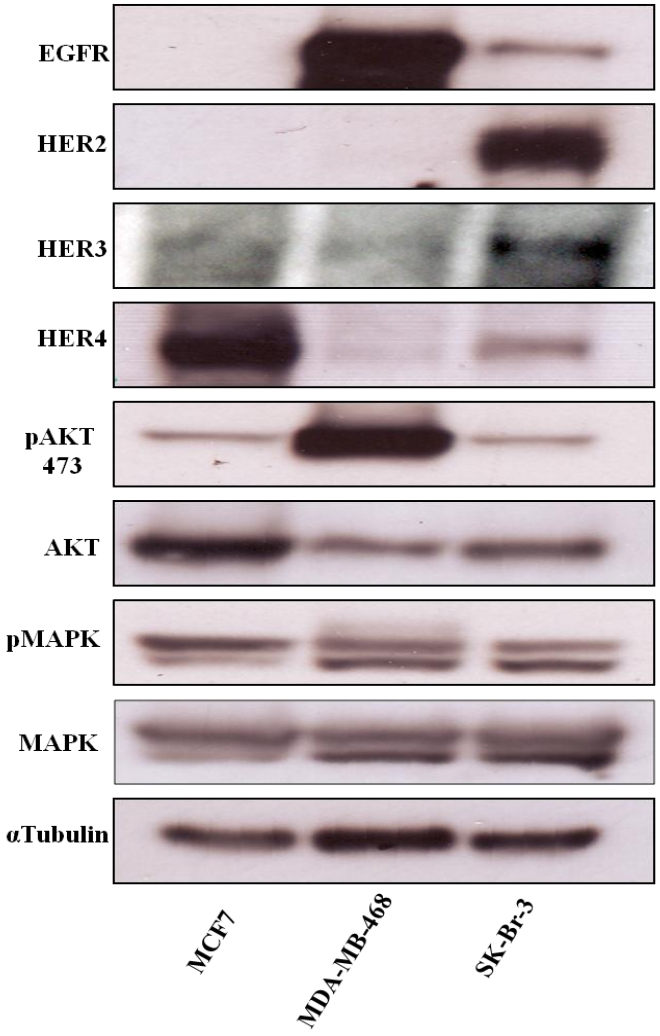

Figure 3.1 HER expression in the MCF-7, MDA-MB-468 and SK-Br-3 cells lines
Expression of the EGFR, HER2, HER3, HER4 and AKT were assessed in three breast cancer cell lines by Western blotting. Proliferating cells were lysed and immunoblotted with antibodies as indicated. αtubulin used as loading control.

3.4 DETERMINATION OF IC_{50} VALUES FOR LAPATINIB, CISPLATIN AND DOXORUBICIN

The SRB assay was used to assess the effects of lapatinib in combination with either cisplatin or doxorubicin on cell proliferation. The SRB assay was first described in 1989 and provides a reproducible and sensitive high throughput technique for assessing cell proliferation (Vichai and Kirtikara, 2006). The results of this assay correlate with the tetrazolium dye3-(4,5-dimethylthiazol-2-yl)-2,5-diphenyltetrazolium bromide (MTT) assay, which assesses cytotoxicity (Vichai and Kirtikara, 2006).

For the investigations described below, cells were plated in 96 well plates at a concentration of 2000-4000 cells per well. This allowed approximately five cell doubling times in 96 hours without saturation of the assay. Drug treatment was added to each well as required, with three wells per drug concentration.

3.4.1 Inhibition of cell proliferation by lapatinib

Lapatinib inhibits cell proliferation in all three cell lines with differing sensitivities (Figure 3.2). The MCF-7 line is the least sensitive (IC_{50} 5.42 µM ((95% CI 4.89-6.00 µM) and Sk-Br-3 the most (IC_{50} 0.1 µM (95% CI 0.079-0.13 µM).

A

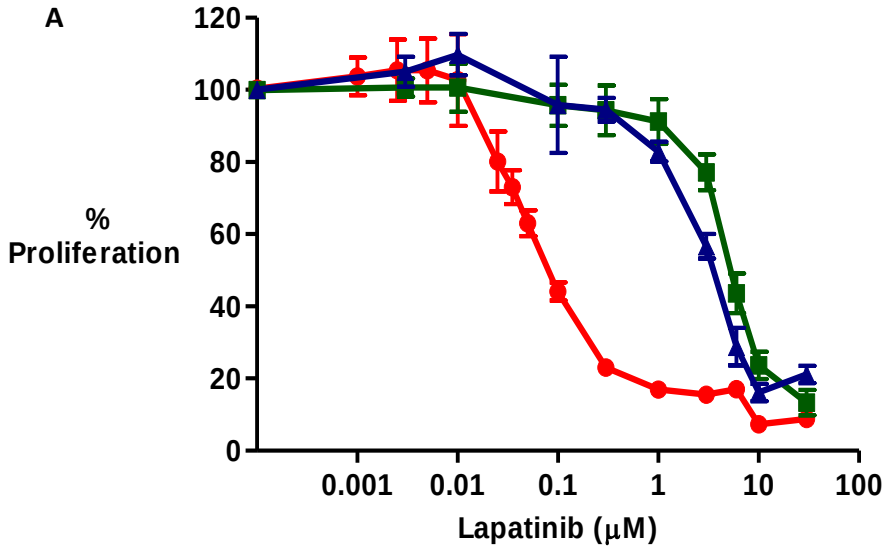

B

Cell line	IC_{50} (95% CI)
SK-Br-3	0.10 µM (0.08-0.13)
MCF-7	5.42 µM (4.89-6.00)
MDA-MB-468	3.38 µM (2.82-4.04)

Figure 3.2 Effect of lapatinib on cell proliferation
(A) The SRB assay was used to assess inhibition of proliferation by lapatinib in SK-Br-3(●), MCF-7(■), and MDA-MB-468(▲) cell lines. Cells were plated in 96-well plates and treated with serial dilutions of lapatinib for 96 hours. Proliferation is expressed as a % of untreated control cell proliferation. Each experiment was repeated in triplicate and observations are presented mean± SD. (B) IC_{50} values for lapatinib in breast cancer cell lines. The IC_{50} and 95% confidence intervals (CI) were calculated using non linear regression, for three replicate experiments.

3.4.2 Inhibition of cell proliferation by chemotherapeutic agents

Prior to conducting combination experiments, the IC_{50} for continuous exposure to cisplatin or doxorubicin was determined, in each cell line (Figure 3.3). The MDA-MB-468 cell line is the most sensitive to cisplatin with an IC_{50} of 0.12 µM (95% CI 0.06-0.24 µM), the SK-Br-3 cell line has an IC_{50} of 0.63 µM (95% CI 0.44-0.90 µM) and the MCF-7 cell line an IC_{50} of 1.54 µM (95% CI 1.10-2.14 µM). For doxorubicin the IC_{50} ranged from 5.39 nM (95% CI 3.34-8.71 nM) in the MDA-MB-468 cell line, 13.61 nM (95% CI 8.82-21 nM) in MCF7 cells and 14.05 nM (95% CI 10.74-18.38 nM) in SK-Br-3 cells.

A

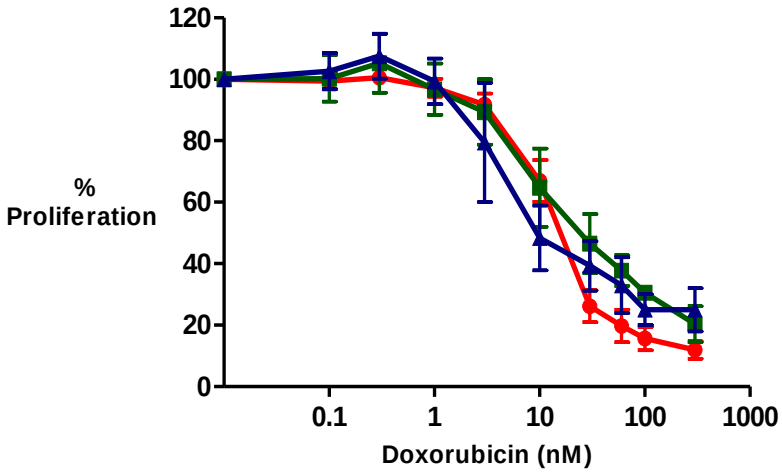

B

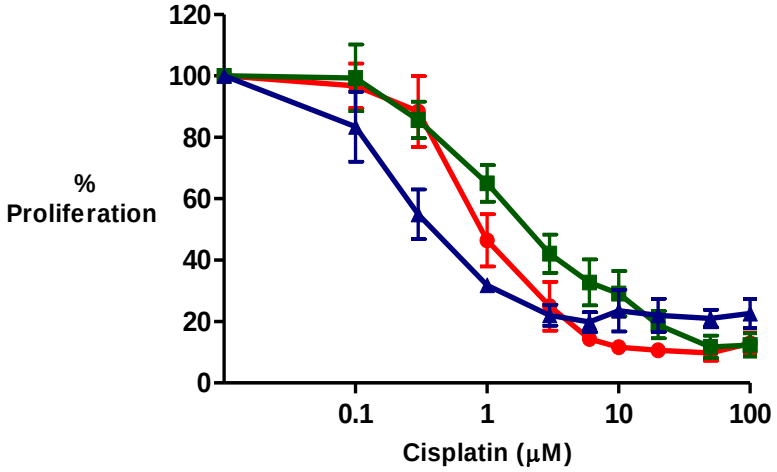

C

IC_{50} (95% CI)	SK-Br-3	MCF-7	MDA-MB-468
Doxorubicin (nM)	14.05 (10.74-18.38)	13.61 (8.82-21.0)	5.39 (3.34-8.71)
Cisplatin (µM)	0.63 (0.44-0.90)	1.54 (1.10-2.14)	0.12 (0.06-0.24)

Figure 3.3 Effect of doxorubicin and cisplatin on cell proliferation

The SRB assay was used to assess the effects of (A) doxorubicin and (B) cisplatin in SK-Br-3(●), MCF-7(■) and MDA-MB-468 (▲) cell lines. Cells were plated in 96-well plates and treated with serial dilutions of (A) doxorubicin and (B) cisplatin for 96 hours. Proliferation is expressed as a % of untreated control cell proliferation. Each experiment was repeated in triplicate and observations are presented mean± SD. (C) IC_{50} values for cisplatin and doxorubicin. The IC_{50} and 95% CI were calculated using non linear regression, for three replicate experiments.

3.5 Combination of lapatinib with chemotherapeutic agents

To investigate the effect of lapatinib in combination with cisplatin or doxorubicin a concentration of lapatinib which inhibited cell proliferation by 20% was studied in three different schedules:

- both drugs continuously for 96 hours (continuous)
- lapatinib treatment for 60 minutes followed by chemotherapy drug -/+ lapatinib for two hours, then drug free media or lapatinib for 96 hours (lapatinib first)
- chemotherapy drug alone for two hours, followed by drug free media or lapatinib for 96 hours (chemotherapy first)

Two techniques were used to assess the interaction between lapatinib and the cytotoxic drugs under investigation, median effect analysis and the normalised isobologram. Median effect analysis, as described by Chou *et al*., is based upon mass-action law and uses the linear regression of dose response data to produce a median effect plot (Figure 3.4) (Chou, 2006). From this a combination index value, which describes the interaction between the two drugs at each dose point studied, can be calculated (Figure 3.4). The experiments described in this chapter use a non-constant ratio design employing a fixed dose of lapatinib which inhibits proliferation by 20%, with an increasing concentration of chemotherapy drug. This means that at each concentration the ratio of the two drugs in relation to each other alters. From this design a combination index value can be calculated for each drug combination investigated which describes the interaction between the two drugs (Figure 3.4B).

3.5.1 Evaluating the impact of drug schedule on cell proliferation

Both the schedules of chemotherapy first and lapatinib first allowed the use of the same concentration of chemotherapy drug, as both schedules utilise a two hour exposure to chemotherapy. For the schedule of continuous exposure, lower concentrations of chemotherapy drugs were used due to the 96 hours long drug treatment. In order to allow comparisons across schedules which use different drug concentrations, a combination index value at an isoeffective concentration is normally used e.g. IC_{20} or IC_{50}. This can be done when experiments are performed using a fixed-ratio design, as median effect analysis allows data simulation to calculate combination indices at isoeffective drug concentrations. Simulation is not possible in experiments

using a non-constant ratio design as presented here, due to the alteration in the ratio of chemotherapy to lapatinib as the concentration of the chemotherapy drug increases. To allow a direct comparison across the three schedules at an isoeffective drug concentration, a normalised isobologram was therefore constructed, with schedules compared at their IC_{50} level (Figure 3.4C).

A

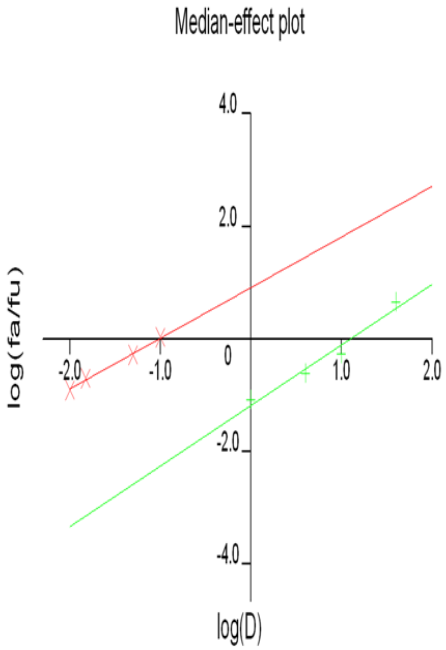

B

Combination Index	Description
<0.10	Very strong synergy
0.10-0.30	Strong synergy
0.30-0.70	Synergy
0.70-0.85	Moderate to slight synergy
0.85-0.90	Slight synergy
0.90-1.10	Nearly additive
1.10-1.20	Slight antagonism
1.20-1.45	Moderate antagonism
1.45-3.30	Antagonism
3.30-10	Strong antagonism
>10	Very strong antagonism

C

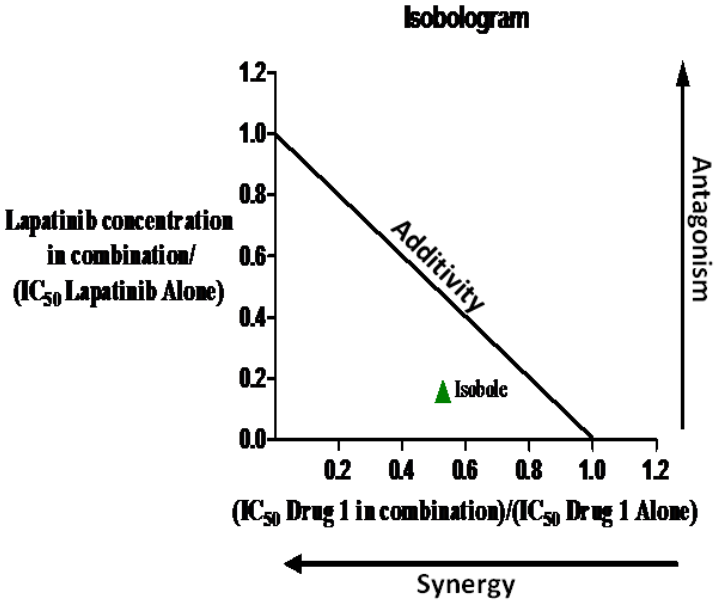

Figure 3.4 Drug interaction analysis
(A) An example of a median effect plot. Cisplatin (×) and lapatinib-cisplatin (×). (B) Description of combination indices as calculated using median effect analysis, adapted from Chou *et al.* (C) Normalised Isobologram demonstrating an isobole for a drug combination.

3.5.2 Lapatinib in combination with doxorubicin

The addition of lapatinib to doxorubicin inhibits cell proliferation producing synergistic effects at all but very high doxorubicin concentrations, in all three cell lines investigated (Figures 3.5, 3.6 and 3.7).

3.5.2.1 SKBr-3 cell line

The impact of schedule is less pronounced in this cell line, with isobologram analysis demonstrating isoboles lying next to each other (Figure 3.5G). Median effect analysis supports this observation with combination indices between 0.45 and 0.89 for all doxorubicin concentrations less than 1 μM in all schedules, indicating a degree of synergy in all the schedules investigated (Figure 3.5).

3.5.2.2 MDA-MB-468 cell line

The schedules of continuous treatment and doxorubicin first, produce the same level of synergy as assessed by isobologram, though combination indices indicate that the schedule of continuous treatment produces the greatest level of synergy (Figure 3.6). The schedule of lapatinib first produces the least synergy of all three schedules investigated, but is still synergistic (Figures 3.6).

3.5.2.3 MCF-7 cell line

The schedule of doxorubicin first produces 'strong synergy/synergy' at 0.1 μM, 0.5 μM and 1.0 μM (combination indices 0.26, 0.29 and 0.34 respectively) which is the highest degree of synergy observed in all three cell lines and for all three schedules (Figure 3.7). The schedule of lapatinib first also produces synergy at the same concentrations of doxorubicin, though to a lesser degree (combination indices 0.45, 0.48 and 0.59) (Figures 3.7). Median effect analysis demonstrates that the least synergy is produced with continuous treatment (Figure 3.7). The importance of schedule is also supported by isobologram analysis with the schedule of doxorubicin first producing the greatest synergy, with an isobole furthest away from the line of additivity (Figure 3.7G).

Therefore, doxorubicin produces synergistic effects in combination lapatinib in all three cell line investigated.

A

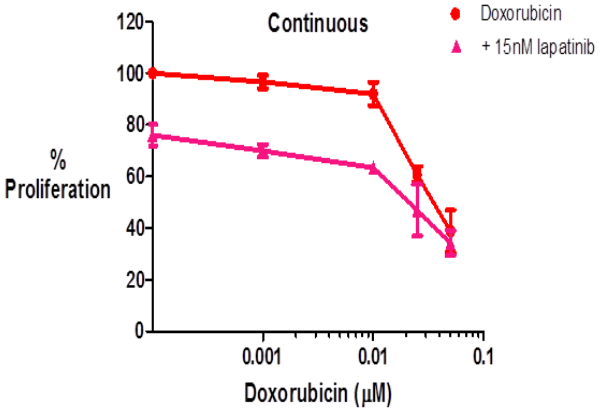

B

Continuous	
Doxorubicin (μM)	Combination index
0.001	0.45
0.01	0.66
0.025	0.60
0.05	0.61

C

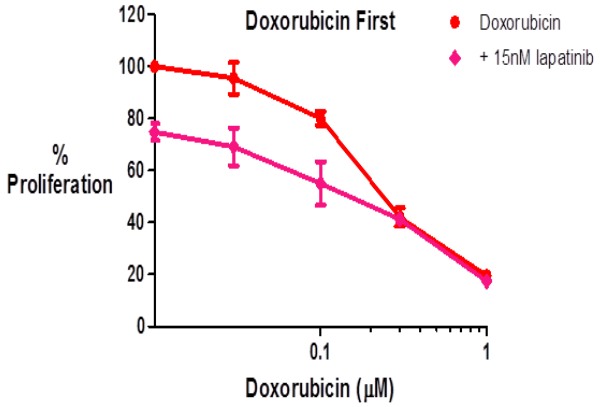

D

Doxorubicin First	
Doxorubicin (μM)	Combination index
0.03	0.58
0.1	0.60
0.3	0.89
1.0	1.07

E

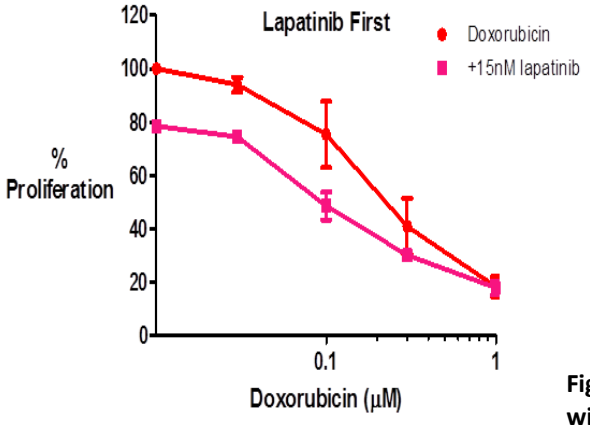

F

Lapatinib First	
Doxorubicin (μM)	Combination index
0.03	0.79
0.1	0.51
0.3	0.64
1.0	1.13

G

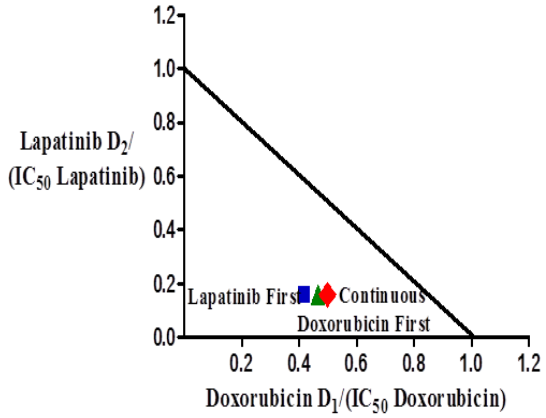

Figure 3.5 Doxorubicin in combination with lapatinib in the SK-Br-3 cell line

The SRB assay was used to assess the combination of lapatinib with doxorubicin compared to doxorubicin alone on cell proliferation over 96 hours. (A) continuous treatment with both drugs, (C) doxorubicin alone for two hours, then lapatinib or DFM (doxorubicin first), (E) lapatinib/DFM for 60 minutes, followed by doxorubicin± lapatinib for two hours, then lapatinib or DFM (lapatinib first),. Experiments were repeated three times and are presented as means ±SD. Combination index values for drug combinations (B, D and E) and isobologram (G).

A

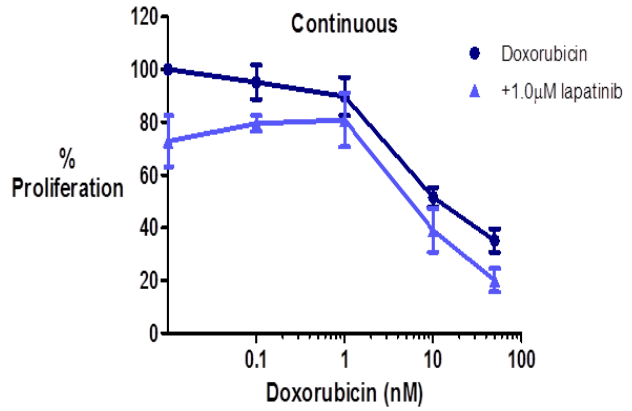

B

Continuous	
Doxorubicin (μM)	Combination index
0.0001	0.54
0.001	1.11
0.01	0.49
0.05	0.44

C

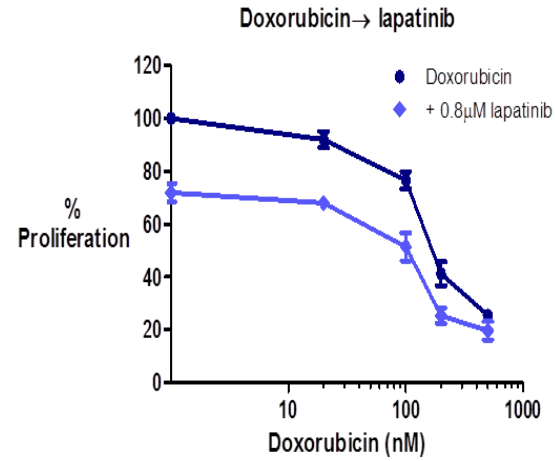

D

Lapatinib First	
Doxorubicin (μM)	Combination index
0.02	0.73
0.1	1.04
0.2	0.75
0.5	0.67

E

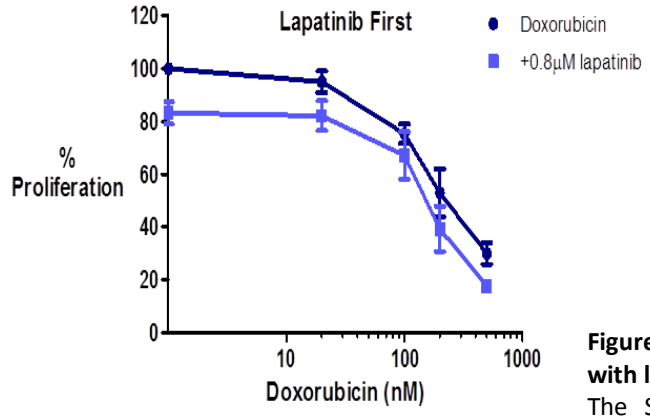

F

Doxorubicin First	
Doxorubicin (μM)	Combination index
0.02	0.50
0.1	0.75
0.2	0.52
0.5	0.86

G

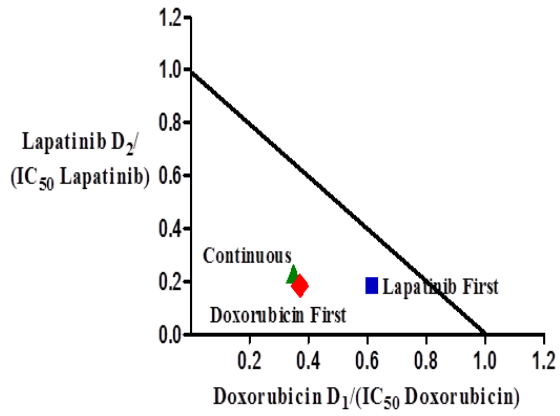

Figure 3.6 Doxorubicin in combination with lapatinib in the MDA-MB-468 cell line
The SRB assay was used to assess the combination of lapatinib with doxorubicin compared to doxorubicin alone on cell proliferation over 96 hours. (A) continuous treatment with both drugs, (C) doxorubicin alone for two hours, then lapatinib or DFM (Doxorubicin first), (E) lapatinib/DFM for 60 minutes, followed by doxorubicin± lapatinib for two hours, then lapatinib or DFM (lapatinib first). Experiments were repeated three times and are presented as means±SD. Combination index values for drug combinations (B, D and F). Normalised isobologram (G).

A

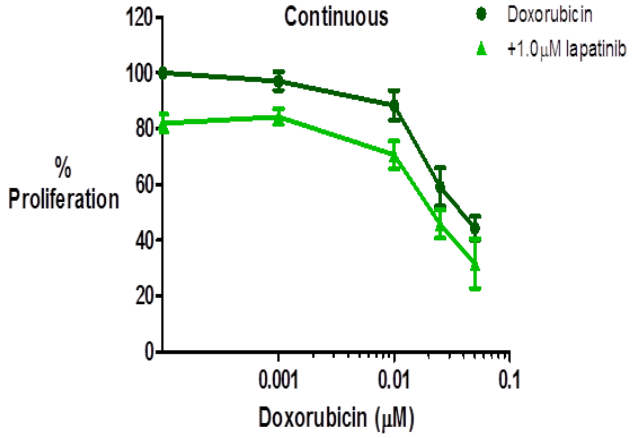

B

Continuous	
Doxorubicin (μM)	Combination index
0.001	1.04
0.01	0.98
0.025	0.63
0.05	0.58

C

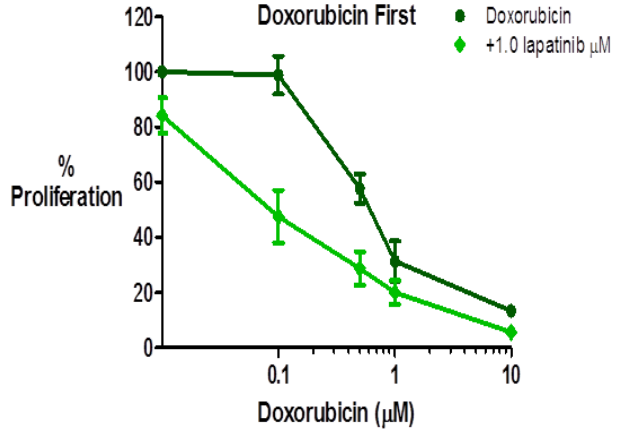

D

Doxorubicin First	
Doxorubicin (μM)	Combination index
0.1	0.26
0.5	0.29
1.0	0.34
10	0.95

E

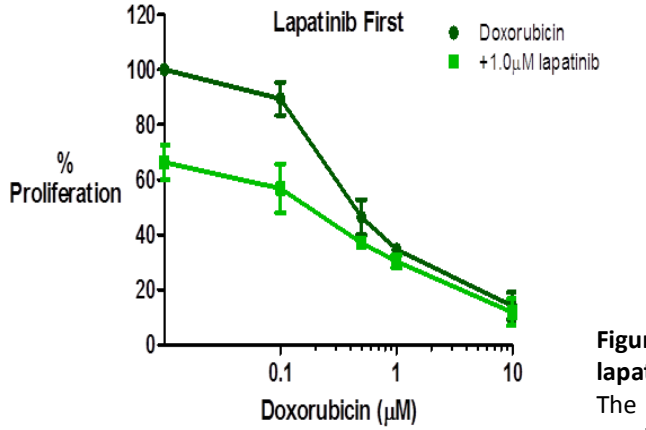

F

Lapatinib First	
Doxorubicin (μM)	Combination index
0.1	0.45
0.5	0.48
1.0	0.59
10	1.23

G

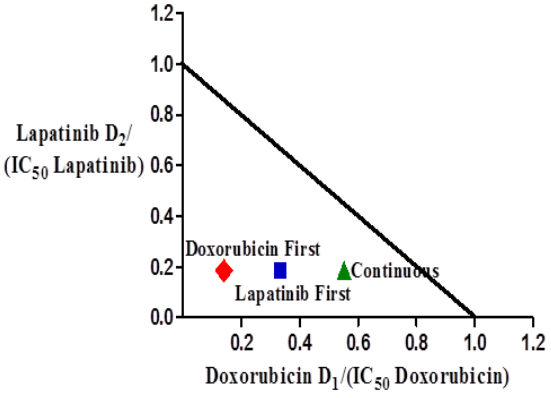

Figure 3.7 Doxorubicin in combination with lapatinib in the MCF-7 cell line

The SRB assay was used to assess the combination of lapatinib with doxorubicin compared to doxorubicin alone on cell proliferation over 96 hours. (A) continuous treatment with both drugs, (C) doxorubicin alone for 2 hours, then lapatinib or DFM (doxorubicin first), (E) lapatinib/DFM for 60 minutes, followed by doxorubicin± lapatinib for 2 hours, then lapatinib or DFM (lapatinib first). Experiments were repeated 3 times and data presented as mean±SD. Experiments were repeated three times and are presented as means ±SD. Combination index values for drug combinations (B, D and F). Normalised isobologram (G).

3.5.3 Lapatinib in combination with cisplatin

Lapatinib also exhibits schedule dependent effects on the inhibition of cell proliferation in combination with cisplatin in all three cell lines investigated, as demonstrated by both changes in combination indices and the shifting of isoboles (Figures 3.8, 3.9 and 3.10).

3.5.3.1 SK-Br-3 cell line

The greatest level of synergy is observed with the schedule of cisplatin first, with a lowest combination index of 0.25, indicating 'strong synergy' (Figures 3.8C and 3.8D). The schedule of lapatinib first produces 'slight synergism' at best with a combination index of 0.87, and 'moderate antagonism' at worst, with a combination index of 1.42 (Figure 3.8E). In a direct comparison between these two schedules, pre-treatment with lapatinib produces 'moderate antagonism' at 4 μM and 10 μM cisplatin (combination indices 1.36 and 1.42 respectively). This alters to synergy when cisplatin is given first (combination index 0.42 and 0.61). Isobologram analysis produces similar results with the greatest level of synergy observed with the schedule of cisplatin first and additive results with the schedule of lapatinib first (Figure 3.8G). Continuous treatment with both lapatinib and cisplatin produces an isobole which lies in between the effects observed with the other two treatment schedules (Figure 3.8G). Therefore, lapatinib in combination with cisplatin produces the greatest level of synergy when lapatinib exposure follows cisplatin treatment in SK-Br-3 cells.

3.5.3.2 MDA-MB-468 cell line

In the MDA-MB-468 cell line, continuous treatment with both lapatinib and cisplatin produces 'moderate antagonism/antagonism' at all cisplatin concentrations investigated as assessed by median effect analysis and the isobologram method at the IC_{50} concentration of cisplatin (Figures 3.9A, 3.9B and 3.9G). The schedules of lapatinib first, or cisplatin first, produce isoboles which lie next to each other on the isobologram (Figure 3.9G). At 0.5 μM and 5.0 μM cisplatin there are no differences between the combination indices produced by these two schedules (Figures 3.9C and 3.9E). This observation is dependent upon cisplatin concentration, as 'moderate synergy' is produced at 1.0 μM and 2.0 μM (combination indices 0.85 and 0.84 respectively), which changes to 'nearly additive' effects when lapatinib is given first

(combination indices 1.04 and 0.99 respectively) (Figures 3.9C and 3.9E). Therefore, in the MDA-MB-468 cell line, the greatest level of synergy is produced when lapatinib follows cisplatin treatment.

3.5.3.3 MCF-7 cell line

Like the MDA-MB-468 cell line, median effect analysis demonstrates that MCF-7 cells treated continuously with lapatinib and cisplatin produce 'nearly additive/moderate antagonism' at all cisplatin concentrations and an isobole which lies on the line of additivity (Figures 3.10A and 3.10G). A lesser degree of synergy is produced with the lapatinib first schedule compared with cells treated with cisplatin first, except at 100 µM (Figures 3.10C and 3.10E). For example, cisplatin 50 µM produces a combination index of 0.60 (indicating synergy) when cisplatin is given first, but 0.92 (near additivity) with the schedule of lapatinib first, an observation supported by the constructed isobologram with the greatest synergy observed with the schedule of cisplatin first (Figure 3.10G). Therefore, like the SK-Br-3 and MDA-MB-468 cell lines, the greatest synergy is observed when lapatinib follows cisplatin exposure.

These data are summarised in Table 3.2 and demonstrate that the effects of cisplatin on cell proliferation are schedule dependent in all three cell lines investigated, with the greatest impact of schedule observed in the SK-Br-3 cell line. Schedule exerts less influence in combination of lapatinib with doxorubicin, with all schedules demonstrating synergy.

	Continuous cisplatin + lapatinib	Cisplatin first → lapatinib	Lapatinib first → cisplatin	Continuous doxorubicin + lapatinib	Doxorubicin first → lapatinib	Lapatinib first → doxorubicin
SK-Br-3 Isobologram (CIX)	Synergy (0.50)	**Synergy (0.25)**	Additive (0.87)	**Synergy (0.45)**	Synergy (0.58)	Synergy (0.51)
MDA-MB-468 Isobologram (CIX)	Antagonism (1.34)	**Synergy (0.73)**	Synergy (0.75)	**Synergy (0.44)**	Synergy (0.73)	Synergy (0.50)
MCF-7 Isobologram (CIX)	Additive (0.93)	**Synergy (0.59)**	Synergy (0.75)	Synergy (0.58)	**Synergy (0.20)**	Synergy (0.45)

Table 3.2 Summary of the effect of lapatinib in combination cisplatin or doxorubicin
Description of the effect of lapatinib on the inhibition of cell proliferation by cisplatin or doxorubicin as determined by analysis by normalised isobologram. The lowest combination index (CIX) value as determined by median effect analysis is shown in brackets for each schedule, with the lowest value across the three schedules highlighted in bold.

A

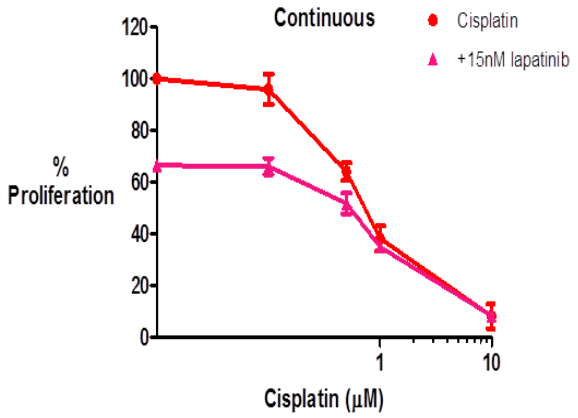

B

Continuous	
Cisplatin (µM)	Combination index
0.1	0.50
0.5	0.70
1.0	0.67
10.0	1.36

C

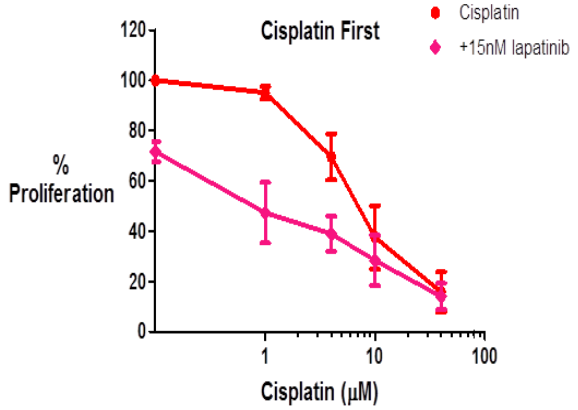

D

Cisplatin First	
Cisplatin (µM)	Combination index
1	0.25
4	0.42
10	0.61
40	1.13

E

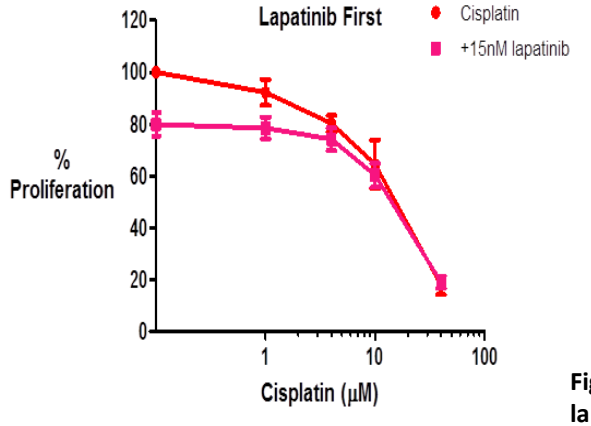

F

Lapatinib First	
Cisplatin (µM)	Combination index
1	0.93
4	1.36
10	1.42
40	0.87

G

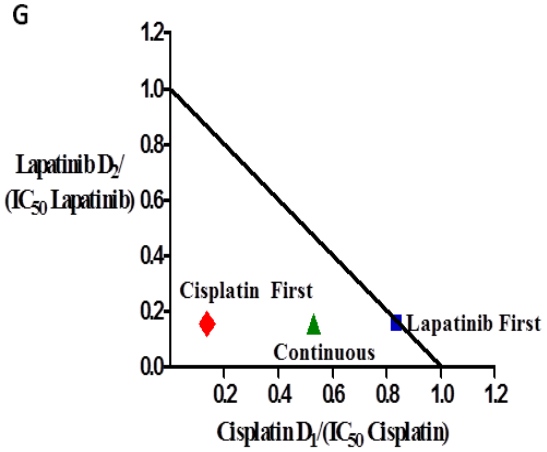

Figure 3.8 Cisplatin in combination with lapatinib in the SK-Br-3 cell line. The SRB assay was used to assess the combination of lapatinib with cisplatin compared to cisplatin alone on cell proliferation over 96 hours. (A) continuous treatment with both drugs, (C) cisplatin alone for two hours, then lapatinib or DFM (cisplatin first), (E) lapatinib/DFM for 60 minutes, followed by cisplatin± lapatinib for two hours, then lapatinib or DFM (lapatinib first) Experiments were repeated three times and are presented as means ±SD. Combination index values for drug combinations (B, D, F). Normalised Isobologram (G).

A

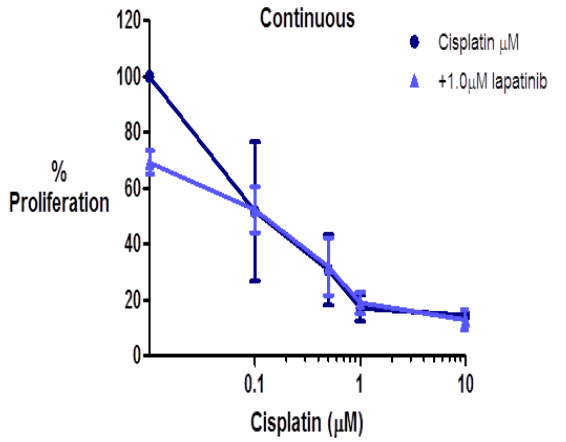

B

Continuous	
Cisplatin (μM)	Combination index
0.1	2.22
0.5	1.34
1.0	1.54
10	1.48

C

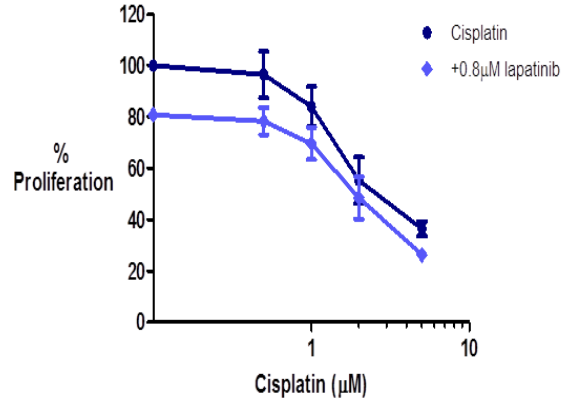

D

Cisplatin first	
Cisplatin (μM)	Combination index
0.5	0.73
1.0	0.85
2.0	0.84
5.0	1.04

E

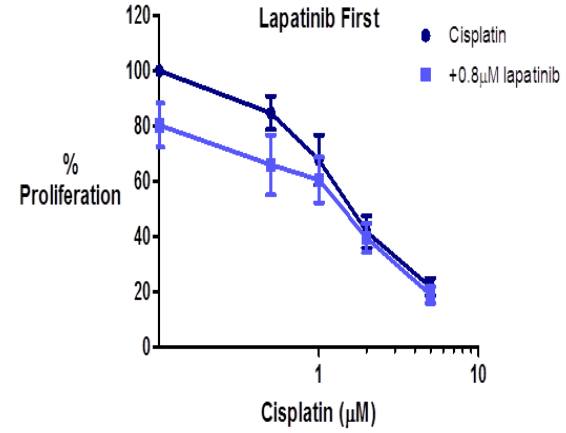

F

Lapatinib First	
Cisplatin (μM)	Combination index
0.5	0.75
1.0	1.04
2.0	0.99
5.0	1.04

G

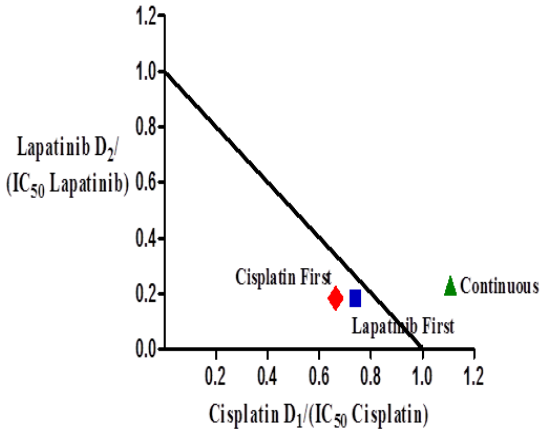

Figure 3.9 Cisplatin in combination with lapatinib in the MDA-MB-468 cell line. The SRB assay was used to assess the combination of lapatinib with cisplatin compared to cisplatin alone on cell proliferation over 96 hours. (A) continuous treatment with both drugs, (C) cisplatin alone for two hours, then lapatinib or DFM (cisplatin first), (E) lapatinib/DFM for 60 minutes, followed by cisplatin± lapatinib for two hours, then lapatinib or DFM (lapatinib first) Experiments were repeated three times and are presented as means ±SD. Combination index values for drug combinations (B, D and F). Normalised isobologram (G).

A

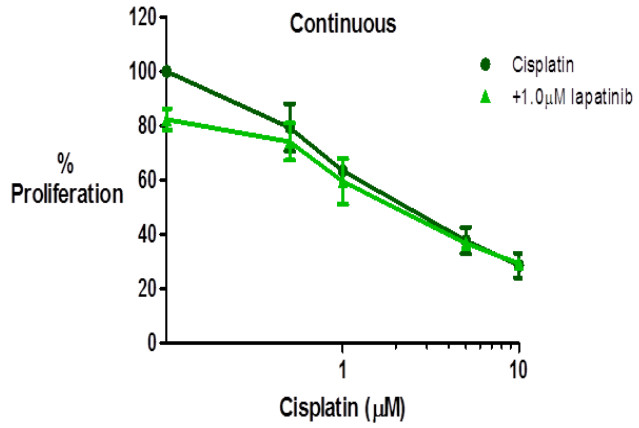

B

Continuous	
Cisplatin (μM)	Combination index
0.5	1.32
1.0	0.93
5.0	1.00
10.0	1.23

C

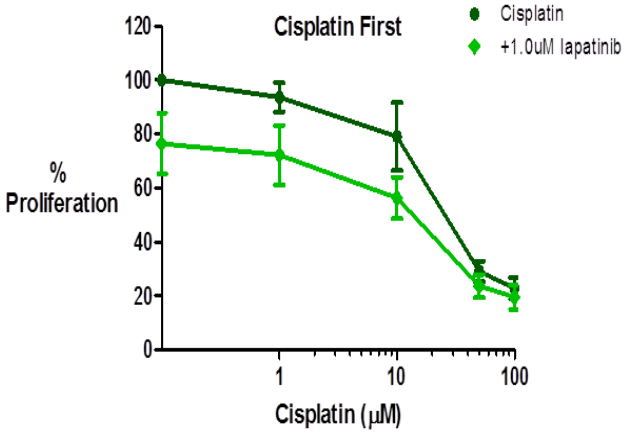

D

Cisplatin First	
Cisplatin (μM)	Combination index
1	0.59
10	0.77
50	0.60
100	0.86

E

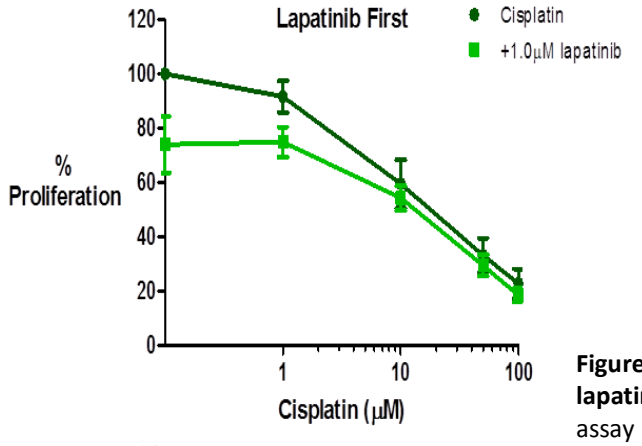

E

Lapatinib First	
Cisplatin (μM)	Combination index
1	0.75
10	0.87
50	0.92
100	0.81

E

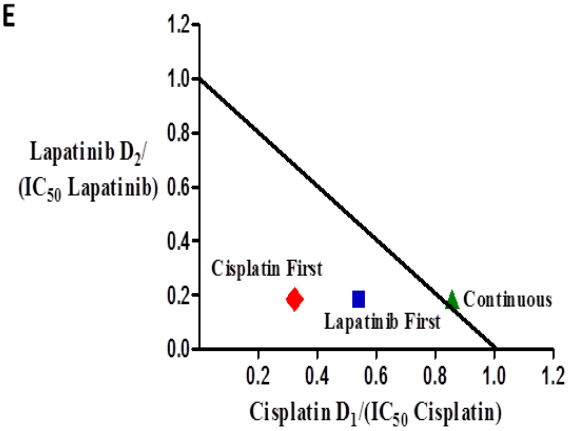

Figure 3.10 Cisplatin in combination with lapatinib in the MCF7 cell line. The SRB assay was used to assess the combination of lapatinib with cisplatin compared to cisplatin alone on cell proliferation over 96 hours. (A) continuous treatment with both drugs, (C) cisplatin alone for two hours, then lapatinib or DFM (cisplatin first), (E) lapatinib/DFM for 60 minutes, followed by cisplatin± lapatinib for two hours, then lapatinib or DFM (lapatinib first). Experiments were repeated three times and are presented as means ±SD. Combination Index values for drug combinations (B, D and F). Normalised isobologram (G).

3.6 DISCUSSION

This chapter describes experiments to investigate the effect of the dual EGFR and HER2 TKI lapatinib on cell proliferation, both as a single agent and in combination with cisplatin or doxorubicin, together with the impact of schedule on combination treatment.

3.6.1 Lapatinib inhibits cell proliferation in breast cancer cell lines

Lapatinib inhibits cell proliferation in all three breast cancer cell lines investigated. The HER2 over-expressing cell line SK-Br-3 was 54 times more sensitive to lapatinib, with an IC_{50} 0.10 μM, than the MCF-7 cell line with an IC_{50} 5.42 μM (Figure 3.2). The EGFR expressing cell line, MDA-MB-468 has an IC_{50} 3.38 μM. These results are in agreement with the published data which supports the determination of sensitivity to lapatinib by the level of expression of HER2 (Konecny *et al.*, 2006; Zhang *et al.*, 2008). The importance of HER2 and sensitivity to lapatinib is also supported by the observation that transfection of HER2 into low HER2 expressing breast cancer cell lines, significantly increases sensitivity to lapatinib. Conversely the knockdown of HER2 with siRNA in HER2 over-expressing cell lines, confers resistance (Konecny *et al.*, 2006; Zhang *et al.*, 2008). In the presence of over-expressed HER2, EGFR plays little role in conferring sensitivity to lapatinib, with knockdown of EGFR in the BT474 and SK-Br-3 breast cancer cell lines, not altering sensitivity to lapatinib (Zhang *et al.*, 2008).

3.6.2 Synergy between lapatinib and DNA interactive agents

The interaction between lapatinib and the two chemotherapy drugs investigated was assessed using the median effect and isobologram methods. Lapatinib produces synergy in combination with doxorubicin and cisplatin, in all cell lines, though the degree is schedule dependent (Table 3.2). In the experiments described in this chapter, the best method of comparing the effect of the addition of lapatinib to chemotherapy across all schedules, is to use the normalised isobologram. We constructed an IC_{50} isobologram which examined the effect on the IC_{50} of the cytotoxic drug under investigation, of the addition of lapatinib.

Lapatinib in combination with cisplatin demonstrates clear schedule dependence when combined with cisplatin in the SK-Br-3 cell line, with the schedule of cisplatin first

producing the greatest level of synergy, and lapatinib pre-treatment prior to cisplatin producing additive results (Figure 3.8). Schedule is also important in the MDA-MB-468 cell line, with continuous treatment with cisplatin and lapatinib producing antagonism at all concentrations investigated as assessed by both median effect analysis and using the isobologram (Figure 3.9); this is not observed in the other schedules. In the MCF-7 cell line, continuous treatment with cisplatin and lapatinib produced additive effects on the inhibition of cell proliferation (Figure 3.10). The schedule of cisplatin followed by lapatinib produced more synergy than when lapatinib was given prior to and during cisplatin treatment.

Schedule is less important when lapatinib is combined with doxorubicin with synergy seen in all schedules as assessed using median effect analysis and all isoboles lie below the line of additivity, in all cell lines and all schedules. The most marked influence of schedule was seen in the MCF-7 cell line, with doxorubicin followed by lapatinib producing strong synergy when compared to doxorubicin alone (Figure 3.7).

Synergy has been shown by others using *in vitro* models (Table 3.3). Budman *et al.* examined the combination of the dual EGFR and HER2 TKI, GW282974X in combination with chemotherapy drugs continuously, using median effect analysis and the calculation of combination indices (Budman *et al.*, 2006). They demonstrated synergy with deoxy-5-fluorouridine (5'-DFUR), an active metabolite of capecitabine, in the three breast cancer cell lines MCF-7, SK-Br-3 and BT474. In combination with epirubicin, GW282974X produced synergy in the SK-Br-3 cell line only with a combination index of 0.5, where as in BT474 cells, which also over-expresses HER2, additivity was produced (combination index 1.1), and antagonism in the MCF-7 cell line (combination index 1.7) (Budman *et al.*, 2006).

Coley *et al*. have also demonstrated synergy using median effect analysis in the ovarian cancer cell line PEO1, with the combination of GW282974A (EGFR and HER2 TKI) and paclitaxel (Coley *et al.*, 2006). In combination with cisplatin, results were additive or antagonistic (Coley *et al.*, 2006). Lapatinib also produces additive results in combination with carboplatin and additive or synergistic results in combination with paclitaxel, docetaxel and doxorubicin in endometrial cancer cell lines (Konecny *et al.*,

2008). Kim *et al.* have shown synergy with a continuous combination of lapatinib with 5-FU, cisplatin, paclitaxel and oxaliplatin in two gastric cancer cell lines, also using median effect analysis (Kim *et al.*, 2008b). Schedule was found to be important in combination with 5-FU, cisplatin and paclitaxel, but not with oxaliplatin, with the schedule of cisplatin or 5-FU followed by lapatinib producing the highest degree of synergy (Kim *et al.*, 2008b).

	Cell Lines (Lapatinib IC_{50} - µM)	Chemotherapy	Combination index level	Drug concentrations
Kim *et al, 2008*	Gastric cancer SNU-216 (0.02) NCI-N87 (0.01)	5-FU, oxaliplatin, cisplatin paclitaxel	FA_{50}	0.1, 1, 3, 9, and 27XIC_{50} lapatinib/ chemotherapy
Coley *et al, 2006*	Ovarian Cancer PEO1 PEOTaxR PEOCarboR	Cisplatin Paclitaxel	Across all FA plus simulation	Lapatinib analogue GW282974A No concentrations given
Konecny *et al, 2006*	Endometrial Cancer USPC1 (0.61) USPC2 (0.05) RL-95-1 (0.93) HEC155 (0.79)	Carboplatin Paclitaxel Doxorubicin Docetaxel	Mean of all FA values.	Lapatinib concentration; USPC1 &2 cell lines-0.031-1.0µM RL-95-1 and HEC155 cell lines-0.31-10µM
Budman *et al, 2006*	Breast cancer BT474 (4.8) MCF7/wt (7.6) MCF7/adr (6.8) SK-Br-3 (0.6)	Docetaxel 5-FU 5'DFUR Epirubicin Gemcitabine	FA_{50}	Lapatinib analogue GW282974X lapatinib/ chemotherapy-0.03125N-8N N= value around IC_{50}
Komoto et al, 2009	Pancreatic cancer MiaPaca-2 PANC-1 Capan-1 Capan-2	S-1 components	Full range FA results plus simulation	4, 2, 1, 0.5, 0.25 and 0.125X 2.5µM lapatinib

Table 3.3 Lapatinib and chemotherapy combination studies.
All studies used median effect analysis in a constant ratio design. IC_{50} values for lapatinib as single agent are given where published. The combination index level is the fraction affected (FA) level at which the drug combinations were assessed.

3.6.3 Problems with *in vitro* drug combination experiments

The studies described above all use a constant ratio design, whereas the experiments presented in this chapter use a non-constant ratio design. A constant ratio experiment,

differs from a non-constant experiment in that the concentration of lapatinib increases in line with the increasing concentration of cytotoxic drug; thereby maintaining the ratio of the two drugs to each other. The studies by Kim *et al*. and Budman *et al*. utilise a combination of EGFR and HER2 TKIs with chemotherapy drugs at their IC_{50} concentrations and Coley *et al.*, a ratio of chemotherapy to lapatinib of 1:1.25 (Budman *et al.*, 2006; Coley *et al.*, 2006; Kim *et al.*, 2008b). This is achieved by serially diluting a solution containing both drugs at four times the desired concentrations by 2, 1, 0.5, 0.25 and 0.125 fold, to give a concentration range. This design is recommended for use with median effect analysis, as it allows the software to undertake mathematical modelling to simulate the interaction across the entire range of drug concentrations investigated. This cannot be done with a non-constant ratio design experiment (Chou, 2010). This is important as the ratio of the two drugs to each other influences the results of any analysis and Chou *et al.* recommend investigating different ratios. This is especially important when investigating drugs in cell lines which are very sensitive, as drug concentrations may lie well below clinically relevant levels (Chou, 2010).

The SK-Br-3 cell line is highly sensitive to lapatinib with inhibition of proliferation occurring with concentrations as low as 10 nM (Figure 3.2). At this concentration HER2 and AKT phosphorylation are only partially reduced by lapatinib and concentrations closer to 50 nM are required to inhibit signalling (Amin *et al.*, 2010). The inhibition of nuclear translocation of EGFR and HER2 by lapatinib has been demonstrated in the gastric cell line SNU-216 (Kim *et al.*, 2008c). This cell line is also highly sensitive to lapatinib with an IC_{50} of 20 nM, though concentrations of both 0.1 µM and 1 µM lapatinib are used to demonstrate inhibition of HER2 nuclear translocation (Kim *et al.*, 2009). Nuclear EGFR was also reduced, but the reduction was greater with 1.0 µM than with 0.1 µM of lapatinib (Kim *et al.*, 2009). These observations are important when considering the experiments presented in this chapter and the SK-Br-3 cell line, when an IC_{20} concentration of lapatinib of 15 nM was used. Whilst synergistic effects were obtained in combination with either doxorubicin or cisplatin, these may have been underestimated as a concentration of 15 nM lapatinib does not fully inhibit HER2 (Amin *et al.*, 2010). Additionally this is not a concentration where the translocation of HER2 to the nucleus, which may be important in DNA repair, has been observed (Kim

et al., 2009). A constant ratio designed experiment could have solved this problem, as the concentration of lapatinib changes in line with the cytotoxic drug under investigation; so combination points where the lapatinib concentration was greater than 0.1 μM or more clinically relevant could have been examined specifically.

Examining the published combination studies discussed above, it can be noted that the study by Kim *et al* only presents combination index values at the IC_{50} combination, when the lapatinib concentration was 0.01 or 0.02 μM (Table 3.3) (Kim *et al.*, 2008b). Coley *et al*. and Komoto *et al*. present the combination indices for all points investigated, plus the graphical simulation, but do not publish the IC_{50} values for lapatinib alone, so the actual concentration of lapatinib investigated cannot be ascertained (Coley *et al.*, 2006; Komoto *et al.*, 2009b). This is important as in both studies, some drug combinations showed increasing antagonism with increasing drug concentration. Konency *et al.* present the mean of the combination index values across different concentration. Whilst this is an acceptable method as suggested by Chou *et al.* it prevents assessment as to whether the interaction between lapatinib and chemotherapy alters with increasing concentrations of both drugs (Chou, 2006).

An alternative design would be to utilise concentrations of lapatinib known to fully affect protein function for short periods of time, then to allow cell growth for the desired duration. For example, 1 μM lapatinib for one hour prior to, in combination with or after chemotherapy. The clonogenic assay, which measures the number of cell colonies formed following exposure to different drugs and combinations, can also be used. We tried this technique, and whilst the cell lines used are reported to form colonies, we were unable to achieve this over the time period required.

Whilst cell based assays may be able to ascertain drug combinations and schedules of interest, they are unable to isolate the mechanisms through which their effects occur. Identification of the key pathways inhibited by lapatinib to produce synergy or antagonism could be achieved using siRNA libraries to target specific proteins or entire pathways, such as those involved in EGFR and HER2 signalling or DNA repair including PI3K-AKT, Ras-Raf-MAPK, HER3, DNA-PK, ERCC1 and RAD51. This would allow a comparison between lapatinib and chemotherapy combinations in wild type and

transfected cell lines. The role of HER2 in the inhibition of cell proliferation by cytotoxic agents could also be investigated using this approach, though this would also result in the reduced expression of HER2. Lapatinib does not reduce the expression of HER2 (Konecny *et al.*, 2006), but inhibits its phosphorylation. The importance of the inhibition of HER2 phosphorylation by lapatinib in the production of synergy in combination with cytotoxic drugs, could be investigated by the creation and transfection of a HER2 which cannot be phosphorylated, into a non-HER2 expressing cell line and comparing the inhibition of cell proliferation by chemotherapy drugs with the same cell line transfected with a fully functioning HER2.

3.7 CONCLUSIONS

Lapatinib inhibits cell proliferation in breast cancer cell lines, with sensitivity determined by the level of expression of HER2. Cells that express low levels of EGFR or HER2 are also sensitive to lapatinib, indicating that the targeting of HER2 is not the sole mechanism through which lapatinib produces its effects.

Lapatinib produces synergistic effects in combination with both cisplatin and doxorubicin, though the degree of synergy is affected by the scheduling of lapatinib. Overall the schedule of chemotherapy first, followed by lapatinib proves to be the most effective at producing synergy, when schedule is important. Cell based assays provide a high throughput method of assessing drug combinations *in vitro*, but fail to identify mechanisms through which these effects are mediated. When using targeted drugs, drug concentration may be important if different cellular effects are produced by different drug concentrations. This should be considered when using highly sensitive cell lines when very low concentrations of targeted drugs are used and it may be necessary to expose cells to higher concentrations of targeted agent, for shorter periods of time to allow the investigation of targeted agents at clinically relevant concentrations.

Investigation into influence of duration of exposure to lapatinib or gefitinib on the cellular effects of DNA damaging agents

4.1 INTRODUCTION

The results presented in Chapter Three demonstrate that lapatinib can synergise with doxorubicin and cisplatin in a schedule dependent manner. Gefitinib in combination with chemotherapy produces similar results *in vitro* (Milano *et al.*, 2008; Solit *et al.*, 2005; Xu *et al.*, 2003). Despite this, such combinations have failed to demonstrate a clinical benefit in phase III trials in lung cancer (Giaccone *et al.*, 2004; Herbst *et al.*, 2004; Herbst *et al.*, 2005; Ready *et al.*, 2010). As discussed in Chapter Three, schedule may be important in mediating synergy between HER targeted TKIs and DNA damaging agents. One possible explanation for this is the reactivation of PI3K/AKT signalling following continued exposure to TKIs and its effect on promoting DNA repair.

4.1.1 HER3 mediated resistance to small molecule tyrosine kinase inhibitors

HER3 is a potent activator of the PI3K/AKT signalling pathway through dimerisation with either EGFR or HER2 and inhibition of either receptor by TKIs leads to inhibition of both HER3 and the PI3K/AKT signalling (Amin *et al.*, 2010; Campbell *et al.*, 2010; Kong *et al.*, 2008). This inhibition is short lived, with phosphorylated HER3 and AKT detectable at 48 hours, despite continued EGFR and HER2 inhibition (Amin *et al.*, 2010; Campbell *et al.*, 2010; Kong *et al.*, 2008; Sergina *et al.*, 2007). This process is driven by the initial inhibition of AKT phosphorylation which leads to an increase in HER3 expression, which is subsequently phosphorylated. In addition to this pathway, increased HER2 expression occurs through TKI induced inhibition of receptor ubiquitination, reducing receptor degradation (Scaltriti *et al.*, 2009) (Figure 4.1).

The initial inhibition of AKT phosphorylation by TKI, reduces the phosphorylation of the FOXO transcription factors, resulting in their transport back into the nucleus where they activate the HER3 promoter, increasing HER3 transcription and hence expression (Amin *et al.*, 2010; Chandarlapaty *et al.*, 2011). This process of negative feedback resulting from the initial inhibition of HER3 and hence AKT phosphorylation is

demonstrated in cells transfected with a 4-hydroxy tamoxifen inducible AKT. The induction of AKT phosphorylation by tamoxifen in these cells reduces HER3 expression and also reduces the degree of increase in HER3 expression induced by lapatinib (Amin *et al.*, 2010). In addition, the use of AKT inhibitors increases the expression and phosphorylation of HER3 (Chandarlapaty *et al.*, 2011). These data demonstrate the regulation of HER3 expression by AKT phosphorylation.

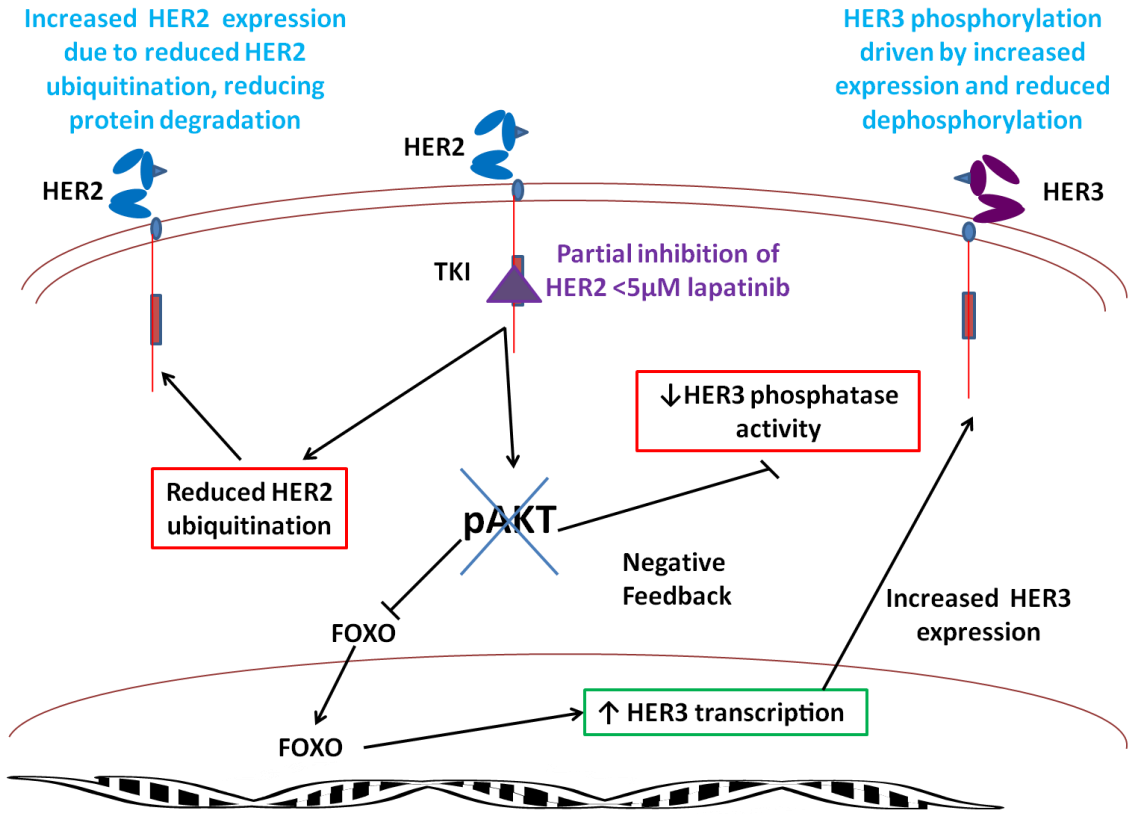

Figure 4.1 Diagram of the proposed mechanism through which HER3 and AKT signalling are reactivated in response to lapatinib concentrations of less than 5 μM
Inhibition of HER2 phosphorylation by lapatinib inhibits the phosphorylation of HER3 and the phosphorylation of AKT initially. This increases transcription of HER3 due to transport of the FOXO transcription factor back into the nucleus. FOXO activated the HER3 promoter leading to increased HER3 expression. In addition, the inhibition of AKT inhibits HER3 phosphatases reducing receptor dephosphorylation as described by Amin *et al*., 2010. HER2 expression is increased due to reduced protein ubiquitination as described by Scaltriti *et al*., 2009. This increases the formation of HER2-HER3 dimers, which when phosphorylated activate AKT signalling.

The increase in expression of HER2 and HER3 drives the formation of HER2-HER3 dimers (Amin *et al.*, 2010; Chandarlapaty *et al.*, 2011; Scaltriti *et al.*, 2009). The mechanism through which the newly produced HER3 proteins are phosphorylated in the presence of continued TKI appears to be dependent upon TKI concentration and whether HER2 function is fully inhibited. Under conditions where only partial or no HER2 kinase inhibition occurs (for example ≤1μM gefitinib), the TKIs gefitinib and AG1478 induce the autocrine release of the HER3 and HER4 ligands, betacellulin and heregulin (Kong *et al.*, 2008). This stimulates the formation of HER2/HER3 and HER3/HER4 dimers thereby negating the effect of low concentrations of TKIs on the inhibition of cell proliferation (Kong *et al.*, 2008).

Higher concentrations of gefitinib (for example 5 μM), induce a forward shift in the dephosphorylation-phosphorylation equilibrium of HER3. This results in an increase in the steady state phosphorylation of HER3, with activation of the PI3K/AKT signalling pathway observed following 48 hours of continuous exposure to gefitinib (Sergina *et al.*, 2007). This process is dependent upon HER2, with the knockdown of HER2 preventing the HER3 phosphorylation (Sergina *et al.*, 2007).

The phosphorylation of HER3 is dependent upon the residual kinase activity of HER2 as the knockdown of HER2 prevents HER3 reactivation (Sergina *et al.*, 2007). High concentrations of lapatinib (≥5 μM) or erlotinib (≥40 μM) prevents the reactivation of HER3 and PI3K/AKT, which is thought to be due to the complete inhibition of HER2 kinase activity (Amin *et al.*, 2010). Another mechanism of HER3 activation is phosphorylation by MET (Engelman *et al.*, 2007) and HER3 may not be completely devoid of kinase activity, able to autophosphorylate though at a lower level than that observed when dimerised with EGFR or HER2 (Di Leo *et al.*).

4.2 AIMS

The reactivation of AKT signalling during prolonged exposure to TKI may explain why combinations of TKIs with DNA damaging agents have also not always translated into the clinical setting, especially as AKT plays a key role in the cellular response to DNA damage as discussed in Chapter One section 1.8.5.1 The results presented in this chapter examine whether the induction and repair of DNA lesions is affected by the duration of exposure to the TKI gefitinib and lapatinib with the following aims:

1. Does continued exposure to lapatinib result in **activation** of HER3 and AKT signalling?
2. Does the duration of exposure to either gefitinib or lapatinib affect the **induction** of DNA lesions produced by Topo IIα poisons, platinum or ionising radiation?
3. Does the duration of exposure to TKI alter the **repair** of DNA lesion induced by Topo IIα poisons, platinum or ionising radiation?
4. Does the duration of exposure to TKI alter the **cytotoxicity** of the chemotherapy agents under investigation?

4.3 DOES THE DURATION OF EXPOSURE TO LAPATINIB ALTER HER3 AND AKT SIGNALLING?

Experiments were carried out in the SK-Br-3 breast cancer cell line as used by Sergina *et al.* They were the first to report the reactivation of HER3 and AKT signalling despite initial inhibition, with continued exposure to gefitinib for 48 hours (Sergina *et al.*, 2007). Initial experiments ascertained a suitable concentration of lapatinib to be investigated. Gefitinib was used at a concentration of 5 µM, as used in the experiments conducted by Sergina *et al.* (Sergina *et al.*, 2007). Cells were treated with either gefitinib or lapatinib for one hour or continuously for 48 hours, with drug replacement at 23 and 47 hours. Replacement of TKI is required as without, HER3 signalling can be detected at 18 hours (Figure 4.2). Drug replacement at 23 hours initially reduces the level of phosphorylated HER3 detected but replacement at 47 hours has a lesser effect and by 72 hours, replacement of gefitinib has no effect.

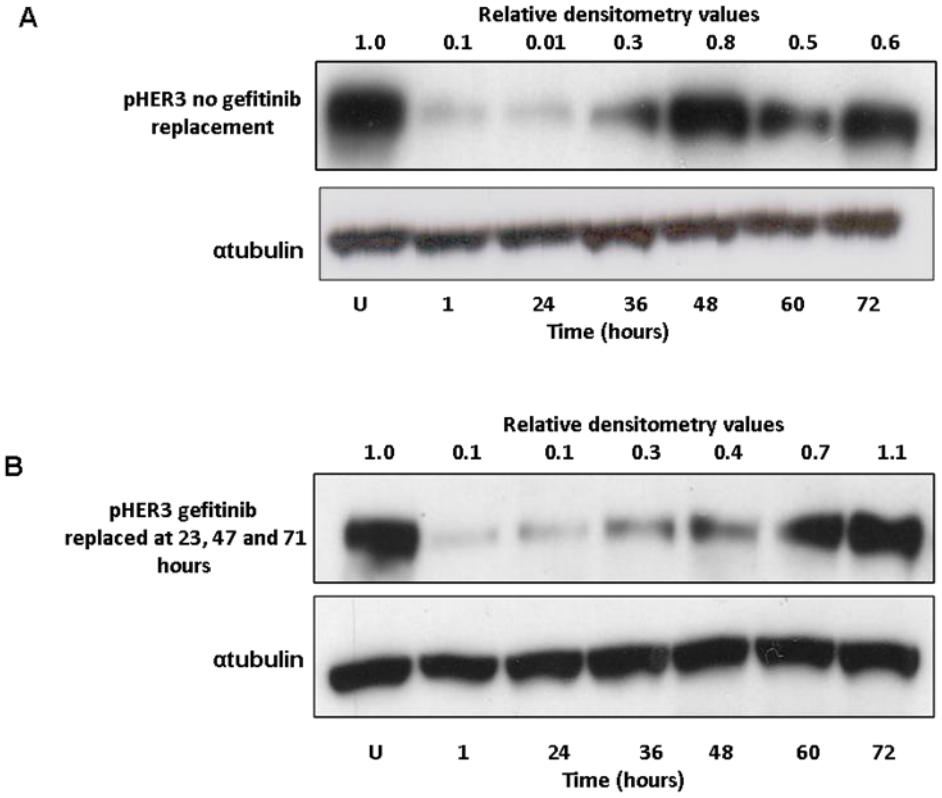

Figure 4.2 Effect of gefitinib replacement on HER3 phosphorylation
The effect of gefitinib replacement on HER3 phosphorylation was assessed in the SK-Br-3 cell line using Western blotting. (A) Cells were treated with 5 µM gefitinib as indicated without drug replacement, (B) gefitinib was replaced at 23, 47 and 71 hours following which cells were lysed and immunoblotted with anti-pHER3. Relative densitometry values are provided to allow comparison of each time point. α tubulin is used as a loading control. Figure representative of two independent experiments.

4.3.1 Inhibition of HER signalling by lapatinib

Lapatinib 0.1 μM reduces HER2 and HER3 phosphorylation with none detectable at concentrations higher than 1.0 μM (Figure 4.3). EGFR is less sensitive, with a reduction in receptor phosphorylation detected at concentrations above 2 μM. A concentration of lapatinib of 2 μM was chosen for further investigation as this inhibits the phosphorylation of EGFR, HER2 and HER3 and is clinically relevant (Lapatinib C_{min} 1.9μM and C_{max} 3.5μM for lapatinib 900mg BD) (Burris *et al.*, 2009).

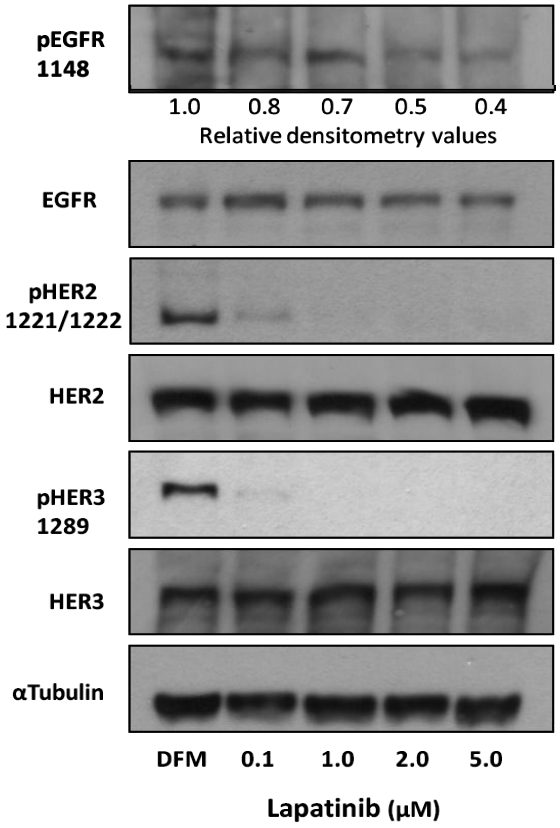

Figure 4.3 Inhibition of HER signalling lapatinib
The effect of lapatinib 0.1- 5.0 μM on EGFR, HER2 and HER3 signalling was assessed in the SK-Br-3 cell line using Western blotting. Cells were treated with the indicated concentration of lapatinib for one hour then lysed and immunoblotted as indicated. α tubulin is used as a loading control. Figure representative of two independent experiments.

4.3.2 The effect of gefitinib and lapatinib on cell viability

The trypan blue assay was used to assess cell viability to ensure that 2 μM lapatinib was a suitable comparison to 5 μM gefitinib (Figure 4.4). Continued treatment with either gefitinib or lapatinib produced a 12±1.4% and 16±1.4% fall in cell viability respectively, compared with untreated cells (98±0.5% for untreated or cells exposed to TKI for one hour, 86±1.4% with exposure to gefitinib for 48 hours and 84±1.4% with

lapatinib, P<0.001). There were no differences in cell viability between gefitinib or lapatinib for 48 hours, confirming 2 µM lapatinib as a suitable comparison to 5 µM gefitinib (Figure 4.4).

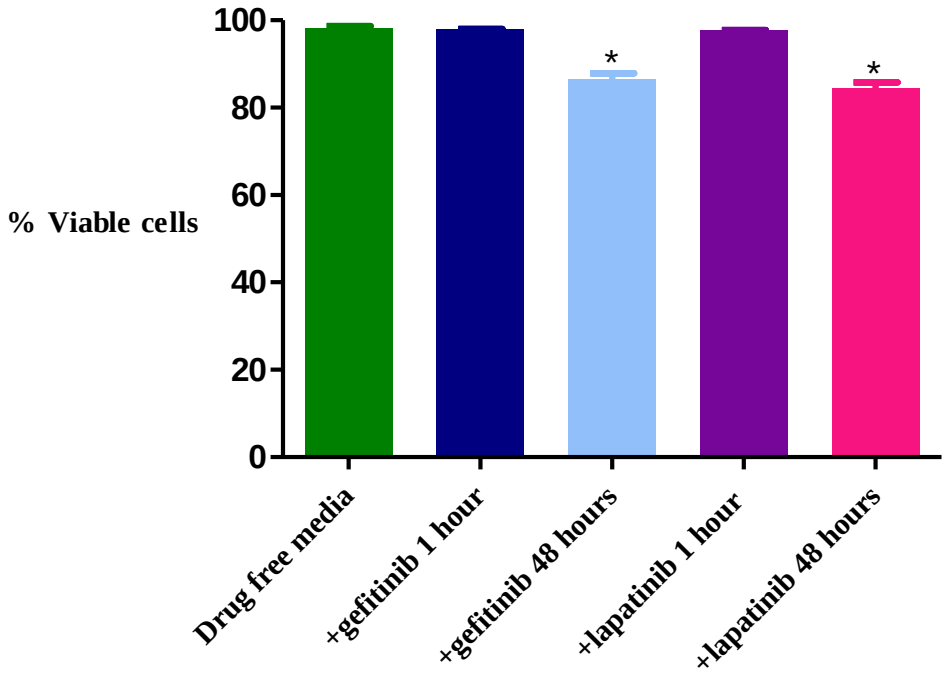

Figure 4.4 Effect of gefitinib and lapatinib exposure on cell viability
Cell viability was assessed using trypan blue to identify dead cells. Cells were pre-treated with either drug free media (■), gefitinib 5 µM for 1 hour (■), lapatinib 2 µM for 1 hour (■), gefitinib 5 µM for 48 hours (■), lapatinib 2 µM for 48 hours (■). Cell suspension was mixed with an equal volume of 0.4% trypan blue and cells counted using haemocytometer four separate times. Data are presented as the mean ±SEM of three experiments. * P< 0.001 compared with the drug free media.

4.3.3 The effect of exposure to gefitinib or lapatinib for 48 hours on HER signalling

The effect of duration of exposure to lapatinib or gefitinib on EGFR, HER2, HER3, AKT and MAPK signalling pathways was assessed by Western blotting. Gefitinib 5 µM inhibits the phosphorylation HER3, AKT and MAPK within an hour (Figure 4.5A). Despite replacement of gefitinib at 23 and 47 hours, HER3 and AKT phosphorylation can be detected at 48 hours, together with phosphorylated MAPK at a lower level (Figure 4.5A).

Like gefitinib, lapatinib 2 µM inhibits the phosphorylation of HER3, AKT and MAPK signalling within one hour. Both AKT and MAPK signalling can be detected following

continuous exposure to lapatinib for 48 hours, though the level of AKT signalling is less than that observed with gefitinib, only detected following prolonged blot exposure (Figure 4.5B). Unlike with continuous exposure to gefitinib, HER3 signalling can be barely detected following 48 hours exposure to lapatinib.

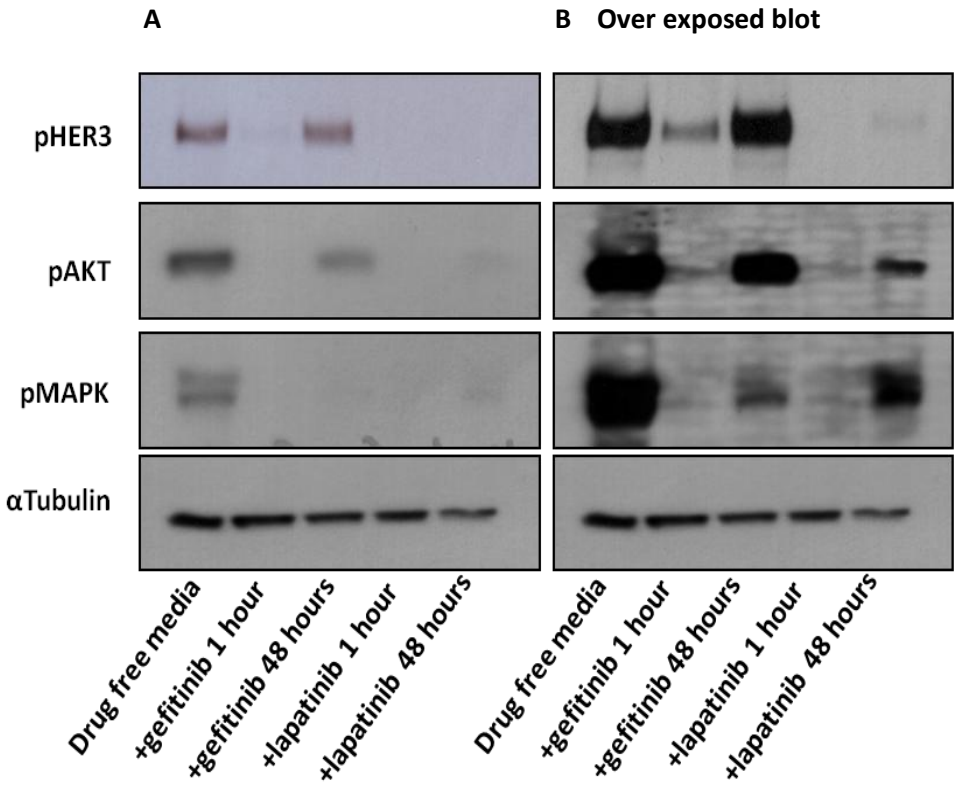

Figure 4.5 Effect of duration of exposure to gefitinib and lapatinib on HER3, AKT and MAPK signalling

The effect of duration of exposure to TKI on HER, AKT and MAPK signalling was investigated in the SK-Br-3 cells by Western blotting. Cells were treated with gefitinib 5 µM or lapatinib 2 µM as indicated for 1 or 48 hours, with replacement of TKI at 23 and 47 hours. Cells were then collected, lysed and immunoblotted as indicated. (B) An over-exposed blot is shown to allow the proteins with lower expression to be visualised. Figure is representative of three independent experiments.

4.4 DOES DURATION OF EXPOSURE TO GEFITINIB OR LAPATINIB ALTER THE INDUCTION OF DNA DAMAGING LESIONS?

As discussed in Chapter One section 1.8.5.1, the PI3K/AKT signalling pathway is involved in the regulation of cell proliferation and can promote resistance to cytotoxic drugs. Having established that this signalling pathway is initially inhibited by gefitinib and lapatinib but then reactivated, we wished to examine whether there are differences in the induction and repair of DNA lesions in cells treated for one or 48

hours with these drugs. DNA damaging agents which induce a variety of different DNA lesions were investigated. Cisplatin was used as inducer of intra and interstrand crosslinks and IR, etoposide and doxorubicin as inducers of DNA single and double strand breaks.

4.4.1 The Induction of interstrand crosslinks by cisplatin

Cells were treated with TKI for one or 48 hours prior to exposure to cisplatin (50 µM) for two hours and collected for analysis nine hours after the removal of cisplatin. This time point was chosen due to data from our laboratory which has demonstrated this is when the formation of crosslinks peaks (Clingen *et al.*, 2008; Friedmann *et al.*, 2004). This concentration of cisplatin was chosen as it produces detectable interstrand crosslinks and is a clinically relevant concentration (Go and Adjei, 1999). Following treatment, and immediately before analysis, cells were irradiated (15 Gy) to deliver a fixed number of DNA strand breaks which could be detected using the alkaline Comet assay as a Comet tail. The presence of an interstrand crosslink retards the migration of IR-induced DNA strand breaks, shortening the Comet tail in comparison to an untreated irradiated control. The difference in tail moment between untreated controls and cisplatin treated samples can be calculated as a percentage reduction compared with the control. Increases in the percentage reduction of the Comet tail, indicates the presence of a greater number of interstrand crosslinks.

Cisplatin-induces interstrand crosslinks with a reduction in tail moment of 48.9±6.2%. Exposure to either gefitinib or lapatinib for one hour produces a non-significant increase in the induction of lesions, with a reduction in tail moment of 63.4±4.9% and 62.4±1.2% respectively ($p>0.05$) (Figure 4.6). Continued exposure to either TKI for 48 hours has no significant effect on the induction of interstrand crosslinks with a reduction in tail moment of 45.4±5.3% with gefitinib and 66.8±2.1% with lapatinib ($p>0.05$). Significantly fewer interstrand crosslinks are produced in cells treated with gefitinib for 48 hours compared with cells treated with lapatinib for the same duration (% reduction in tail moment 45.4±5.3% vs. 66.8±2.1 % $p\leq 0.05$). These data indicate that the number of interstrand crosslinks induced by cisplatin is not significantly altered by either gefitinib or lapatinib or the duration of exposure to these drugs.

However, fewer lesions are induced in cells treated with gefitinib for 48 hours compared with cells treated with lapatinib for 48 hours.

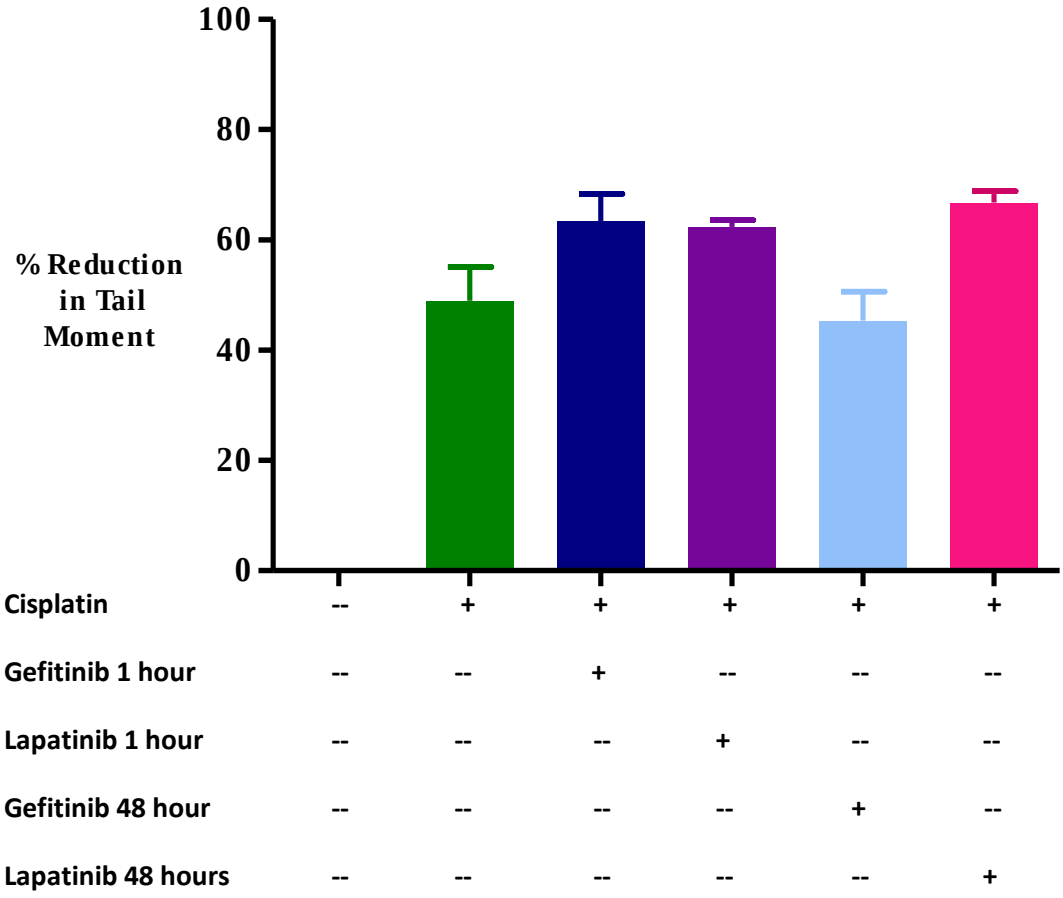

Figure 4.6 Effect of duration of exposure to gefitinib or lapatinib on the induction of interstrand crosslinks by cisplatin.
The modified alkaline comet assay was used to assess the induction of interstrand crosslinks by cisplatin in the SK-Br-3 cell line. Cells were pre-treated with either drug free media (■), gefitinib 5 µM for 1 hour (■), lapatinib 2 µM for 1 hour (■), gefitinib 5 µM for 48 hours (■), lapatinib 2 µM for 48 hours (■), before exposure to cisplatin (50 µM), After two hours the media was replaced with DFM or media containing TKI and cells collected after nine hours. Each experiment was repeated three times. Data are presented as mean±SEM * P≤ 0.05 compared with cisplatin alone.

4.4.2 Induction of DNA strand breaks

IR produces both single and double strand DNA breaks which can be quantified using alkaline Comet assay as described in Chapter Two section 2.5, with an increase in the measured tail moment indicating a greater number of DNA strand breaks (Olive and Banath, 2006). The Topo II poisons doxorubicin and etoposide induce single and

double DNA strand breaks, which can also be measured using the alkaline Comet assay.

4.4.2.1 The induction of DNA strand breaks by ionising radiation

Following exposure to TKI cells were irradiated (20 Gy) and processed immediately. This dose was chosen as it produces a tail moment of 12.3±0.34 which lies below the maximum sensitivity of the assay, allowing both decreases and increases in tail moment to be detected (Figure 4.7).

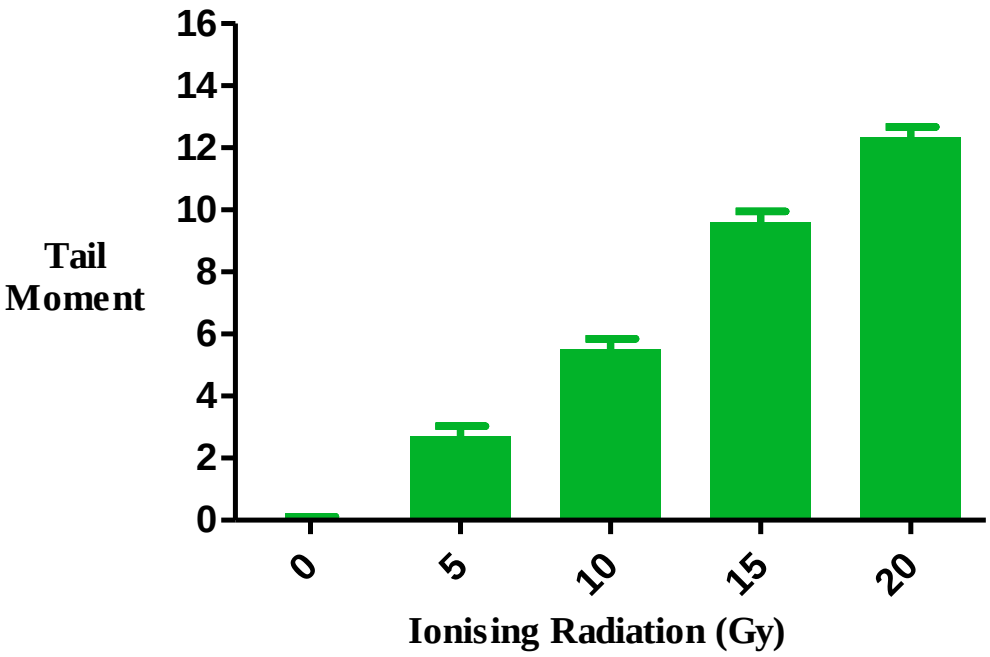

Figure 4.7 Induction of DNA strand breaks by ionising radiation
The alkaline comet assay was used to assess the induction of strand breaks by IR in the SK-Br-3 cell line. Cells were grown in DFM for 24 hours prior to exposure to IR, after which cells were collected, and analysed. Data represents mean±SEM of 50 cells per dose point.

The induction of DNA strand breaks by IR was not affected by either TKI or duration of TKI treatment. IR alone produces a tail moment of 9.7±1.0, a tail moment of 9.2±0.5 in cells treated with gefitinib for one hour and 10.2±0.4 following gefitinib treatment for 48 hours ($p>0.05$) (Figure 4.8). Pre-treatment with lapatinib also has no significant effect, with a tail moment of 8.5±0.7 in cells treated with lapatinib for one hour and 11.0±0.2 in cells treated with lapatinib for 48 hours ($p>0.05$) (Figure 4.8). Therefore,

the induction of DNA strand breaks by IR is not affected by either the gefitinib or lapatinib or the duration of exposure to the drug.

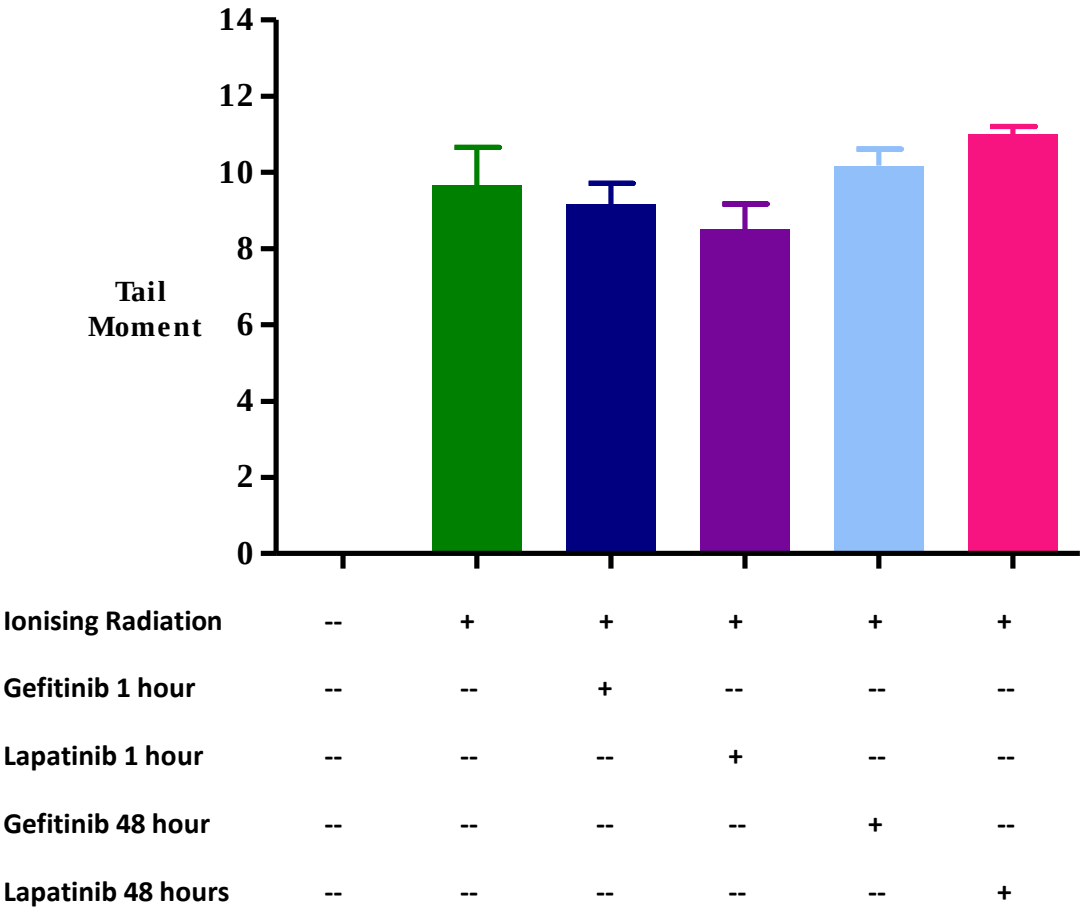

Figure 4.8 Effect of duration of exposure to gefitinib or lapatinib on the induction of DNA strand breaks by ionising radiation
The alkaline comet assay was used to assess the induction of strand breaks by IR in the SK-Br-3 cell line. Cells were pre-treated with drug free media (■), gefitinib 5 µM for 1 hour (■), lapatinib 2 µM for 1 hour (■), gefitinib 5 µM for 48 hours (■), lapatinib 2 µM for 48 hours (■). before exposure to IR (20 Gy), after which cells were collected, and analysed. Data represents mean±SEM of three independent experiments.

4.4.2.2 The induction of DNA stand breaks by doxorubicin and etoposide

The induction of DNA strand breaks by doxorubicin was investigated across a range of concentrations from 2.5-50 µM. Doxorubicin produced strand breaks at all concentrations, with a concentration-dependent increase in strand breaks observed between 2.5-10 µM; 50 µM doxorubicin produced the fewest strand breaks (Figure 4.9A).

Exposure to TKI for one hour has no significant effect on the induction of DNA strand breaks and there are no significant differences between lapatinib and gefitinib (for example at 5 μM doxorubicin alone- tail moment 4.4±0.8, plus gefitinib one hour 3.9±0.2, and lapatinib 4.2±0.6 $P>0.05$). Exposure to either TKI for 48 hours significantly reduces the ability of doxorubicin to induce DNA strand breaks at all drug concentrations investigated (for example 5 μM doxorubicin plus gefitinib 48 hours produces a tail moment 0.43±0.19 and lapatinib 48 hours 0.10±0.17 $p\leq0.01$) (Figure 4.9A).

Etoposide also produces DNA strand breaks in a concentration-dependent manner over a range of 50-200 μM, with 50 μM etoposide producing a tail moment of 3.0±0.3 and 200 μM, a tail moment of 10.9±1.0 (Figure 4.9B). Exposure to TKI for one hour has no significant effect on the induction of DNA strand breaks (for example 100 μM etoposide alone produces a tail moment of 8.5±0.9, gefitinib 8.3±1.1 and lapatinib 8.4±1.3 $p>0.05$) (Figure 4.9B). As with doxorubicin, exposure to TKI for 48 hours significantly reduces the number of DNA strand breaks produced at all etoposide concentrations (for example at 100 μM etoposide plus gefitinib tail moment 3.9±0.8 and lapatinib 4.2±0.2 $p\leq0.05$) (Figure 4.9B), though a concentration-dependent increase in tail moment can be observed. This indicates that the ability of doxorubicin and etoposide to induce DNA strand breaks is significantly inhibited by continued exposure to either gefitinib or lapatinib for 48 hours.

Taken together these data indicate that continuous exposure to the TKI gefitinib or lapatinib, inhibits the production of DNA damage by the Topo IIα poisons but not cisplatin or IR.

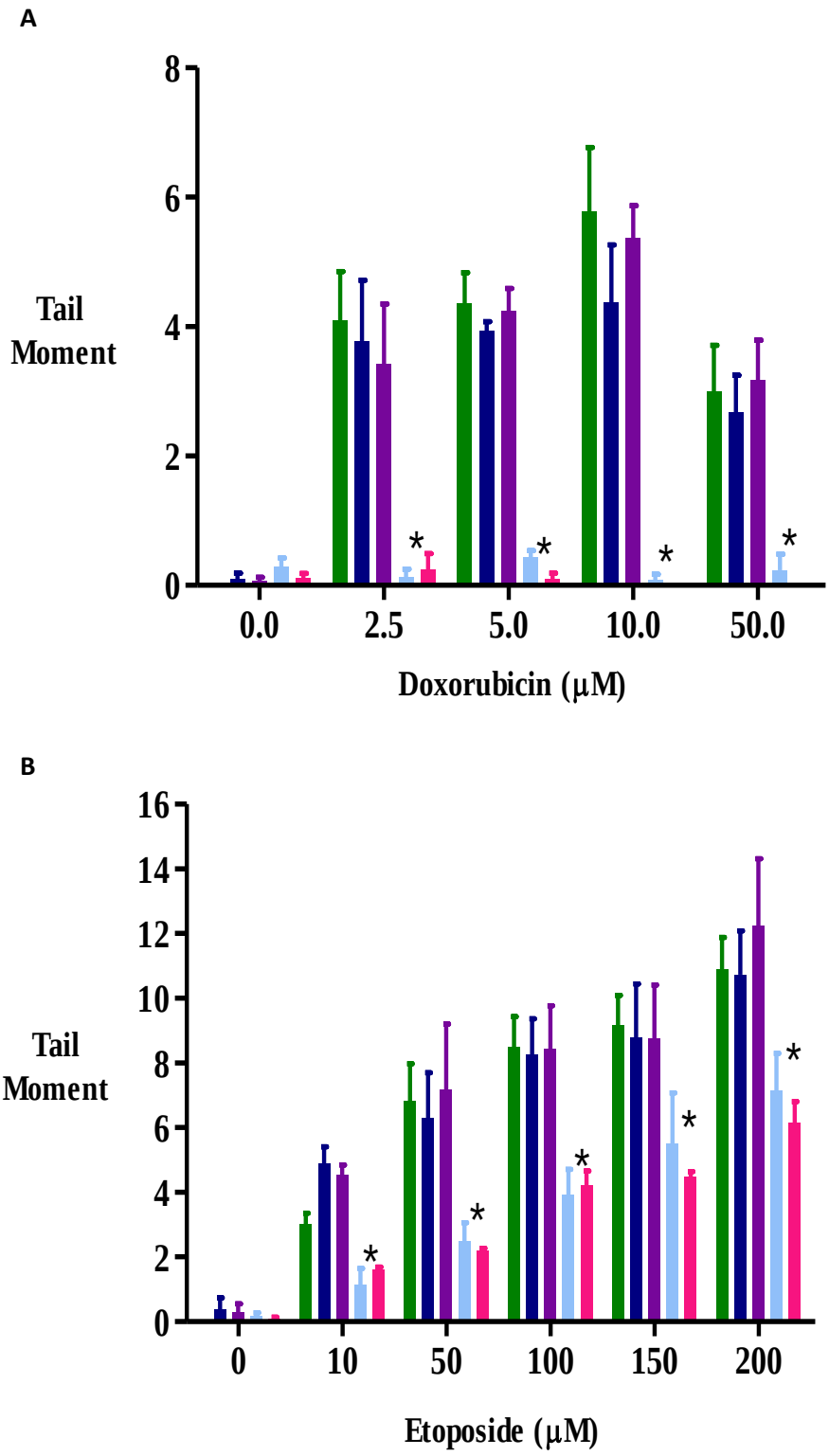

Figure 4.9 Effect of duration of exposure to gefitinib or lapatinib on the induction of DNA strand breaks by doxorubicin or etoposide.

The alkaline comet assay was used to assess the induction of strand breaks by (A) doxorubicin, (B) etoposide in the SK-Br-3 cell line. Cells were pre-treated with either drug free media (■), gefitinib (■) or lapatinib (■) for one hour, gefitinib (■) or lapatinib (■) for 48 hours prior to exposure to doxorubicin or etoposide at the stated concentration for 2 hours in the presence of TKI, after which cells were collected, and analysed. Each experiment was repeated in triplicate. * P≤ 0.05 compared with Topo II poison alone.

4.5 DOES THE DURATION OF EXPOSURE TO GEFITINIB OR LAPATINIB MODULATE DNA REPAIR?

The effect of duration of exposure to gefitinib or lapatinib on the ability of cells to repair DNA lesions was investigated using the alkaline Comet assay plus measurement of γH2AX and RAD51 foci. For all assays, multiple time points were examined following removal of the cytotoxic drug under investigation, allowing the repair of DNA strand breaks to be investigated.

The protein H2AX is phosphorylated at serine 139 to form γH2AX foci at sites flanking DNA DSBs, signalling their presence, location and recruiting repair proteins (Banath and Olive, 2003; Clingen *et al.*, 2008). γH2AX foci can be induced either by agents that cause DSBs directly (for example IR or Topo II poisons), indirectly through the collision of replication forks with interstrand crosslinks, single strand breaks or damaged DNA bases, or during DNA repair (Banath *et al.*, 2010; Clingen *et al.*, 2008). Foci can be visualised and counted using confocal microscopy as described in Chapter Two, sections 2.6. The resolution of γH2AX foci over time following removal of the DNA damaging agent can be studied, with persistence of foci at 24 hours correlating with cytotoxicity (Banath *et al.*, 2010). Due to the sensitivity of this assay, lower concentrations of DNA damaging agents were used in comparison to those used in the Comet assays.

RAD51 plays a key role in the process of DNA repair by HR and is involved in the repair of DNA DSBs, including those produced as a result of stalled replication forks due to interstrand crosslinks. RAD51 is involved in presynapsis during which free single stranded DNA is processed and a presynaptic filament formed through binding of RPA, allowing the loading of RAD51 onto single stranded DNA (Scott and Pandita, 2006). RAD51 foci form in the same cells as γH2AX foci, though the two proteins are not co-localised (Banath *et al.*, 2010) and by examining their formation and resolution, insights into the role of HR in DNA repair can be gained.

4.5.1 Repair of cisplatin-induced DNA damage

The repair of cisplatin-induced DNA damage involves both NER and HR as discussed in Chapter One, section 1.7.5.1. The modified alkaline Comet assay allows the detection

of the unhooking a interstrand crosslink from one or both strands of DNA; this is the first step in the repair of this type of lesion (Muniandy *et al.*, 2010). This unhooking step can be detected by the modified alkaline Comet assay as a fall in the percentage reduction in tail moment, as the unhooked interstrand crosslink no longer retards the migration of DNA (Hartley *et al.*, 1999). The measurement of γH2AX foci allows the assessment of DNA damage signalling and RAD51 the role of HR in the repair of cisplatin-induced DNA damage. Cisplatin was used at a concentration of 50 μM for two hours in the alkaline Comet assay and 1 μM for two hours to assess γH2AX and RAD51 foci induction and resolution.

4.5.1.1 Repair of cisplatin-induced DNA interstrand crosslinks

Cells were pre-treated for the required duration, exposed to cisplatin for two hours and the culture media replaced every 24 hours for the duration of the experiment. To allow comparison between treatments data are normalised to the nine hour time point, which is the time point at which the greatest number of interstrand crosslinks are observed in cells treated with cisplatin only. Therefore, the nine hour time point becomes 100% for each drug combination investigated and other time points are expressed as a percentage of this point, so that a fall in the 'percentage of peak tail moment' represents the unhooking of interstrand crosslinks (Figure 4.10).

The number of interstrand crosslinks increases following incubation with cisplatin peaking nine hours following removal of cisplatin (Figure 4.10). From 24 hours onwards fewer interstrand crosslinks are detected, indicating their unhooking. In cells treated with cisplatin alone 25.4±8.0% of the interstrand crosslinks present at nine hours remain at 72 hours (Figure 4.10).

Exposure to gefitinib for one hour prior to cisplatin treatment slows the rate of unhooking of interstrand crosslinks, reaching a statistical significant difference from cisplatin only treated cells at 72 hours (cisplatin alone 25.4±8.0%, gefitinib one hour 64.2±5.5 $p \leq 0.01$) (Figure 4.10). Exposure to gefitinib for 48 hours prior to cisplatin, significantly inhibits the unhooking of interstrand crosslinks, with no reduction in tail moment detected from 24 hours onwards (Figure 4.10).

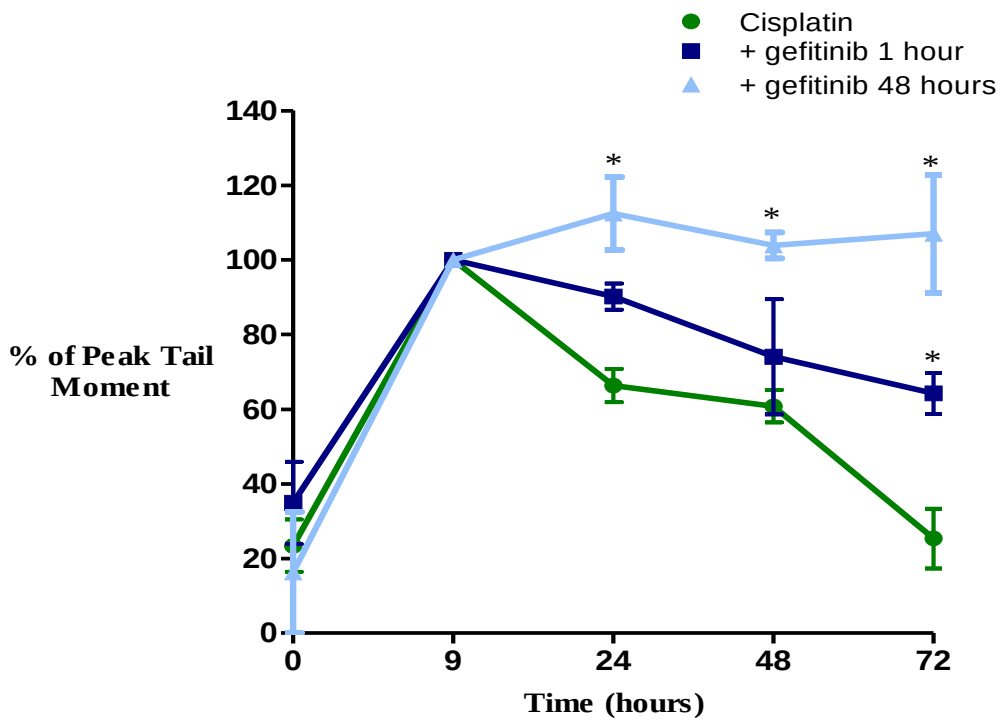

Figure 4.10 Effect of duration of exposure to gefitinib on the repair of cisplatin-induced DNA damage

The alkaline comet assay was used to assess the modulation of the repair of cisplatin-induced interstrand crosslinks by gefitinib. Cells were pre-treated with drug free media or gefitinib for one hour or 48 hours, followed by the addition of cisplatin (50 µM) for two hours. Media was then replaced with either fresh DFM or media containing gefitinib which was replaced every 24 hours, and cells collected at the time points as indicated. Data are presented as mean±SEM of three independent experiments. * P≤ 0.05 compared with cisplatin alone.

Like gefitinib, pre-treatment with lapatinib inhibits the unhooking of cisplatin-induced interstrand crosslinks with 77.3±11.0% remaining at 72 hours (Figure 4.11A). In cells treated with lapatinib for 48 hours, there was a notable increase in dead cells 72 hours after exposure to cisplatin, making the unhooking of interstrand crosslinks difficult to study at 72 hours. In the first 48 hours following cisplatin exposure, lapatinib pre-treatment for 48 hours does not significantly alter the unhooking of cisplatin-induced interstrand crosslinks (Figure 4.11B). This is in contrast to the effect of gefitinib exposure for 48 hours as demonstrated in Figure 4.12.

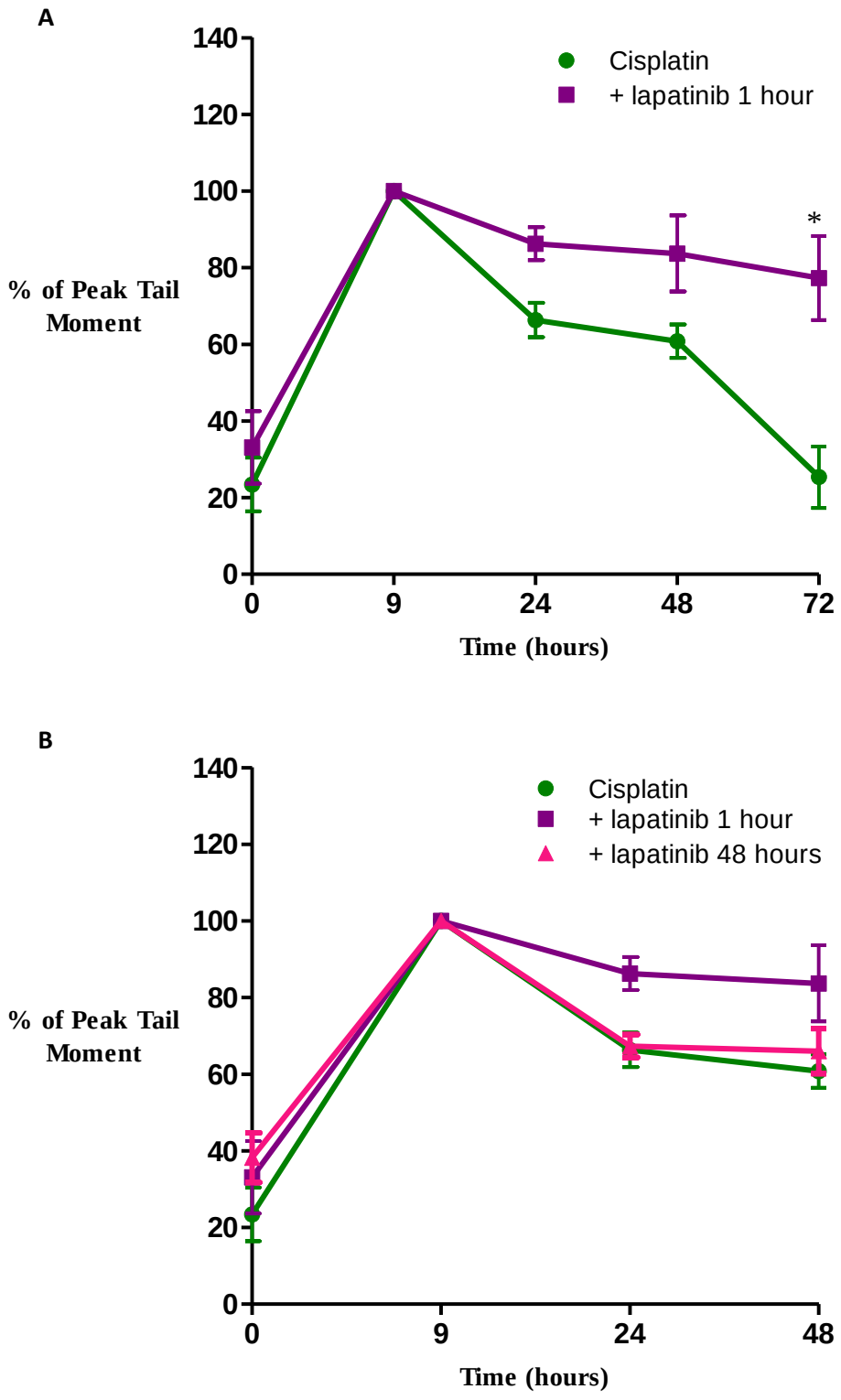

Figure 4.11 Effect of duration of exposure to lapatinib on the repair of cisplatin-induced DNA damage

The alkaline comet assay was used to assess the modulation of the repair of cisplatin-induced interstrand crosslinks by lapatinib. Cells were pre-treated with drug free media or lapatinib for one hour or 48 hours, followed by the addition of cisplatin (50 μM) for two hours. Media was then replaced with either fresh DFM or media containing lapatinib, which was replaced every 24 hours and cells collected at the time points as indicated. Data presented as mean±SEM of three independent experiments. * P≤ 0.05 compared with cisplatin alone.

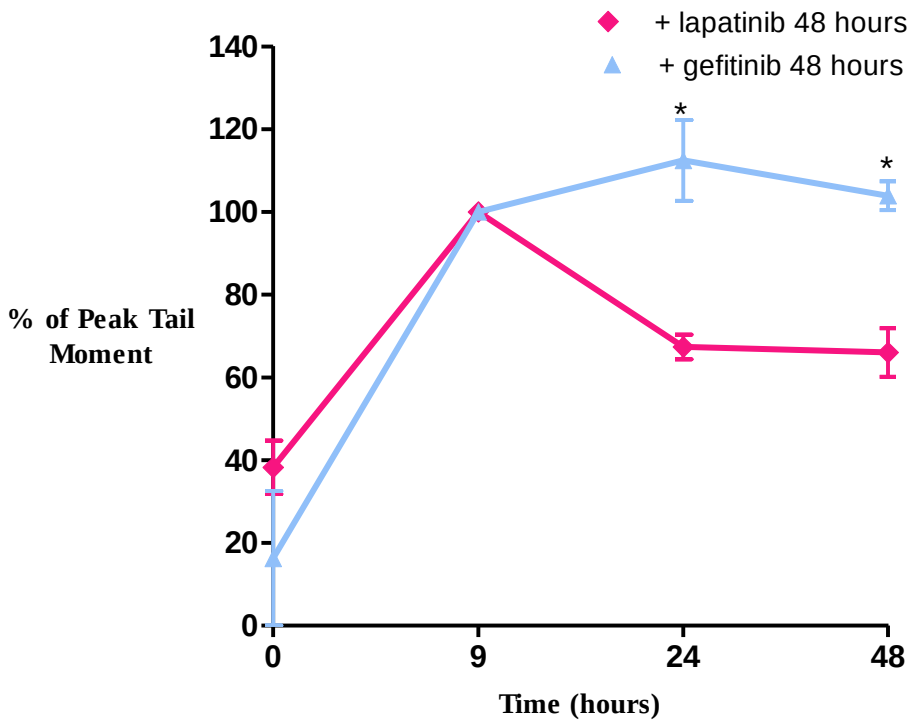

Figure 4.12 Differences in the effect of gefitinib and lapatinib for 48 hours on the unhooking of interstrand crosslinks.
SK-Br-3 cells were pre-treated with gefitinib or lapatinib for 48 hours prior to treatment with cisplatin (50 µM) for two hours. Media containing TKI was replaced every 24 hours, and cells collected for analysis at the time points indicated. Data are presented as mean±SEM of three independent experiments. * P≤ 0.05.

4.5.1.2 Modulation of cisplatin-induced γH2AX foci by gefitinib

γH2AX foci induction peaks 10 hours following removal of cisplatin and then falls (data not shown). The peak number of foci produced is not significantly altered by gefitinib, regardless of duration of treatment (Figure 4.13). Pre-treatment with gefitinib for one hour slows the resolution of γH2AX foci with significantly more foci persisting at 48 hours compared with cells treated with cisplatin alone (cisplatin alone 3.2±0.2 foci/cell vs. one hour gefitinib 11.8±2.8 foci/cell p≤0.05), though by 72 hours there are no significant differences (Figure 4.13). In cells pre-treated with gefitinib for 48 hours, a reduction in γH2AX foci is observed at 24 hours after which no further resolution of foci can be detected with significantly more foci persisting at, 24, 48 and 72 hours compared with cells treated with cisplatin alone (Figure 4.13).

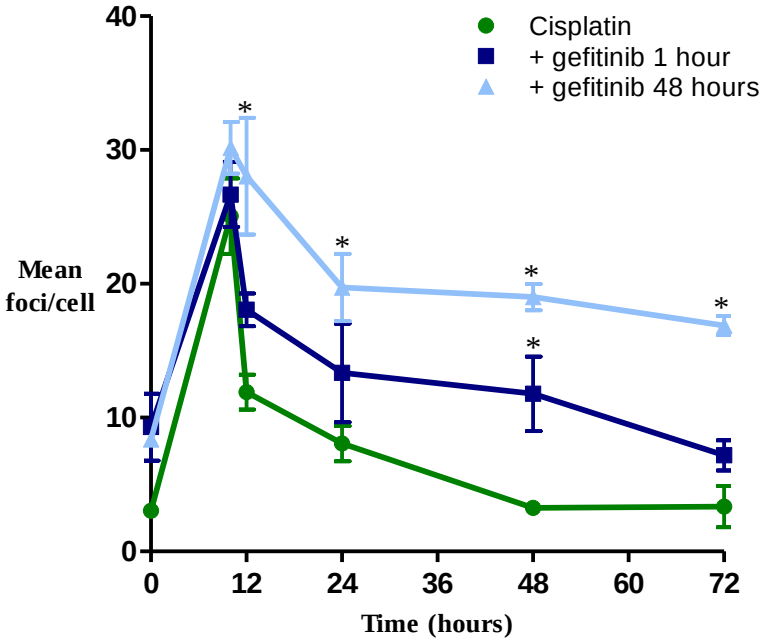

Figure 4.13 Effect of duration of exposure to gefitinib on the resolution of γH2AX foci
Measurement of γH2AX foci was used to assess the repair of cisplatin-induced DNA damage following pre-treatment with DFM, gefitinib for one hour or 48 hours prior to the addition of cisplatin (1 μM). Following incubation with cisplatin for two hours the media was replaced with fresh DFM or gefitinib for the duration of the experiment. Data are presented as mean ±SEM of three independent experiments. * P≤ 0.05 compared with cisplatin alone.

4.5.1.3 Modulation of cisplatin-induced RAD51 foci by gefitinib

RAD51 foci induction peaks at a level of 20.6±1.2 foci/cell at 24 hours in cells treated with cisplatin alone and then falls, reaching baseline at 48 hours (Figure 4.14). In cells treated with gefitinib for one hour prior to cisplatin exposure, the peak level of RAD51 foci is lower than that observed in cells treated with cisplatin alone at 13.3±6.0 foci/cell, and takes 72 hours to reach baseline levels. Pre-treatment of cells with gefitinib for 48 hours prior to cisplatin alters the peak of Rad51 foci, which occurs later at 48 hours and at a lower number of 20.0±0.2 foci/cell, with no resolution of foci observed in the 72 hour duration of the experiment (Figure 4.14).

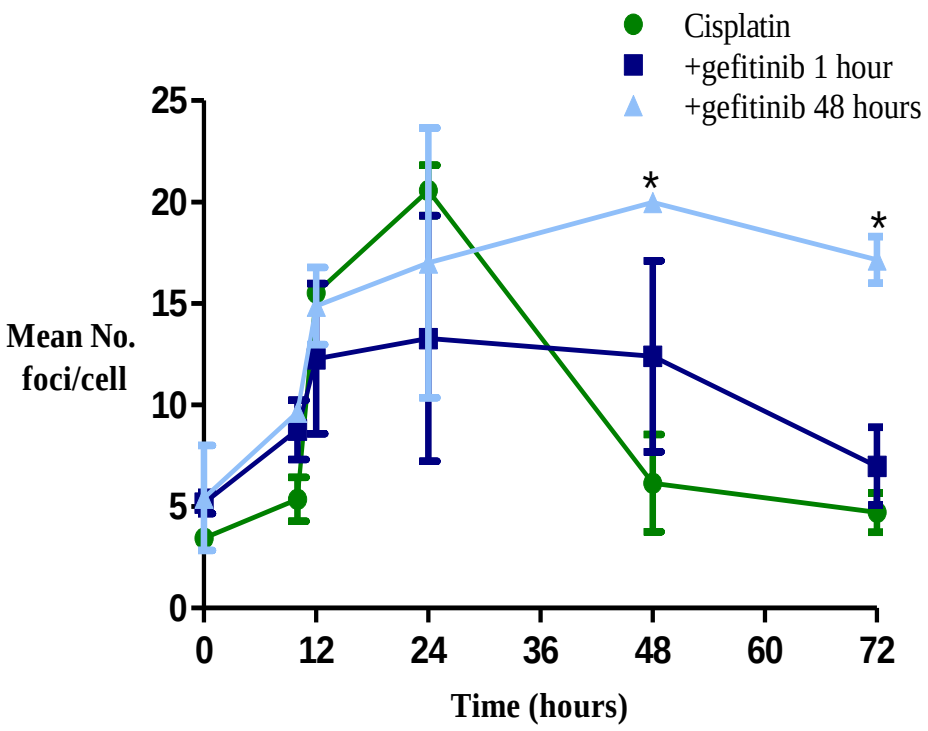

Figure 4.14 Effect of duration of exposure to gefitinib on the resolution of RAD51 foci
Measurement of RAD51 foci was used to assess the repair of cisplatin-induced DNA damage following pre-treatment with DFM, gefitinib for one hour or 48 hours prior to the addition of cisplatin (1 μM). Following incubation with cisplatin for two hours the media was replaced with fresh DFM or gefitinib for the duration of the experiment, and cells collected for analysis over 72 hours. Data are presented as mean±SEM of two independent experiments. *P≤ 0.05 compared with cisplatin alone.

4.5.2 The modulation of the repair of DNA single and double strand breaks by duration of exposure to lapatinib and gefitinib

The repair of DNA strand breaks produced by IR was studied using the alkaline Comet assay together with measurement of γH2AX and RAD51 foci. To investigate the repair of doxorubicin and etoposide-induced DSBs the alkaline Comet assay and measurement of γH2AX foci were used. As with the assessment of cisplatin-induced DNA damage, multiple time points after the removal of the DNA damaging agent were examined.

4.5.2.1 The repair of ionising radiation-induced DNA damage

4.5.2.1.1 Repair of DNA strand breaks

The repair of IR-induced DNA strand breaks was investigated over four hours using the alkaline Comet assay. These data were normalised to the tail moment observed

directly after irradiation. This allows the comparison between the different treatment combinations.

DNA strand breaks induced by IR (20 Gy) were repaired rapidly with 78.7±3.9% repaired within 30 minutes and only 2.7±1.7% of strand breaks remaining at four hours (Figure 4.15A). Exposure to lapatinib, regardless of duration, does not alter the repair of IR-induced DNA strand breaks compared with treated with IR alone (Figure 4.15A).

Pre-treatment of cells with gefitinib delays the repair of IR-induced strand breaks compared with cells treated with IR alone (Figure 4.15B). At one hour significantly fewer DNA strand breaks are repaired in cells pre-treated with gefitinib for one hour (66.2±4.4%) compared with cells treated with IR alone (87.9±5.4% $p \leq 0.05$), though there are no significant differences at 30 minutes, two and four hours (Figure 4.15B). Exposure to gefitinib for 48 hours prior to IR produces a greater inhibition of repair with 34.2±6.4% of lesions repaired at 30 minutes, compared with 68.7±3.9% repaired in cells treated with IR alone ($p<0.001$), and 60.8±7.2% repaired at one hour compared with 87.9±5.4% repaired in cells treated with IR alone ($p \leq 0.01$). Four hours following exposure to IR nearly all DNA strand breaks are repaired regardless of the duration of gefitinib treatment (Figure 4.15B).

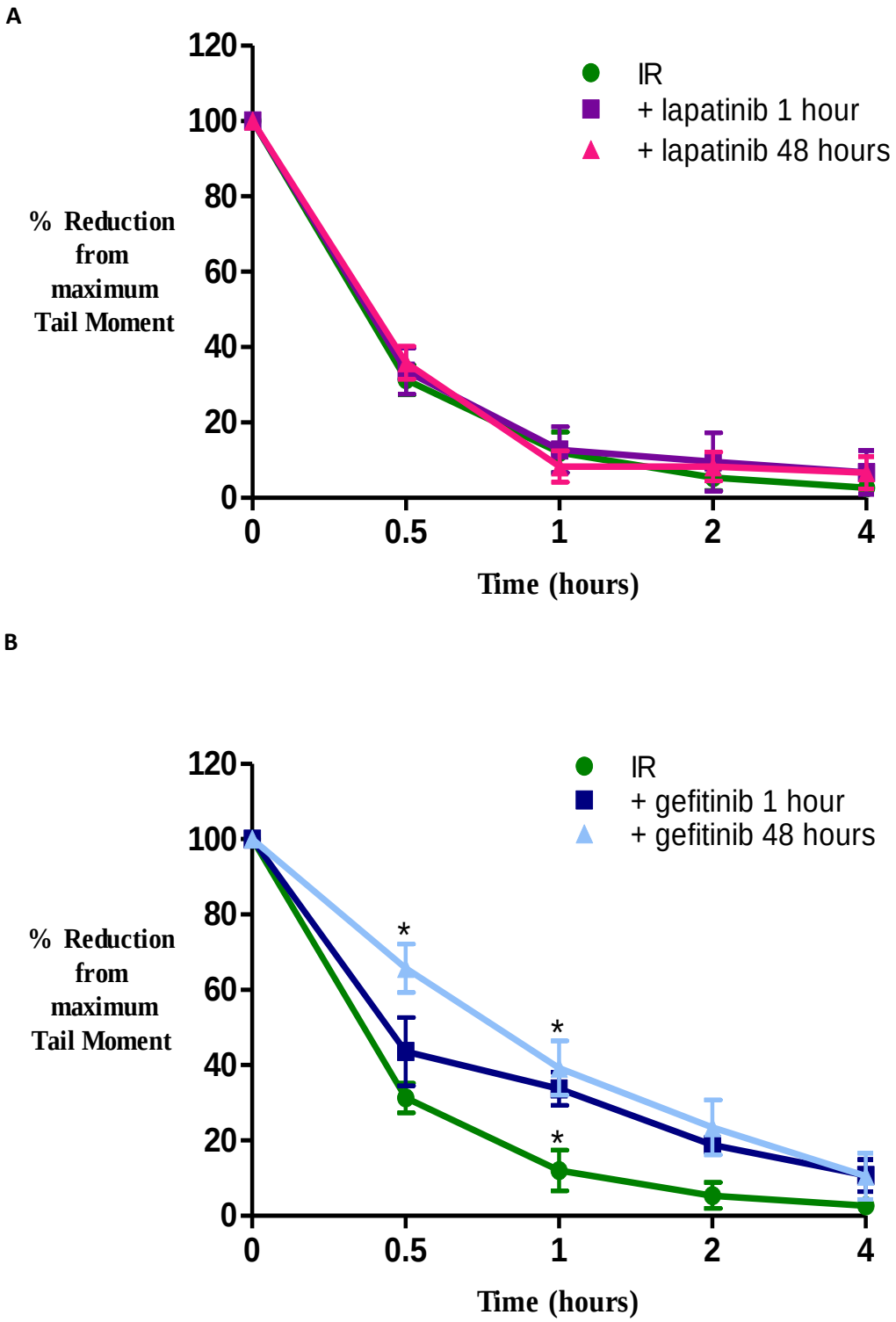

Figure 4.15 Effect of duration of exposure to lapatinib or gefitinib on the repair of ionising radiation-induced DNA strand breaks

The modulation of repair of IR-induced strand breaks by (A) lapatinib and (B) gefitinib was assessed in the SK-Br-3 cell line. Cells were pre-treated with drug free media, lapatinib or gefitinib for one hour or 48 hours, before exposure to IR (20 Gy), and then collected at the times indicated and analysed using the alkaline Comet assay. Data are presented as mean±SEM of three independent experiments. * P< 0.05 compared with IR alone.

4.5.2.1.2 Modulation of ionising radiation-induced γH2AX foci by gefitinib

To investigate the repair of IR-induced lesions by measuring γH2AX foci, IR 2 Gy was investigated over 24 hours (Figure 4.16A). As with previous experiments, a lower dose of IR was used to enable individual foci to be counted. There are no significant differences in the induction of γH2AX foci in cells treated with IR alone and those pre-treated with gefitinib for one or 48 hours. Near complete resolution of foci is observed in all treatment arms by 24 hours, with 4.5±1.4 foci/cell remaining in cells treated with IR alone compared with 2.2±2.0 foci/cell with gefitinib one hour and 1.7±0.9 foci/cell with gefitinib 48 hours ($p>0.05$) (Figure 4.16A). Closer examination of Figure 4.16A suggests that there may be differences in γH2AX foci resolution in the first two hours following IR, which have been missed due to the time points examined. To examine this further the resolution of γH2AX foci was investigated over a five hour period. As this experiment was conducted only once no statistical analysis can be conducted, but it appears that treatment with gefitinib, regardless of duration, slows the resolution of γH2AX compared to cells treated with IR alone over five hours (Figure 4.16B).

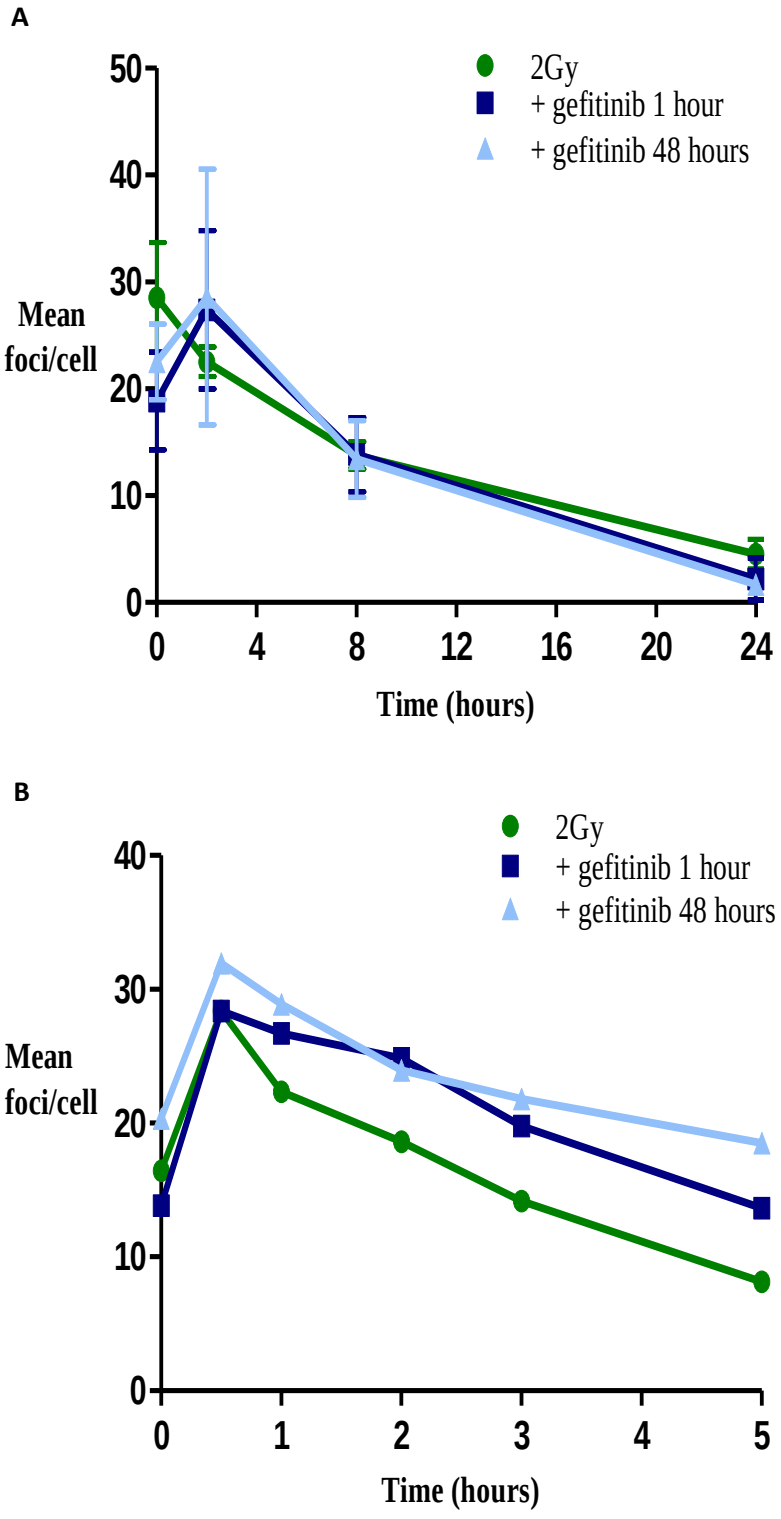

Figure 4.16 Effect of the duration of exposure to gefitinib on the resolution of ionising radiation-induced γH2AX foci

The induction and resolution of γH2AX foci following IR was studied in cells pre-treated with DFM, gefitinib for one hour or 48 hours over (A) over 24 hours and (B) over 5 hours. For Figure A, data are presented as mean±SEM of three independent experiments. * P< 0.05 compared with IR alone. Figure B was performed once and is presented as the mean foci of 50 cells.

4.5.2.1.3 Modulation of ionising radiation-induced RAD51 foci

In cells treated with IR alone, RAD51 foci peaks four hours later at 24.9±4.0 foci/cell, and falls to baseline at 24 hours (Figure 4.17). Pre-treatment of cells with gefitinib for one hour results in a similar modulation of RAD51 foci, peaking at 23.9±5.1 foci/cell and a falling to baseline expression at 24 hours. In cells pre-treated with gefitinib for 48 hours prior to exposure to IR, RAD51 foci fail to resolve within the 24 hours duration of the experiment, with 21.5±1.8 foci/cell remaining at 24 hours (Figure 4.17).

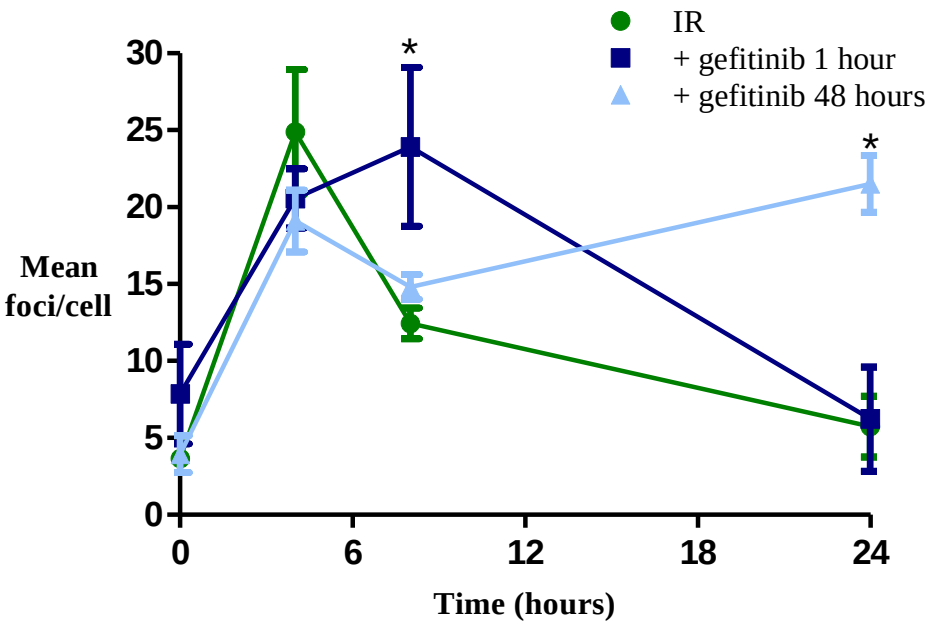

Figure 4.17 Effect of the duration of exposure to gefitinib on the resolution of ionising radiation-induced RAD51 foci

The induction and resolution of RAD51 foci following IR was studied in cells pre-treated with DFM, gefitinib for one hour or 48 hours over 24 hours. Data are presented as mean±SEM of three independent experiments. * P< 0.05 compared with IR alone.

4.5.2.2 The repair of Topoisomerase II poison-induced DNA strand breaks

4.5.2.2.1 Repair of doxorubicin-induced DNA damage

4.5.2.2.1.1 Repair of doxorubicin-induced DNA strand breaks

The effect of lapatinib or gefitinib on the repair of doxorubicin-induced DNA strand breaks was investigated using the alkaline Comet assay. A concentration of 5 µM doxorubicin was chosen for investigation as this is a clinically achievable concentration *in vivo* and a concentration at which Topo IIα poisoning occurs, producing DNA single and double strand breaks (Gewirtz, 1999).

As with IR, data are expressed as a percentage of the tail moment achieved immediately following removal of the Topo II poison under investigation. In order to investigate the formation and resolution of γH2AX foci, a tenth of the dose of Topo IIα poison used for the Comet assay was investigated.

Following doxorubicin treatment 41.8±4.3% of strand breaks are repaired within the first four hours and by 10 hours, 62.8±7.7% of strand breaks are repaired (Figure 4.18A).

Lapatinib exposure for one hour has no effect on repair of DNA lesions within the first four hours (Figure 4.18A). By eight and 10 hours an increase in DNA strand breaks can be observed in cells these cells compared with cells treated with doxorubicin alone, reaching a statistically significant difference at 10 hours (Figure 4.18A). Prior exposure to gefitinib for one hour also has no effect on the initial repair of doxorubicin-induced DNA lesions, but an increase in DNA strand breaks can be observed at 10 hours (Figure 4.18B).

Doxorubicin produced few detectable strand breaks in cells treated with either gefitinib or lapatinib for 48 hours, for the duration of the experiment, so their repair cannot be studied (data not shown).

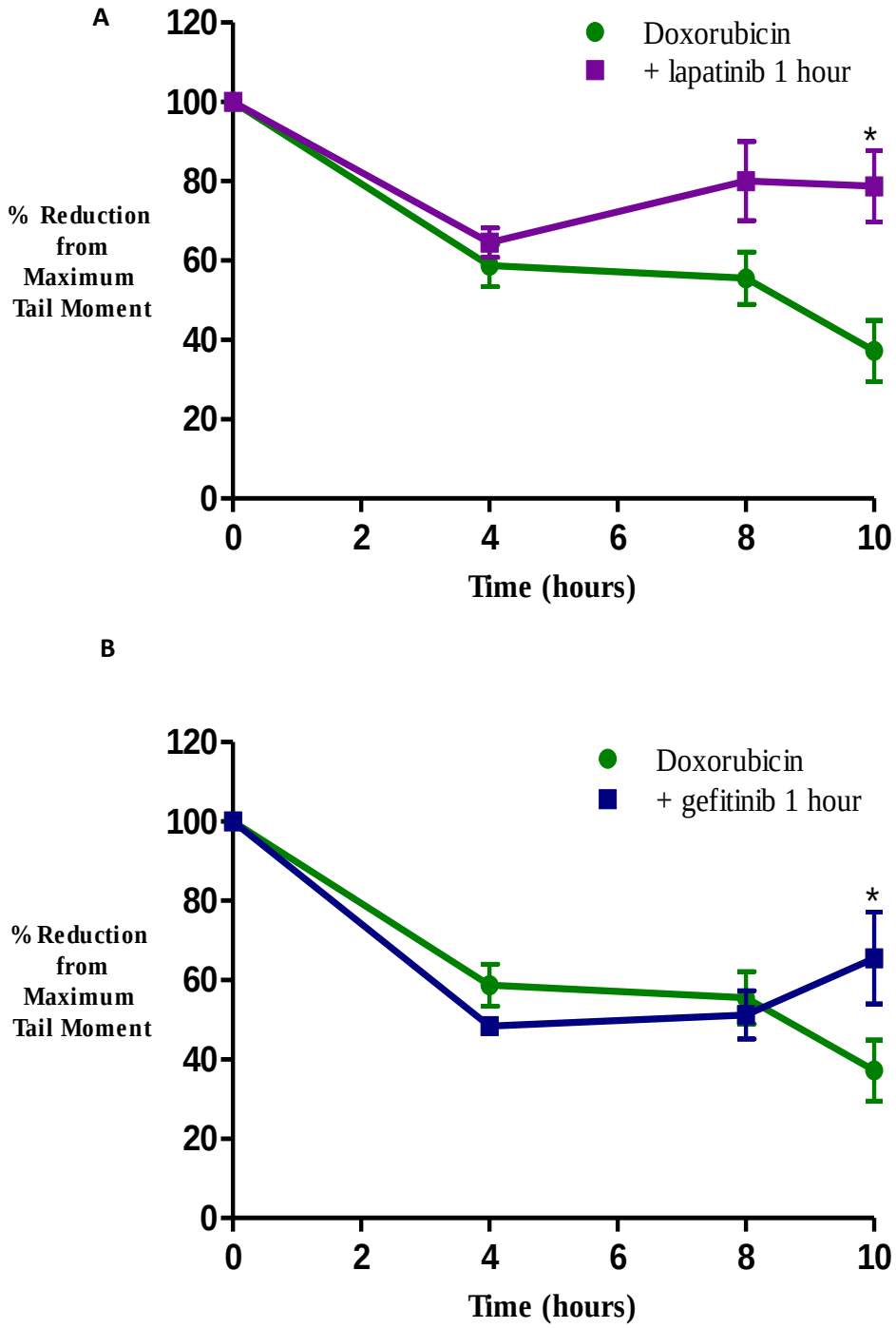

Figure 4.18 Effect of duration of exposure to lapatinib or gefitinib on the repair of doxorubicin-induced DNA strand breaks

The alkaline comet assay was used to assess the repair doxorubicin-induced DNA strand breaks in cells treated with (A) lapatinib and (B) gefitinib. Cells were pre-treated with drug free media, lapatinib or gefitinib for one hour, before incubation with doxorubicin (5 µM) for two hours. Media was removed and replaced with fresh DFM or TKI and cells collected at the times indicated. Data are presented as mean±SEM of three independent experiments. * P< 0.05 compared with doxorubicin alone.

4.5.2.2.1.2 Modulation of doxorubicin-induced γH2AX foci by gefitinib

γH2AX foci formation peaks six hours after removal of doxorubicin at 61.1±7.0 foci/cell and remains elevated for the duration of the experiment (Figure 4.19). Following gefitinib treatment for one hour, the peak of doxorubicin-induced γH2AX occurs earlier at four hours, with fewer foci 48.3±9.6 foci/cell and then falls so that at six hours cells have 53% fewer foci than cells treated with doxorubicin alone (29.0±4.1 vs. 61.1±7.0 foci/cell respectively p ≤0.01) (Figure 4.19). Following this initial fall in foci, no further resolution is observed so that 24 hours following exposure to doxorubicin, 43% fewer foci are present in cells pre-treated with gefitinib for one hour compared with cells treated with doxorubicin only (gefitinib one hour 31.9±8.2 foci/cell vs. doxorubicin alone 56.5±7.0 foci/cell P≤0.05). Significantly fewer foci are produced by doxorubicin in cells pre-treated with gefitinib for 48 hours at all time points investigated (Figure 4.19).

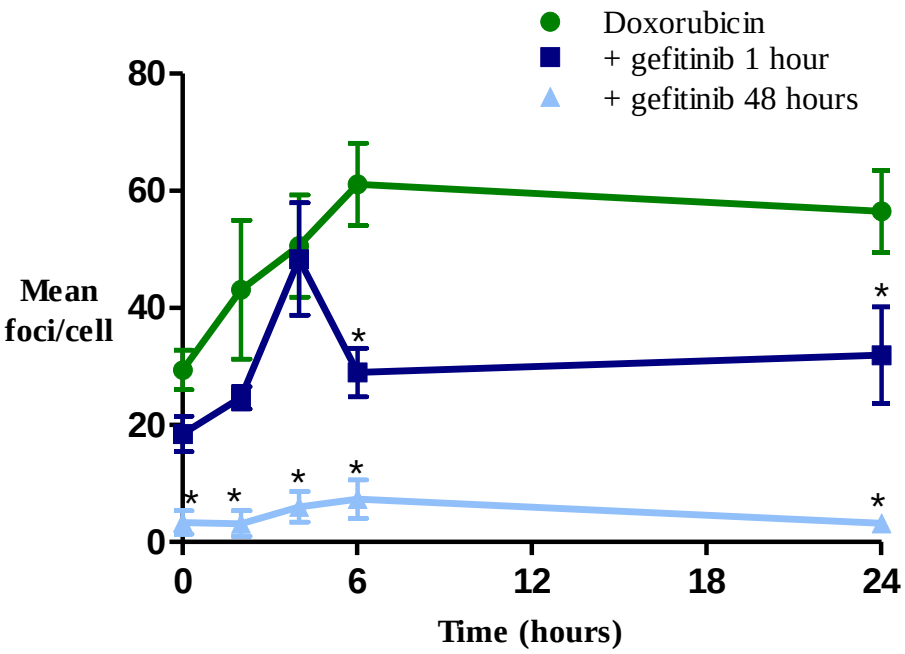

Figure 4.19 Effect of duration of exposure to gefitinib on the resolution of doxorubicin-induced γH2AX foci

γH2AX foci following doxorubicin was studied in cells pre-treated with DFM, gefitinib for one hour or 48 hours prior to the addition of doxorubicin (0.5μM) for two hours. Media was then replaced with fresh DFM or TKI and cells collected at the time points indicated Data are presented as mean±SEM of three independent experiments. *P< 0.05 compared with doxorubicin alone

4.5.2.2.2 Repair of etoposide induced DNA damage

4.5.2.2.2.1 Repair of etoposide-induced DNA strand breaks

Etoposide is used at a concentration of 150 μM, which is far higher than that achievable clinically. This concentration was chosen as it allows the repair of DNA strand breaks produced after TKI exposure for 48 hours to be investigated, given the rapid rate of repair of these lesions.

Etoposide-induced DNA strand breaks are repaired rapidly with 8.5±1.6% of the peak number of foci, remaining four hours after the removal of etoposide and 5.2±1.1% at 10 hours (Figure 4.20A). Pre-treatment with lapatinib for one hour significantly delays the repair of etoposide-induced DNA strand breaks (Figure 4.20A), at 30 minutes 28.2±4.5% are repaired compared with 49.8±5.3% in cells treated with etoposide alone ($p<0.001$). This trend continues with 55.3±4.4% repaired at two hours in cells pre-treated with lapatinib for one hour, compared with 76.3±2.7% in etoposide only treated cells ($p <0.001$) and 78.1±5.9% repaired at four hours compared with 91.5±1.6% ($p\leq0.05$); by 10 hours there are few remaining DNA strand breaks.

In cells treated with lapatinib for 48 hours, the etoposide-induced DNA strand breaks are repaired more rapidly, with 83.5±5.1% repaired within the first 30 minutes, compared with 49.8±5.3% in cells treated with etoposide alone ($p<0.001$) and all strand breaks are repaired by two hours (Figure 4.20A).

Like lapatinib, exposure to gefitinib for one hour delays the repair of etoposide-induced DNA strand breaks (Figure 4.20B). Two hours after exposure to etoposide 64.4±2.5% of strand breaks are repaired in cells pre-treated with gefitinib for one hour compared with 76.3±2.7% in cells treated with etoposide alone ($p\leq0.05$). This difference is greater at four hours, when 76.5±4.6% of strand breaks are repaired in cells with prior exposure to gefitinib for one hour, compared with 91.5±1.6% repaired in etoposide only treated cells ($P\leq0.01$) (Figure 4.20B). Like lapatinib, gefitinib exposure for 48 hour hours prior to etoposide treatment increases the rate of repair of DNA strand breaks, with all strand breaks repaired by two hours (Figure 4.20B).

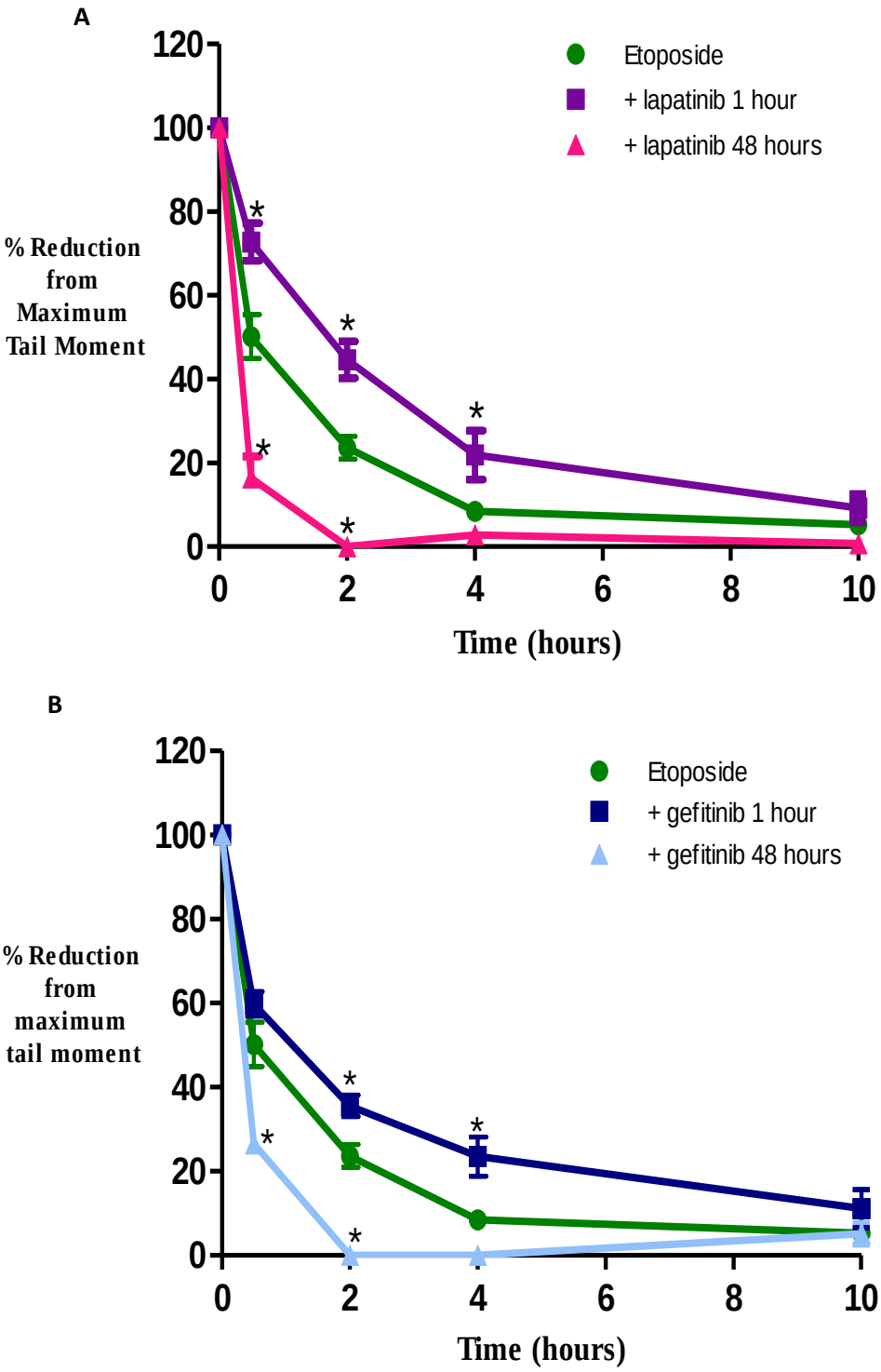

Figure 4.20 Effect of duration of exposure to lapatinib or gefitinib on the repair of etoposide-induced DNA strand breaks

The alkaline comet assay was used to assess the repair doxorubicin-induced DNA strand breaks in cells treated with (A) lapatinib and (B) gefitinib. Cells were pre-treated with drug free media, lapatinib or gefitinib for one hour or 48 hours before incubation with etoposide (150 µM) for two hours. Media was removed and replaced with fresh DFM or TKI and cells collected at the times indicated. Data are presented as mean±SEM of three independent experiments. * P< 0.05 compared with etoposide alone.

4.5.2.2.2.2 Modulation of etoposide-induced γH2AX foci by gefitinib

Measurement of γH2AX foci following etoposide (15 μM) peaks at two hours with 64.4±11 foci/cell and then falls to 30.6±9.3 foci/cell by eight hours (Figure 4.21). The peak of foci production is not altered by gefitinib pre-treatment for one hour, though there are 50% fewer foci at 24 hours compared with cells treated with etoposide alone (23.3±5.4 vs. 46.6±5.3 foci per cell $p< 0.05$). Continuous gefitinib exposure for 48 hours results in significantly fewer γH2AX foci produced following etoposide treatment at all time point investigated (Figure 4.21).

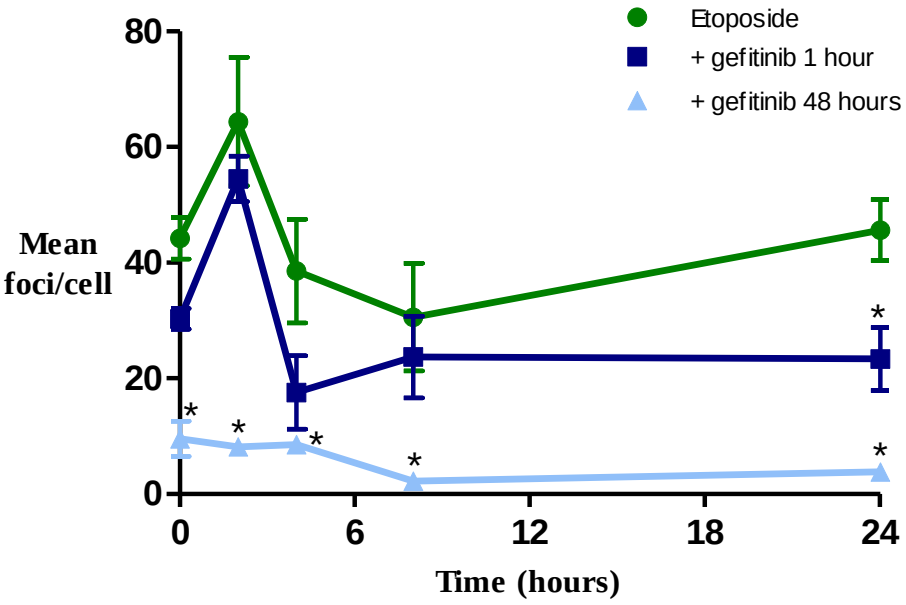

Figure 4.21 Effect duration of exposure to gefitinib on the resolution of etoposide-induced γH2AX foci

γH2AX foci following etoposide was studied in cells pre-treated with DFM, gefitinib for one hour or 48 hours prior to the addition of etoposide (15μM) for two hours. Media was then replaced with fresh DFM or TKI and cells collected at the time points indicated Data are presented as mean±SEM of three independent experiments. *P< 0.05 compared with etoposide alone.

4.6 DOES THE DURATION OF EXPOSURE TO GEFITINIB OR LAPATINIB MODULATE THE CELL CYCLE RESPONSE TO DNA DAMAGING AGENTS?

Cell cycle arrest plays a key role in the cellular response to DNA damage, creating time to repair damage and preventing the passage of damaged DNA to daughter cells (Dai and Grant, 2010). The cell cycle also determines which mechanism of DNA repair cells

have available, with HR limited to late S and G2M-phases of the cell cycle (Dai and Grant, 2010). In order to assess the effect of gefitinib and lapatinib on the cell cycle response to cytotoxic chemotherapy, FACS as described in Chapter Two section 2.7 was used to assess the cell cycle. To enable direct correlation with the Comet assay data presented above, cells were treated in exactly the same way. Cells were collected for analysis 24 hours after removal of the cytotoxic agent under investigation.

4.6.1 The effect of gefitinib and lapatinib on the cell cycle

Exposure to either gefitinib or lapatinib increases number of cells in the G0/G1-phase of the cell cycle. In cells treated with gefitinib for 25 hours (one hour followed by incubation for 24 hours), 81.6±5.2% cells are in G0/G1 compared with 69.9±0.3% of untreated cells (Table 4.1 and Figure 4.22). This increases to 87.5±1.2% in cells treated with gefitinib for 72 hours (48 hours followed by 24 hours incubation). Lapatinib treatment for 25 hours results in 88.1±1.2% of cells in G0/G1. Fewer cells are in this phase following treatment with lapatinib for 72 hours (73.6±1.1%) due to an increase in the number of cells in sub-G1. In untreated cells, 3.3±1.4% of cells are identified in sub-G1, 4.9±0.5% in cells treated with lapatinib for 25 hours and 19.0±1.4% in cell treated with lapatinib for 72 hours.

Cell cycle phase	Sub-G1 (%)	G0/G1 (%)	S (%)	G2M (%)
DFM	**3.3±1.5**	**70.0±0.3**	**11.1±1.6**	**15.7±2.6**
Gefitinib 1 hour (25 hours in total)	**10.6±3.8**	**81.6±5.2**	**3.1±0.1**	**5.1±1.0**
Gefitinib 48 hours (72 hours in total)	**5.1±0.6**	**87.5±1.2**	**2.4±0.6**	**5.4±0.1**
Lapatinib 1 hour (25 hours in total)	**4.9±0.5**	**88.1±1.2**	**2.4±0.3**	**4.8±0.8**
Lapatinib 48 hours (72 hours in total)	**19.0±1.4**	**73.6±1.1**	**3.2±0.6**	**4.6±1.2**

Table 4.1 Effect of duration of exposure to gefitinib or lapatinib on the cell cycle
Cells were plated in cell culture flasks and left overnight to adhere. Cells were then treated with DFM or TKI with replacement of media±TKI every 24 hours. All cells were grown for 72 hours in total and collected at the same time for analysis 24 hours after drug treatment.

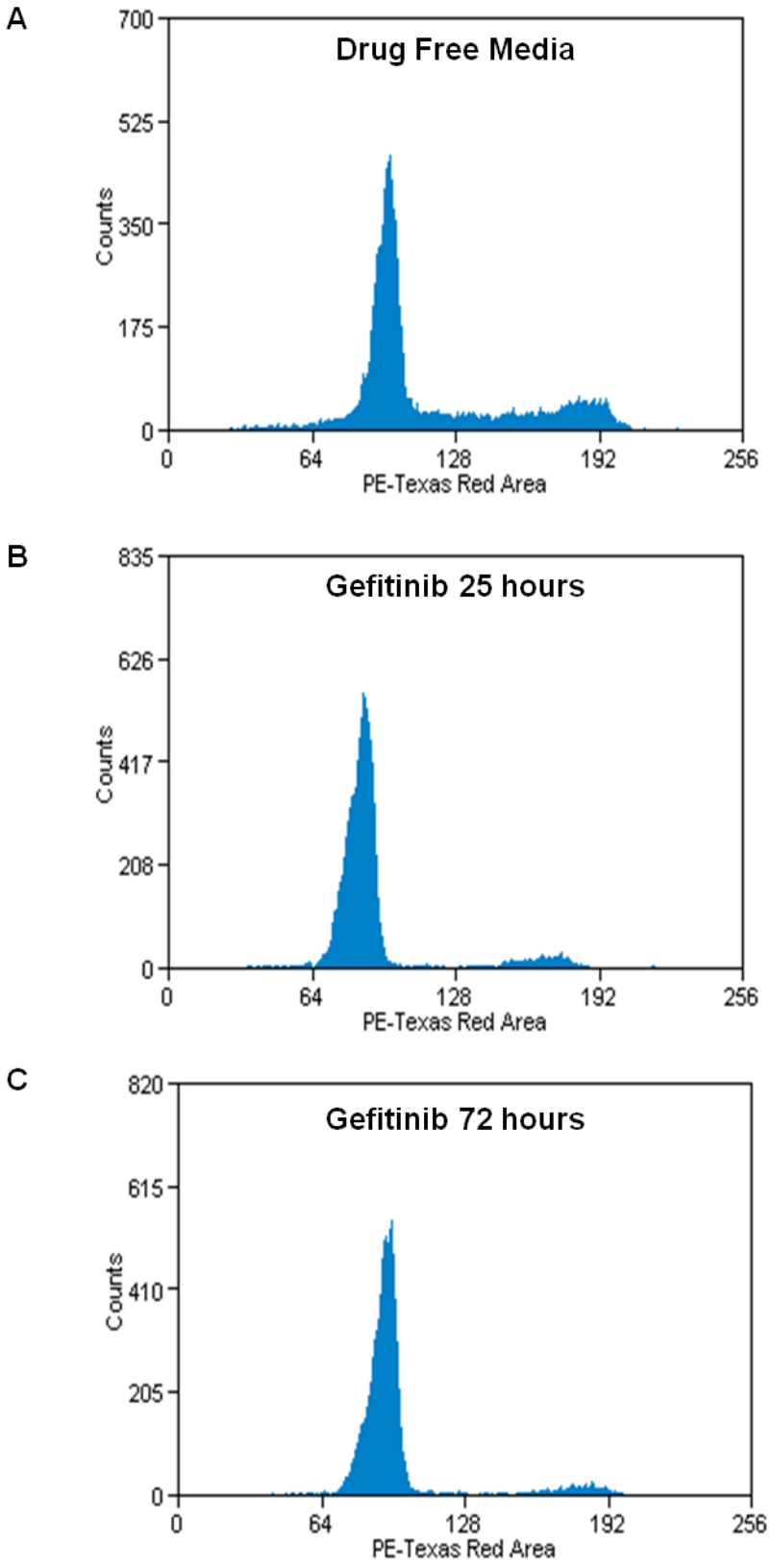

Figure 4.22 Example of cell cycle analysis obtained using FACS
SK-Br-3 cells were treated with gefitinib 5 µM for the duration indicated. Cells were collected 24 hours following drug treatment. Therefore for gefitinib treatment for one hour, cells were collected for analysis after a further 24 hours, making a total 25 hours of exposure to gefitinib.

4.6.2 The effect of duration of exposure to gefitinib or lapatinib on the modulation of the cell cycle by cisplatin

Cisplatin treatment increases the number of cells in S-phase of the cell cycle to 14.4±2.5% compared with 11.1±1.8% in untreated cells (Figure 4.23A). This is also observed in cells pre-treated with TKI for one hour, with cisplatin treatment of cells exposed to gefitinib for one hour inducing 19.7±0.2% of cells into S-phase compared with 3.1±0.1% in cells treated with gefitinib alone. Similar results are observed with lapatinib pre-treatment for one hour with 12.3±1.7% cells in S-phase following cisplatin compared with 2.4±0.3% in cells treated with lapatinib alone (Figure 4.23A).

The pre-treatment of cells with TKI for 48 hours produces different results to those described above. In cells pre-treated with gefitinib for 48 hours, smaller increases in the number of cells in the sub-G1 (gefitinib alone 5.1±0.6% vs. gefitinib+cisplatin 8.9±1.6%) and S-phases (gefitinib alone 2.4±0.6% vs. gefitinib+cisplatin 6.8±4.4%) of the cell cycle are observed. Cisplatin does not significantly alter the cell cycle of cells pre-treated with lapatinib for 48 hours compared with cells treated with lapatinib alone for 48 hours (Figure 4.23A).

4.6.3 The effect of duration of exposure to gefitinib or lapatinib on the modulation of the cell cycle by ionising radiation

IR doubles the number of cells in the S (11.1±1.6% to 21.2±7.7%) and G2/M (15.9±2.6% to 38.5±12.0%) phases of the cell cycle compared with untreated cells (Figure 4.23B). In cells pre-treated with either gefitinib or lapatinib prior to IR, fewer cells arrest in the G2/M (gefitinib+IR 22.1±1.3%, lapatinib+IR 22.7±3.4% and IR alone 38.5±12.0%) or S phase of the cell cycle (gefitinib+IR 6.5±1.7%, lapatinib+IR 6.1±2.4% and IR alone 21.2±7.7%). The pre-treatment of cells with either gefitinib or lapatinib for 48 hours prior to IR, prevents an IR-induced alteration in the cell cycle distribution of cells except for an increase in the number of cells in the sub-G1 phase in cells pre-treated with lapatinib from 19.7±1.1% with lapatinib alone to 28.2±4.1% following IR.

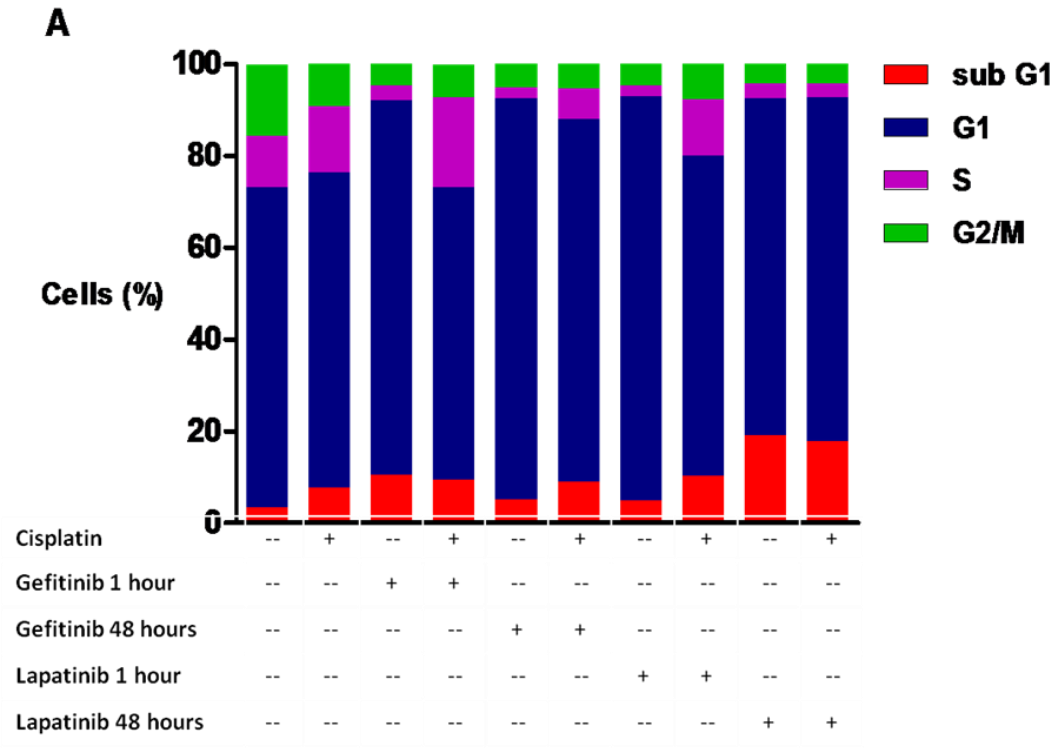

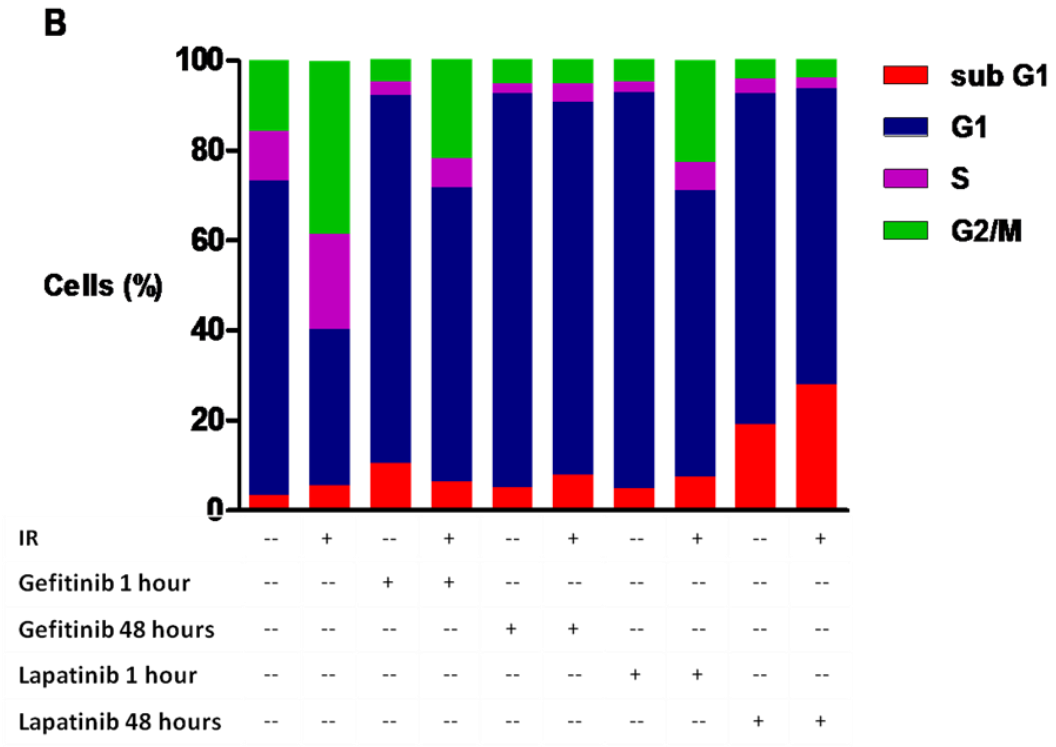

Figure 4.23 Modulation of the cell cycle response to cisplatin and ionising radiation by duration of exposure to gefitinib and lapatinib

Cells were treated with drug free, media, gefitinib or lapatinib for one or 48 hours prior to the addition of (A) cisplatin (50 μM) for two hours or (B) IR (20 Gy), after which media was replaced +/- TKI. Cells were then incubated for a further 24 hours, prior to collection, fixation and staining with propidium iodide. The fluorescence of 10, 000 cells was measured using FACS. Data presented as the mean of three independent experiments.

4.6.4 The effect of duration of exposure to gefitinib or lapatinib on the modulation of the cell cycle by doxorubicin

Doxorubicin increases the number of cells in S-phase from 11.1±1.6% in untreated cells to 21.2±7.2% (Figure 4.24A). An increase in S-phase cells is also observed in cells pre-treated with TKI for one hour (gefitinib alone 3.1±1.0% to 12.3±2.0% with gefitinib+doxorubicin, and lapatinib alone 2.4±0.3% to 14.3±1.7% with lapatinib+doxorubicin) (Figure 4.24A). An increase in the number of cells in sub-G1 is observed, both in cells treated with doxorubicin alone and those pre-treated with TKI for one hour (DFM 3.3±1.4% to 11.4±4.5%, gefitinib 10.6±3.8% to 17.0±8.6% and lapatinib 4.6±0.5% to 30.1±4.5%); this does not occur in cells 6pre-treated with TKI continuously for 48 hours (gefitinib 5.1±0.6% to 6.2±0.5% and lapatinib 19.0±1.4% to 15.4±2.4% (Figure 4.24A).

Overall doxorubicin does not significantly alter the cell cycle distribution of cells treated with either gefitinib or lapatinib continuously for 48 hour, prior to doxorubicin exposure (Figure 4.24A).

4.6.5 The effect of duration of exposure to gefitinib or lapatinib on the modulation of the cell cycle by etoposide

Etoposide increases the percentage of cells in S-phase from 11.1±1.6% to 34.0±2.3% (Figure 4.24B). This is also observed in cells treated with either gefitinib or lapatinib for one hour though, as with doxorubicin, the number of cells in S-phase is lower than that induced by etoposide alone (gefitinib alone 3.1±1.0.% to 12.4±4.4% with gefitinib+doxorubicin, and lapatinib alone 2.4±0.3% to 10.8±1.0% with lapatinib+doxorubicin). Etoposide increases the number of cells in sub-G1 in both untreated cells and those pre-treated with TKI for one hour. Again like with doxorubicin, this increase is not observed in cells pre-treated with either TKI for 48 hours (DFM 3.3±1.4% to 11.5±1.1%, gefitinib one hour 10.6±3.8% to 16.4±2.7%, lapatinib one hour 4.6±0.5% to 16.7±4.1%, gefitinib 48 hours 5.1±0.6% to 8.3±2.5%, and lapatinib 48 hours 19.0±1.4% to 13.5±2.8%) (Figure 4.24B). Like doxorubicin, etoposide does not alter the cell cycle distribution of cells which have been treated with either gefitinib or lapatinib for 48 hours.

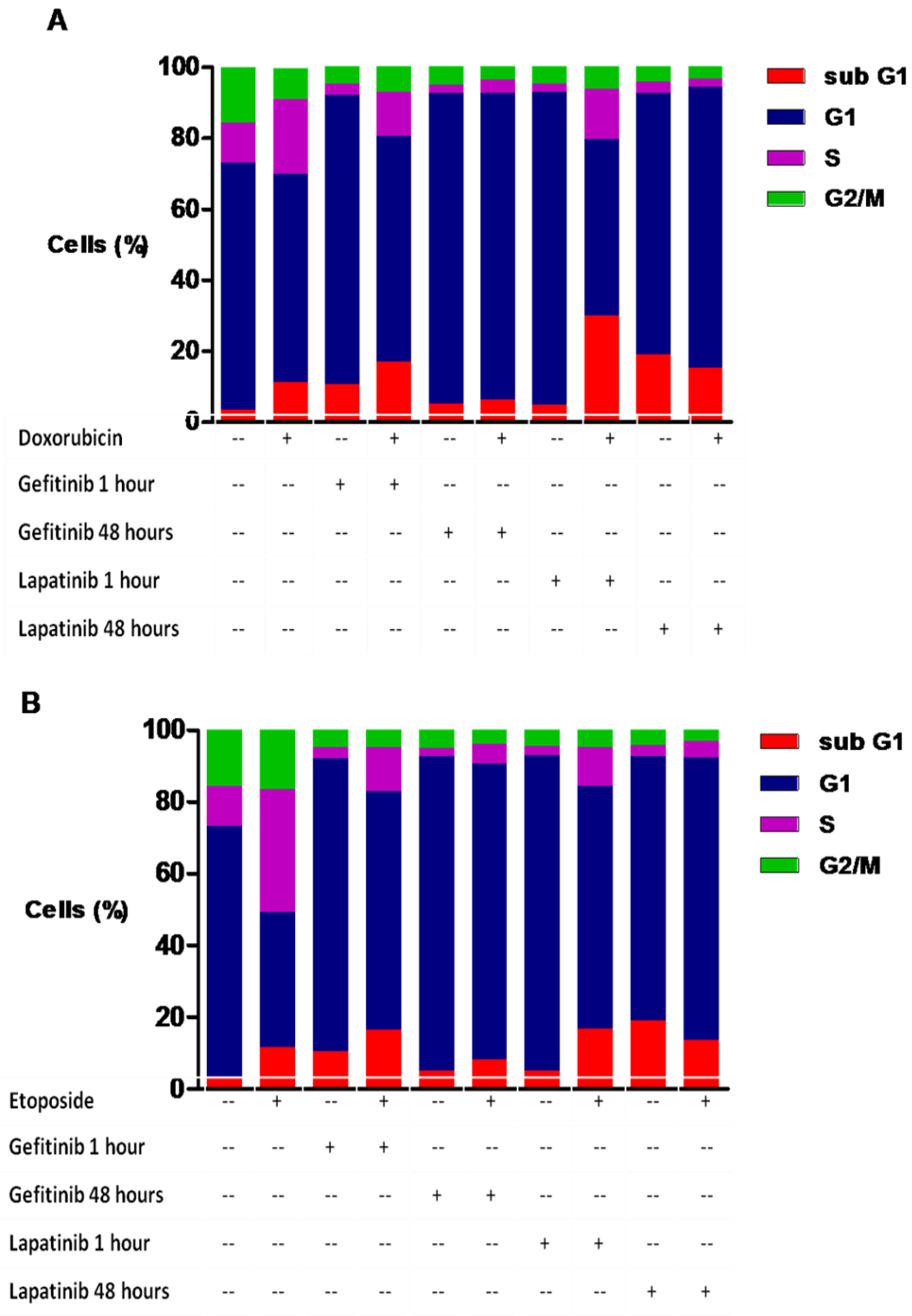

Figure 4.24 Modulation of the cell cycle response to doxorubicin and etoposide by duration of exposure to gefitinib and lapatinib

Cells were treated with drug free ,media, acute or chronic gefitinib or lapatinib prior to the addition of (A) doxorubicin (5 µM) for two hours or (B) etoposide (50 µM) for two hours, after which media was replaced +/- TKI. Cells were then incubated for a further 24 hours, prior to collection, fixation and staining with propidium iodide. The fluorescence of 10, 000 cells was measured using FACS. Data presented as the mean of three independent experiments.

4.7 THE EFFECT OF DURATION OF EXPOSURE TO GEFITINIB OR LAPATINIB ON THE INDUCTION OF APOPTOSIS BY ETOPOSIDE AND DOXORUBICIN

Section 4.4.2.2 demonstrates that cells treated with gefitinib or lapatinib continuously for 48 hours are resistant to the induction of DNA strand breaks by the Topo II poisons doxorubicin and etoposide. In order to investigate if these effects result in resistance to the cytotoxic effects of doxorubicin and etoposide, the induction of apoptosis was assessed by measuring annexin V expression.

4.7.1 The Annexin V assay

Annexins are a family of proteins which bind to negatively charged phospholipids in a calcium dependent manner (Huerta *et al.*, 2007). Phosphatidylserine residues are negatively charged phospholipids which make up the cytoplasmic surface of cell membranes (Huerta *et al.*, 2007). Cells undergoing apoptosis develop membrane asymmetry resulting in the transport of phosphatidylserine residues to the cell surface, thus allowing the identification of apoptotic cells. Annexin V specifically binds to phosphatidylserine residues and through the conjugation annexin V to a fluorochrome, FACS can be used to identify fluorescent and therefore apoptotic cells. Dual staining of cells with both annexin V and a DNA binding dye allows differentiation between cells undergoing early and late apoptosis (Huerta *et al.*, 2007) as during late apoptosis the cell membrane is disrupted, allowing the penetration of DNA binding dyes. Cells which have undergone non-apoptotic cell death are stained by the DNA binding dye due to a permeable cell membrane but do not bind annexin V and cells which are alive, remain unstained (Huerta *et al.*, 2007). Classically propidium iodide is used in combination with annexin V conjugated to a fluorochrome. Propidium iodide emits fluorescence at 615 nm, but doxorubicin also emits fluorescence at this wavelength, so propidium iodide could not be used in cells treated with doxorubicin (Figure 4.25C). Doxorubicin fluorescence is not detected at 660 nm allowing the use of the red fluorescent dye Sytox red, to be used as DNA stain instead (Figure 4.25D).

4.7.1.1 Drug fluorescence

Cells treated with either gefitinib or lapatinib for 48 hours emit a fluorescence which is detected in all four channels available for FACS (Figures 4.25E, F, G and H). This meant

that the boundaries denoting unstained and alive cells had to be altered for cells treated with either gefitinib or lapatinib for 48 hours. This potentially introduces inconsistencies when comparing cell treated with chemotherapy alone with cells pre-treated with TKI followed by chemotherapy. However, comparisons can be made between cells which have been treated with the same TKI for the same duration.

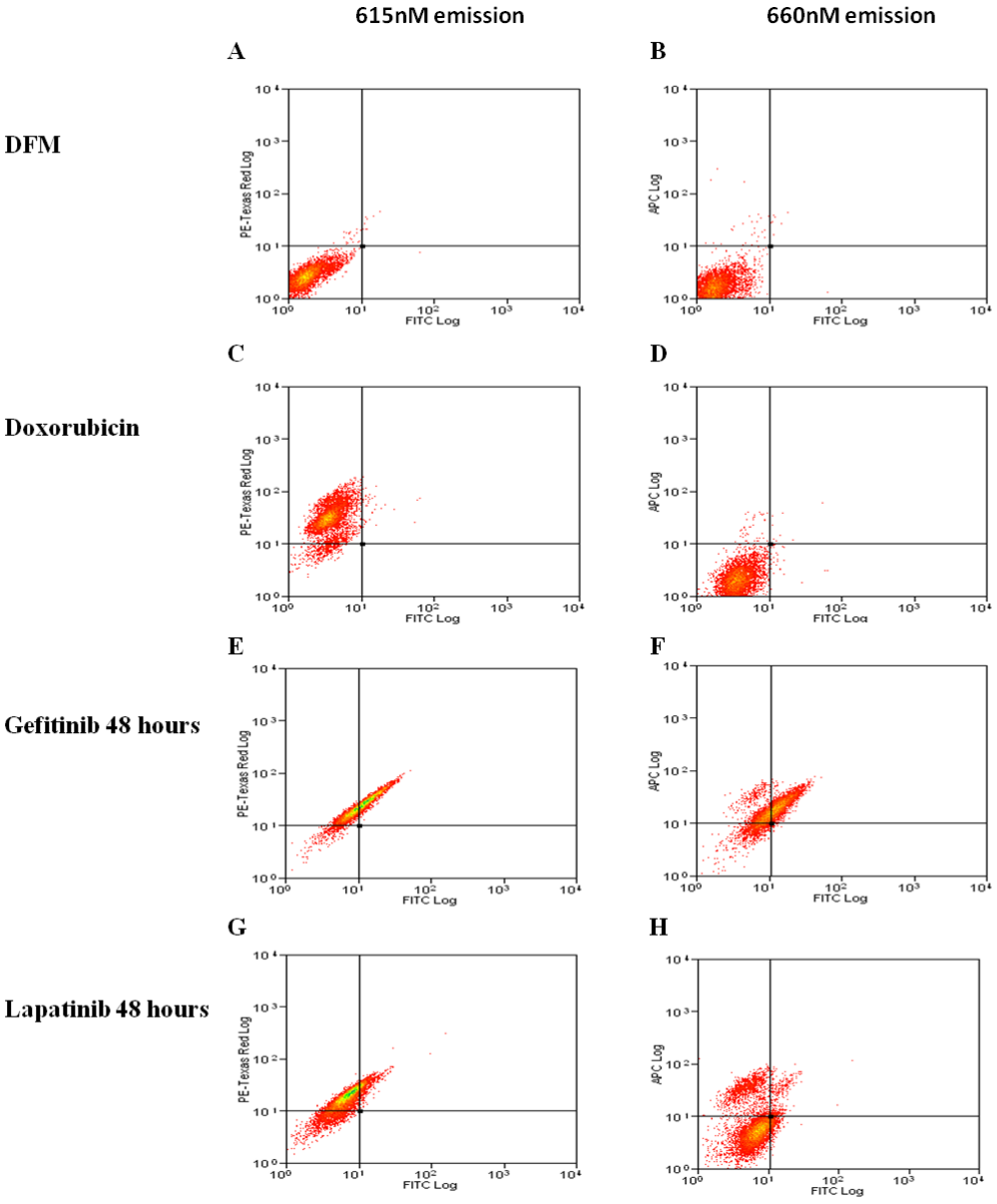

Figure 4.25 Fluorescence of doxorubicin, gefitinib and lapatinib
The fluorescence of unstained cells following treatment with TKI was detected by the FACS machine. Two channels were assessed, PE-Texas red which detects emission at a peak of 615nm and APC, which measures peak emission at 660nm. 10,000 cells were assessed following treatment with (A + B) DFM, (C+D) doxorubicin 5 µM for 2 hours, (E+F) 5 µM gefitinib 48 hours and (G+H) 2 µM lapatinib 48 hours. Images are representative of two independent experiments.

4.7.2 The induction of apoptosis by tyrosine kinase inhibitors

In untreated cells, 17.1±3.8% of cells are identified as undergoing apoptosis, compared with 20.3±0.4% and 19.6±0.6% in cells treated with gefitinib one or 48 hours respectively. A greater degree of apoptosis is detected in cells treated with lapatinib for one hour (25.7±0.1%) and 48 hours (45.6±1.9%) than gefitinib treated cells (Figure 4.26).

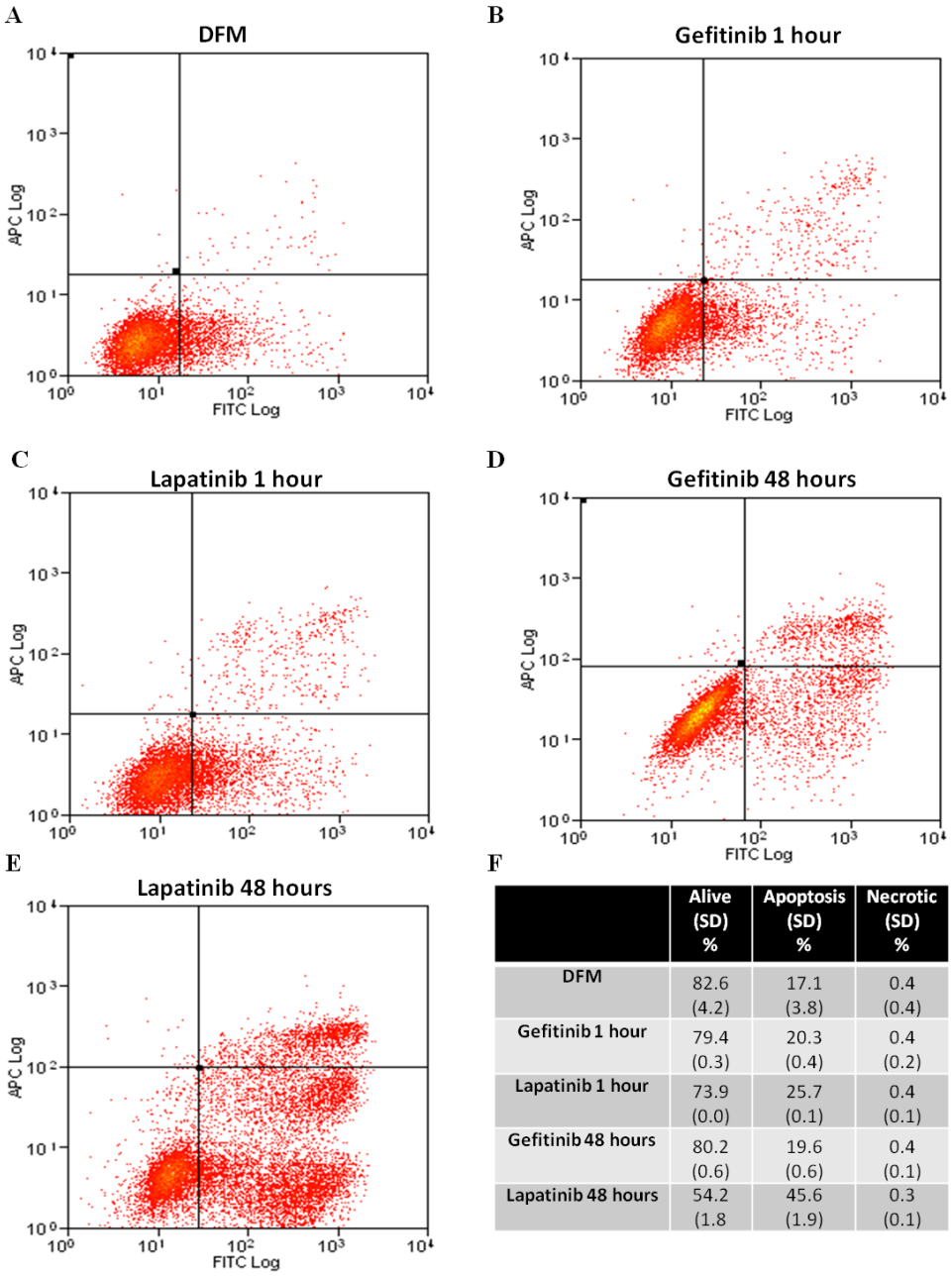

F

	Alive (SD) %	Apoptosis (SD) %	Necrotic (SD) %
DFM	82.6 (4.2)	17.1 (3.8)	0.4 (0.4)
Gefitinib 1 hour	79.4 (0.3)	20.3 (0.4)	0.4 (0.2)
Lapatinib 1 hour	73.9 (0.0)	25.7 (0.1)	0.4 (0.1)
Gefitinib 48 hours	80.2 (0.6)	19.6 (0.6)	0.4 (0.1)
Lapatinib 48 hours	54.2 (1.8	45.6 (1.9)	0.3 (0.1)

Figure 4.26 Induction of apoptosis by gefitinib or lapatinib
Cells were treated with (A) DFM, (B) 5 µM gefitinib 1 hour (C) 2 µM lapatinib 1 hour, (D) 5 µM gefitinib 48 hours and (E) 2 µM lapatinib 48 hours. The fluorescence of 10, 000 cells was measured using FACS. Representative images for each experiment are presented. Data are presented as the mean±SD % of 10,000 cells from two independent experiments.

4.7.3 The induction of apoptosis by doxorubicin and etoposide

In cells grown in the absence of any drug for the 72 hours duration of the experiment, 17.1±3.8% of cells are identified as undergoing apoptosis (Figure 4.27). This number increases with the addition of 5 µM doxorubicin to 59.5%±3.0% and to 43.0±8.1% with etoposide 50 µM (Figure 4.27).

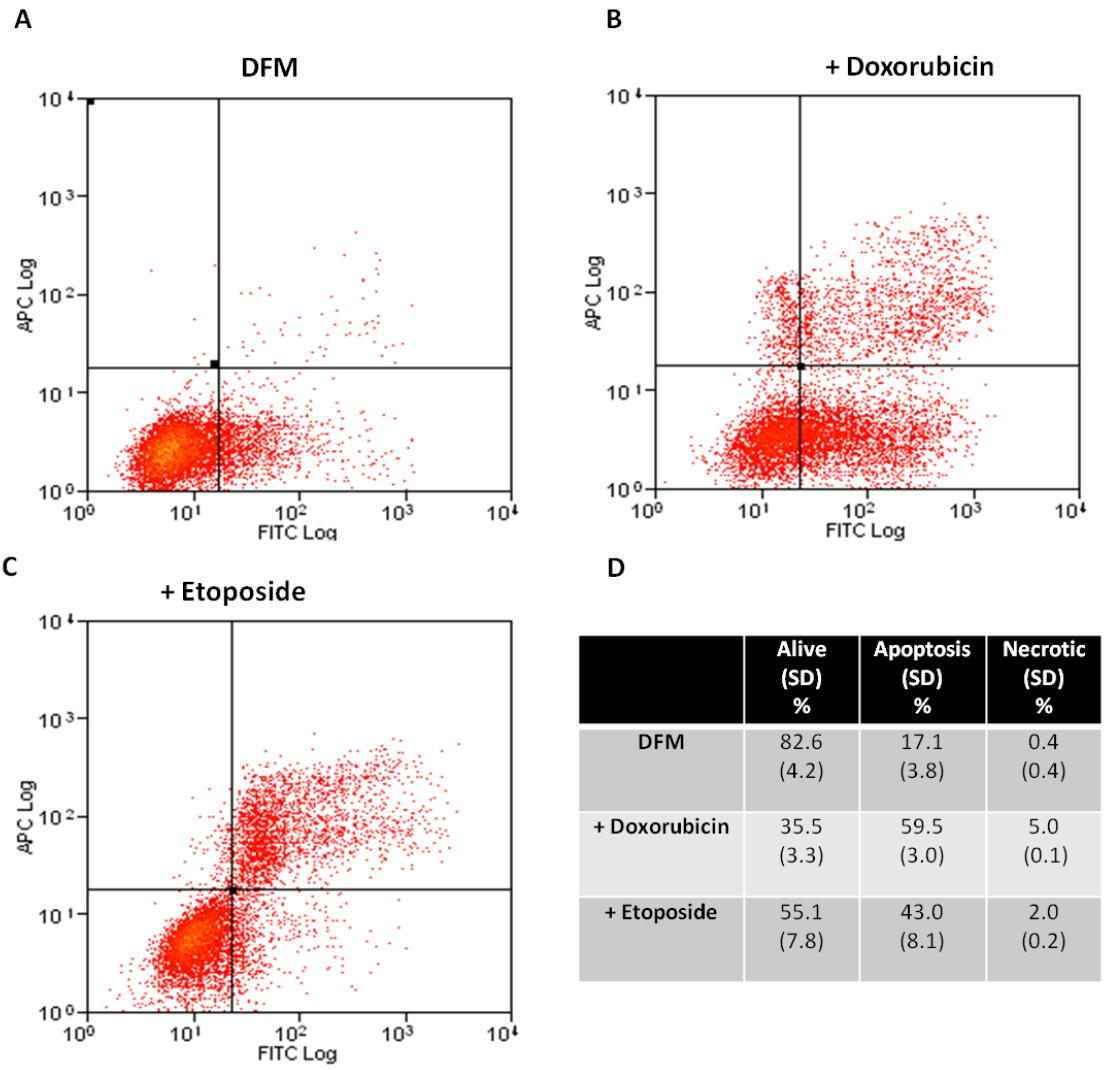

	Alive (SD) %	Apoptosis (SD) %	Necrotic (SD) %
DFM	82.6 (4.2)	17.1 (3.8)	0.4 (0.4)
+ Doxorubicin	35.5 (3.3)	59.5 (3.0)	5.0 (0.1)
+ Etoposide	55.1 (7.8)	43.0 (8.1)	2.0 (0.2)

Figure 4.27 Induction of apoptosis by doxorubicin and etoposide
Cells were grown for 48 hours prior to treatment with (A) DFM, (B) doxorubicin (5 µM) or (C) etoposide (50 µM) for 2 hours. Cells were then incubated for a further 24 hours in DFM, prior to collection and processing. The fluorescence of 10, 000 cells was measured using FACS. Representative images for each experiment are presented. Data are presented as the mean±SD % of 10,000 cells from two independent experiments

4.7.4 The induction of apoptosis by doxorubicin and etoposide in cells treated gefitinib or lapatinib for one hour

Following gefitinib treatment for one hour, 20.3±0.4% of cells are identified as undergoing apoptosis (Figure 4.28A). Though doxorubicin increases this to 62±4.7%,

this is not higher that the 59.5±3.0% of cell identified as apoptotic with doxorubicin alone. Etoposide is able to increase the degree of apoptosis observed in gefitinib pre-treated cells to 55.2±15.6%, which is greater than that produced by etoposide alone (43.0±8.1%) (Figure 4.28).

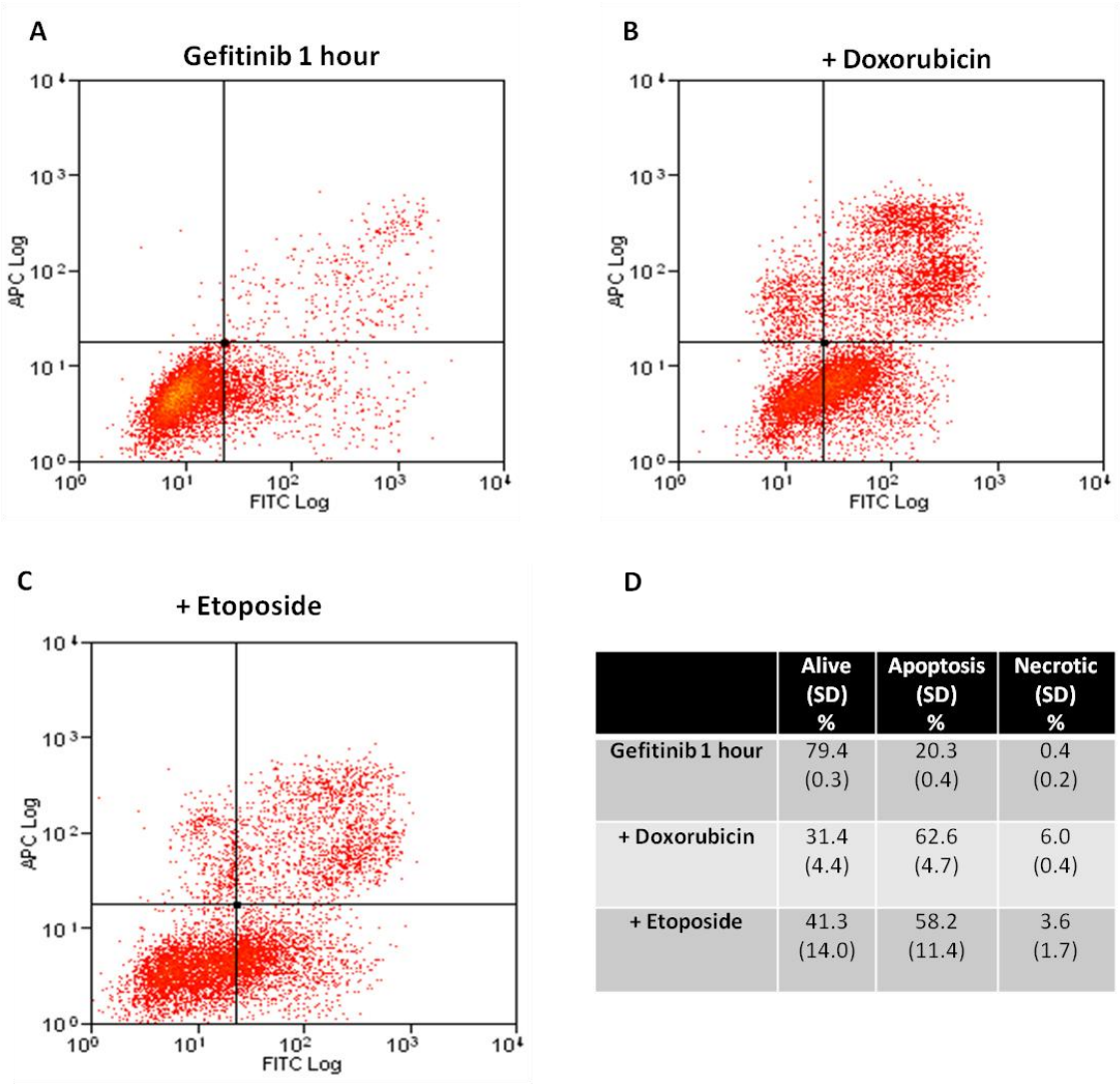

	Alive (SD) %	Apoptosis (SD) %	Necrotic (SD) %
Gefitinib 1 hour	79.4 (0.3)	20.3 (0.4)	0.4 (0.2)
+ Doxorubicin	31.4 (4.4)	62.6 (4.7)	6.0 (0.4)
+ Etoposide	41.3 (14.0)	58.2 (11.4)	3.6 (1.7)

Figure 4.28 Induction of apoptosis by doxorubicin and etoposide following gefitinib exposure for one hour

Cells were grown for 48 hours prior to treatment with gefitinib 5 µM for one hour (A) followed by the addition doxorubicin (5 µM) (B) or etoposide (50 µM) (C) for two hours. Cells were then incubated for a further 24 hours in fresh media +/- gefitinib, prior to collection and processing. The fluorescence of 10, 000 cells was measured using FACS. Representative images for each experiment are presented. Data are presented as the mean±SD % of 10,000 cells from two independent experiments.

Lapatinib treatment alone induces 25.7±0.1% of cells to undergo apoptosis (Figure 4.29A). This increases to 50.6±1.5% in cells treated with doxorubicin following lapatinib for one hour, though this is lower than 59.5±3.0% of cells which are identified as apoptotic with doxorubicin alone. Etoposide increases the number of apoptotic cells

over both lapatinib alone (25.7±0.1%) and etoposide alone (43.0±8.1%) to 64.5±7.6% in cells pre-treated with lapatinib for one hour (Figure 4.29).

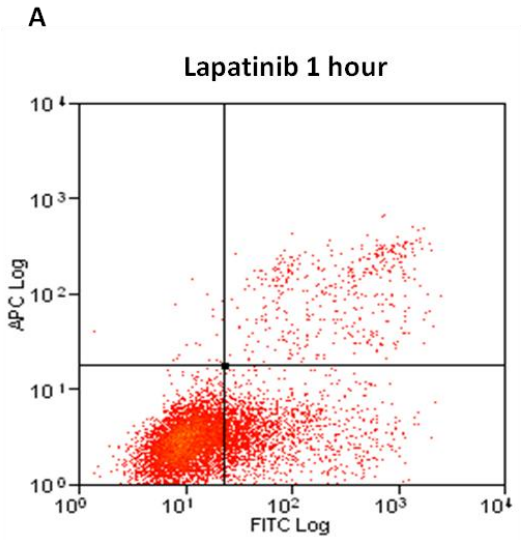

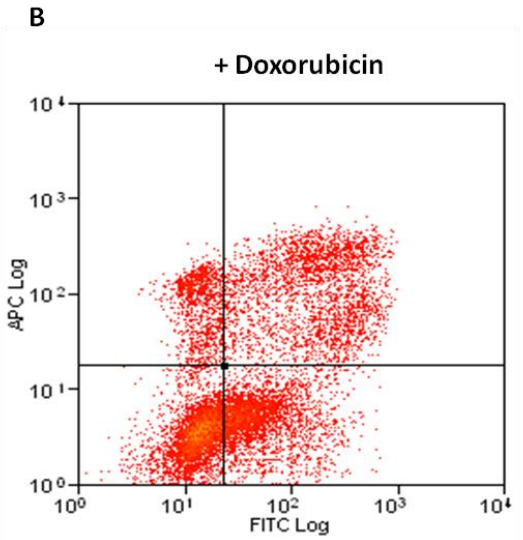

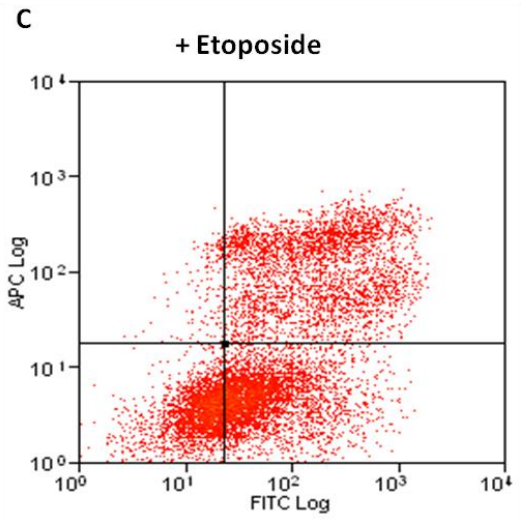

D

	Alive (SD) %	Apoptosis (SD) %	Necrotic (SD) %
Lapatinib 1 hour	73.9 (0.0)	25.7 (0.1)	0.4 (0.1)
+Doxorubicin	40.0 (2.7)	50.6 (1.5)	10.9 (4.2)
+ Etoposide	32.6 (5.2)	64.5 (7.6)	2.9 (2.4)

Figure 4.29 Induction of apoptosis by doxorubicin and etoposide following lapatinib exposure for one hour

Cells were grown for 48 hours prior to treatment with lapatinib 2 µM for one hour (A) followed by the addition doxorubicin (5 µM) (B), or etoposide (50 µM) (C) for two hours. Cells were then incubated for a further 24 hours in media +/- lapatinib, prior to collection and processing. The fluorescence of 10, 000 cells was measured using FACS. Representative images for each experiment are presented. Data are presented as the mean±SD % of 10,000 cells from two independent experiments.

4.7.5 The induction of apoptosis by doxorubicin and etoposide in cells treated with gefitinib or lapatinib for 48 hours

Gefitinib exposure for 48 hours induces 19.6±0.6% of cells to undergo apoptosis. The addition of doxorubicin reduces this figure to 11.3±2.1% and 15.4±2.0% with etoposide (Figure 4.30). Similar results were seen in cells treated with lapatinib for 48 hours with

45.6±1.9% of cells treated with lapatinib alone undergoing apoptosis (Figure 4.31). This number is reduced by treatment with doxorubicin, to 22.3±7.7% and is unaltered by treatment with etoposide 45.6±7.2% (Figure 4.31).

These results indicate that cells pre-treated with either gefitinib or lapatinib are rendered resistant to the cytotoxic effects of both doxorubicin and etoposide. Short exposure to gefitinib or lapatinib for one hour increases the cytotoxicity of etoposide but has little effect on doxorubicin-induced apoptosis 24 hours after exposure to the drug.

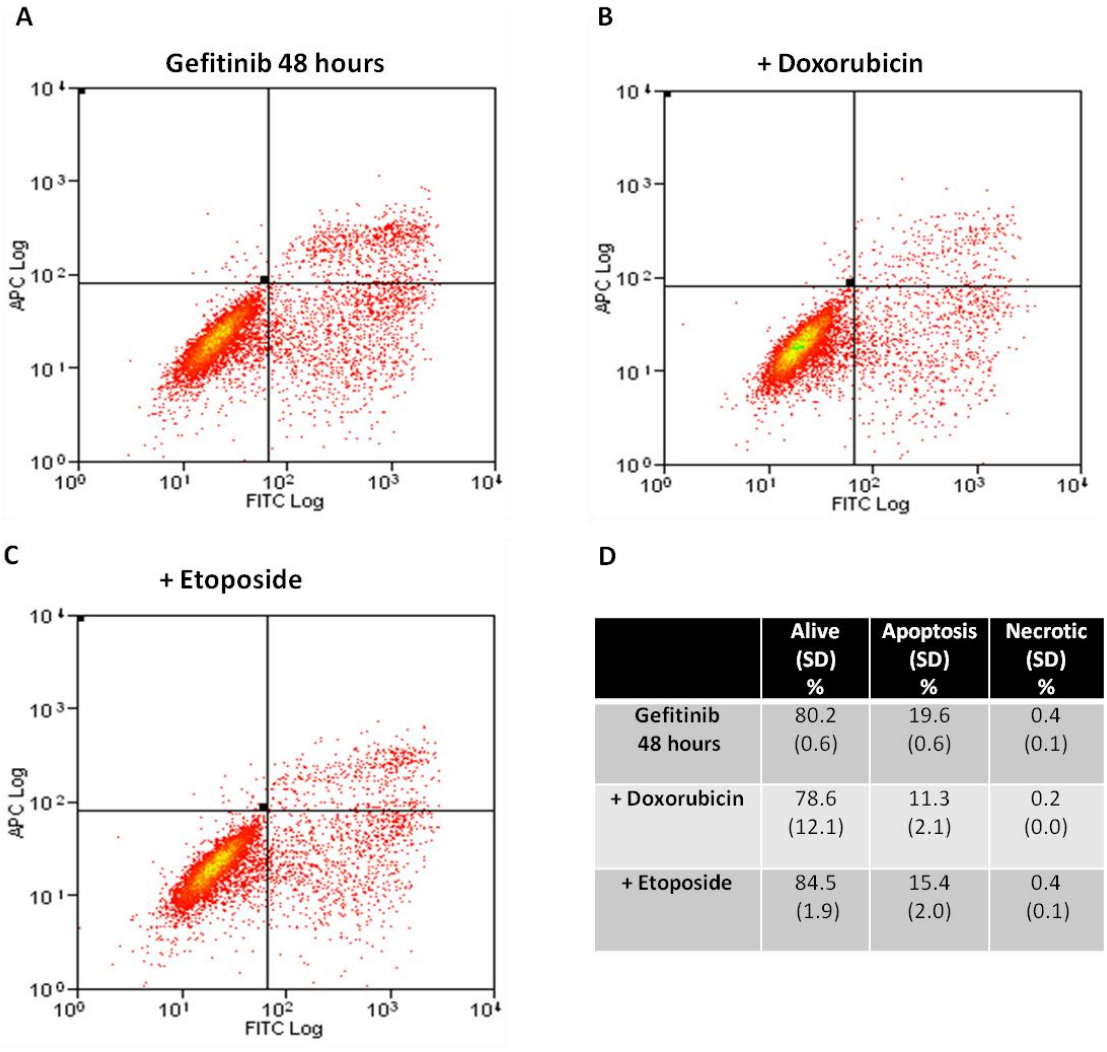

	Alive (SD) %	Apoptosis (SD) %	Necrotic (SD) %
Gefitinib 48 hours	80.2 (0.6)	19.6 (0.6)	0.4 (0.1)
+ Doxorubicin	78.6 (12.1)	11.3 (2.1)	0.2 (0.0)
+ Etoposide	84.5 (1.9)	15.4 (2.0)	0.4 (0.1)

Figure 4.30 Induction of apoptosis by doxorubicin and etoposide in cells treated with gefitinib continuously for 48 hours
Cells were grown for 48 hours prior to treatment with gefitinib 5 µM for one hour (A) followed by the addition doxorubicin (5 µM) (B), or etoposide (50 µM) (C) for two hours. Cells were then incubated for a further 24 hours in media +/- gefitinib, prior to collection and processing. The fluorescence of 10, 000 cells was measured using FACS. Representative images for each experiment are presented. Data are presented as the mean±SD % of 10,000 cells from two independent experiments.

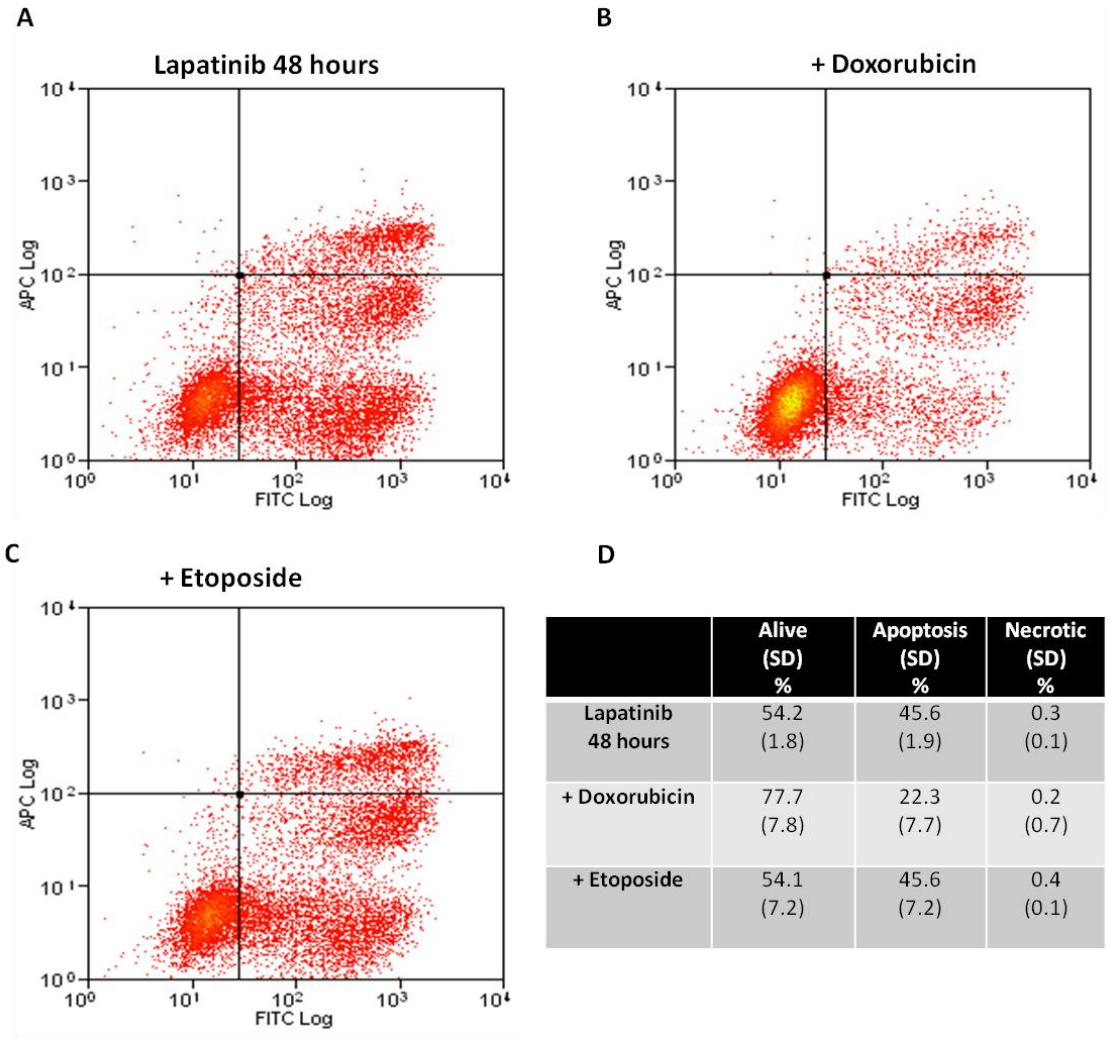

	Alive (SD) %	Apoptosis (SD) %	Necrotic (SD) %
Lapatinib 48 hours	54.2 (1.8)	45.6 (1.9)	0.3 (0.1)
+ Doxorubicin	77.7 (7.8)	22.3 (7.7)	0.2 (0.7)
+ Etoposide	54.1 (7.2)	45.6 (7.2)	0.4 (0.1)

Figure 4.31 Induction of apoptosis by doxorubicin and etoposide in cells treated with lapatinib continuously for 48 hours

Cells were grown for 48 hours prior to treatment with lapatinib 2 μM for one hour (A) followed by the addition doxorubicin (5 μM) (B), or etoposide (50 μM) (C) for two hours. Cells were then incubated for a further 24 hours in media +/- lapatinib, prior to collection and processing. The fluorescence of 10, 000 cells was measured using FACS. Representative images for each experiment are presented. Data are presented as the mean±SD % of 10,000 cells from two independent experiments.

4.8 DISCUSSION

This chapter describes the results of investigations examining the effect of duration of exposure to gefitinib or lapatinib on the induction and repair of DNA lesions induced by cisplatin, IR, doxorubicin and etoposide. These data demonstrate that both lapatinib and gefitinib produce similar effects on the induction and repair of DNA lesions by doxorubicin and etoposide, but differ in their effects on cisplatin and IR-induced DNA lesions. The duration of exposure to either gefitinib or lapatinib prior to the addition of

DNA damaging agent alters the ability of doxorubicin and etoposide to induce DNA damage and alters the rate of repair of etoposide-induced DSBs.

4.8.1 The alteration of HER3, AKT and MAPK signalling by duration of lapatinib exposure

Lapatinib inhibits the phosphorylation of HER3, AKT and MAPK within one hour (Figure 4.5). With continued lapatinib treatment, both AKT and MAPK signalling resume at 48 hours, though at a lower level than observed in untreated cells. Amin *et al.* have examined the effect of varying concentrations of lapatinib on HER, AKT and MAPK signalling (Amin *et al.*, 2010). They report that concentrations of lapatinib as low as 50 nM inhibit HER2, HER3, AKT and MAPK signalling within one hour. Despite continuous replacement of lapatinib every 24 hours, HER3, AKT and MAPK signalling resumes at 48 hours onwards. However, this signalling is dependent upon the concentration of lapatinib used with 50 nM and 200 nM lapatinib allowing the full resumption of HER3, AKT and MAPK signalling. Concentrations of 1 μM lapatinib reduce the strength of signalling detected at 48 hours and 5 μM prevents HER3 and AKT phosphorylation with only slight MAPK phosphorylation detected at 48 hours; at all concentrations of lapatinib, no HER2 phosphorylation is detected (Amin *et al.*, 2010). The mechanism through which HER3 is phosphorylated in the presence of HER2 inhibition is unresolved, but Amin *et al.* demonstrate an increase in HER2 and HER3 expression and that the reactivation of HER3 is driven by the initial reduction in AKT signalling induced by lapatinib (Amin *et al.*, 2010).

4.8.2 The modulation of the induction and repair of cisplatin-induced interstrand crosslinks by duration of exposure to gefitinib or lapatinib

Cisplatin produces DNA interstrand and intrastrand crosslinks and DNA DSBs (Clingen *et al.*, 2008). The pre-treatment of cells with TKI either for one or 48 hours does not significantly alter the number of interstrand crosslinks produced by cisplatin compared with those produced by cisplatin alone (Figure 4.6).

One of the determinants of resistance to cisplatin is the ability to remove and repair the DNA damage produced by interstrand crosslinks. An early step in their repair is the unhooking of the crosslink from one strand of DNA (Clingen *et al.*, 2008). The modified

alkaline Comet assay detects the unhooking of these lesions, allowing the investigation of this step in the repair process. γH2AX foci are also formed in response to cisplatin, due to the production of DNA DSBs produced by the collision of replication forks with interstrand crosslinks, and in response to their direct removal and repair (Clingen *et al.*, 2008). The modulation of repair of cisplatin-induced DNA damage by gefitinib or lapatinib was investigated using the alkaline Comet assay together with the measurement of RAD51 and γH2AX foci induction and resolution.

The pre-treatment of cells continuously with gefitinib for 48 hours markedly inhibits the unhooking of cisplatin-induced interstrand crosslinks (Figures 4.10). This observation is supported by the examination of γH2AX foci with persistence of foci for 72 hours in cells pre-treated with gefitinib for 48 hours, in comparison with cells treated with cisplatin where the numbers of foci falls to baseline levels within 24 hours (Figure 4.13). The measurement of RAD51 foci indicates that these cells are unable to be repaired by the process of HR, as the number of foci remains raised for the 72 hours duration of the experiment (Figure 4.14). Gefitinib treatment for one hour has a lesser effect on the unhooking of interstrand crosslinks with a significant difference only detected at 72 hours (Figure 4.11). The resolution of γH2AX foci indicates a delay in the repair process though by 72 hours there are no significant differences in the number of residual foci compared with cells treated with cisplatin alone (Figure 4.13). The process of HR is active in cells pre-treated with gefitinib for one hour as demonstrated by a return to baseline levels of RAD51 foci within 72 hours (Figure 4.14). Though these data suggest that the process of HR maybe attenuated in these cells, as the peak number of foci is reduced compared with cells treated with cisplatin alone (Figure 4.14).

These data require careful consideration regarding the effect of cell cycle on cellular repair processes. It is established that the repair of interstrand crosslinks in replicating cells utilises different processes to those used in non-replicating cells (Knipscheer *et al.*, 2009; Muniandy *et al.*, 2010). In replicating cells, cells treated with cisplatin alone accumulate in the S-phase of the cell cycle (Figure 4.23A). This indicates that recognition and repair is ongoing with activation of the S-phase checkpoint. Within S-phase, replication coupled repair dominates and involves the collision of replication

forks with interstrand crosslinks to form a DSB and the attraction of proteins belonging to the Fanconi anaemia pathway to stalled replication forks (Knipscheer *et al.*, 2009; Muniandy *et al.*, 2010). Replication coupled repair has been demonstrated to involve multiple processes including NER, HR and TLS (Muniandy *et al.*, 2010). In cells pre-treated with either gefitinib or lapatinib for one hour, cell cycle analysis 24 hours after removal of cisplatin demonstrates a greater percentage of cells in S-phase compared with cells treated with either TKI alone (Figure 4.23A), indicating the activation of the S-phase check point and possibly that an attempt at repair is occurring even in the presence of TKI. This is supported by the Comet assay, γH2AX and RAD51 data which show gradual falls in the number of interstrand crosslinks, γH2AX and RAD51 foci (Figures 4.10, 4.13 and 4.14).

In non-replicating cells, the presence of an interstrand crosslink can be detected by both the recognition of its distorting effect on the helical structure of DNA and during transcription, attracting recognition proteins linked to the NER, BER and MMR pathways (Muniandy *et al.*, 2010). Cell cycle analysis demonstrates that cells treated with TKI for 48 hours alone enter G0/G1 cell cycle arrest, which is not altered by cisplatin (Figure 4.23A). In cells treated with gefitinib for 48 hours, no unhooking of interstrand crosslinks can be detected (Figure 4.10) and γH2AX and RAD51 foci do not resolve (Figures 4.13 and 4.14). Unlike the modified alkaline Comet assay, the measurement of γH2AX foci is not specific for the presence of an interstrand crosslink as they can be induced by the repair of other DNA damage, including DNA base repair (Banath *et al.*, 2010; Clingen *et al.*, 2008). This potentially explains why despite no unhooking of interstrand crosslinks is detected with gefitinib treatment for 48 hours, though around a third of γH2AX foci resolve (Figures 4.10 and 4.13).

Lapatinib differs from gefitinib in its modulation of the repair of cisplatin-induced interstrand crosslinks. The Comet assay demonstrates that there is no significant inhibition of the unhooking interstrand crosslinks in cells pre-treated with lapatinib for 48 hours, in comparison with no unhooking detected in cells treated with gefitinib for the same duration (Figure 4.12).

4.8.3 The modulation of the induction and repair of ionising radiation-induced DNA strand breaks by duration of exposure to gefitinib or lapatinib

The induction of DNA stand breaks by IR is not altered by either gefitinib or lapatinib, or the duration of exposure (Figure 4.8). Marked differences are observed between the effects of gefitinib and lapatinib on the repair of IR-induced strand breaks (Figure 4.15). Lapatinib, regardless of the length of treatment, has no effect on the repair of IR-induced DNA strand breaks (Figure 4.15A), though gefitinib for one or 48 hours exposure slows the repair of DNA strand breaks as assessed using the alkaline Comet assay (Figure 4.15B). These results cannot be explained by alterations in cell cycle as both lapatinib and gefitinib produced similar effects when given for one hour or continuously for 48 hours (Figure 4.23) indicating that the modulation of the repair by gefitinib but not lapatinib may be due to differences between the two drugs.

4.8.4 Differences between the effects of gefitinib and lapatinib?

Data examining the repair of cisplatin-induced interstrand crosslinks and IR-induced DNA strand breaks following treatment with TKI for 48 hours provides evidence that the effect of lapatinib and gefitinib are not the same, despite both inhibiting EGFR and HER2 signalling and producing similar effects on the cell cycle.

Differences between the effects of EGFR targeted TKIs (gefitinib, erlotinib, AG1487) and HER2 targeted TKIs (lapatinib and AG825) are supported by the literature. Firstly AG1487 and gefitinib, whilst inhibiting the phosphorylation of EGFR, induce the formation of EGFR homo and heterodimers and the binding of EGF (Arteaga *et al.*, 1997; Liao and Carpenter, 2009; Lichtner *et al.*, 2001) whereas lapatinib does not (Liao and Carpenter, 2009). Liao *et al*. demonstrate that the anti-EGFR antibody cetuximab promotes the internalisation and nuclear transport of EGFR, which is further enhanced by the EGFR targeted TKIs erlotinib, gefitinib and AG1478 (Liao and Carpenter, 2009). However, lapatinib (1 μM) is not able to enhance cetuximab-induced nuclear transport, but actually blocks it (Liao and Carpenter, 2009).

Further differences between HER2 targeted TKIs and EGFR targeted TKIs can be derived from differences in their ability to sensitise cells to IR. Erlotinib (5 μM) is able to sensitise cells to the effects of IR as measured by the ability of two lung cancer cell

lines to form colonies, yet the HER2 TKI AG825 (10 μM) has no effect on colony formation over IR alone (Toulany *et al.*, 2010). At the concentrations of erlotinib and AG825 investigated both drugs produce similar effects on HER and PI3K/AKT signalling when given as single agents (Sergina *et al.*, 2007), yet erlotinib inhibits IR-induced AKT activation, but AG825 does not (Toulany *et al.*, 2010).

Differences also occur in the production of HER2 cleavage products by IR with IR-induced activation of HER2 occurring through dimerisation with EGFR, producing the phosphorylated HER2 cleavage products p95 and p135 (Toulany *et al.*, 2010). Inhibition of EGFR by the TKI BIBX13682BS inhibits their production yet the HER2 targeted TKI AG825 does not, suggesting that despite EGFR and HER2 inhibition, dimerisation and the production of HER2 cleavage products can still occur (Toulany *et al.*, 2010). Together these data may indicate that gefitinib and lapatinib have different effects on cellular process, despite both inhibiting EGFR, HER2 and HER3 phosphorylation.

Resistance to the cytotoxic effects of IR have been linked to the ability to modulate the localisation and activity of DNA-PK (Dittmann *et al.*, 2005a; Dittmann *et al.*, 2005b; Mahaney *et al.*, 2009). IR-induced DNA-PK activity is reduced by cetuximab (Dittmann *et al.*, 2005b) and gefitinib (Friedmann *et al.*, 2006) and phosphorylation of DNA-PK catalytic subunit can be inhibited by erlotinib or the knockdown of HER2 by siRNA, but not by the TKI, AG825 (Toulany *et al.*, 2010). Treatment with cetuximab inhibits the nuclear transport of both EGFR and DNA-PK in response to IR, with immunoprecipitation experiments demonstrating their co-localisation in the cytoplasm (Dittmann *et al.*, 2005b). Additionally, DNA-PK is involved in the repair of cisplatin-induced DNA damage (Friedmann *et al.*, 2006; Shao *et al.*, 2008) and nuclear EGFR promotes resistance to cisplatin (Hsu *et al.*, 2009).

Together these data suggest that differences between the effects of gefitinib and lapatinib on EGFR dimerisation, nuclear transport and activation of DNA-PK may explain the TKI dependent differences on the repair of cisplatin and IR-induced DNA damage presented in this chapter. NHEJ is the main pathway in mammalian cells, at all stages of the cell cycle, by which IR-induced DNA damage is repaired and DNA-PK plays a key role in this system (Mahaney *et al.*, 2009). The fact that lapatinib, regardless of

duration, has no effect on the repair of IR-induced DNA strand breaks could be due to the failure of lapatinib to inhibit the phosphorylation of DNA-PK_{cs} as demonstrated by Toulany *et al.* (Toulany *et al.*, 2010).

The repair of interstrand crosslinks is more complicated utilising a number of different DNA repair pathways. The increase in cells in S-phase following cisplatin alone and following TKI exposure for one hour, suggests involvement of the Fanconi anaemia DNA repair proteins which activate the S-phase checkpoint (Knipscheer *et al.*, 2009; Muniandy *et al.*, 2010). This is not observed following TKI exposure for 48 hours, when cells are in G0/G1 arrest. This may mean that cells are more reliant upon DNA-PK to repair cisplatin-induced DNA damage, explaining why cells treated with lapatinib for 48 hours are able to repair interstrand crosslinks (DNA-PK_{cs} still active) in contrast to gefitinib where no repair is seen (DNA-PK_{cs} inhibited).

Data from our own laboratory demonstrates that EGFR needs to be in an active conformation in order to bind the DNA-PK catalytic subunit (Liccardi *et al.*, 2011). Gefitinib, erlotinib and AG1487 also bind and stabilise EGFR when it is in an active conformation (Johnson, 2009). However, lapatinib only binds to EGFR when it is in an inactive conformation (Johnson, 2009) and therefore is not able to bind EGFR which is bound to the DNA-PK catalytic subunit, which may explain why no alteration in the repair of IR-induced DNA lesion is observed in lapatinib treated cells.

4.8.5 The modulation of the induction and repair of doxorubicin and etoposide-induced DNA strand breaks by duration of exposure to gefitinib or lapatinib

In contrast to cisplatin and IR, both doxorubicin and etoposide induce fewer DNA strand breaks in cells treated with TKI for 48 hours, as detected by both the alkaline Comet assay and measurement of γH2AX foci (Figure 4.9, 4.19 and 4.20). This translates into resistance to Topo II poison-induced apoptosis, with fewer cells undergoing apoptosis following treatment with TKI for 48 hours, than observed with TKI alone (Figures 4.30 and 4.31). Therefore, the treatment of cells with TKI for 48 hours renders them resistant to the cytotoxic effects of doxorubicin and etoposide through the inhibition of the production of DNA strand breaks.

Another interesting observation is that doxorubicin, at all concentrations examined, is unable to induce significant numbers of DNA strand breaks in cells treated with TKI for 48 hours. However, etoposide induces strand breaks in a concentration-dependent manner, though at a significantly lower level than produced by etoposide alone, or in cells pre-treated with TKI for one hour (Figure 4.9). These breaks are also repaired more quickly than those produced by etoposide alone or in cells pre-treated with TKI for one hour (Figures 4.20). This indicates that either the mechanism of repair, or the type of DNA lesions produced by etoposide following TKI treatment for 48 hours, are different. The latter hypothesis is supported by data from analysis of γH2AX foci. Etoposide-induced DNA DSBs correlate with the induction of γH2AX foci, allowing its use as a surrogate marker for DSBs (Smart *et al.*, 2008). In cells pre-treated with gefitinib for 48 hours, significantly fewer foci are induced by etoposide or doxorubicin (Figures 4.19 and 4.21). This observation is not due to inhibition of γH2AX foci production in cells treated gefitinib for 48 hours, as both cisplatin and IR induce similar peak levels of foci in cells treated under the same conditions (Figures 4.13 and 4.16) nor is it due to the reduced concentration of chemotherapy drug used, as significantly more foci are induced in cells treated with chemotherapy drug alone, than in cells pre-treated with gefitinib for 48 hours (Figures 4.19 and 4.21). Therefore, these data indicate that following gefitinib treatment for 48 hours, etoposide is unable to induce DNA DSBs, as indicated by a fall in peak foci production from 64.3±11 foci/cell with etoposide alone, to 9.6±3.0 foci/cell in cells pre-treated with gefitinib for 48 hours, representing an 85% fall in the production of DNA DSBs (Figure 4.21). The production of DNA DSBs by etoposide is reported to represent only 3% of the strand breaks produced by the drug, with the remaining 97% accounted for by single strand breaks (Muslimovic *et al.*, 2009). This may explain why the alkaline Comet assay continues to detect etoposide-induced strand breaks in cells treated with TKI for 48 hours but there is a marked reduction in the production of γH2AX foci under the same conditions (Figure 4.21).

The alkaline Comet assay data does not demonstrate any modulation of the repair of doxorubicin-induced strand breaks by TKI exposure for one hour, though there are significantly more strand breaks at 10 hours compared with doxorubicin alone, indicating a second process which produces strand breaks coming into play (Figure

4.18). γH2AX foci following gefitinib for one hour also produces an interesting observation, with the peak of foci occurring earlier and at a lower level than in cells treated with doxorubicin alone (Figure 4.19). Additionally, γH2AX foci start to fall six hours after removal of doxorubicin in gefitinib pre-treated cells, indicating a delay but not inhibition of foci resolution (Figure 4.19). The significance of the resolution of γH2AX foci in terms of cell survival is unclear, as foci are part of a signalling system and their removal does not necessarily indicate that DNA has been fully repaired. However, persistence of γH2AX foci at 24 hours is linked to cell death (Banath *et al.*, 2010).

Pre-treatment of cells with TKI for one hour modulates the repair of etoposide induced DNA strand breaks by delaying, but not inhibiting their repair as assessed by the alkaline Comet assay (Figure 4.20). This indicates that TKIs interfere with DNA repair processes though these can be overcome, as demonstrated by near complete repair of strand breaks by 10 hours, fewer residual γH2AX foci at 24 hours and no increase in apoptosis (Figures 4.20, 4.21, 4.30 and 4.31).

4.8.6 The induction of DNA strand breaks by doxorubicin

Doxorubicin produces DNA strand breaks through interaction with Topo IIα directly and through non-Topo IIα methods, with strand breaks produced after the removal of the drug through production of ROS for example (Binaschi *et al.*, 1990; Yan *et al.*, 2009). This may explain the observed increase in DNA strand breaks after removal of doxorubicin observed in cells pre-treated with TKI for one hour and would be expected in cells pre-treated with TKI for 48 hours (Figure 4.18). The fact that in cells pre-treated with TKI for 48 hours, significant numbers of DNA strand breaks are not induced by doxorubicin, even at 24 hours indicates that not only is doxorubicin unable to poison Topo IIα, it is also unable to produce non-Topo IIα mediated DNA damage in these cells.

4.9 CONCLUSIONS

Continuous exposure to the TKI gefitinib or lapatinib for 48 hours induces the reactivation of both AKT and MAPK signalling, despite initial inhibition. TKIs modulate both the induction and repair of DNA lesions, in a manner dependent upon the TKI drug, the duration of TKI inhibition and the type of DNA damaging agent. Cells pre-

treated with TKIs for 48 hours are resistant to the DNA damaging effects of doxorubicin and etoposide but not the induction of DNA lesions by IR or cisplatin.

Lapatinib and gefitinib differ in their ability to modulate the repair of cisplatin-induced interstrand crosslinks and IR-induced DNA damage. Lapatinib does not affect the repair of IR-induced DNA damage and its inhibition of the repair of cisplatin-induced interstrand crosslinks is less pronounced than gefitinib, which inhibits the repair of both cisplatin and IR-induced DNA damage in cells pre-treated for 48 hours.

Both TKIs investigated produce similar effects on the repair of DNA lesions induced by etoposide and doxorubicin, with TKI treatment for one hour inhibiting repair. In contrast, fewer DNA strand breaks were induced in cells treated with either TKI continuously for 48 hours and these breaks were repaired more quickly. This observation may be explained by an alteration in the type of lesion induced by Topo II poisons in cells following exposure to gefitinib or lapatinib continuously for 48 hours.

Further work is needed to elucidate the reasons why gefitinib is able to modulate the repair interstrand crosslinks and IR-induced DNA damage yet lapatinib is not, and whether this translates into differences in cytotoxicity. If the inhibition of DNA interstrand crosslinks and DNA repair by gefitinib translates into increased cytotoxicity, a greater level of apoptosis should be observed in cells pre-treated with gefitinib prior to cisplatin or IR, compared with either agent alone or cells treated with lapatinib for 48 hours. The induction of γH2AX foci by cisplatin or IR in cells pre-treated with lapatinib for 48 hours would also be expected to demonstrate no significant alteration in the peak number of foci or their resolution. If these results confirmed that gefitinib inhibits the repair of cisplatin and IR-induced DNA damage but lapatinib does not, one potential explanation is a difference in the modulation of DNA-PK by EGFR between the two drugs. A direct comparison between the two TKIs on DNA-PK_{cs} phosphorylation, activity and nuclear transport in response to cisplatin or IR would be expected to demonstrate inhibition by gefitinib but not lapatinib.

The modulation of the cellular effects of topoisomerase II poisons by duration of exposure to gefitinib or lapatinib

5.1 INTRODUCTION

The results presented in Chapter Four demonstrate that continuous exposure to gefitinib or lapatinib induces resistance to the cytotoxic effects of the Topo II poisons doxorubicin and etoposide, in part through the inhibition of DNA strand break production. Resistance to Topo II poisons can be mediated through a reduction in intracellular drug concentration, Topo II expression or Topo II activity as discussed in Chapter One section 1.7.3. This chapter describes investigations into the mechanism by which exposure to TKIs renders cells resistant to the cytotoxic effects of Topo II poisons.

5.1.1 Topoisomerase II poisons

A number of chemotherapy drugs used in the management of a wide variety of cancers poison Topo II, including doxorubicin, epirubicin, etoposide, mitoxantrone and m-AMSA. These drugs can be grouped according to their dependence on ATP or their ability to intercalate DNA (Nitiss, 2009b). Both doxorubicin and etoposide are classified as ATP-dependent Topo II poisons, with ATP depletion preventing their poisoning of Topo II and the induction of DNA breaks (Sorensen *et al.*, 1999). Doxorubicin is an intercalating Topo II poison in contrast with etoposide, which is an non-intercalating drug (Nitiss, 2009b). In order to investigate whether TKI-induced resistance to the DNA damaging effects of Topo II poisons is due to their dependence on ATP, two further drugs m-AMSA and menadione were investigated.

5.1.1.1 M-AMSA

M-AMSA is an intercalating Topo II poison and is used in the systemic management of acute myeloid leukaemia (Nitiss, 2009b). Its dependence on ATP is not clear with *in vitro* studies demonstrating both ATP-independence (Sorensen *et al.*, 1999) and ATP-dependence (Wang *et al.*, 2001).

5.1.1.2 Menadione (vitamin K3)

Menadione is a synthetic compound that was chosen for investigation due to its classification as an ATP-independent Topo II poison (Sorensen *et al.*, 1999; Wang *et al.*, 2001). However, recent reports have confirmed that the drug's main mechanism of action is through the depletion of glutathione, increasing the production of ROS producing single stranded DNA breaks (Marchionatti *et al.*, 2009).

5.1.2 Inhibition of the induction of DNA double strand breaks

The γH2AX data presented in Chapter Four indicates that exposure to either gefitinib or lapatinib for 48 hours reduces the induction of γH2AX in response to doxorubicin and etoposide. DNA DSBs induce γH2AX foci and are often used as a surrogate marker for the identification of these lesions (Bonner *et al.*, 2008). However, γH2AX foci induction is reliant upon the activity of PI3K-like kinases including DNA-PK, ATM and ATR (Bonner *et al.*, 2008). The data presented in Chapter Four demonstrates that the induction of γH2AX foci by cisplatin or IR is not significantly altered by the duration of exposure to gefitinib, indicating that the mechanism for the formation of foci is not inhibited. Therefore, a reduction in the number of γH2AX foci induced by doxorubicin and etoposide observed in cells treated with TKI for 48 hours may indicate a reduction in the numbers of DNA DSBs produced under these conditions.

A mechanism for assessing the presence of DNA DSBs more directly is the neutral Comet assay (discussed further in section 5.9.1). This assay was used to assess the modulation of the ability of Topo II poisons to induce DNA DSBs in cells treated with gefitinib for one or 48 hours.

5.1.3 Modulation of topoisomerase II expression and activity by tyrosine kinase inhibitors

Resistance to Topo II poisons can be mediated by a variety of methods and the literature supports two possible connections with HER inhibition. As demonstrated in Chapter Four, TKIs induce a G0/G1 cell cycle arrest, a state which is linked to reduced expression of Topo IIα (Pommier *et al.*, 2010), which may be one mechanism through which resistance to doxorubicin and etoposide is mediated. The second mechanism is through an alteration in Topo II activity. Active Topo II, producing cleavable complexes,

is essential for Topo II poisons to function as they prevent the religation of the DNA DSB contained within the cleavable complex. Topo II poison activity is associated with the phosphorylation of Topo IIα at serine 1106 with hypophosphorylation at this site inducing resistance to the cytotoxic effects of both m-AMSA and etoposide (Chikamori *et al.*, 2003). Serine 1106 is phosphorylated by casein kinase Iδ (Grozav *et al.*, 2009) an enzyme which is inhibited by gefitinib (Brehmer *et al.*, 2005). Therefore, TKIs may inhibit the activity of the Topo II enzyme and induce resistance to Topo II poisons.

5.2 AIMS

1. Does the duration of exposure to gefitinib or lapatinib modulate the **induction** of DNA strand breaks by m-AMSA and menadione?
2. Does duration of exposure to gefitinib and lapatinib modulate the **expression** and **activity** of Topo II?
3. Does the reduction of Topo IIα expression modulate the **production** of DNA strand breaks by Topo II poisons?
4. Does the duration of exposure to gefitinib modulate the **production** of DNA DSBs by Topo II poisons as detected by the neutral Comet assay?

5.3 THE EFFECT OF DURATION OF EXPOSURE TO GEFITINIB OR LAPATINIB ON THE DNA DAMAGING EFFECTS OF M-AMSA AND MENADIONE

The ability of m-AMSA and menadione to induce DNA strand breaks in SK-Br-3 cells following exposure to gefitinib or lapatinib was assessed using the alkaline Comet assay.

5.3.1 Induction of DNA strand breaks by m-AMSA and menadione

M-AMSA induces strand breaks in a concentration dependent manner which is not significantly altered by the duration of exposure to either gefitinib or lapatinib (Figure 5.1).

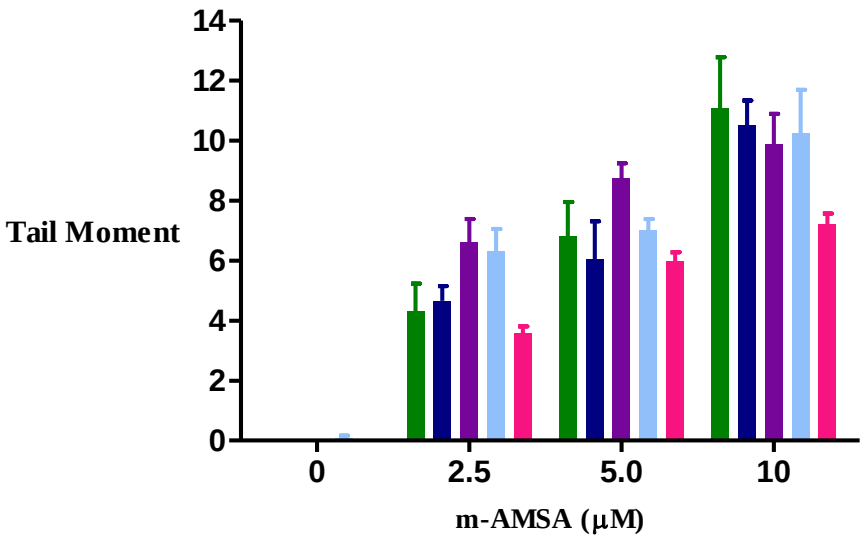

Figure 5.1 Effect of duration of exposure to gefitinib or lapatinib on the Induction of DNA strand breaks by m-AMSA
The alkaline comet assay was used to assess the induction of DNA strand breaks by m-AMSA. Cells were pre-treated with either DFM (■), gefitinib 1 hour (■), gefitinib 48 hours (■), lapatinib 1 hour (■), or lapatinib 48 hours (■), before addition of m-AMSA one hour. Data are presented as the mean±SEM, *p<0.05 compared with m-AMSA.

The inducer of ROS, menadione, also induces DNA strand breaks in a concentration dependent manner. This is not altered by the pre-treatment of cells with gefitinib for one hour, though significantly more strand breaks are induced in cells treated with gefitinib for 48 hours; this meant that concentrations above 25 μM could not be

examined due to the high levels of dead cells detected using the Comet assay following pre-treatment with gefitinib for 48 hours (Figure 5.2).

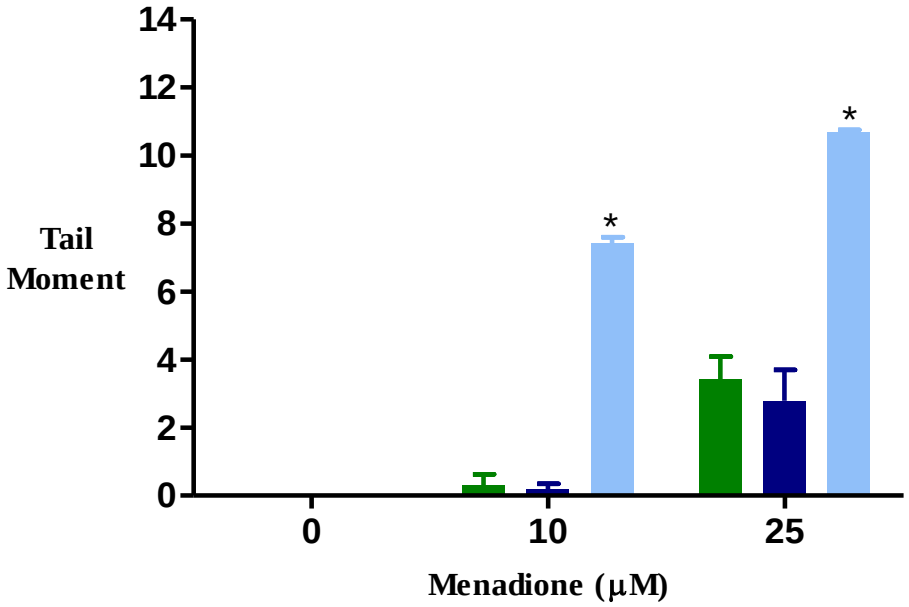

Figure 5.2 Effect of duration of exposure to gefitinib on the induction of DNA strand breaks by menadione
The alkaline comet assay was used to assess the induction of DNA strand breaks by menadione Cells were pre-treated with either DFM (■), one hour gefitinib (■), 48 hours gefitinib (■) before the addition of menadione for one hour. Data are presented as the mean±SEM, *p<0.05 compared with menadione alone

5.3.2 Repair of m-AMSA-induced DNA damage

The repair of DNA strand breaks was assessed by examining the resolution of Comet tails as detected by the alkaline Comet assay and γH2AX foci following the treatment of cells with m-AMSA.

5.3.2.1 Repair of m-AMSA-induced DNA strand breaks

For the assessment of the repair of m-AMSA–induced DNA strand breaks, data are expressed as a percentage of the tail moment obtained immediately following incubation with m-AMSA. The repair of all strand breaks is completed within 72 hours in all drug combinations (Figure 5.3). Pre-treatment with TKI increases the rate of repair with 57.3±2.3% and 68.6±6.1% of strand breaks repaired within 30 minutes in cells treated with gefitinib for one or 48 hours and 46.5±7.0% and 54.5±1.2% of strand breaks in cells treated with lapatinib for one or 48 hours. This compares with only 32.2±3.8% in cells treated with m-AMSA alone (P<0.05) (Figure 5.3). Therefore,

exposure to gefitinib or lapatinib, regardless of duration, increases the rate of repair of m-AMSA-induced DNA strand breaks as detected by the alkaline Comet assay.

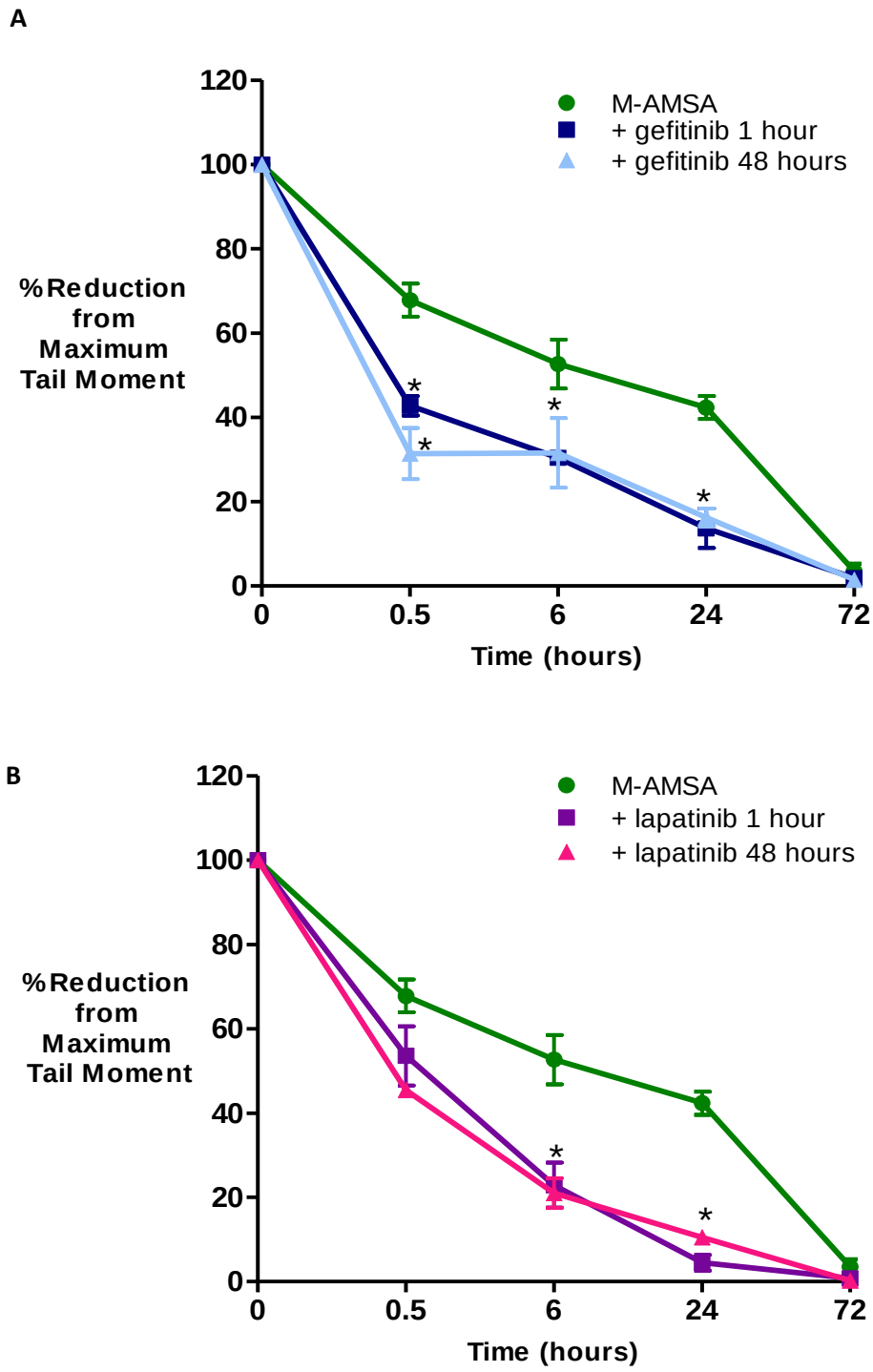

Figure 5.3 Effect of duration of exposure to gefitinib or lapatinib on the repair of m-AMSA-induced DNA strand breaks

The repair of DNA strand breaks was assessed using the alkaline comet assay. Cells were pre-treated with either DFM, (A) gefitinib or (B) lapatinib for one or 48 hours before the addition of m-AMSA (5 μM) for one hour. Media was replaced ±TKI and cells harvested at the indicated time points. Data are presented as the mean±SEM of three independent experiments. *p>0.05 compared with m-AMSA alone.

5.3.2.2 Modulation of m-AMSA-induced γH2AX foci by gefitinib

The induction of γH2AX foci by m-AMSA (0.5 µM) peaks at four hours at 39.3±3.5 foci/cell. A small fall in foci occurs between four and six hours but then no further resolution of foci is observed (Figure 5.4). Exposure to gefitinib for one hour reduces the peak number of γH2AX foci to 29.1±4.5foci/cell, though this is not statistically significant. There is also no significant difference in the rate of resolution of γH2AX foci between cells treated with m-AMSA only and those pre-treated gefitinib for one hour (Figure 5.4). In cells treated with gefitinib for 48 hours, the peak of γH2AX foci induction is significantly reduced to 2.1±0.8 foci/cell ($p<0.01$), with significantly fewer foci observed at all time points for the duration of the experiment (Figure 5.4). These data indicate that fewer γH2AX foci are produced in cells pre-treated with gefitinib for 48 hours at all time points investigated suggesting that fewer DNA DSBs are produced under these conditions.

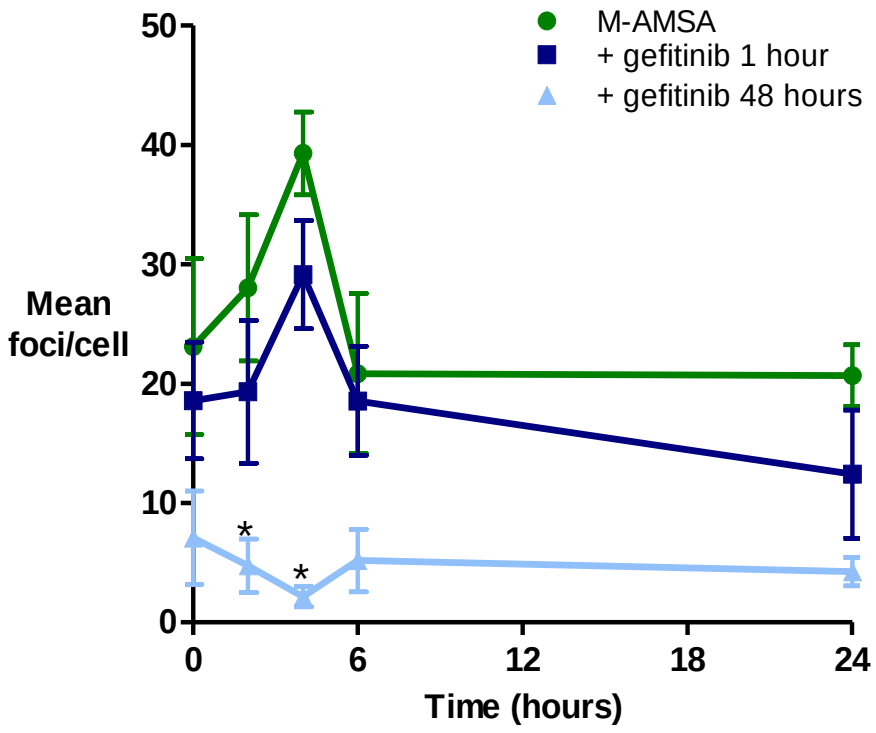

Figure 5.4 Effect of the duration of exposure to gefitinib on the induction and resolution of m-AMSA-induced γH2AX foci

The induction and resolution of γH2AX foci following m-AMSA was studied in cells pre-treated with DFM or gefitinib for one or 48 hours before the addition of m-AMSA (0.5 µM) for one hour. Media was replaced±TKI and cells harvested at the indicated time points. Data are presented as the mean±SEM of three independent experiments. *$p>0.05$ compared with m-AMSA alone.

5.4 THE MODULATION OF M-AMSA-INDUCED CELL CYCLE ARREST AND CYTOTOXICITY BY TYROSINE KINASE INHIBITION

5.4.1 Modulation of m-AMSA-induced cell cycle arrest by gefitinib or lapatinib

The effects of m-AMSA on the cell cycle were assessed in cells 24 hours after exposure to m-AMSA for one hour. M-AMSA (5 µM) increases the number of cells in S-phase to 40.9±6.9% from 11.1±1.6% in untreated cells (Figure 5.5). An m-AMSA-induced increase in S-phase is also observed in cells pre-treated with gefitinib for one hour with 13.2±2.0% cells in S-phase compared with 3.1±1.0% in cells treated with gefitinib alone, though this is lower than the 40.9±6.9% of cells in S-phase following m-AMSA alone (Figure 5.5). Similar results are obtained with exposure to lapatinib for one hour with 2.3±0.3% of lapatinib only treated cells in S-phase compared with 11.8±2.8% in cells treated in combination with m-AMSA. M-AMSA does not alter the cell cycle in cells pre-treated with either gefitinib or lapatinib continuously for 48 hours (Figure 5.5).

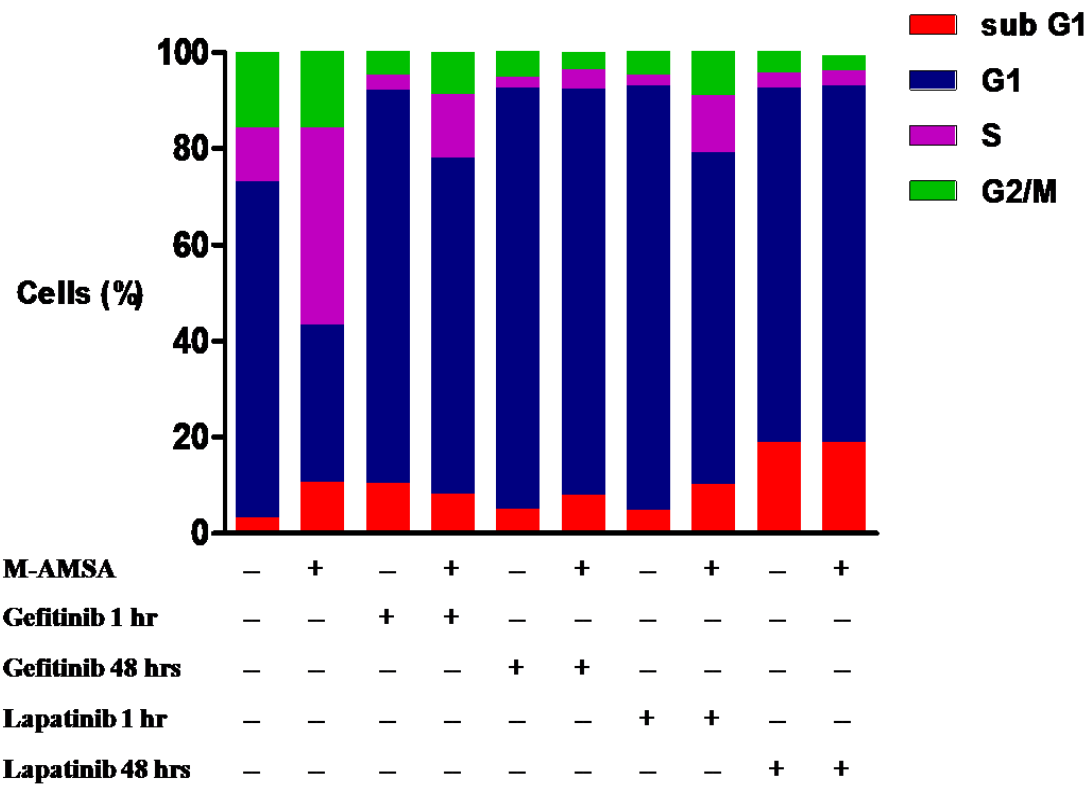

Figure 5.5 Effect of m-AMSA on the cell cycle
SK-Br-3 cells were treated with gefitinib or lapatinib for one or 48 hours prior to the addition of 5 µM m-AMSA for one hour. Cells were collected 24 hours later and the DNA content analysed by staining with propidium iodide. Data presented as the mean of three independent experiments.

5.4.2 Modulation of m-AMSA-induced apoptosis by gefitinib or lapatinib

M-AMSA induces 56.5±4.7% of cells to undergo apoptosis 24 hours after exposure, compared with 17.1±3.8% in untreated cells, as assessed by the measurement of annexin V (Table 5.1 and Figure 5.6). In cells pre-treated with gefitinib or lapatinib for one hour, 64.1±13.9% or 64.8±10.3% of cells respectively are undergoing apoptosis, compared with 20.3±0.4% and 25.7±0.1% with either TKI alone. M-AMSA is unable to induce apoptosis in cells treated with continuously either TKI for 48 hours over that produced by TKI alone, with 18.1±1% and 43.0±8.3% of cells treated with gefitinib or lapatinib respectively undergoing apoptosis compared with 19.6±0.6% and 45.6±1.9% apoptosis observed in cells treated with TKI alone (data for TKI alone presented in Chapter 4, 4.7.2).

m-AMSA 5 µM +	Alive±SD (%)	Apoptosis±SD (%)	Necrotic±SD (%)
DFM	41.5±4.6	56.5±4.7	2.1±0.1
Gefitinib 1 hour	34.7±13.6	64.1±13.9	1.2±0.4
Gefitinib 48 hours	81.6±1.9	18.1±1.9	0.3±0.1
Lapatinib 1 hour	34.0±9.5	64.8±10.2	1.2±0.7
Lapatinib 48 hours	55.3±10.4	43.0±8.3	1.6±2.1

Table 5.1 Induction of apoptosis by m-AMSA in cells treated with gefitinib or lapatinib
Cells were treated with drug free media, gefitinib for 1 or 48 hours or lapatinib for 1 or 48 hours hour. Cells were then treated with m-AMSA 5 µM for two hours. The media was then replaced with fresh media +/- TKI and cells collected 24 hours after exposure to m-AMSA. Cells were dual stained with sytox red and anti-annexin V antibody conjugated to a fluorochrome to identify apoptotic and necrotic cells (see Figure 5.6). The fluorescence of 10, 000 cells was measured using FACS. Data are presented as the mean±SD% of 10,000 cells from two independent experiments.

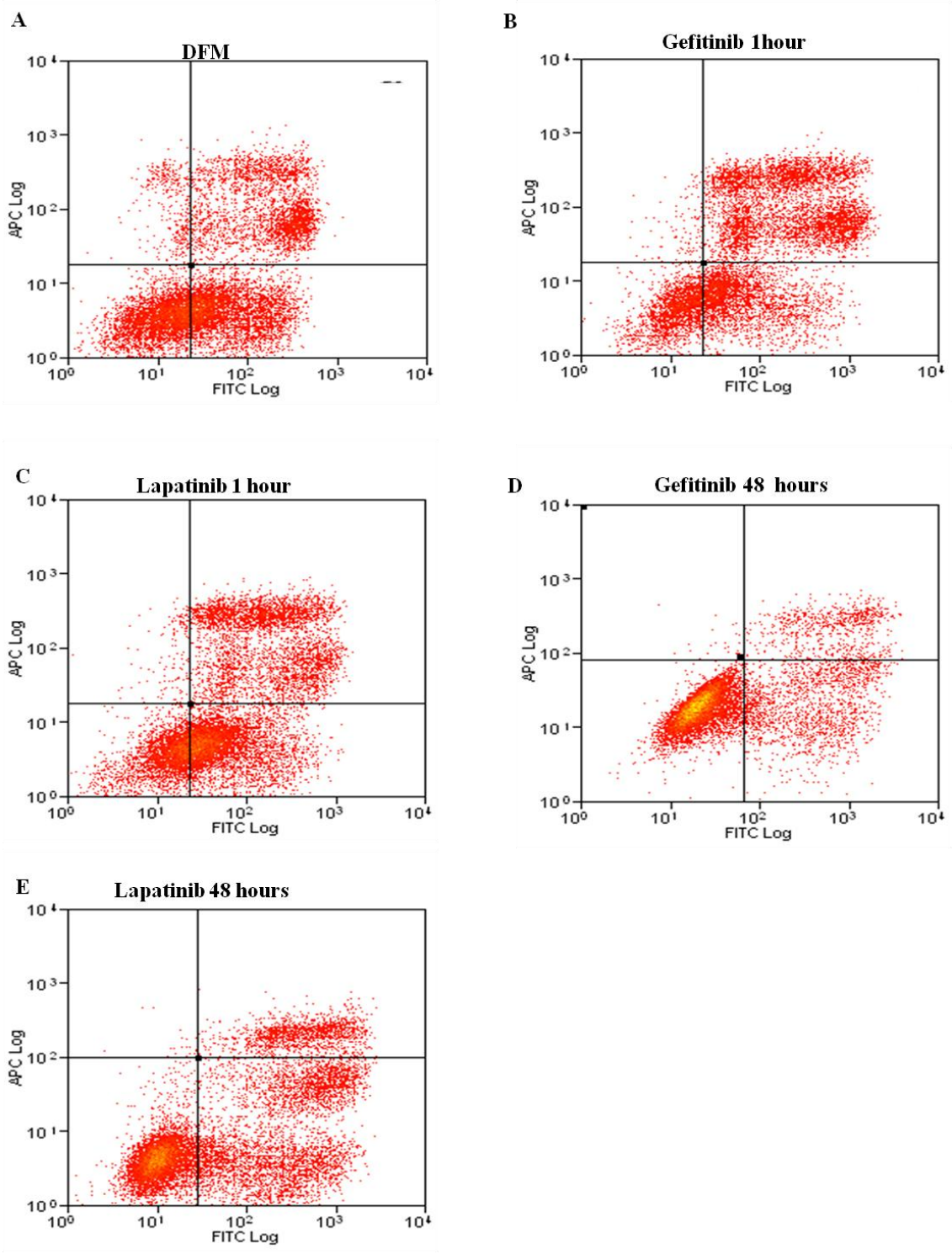

Figure 5.6 Induction of apoptosis by m-AMSA

Cells were treated with (A) drug free media, (B) gefitinib 1 hour (C) lapatinib 1 hour, (D) gefitinib 48 hours and (E) lapatinib 48 hours, followed by m-AMSA 5 µM for two hours. The media was then replaced with fresh media +/- TKI and cells collected 24 hours after exposure to m-AMSA. Cells were dual stained with sytox red and anti-annexin V antibody conjugated to a fluorochrome. The fluorescence of 10, 000 cells was measured using FACS. Representative images for each experiment are presented. Data are presented as the mean±SD% of 10,000 cells from two independent experiments.

5.5 Modulation of the intracellular uptake of doxorubicin by gefitinib or Lapatinib

As discussed in Chapter One section 1.7.1, multi-drug resistance transporters can induce resistance to many chemotherapy drugs, including doxorubicin and etoposide (Gottesman *et al.*, 2002). Both gefitinib (Kitazaki *et al.*, 2005; Leggas *et al.*, 2006; Nakamura *et al.*, 2005; Yang *et al.*, 2005) and lapatinib (Dai *et al.*, 2008; Kuang *et al.*, 2010) are able to inhibit multi-drug resistance transporters increasing intracellular chemotherapy concentrations as discussed in Chapter One section 1.8.2. These studies used short exposure to TKI, measured in hours, to demonstrate an increase in substrate uptake and the effect of longer exposure is not known. Whilst the SK-Br-3 cell line is not reported to express a multi-drug resistance transporter, the intracellular concentration of doxorubicin following exposure of cells to TKI was investigated using FACS to examine if TKI exposure was modulating the intracellular concentration of doxorubicin.

As demonstrated in Chapter Four Figure 4.25, doxorubicin emits a fluorescence that can be detected using FACS. The level of doxorubicin fluorescence was measured in cells treated with doxorubicin (5 μM) alone, or following TKI exposure for one or 48 hours. Intracellular doxorubicin is detected as an increase in fluorescence which shifts cells to the right on the FACS dot plot and the mean cell fluorescence (MFI) can be calculated (Figure 5.7). As also demonstrated in Chapter Four, both lapatinib and gefitinib emit fluorescence in cells treated for 48 hours and the MFI of TKI only treated cells was used to normalise the doxorubicin fluorescence data, which is expressed as a percentage of the MFI obtained from cells treated with doxorubicin alone (Figures 5.7 and 5.8).

These results demonstrate that there is no increase in the doxorubicin fluorescence in cells treated with either gefitinib or lapatinib for one hour (Figure 5.7). Whilst the MFI of doxorubicin in cells treated with gefitinib for 48 hours is reduced by 17.4±1.1% and by 10.2±13.6% in cells treated with lapatinib for 48 hours, compared with cells treated with doxorubicin alone, this is non-significant difference (Figure 5.8).

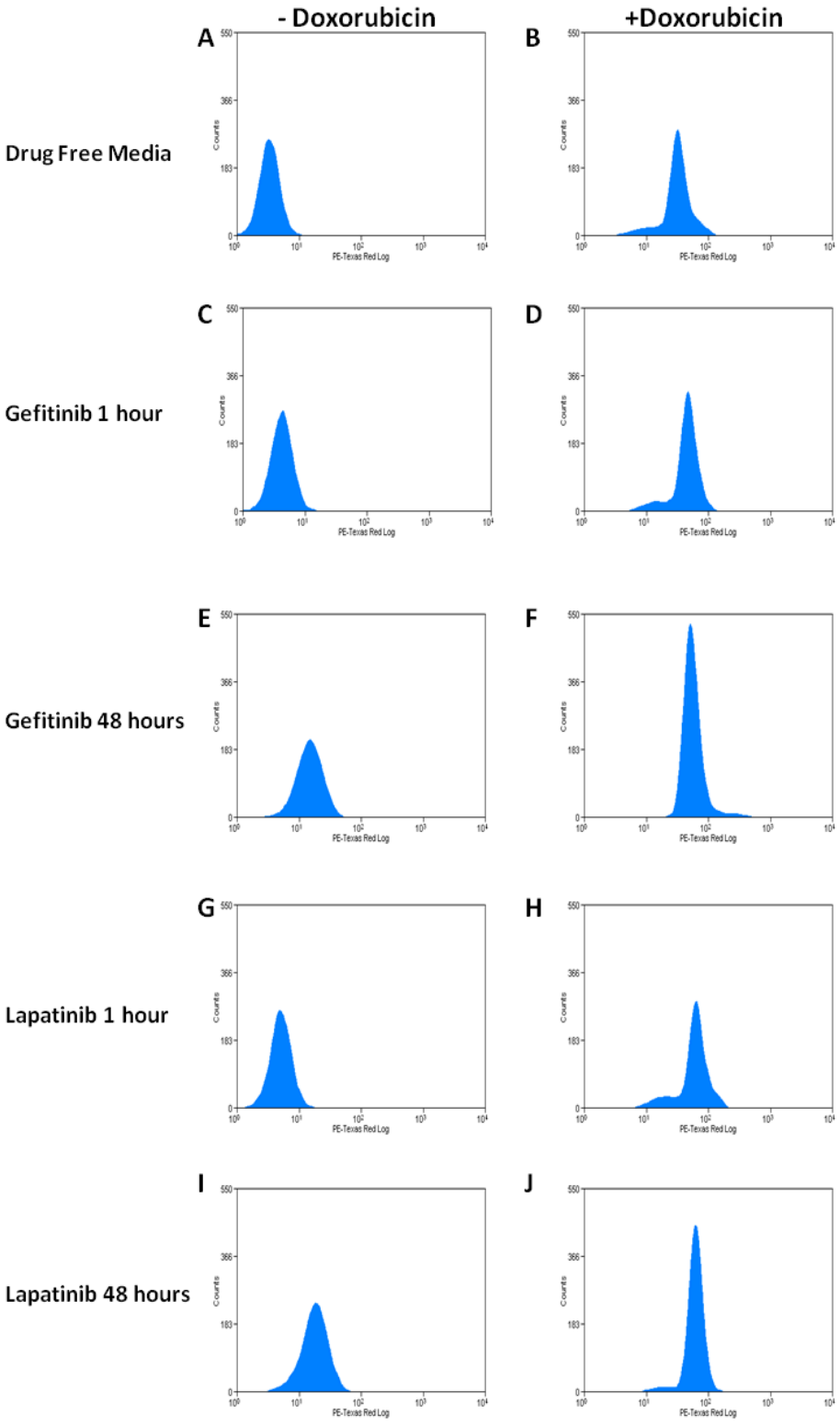

Figure 5.7 Measurement of doxorubicin fluorescence

Drug fluorescence was measured using FACS, in SK-Br-3 cells treated with (B,D,F,H,J) and without (A,C,E,G,I) doxorubicin 5µM for 2 hours. Figure representative of three independent experiments.

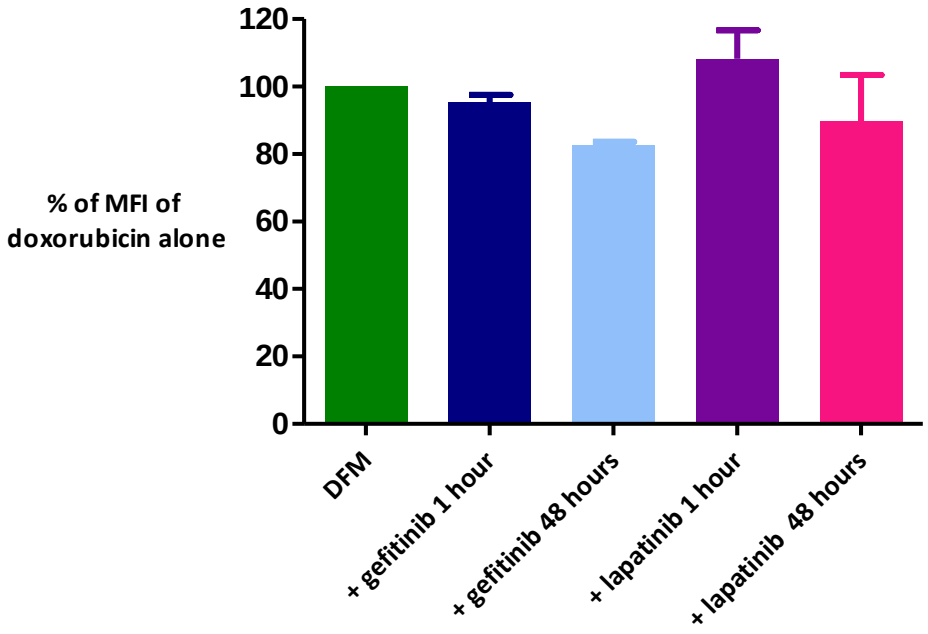

Figure 5.8 Modulation of intracellular doxorubicin by gefitinib or lapatinib
FACS as used to measure the fluorescence of doxorubicin in SK-Br-3 cells pre-treated with DFM, gefitinib or lapatinib for one or 48 hours before addition of 5 µM doxorubicin for two hours, after which cells were collected and analysed. Data are presented as the mean±SEM of three independent experiments.

5.6 DOES DURATION OF EXPOSURE TO GEFITINIB AND LAPATINIB MODULATE THE ACTIVITY AND EXPRESSION OF TOPOISOMERASE II?

As discussed in Chapter One section 1.7.3 resistance to Topo II poisons can be produced through a reduction in Topo II enzyme activity through inhibition of enzyme phosphorylation or down-regulation of expression (Nitiss, 2009b). Topo II expression as measured using Western blotting demonstrates that Topo IIα expression is reduced in cells treated with either gefitinib or lapatinib continuously for 48 hours; Topo IIβ expression is unaffected (Figure 5.9A).

To investigate Topo II activity, nuclear extracts were prepared from cells treated with TKI; these extracts contain both Topo IIα and Topo IIβ and their ability to decatenate kinetoplast DNA was assessed in an *in vitro* assay. Kinetoplast DNA is the mitochondrial DNA from the Kinetoplastid class of protozoa, which forms interlinked circles of DNA (Figure 5.9B). This assay examines the ability of extracted Topo II to separate the interlinked circles, which can be visualised as separate bands following gel electrophoresis. The results demonstrate that continuous exposure to either gefitinib

or lapatinib for 48 hours reduces the ability of cells to decatenate DNA, with a smaller fall occurring in cells treated for one hour (Figure 5.9C).

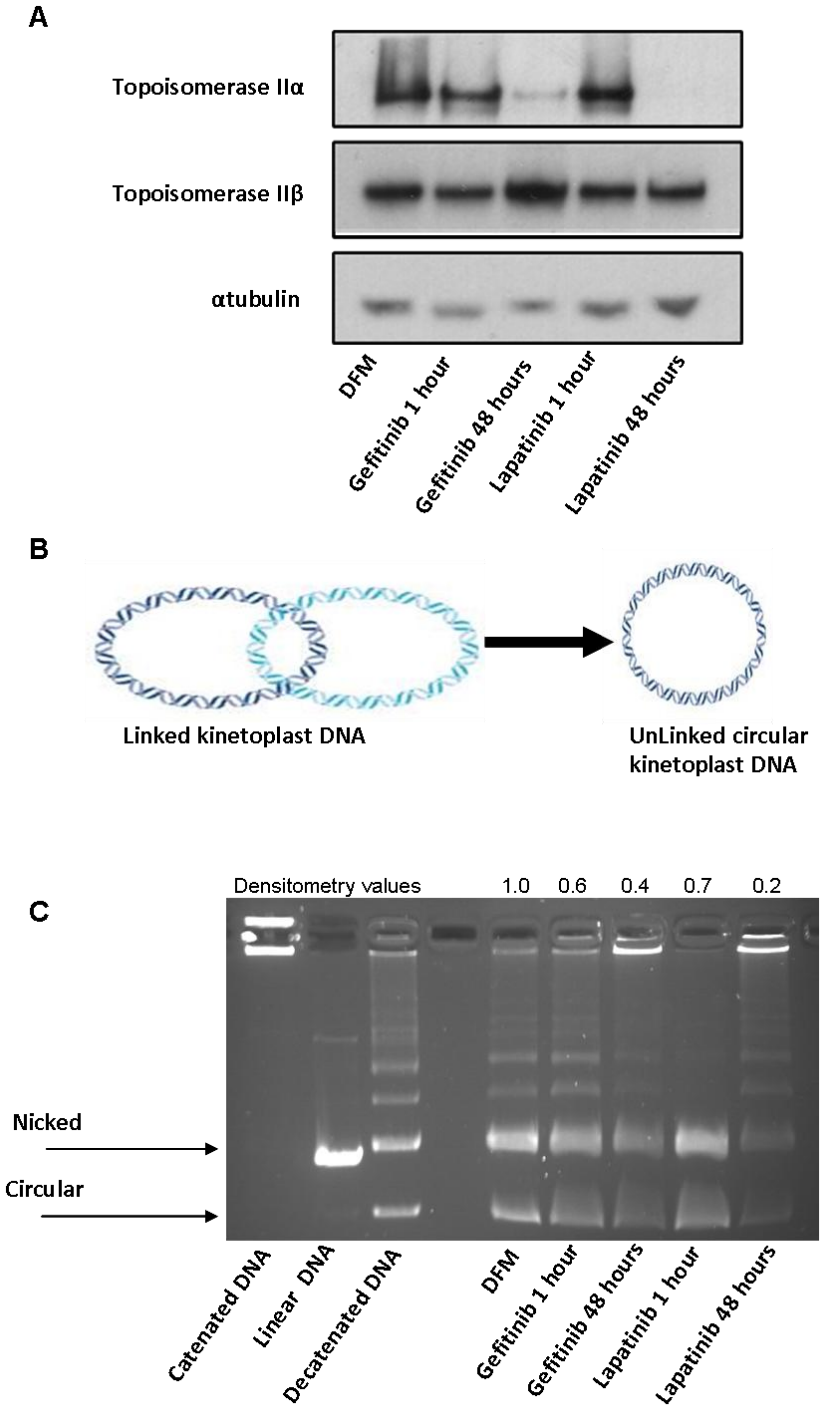

Figure 5.9 Modulation of expression and activity of topoisomerase II by gefitinib or lapatinib
(A) The effect of TKI on the expression of Topo IIα and Topo IIβ was investigated using Western blotting. Cells were treated as indicated, lysed and immunoblotted. Loading control is provided by αtubulin. (B) Representation of decatenation of kinetoplast DNA. (C) Nuclear extracts were prepared from cells treated with TKI and their ability to decatenate DNA *in vitro* assessed. Controls indicate the location of catenated, linear and decatenated DNA. Figure representative of three independent experiments and quantisation by densitometry as demonstrated.

5.7 DOES REDUCED TOPOISOMERASE IIα EXPRESSION MODULATE DNA STRAND BREAK INDUCTION BY TOPOISOMERASE II POISONS?

Etoposide, doxorubicin and m-AMSA poison both Topo IIα and Topo IIβ (Pommier *et al.*, 2010). As discussed above Topo IIα expression falls in cells treated TKI for 48 hours, though Topo IIβ expression is unaffected. The relative targeting of each isoform of Topo II by doxorubicin, etoposide and m-AMSA varies depending upon the method of assessment. Using purified Topo II in decatenation assays, both doxorubicin and m-AMSA target both Topo II isoforms equally, with etoposide demonstrating a preference for Topo IIα (Perrin *et al.*, 1998). However, cytotoxicity assays indicate that etoposide and doxorubicin are dependent upon Topo IIα expression to induce cell death (de Campos-Nebel *et al.*, 2010; Toyoda *et al.*, 2008), in contrast to m-AMSA, to which resistance can be mediated by the knockdown of Topo IIβ (Toyoda *et al.*, 2008; Willmore *et al.*, 2002).

The trapped in agarose DNA immunostaining assay (TARDIS), which examines the formation of Topo IIα or Topo IIβ cleavable complexes specifically, demonstrates the targeting of both Topo II isoforms by doxorubicin, etoposide and m-AMSA. However, this assay does not allow the relative contributions of each enzyme to be compared due to possible differences in the efficacies of the Topo IIα antibody compared with the Topo IIβ antibody used in the assay (Errington *et al.*, 2004; Willmore *et al.*, 2002).

In order to investigate the effect of the Topo II poisons used in this study on the formation of Topo IIβ-induced DNA strand breaks, a cell system in which Topo IIα expression can be reduced was utilised. The HTETOP cell line is derived from a human fibrosarcoma cell line in which endogenous Topo IIα has been disrupted and a tetracycline controlled exogenous Topo IIα transfected. This allows the suppression of Topo IIα expressing by the addition of a tetracycline (Carpenter and Porter, 2004).

Doxycycline 1 μg for 24 hours reduces, but does not abolish the expression of Topo IIα (Figure 5.10A). The ability of doxorubicin, etoposide and m-AMSA to induce DNA strand breaks following reduction in Topo IIα expression using the alkaline Comet assay was assessed in cells treated with and without doxycycline.

Significantly fewer DNA strand breaks are produced by all three Topo II poisons in cells with treated with doxycycline (Topo IIα reduced) compared with untreated cells (Topo IIα expressing) (Figure 5.10 and Table 5.2). The greatest effect on the induction of DNA strand breaks of the reduced expression of Topo IIα is observed with doxorubicin, with an 87-95% reduction in strand breaks (Figure 5.10B). Fewer DNA strand breaks are induced by both etoposide and m-AMSA, with a 74-86% reduction in DNA strand breaks when Topo IIα expression is reduced (Figure 5.10C & 5.10D).

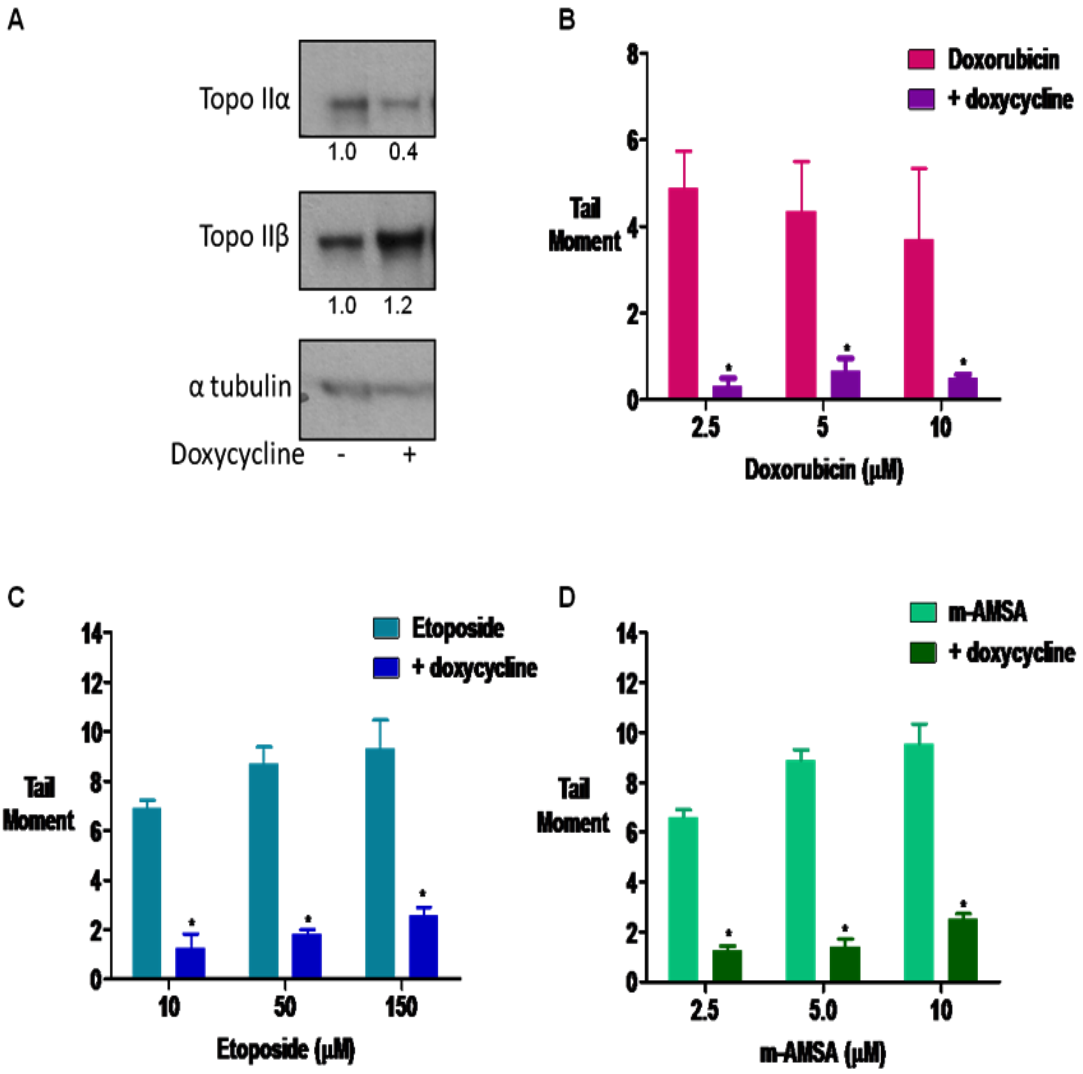

Figure 5.10 Effect of reduced topoisomerase IIα expression on the production of DNA strand breaks

(A) Western blotting was used to assess the expression of Topo IIα and Topo IIβ following treatment with doxycycline in HTETOP cells. Densitometry values are as shown. The alkaline comet assay was used to assess the induction of DNA strand breaks by (B) doxorubicin 2 hours, (C) etoposide 2 hours, (D) m-AMSA 1 hour. Data are presented as mean±SEM of three independent experiments. *p<0.05.

Drug Concentration (μM)	Percentage of tail moment		
	Doxorubicin (%)	Etoposide (%)	m-AMSA (%)
2.5	4.8±2.4		16.2±2.5
5.0	13.1±6.1		14.4±4.0
10	11.4±4.0	16.6±7.9	24±2.4
50		18.5±1.5	
150		25.8±4.8	

Table 5.2 Percentage reduction in tail moment by knockdown of topoisomerase IIα
Data from Figure 5.10 are presented as the tail moment in HETOP cells which have been treated with doxycycline to reduce the expression of Topo IIα expressed as a percentage of that produced in cells with normal expression of Topo IIα. Data are presented as the mean±SEM of three independent experiments.

5.8 The effect of gefitinib on topoisomerase II expression and the cell cycle

Topo IIα expression alters with the cell cycle with the highest levels observed during G2/M (Pommier *et al.*, 2010). In order to assess if the reduction in Topo IIα expression is due to cell cycle arrest, the effect of gefitinib (5 μM) on the cell cycle and Topo II expression was assessed over 72 hours, with gefitinib replaced daily. Gefitinib treatment for six hours has no effect on the cell cycle but by 24 hours, an increase in cells in G0/G1-phase can be detected at 83.6±3.4% from 62.8±1.5% in untreated cells (Figure 5.11). Despite G0/G1-phase cell cycle arrest, a small percentage of cells are able to progress through to G2/M over 72 hours with a constant number in S-phase (Figure 5.11).

Western blotting demonstrates that Topo IIα levels start to fall after 24 hours exposure to gefitinib, with a marked reduction at 48 hours (Figure 5.11F).

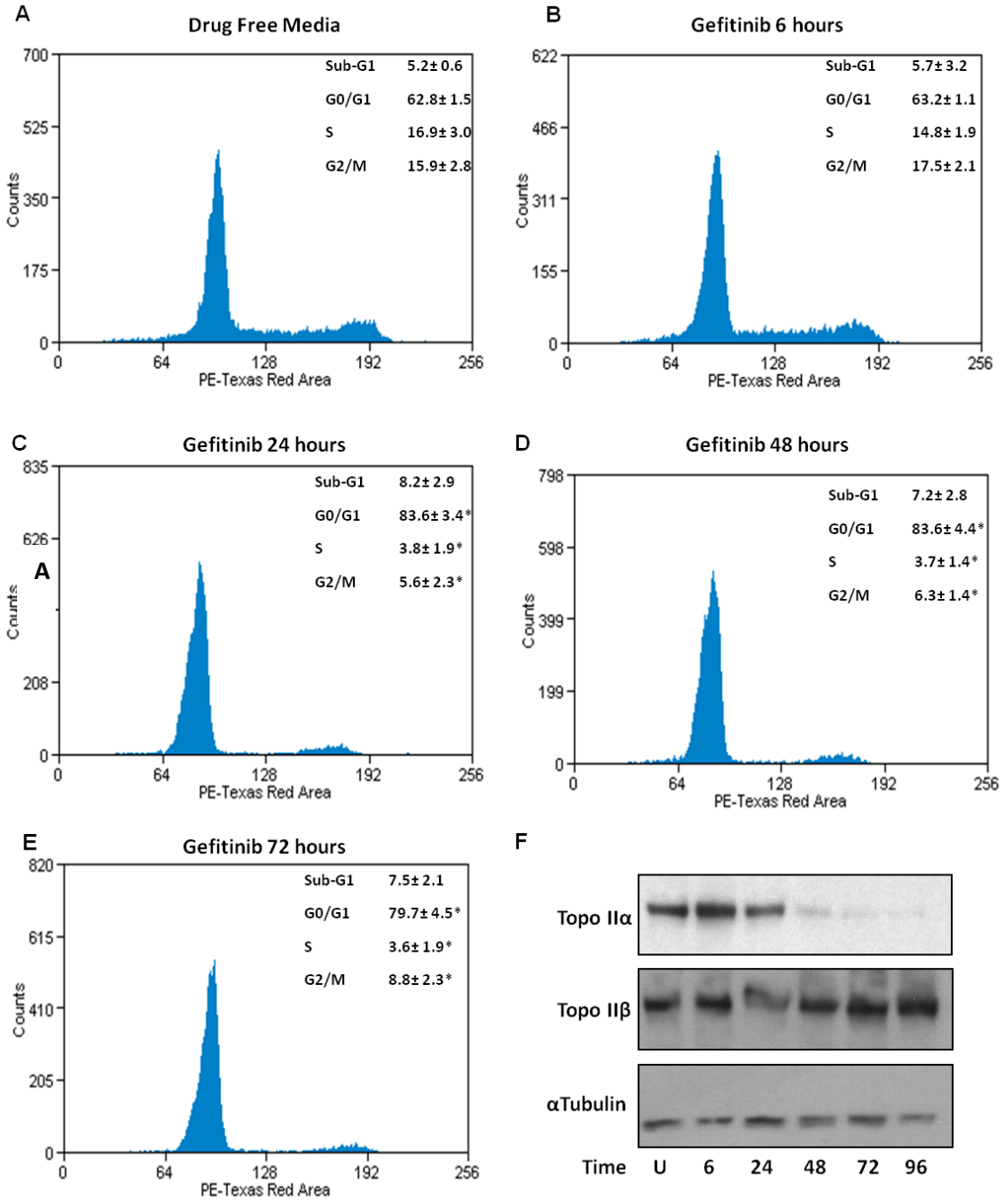

Figure 5.11 Effect of gefitinib on the cell cycle and topoisomerase II expression
SK-Br-3 cells were treated continuously with 5 µM gefitinib with replacement every 24 hours and the effect on cell cycle and Topo II expression investigated. (A-E) Cell cycle was assessed using FACS for 10, 000 cells over 72 hours. Data are presented as mean±SD of three independent experiments. *P<0.05 compared with cell treated with drug free media. (F) Topo II expression was assessed using Western blotting. αTubulin is used as a loading control. Image is representative of three independent experiments

5.9 DOES THE DURATION OF EXPOSURE TO GEFITINIB MODULATE THE PRODUCTION OF DNA DSBS BY TOPOISOMERASE II POISONS?

The Topo II poison m-AMSA induces the same numbers of DNA strand-breaks, regardless of the duration of exposure to gefitinib or lapatinib. However, measurement of γH2AX foci indicates that following exposure to gefitinib for 48 hours, fewer DNA DSBs are produced, matching the findings with doxorubicin and etoposide. As discussed in Chapter Four, this observation cannot be explained by inhibition of γH2AX foci formation by gefitinib, as foci are formed in response to both cisplatin and IR despite exposure to gefitinib. This observation suggests that Topo II poisons are unable to produce DNA DSBs following continued TKI treatment but continue to produce single strand DNA breaks, which are detected by the alkaline Comet assay. As γH2AX foci are a surrogate marker for DNA DSBs (Bonner *et al.*, 2008), the neutral Comet assay was used to confirm the hypothesis that gefitinib exposure for 48 hours reduces the production of DNA DSBs by Topo II poisons.

5.9.1 Differences between the alkaline and neutral Comet assays

The alkaline Comet assay uses an alkaline buffer to relax, unwind and denature DNA, with the presence of DNA single or double strand breaks producing fragmentation of DNA (Olive and Banath, 2006). During electrophoresis these DNA fragments migrate further producing a Comet tail. As the number of single and double DNA strand breaks increases, DNA becomes more fragmented resulting in the production of a longer Comet tail. The neutral Comet assay employs a neutral non-denaturing buffer which maintains DNA super coiling. When the cells are electrophoresed the super coiled DNA is pulled to one side, producing the visualised Comet tail that can be seen even in untreated cells (Figure 5.12). The presence of single or double DNA strand breaks causes relaxation of the super coils allowing DNA migration, producing a longer Comet tail due to the greater the degree of relaxation. Due to maintenance of the super coiled structure, a DNA DSB break produces a greater degree of relaxation and migration than a single strand break (Olive and Banath, 2006). This can be tested by using hydrogen peroxide which produces a 1,000 fold more single strand breaks than double strand breaks (Wojewodzka *et al.*, 2002). In the alkaline comet assay hydrogen

peroxide produces a long comet tail whereas in the neutral version, the tail is not significantly longer than that produced in untreated cells (Figure 5.12).

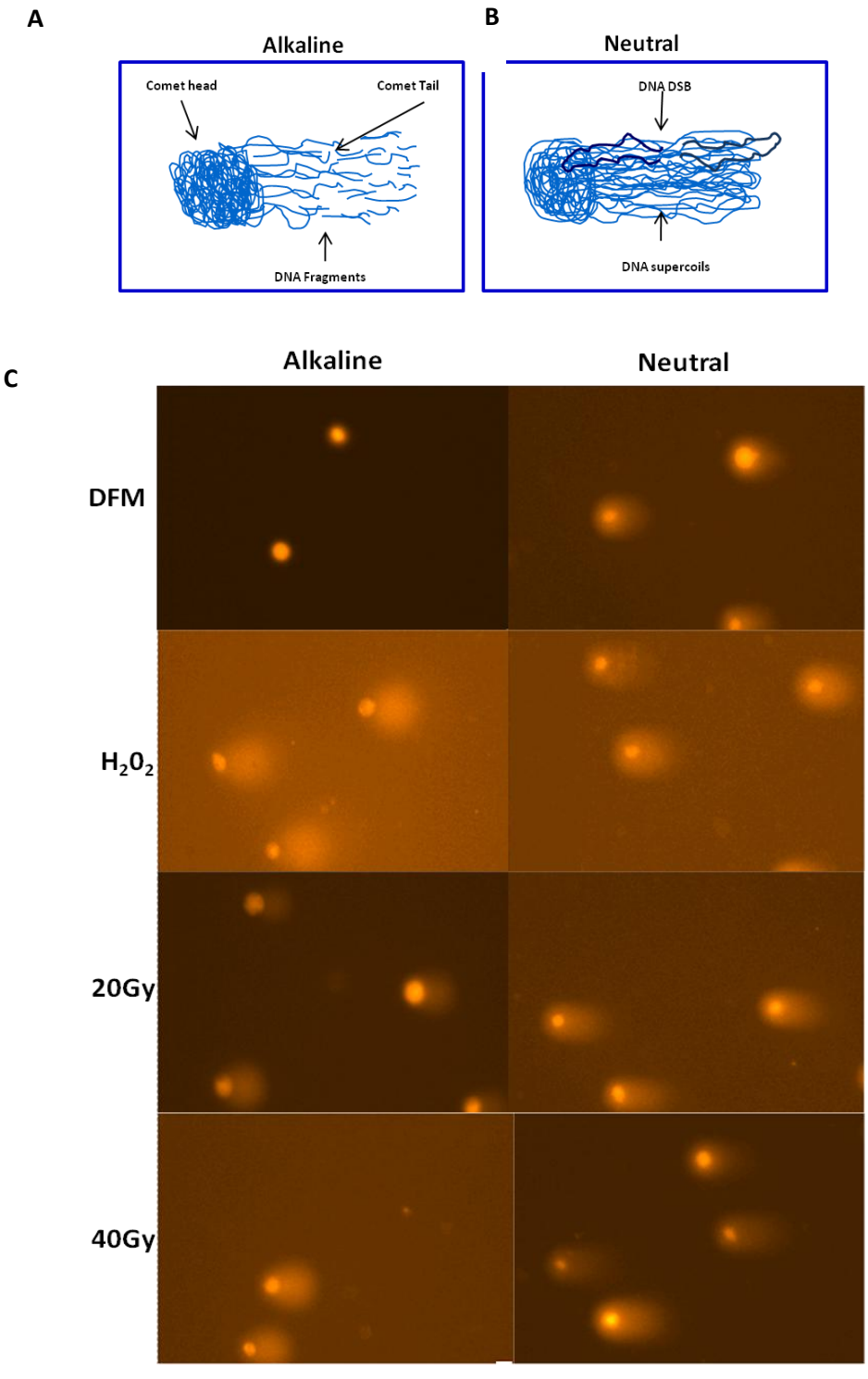

Figure 5.12 Differences between the alkaline and neutral Comet assays
In the alkaline comet assay DNA is relaxed and unwound by alkaline buffer, allowing DNA fragments to migrate during electrophoresis. (B) In the neutral assay, the DNA supercoils remain intact and are pulled towards the cathode during electrophoresis. The presence of a DNA DSB increases the migration of DNA. (C) Cells treated with hydrogen peroxide or ionising radiation, collected and analysed using the alkaline and neutral Comet assays.

5.9.2 Modulation of topoisomerase II poison-induced DNA double strand breaks by duration of exposure to gefitinib

The ability of the Topo II poisons doxorubicin, etoposide and m-AMSA to induce DNA DSBs was investigated over a range of concentrations. Both etoposide and m-AMSA induce DSBs in a concentration dependent manner, which is not observed with doxorubicin (Figure 5.13). Gefitinib exposure for one hour has no significant effect on the induction of DSBs by doxorubicin, etoposide or m-AMSA, except at the concentration of 10 µM (m-AMSA alone tail moment of 8.2±0.7, compared with 5.2±0.9 in combination with gefitinib for one hour $p<0.05$) (Figure 5.13).

Gefitinib treatment for 48 hours significantly inhibits the ability of all Topo II poisons to induce DNA DSBs with doxorubicin (5 µM) inducing 84% fewer DNA DSBs compared with cells treated with doxorubicin alone, etoposide (50 µM) 77% and m-AMSA (5 µM) 58% fewer (Figure 5.13). In these cells etoposide retains its ability to increase the number of DSB with increasing drug concentration but this is lost with m-AMSA with similar tail moments measured across all concentrations of the drug investigated (Figure 5.13).

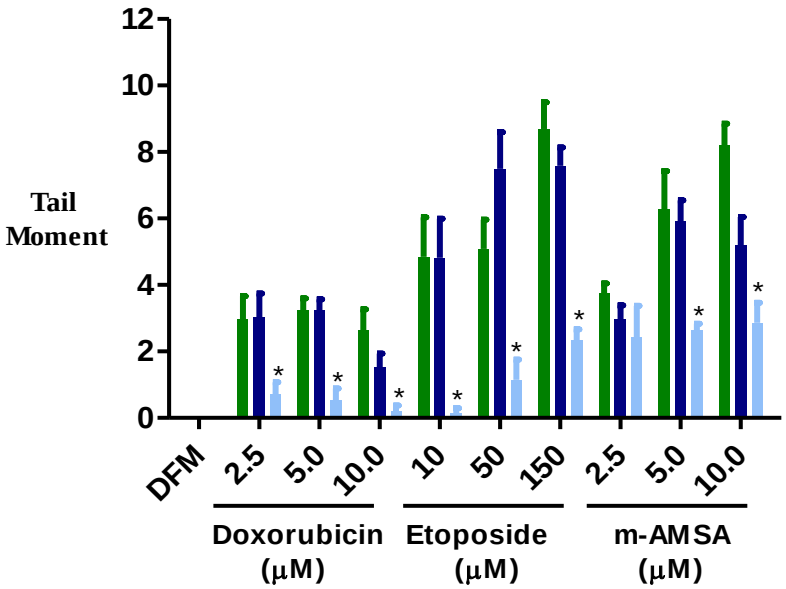

Figure 5.13 Induction of DNA double strand breaks by topoisomerase Iiα poisons
The neutral Comet assay was used to assess the induction of DNA DSB strand breaks in the SK-Br-3 cell line. Cells were pre-treated with either DFM (■), gefitinib 1 hour (■), gefitinib 48 hours (■) before the addition of doxorubicin, etoposide or m-AMSA for one or two hours, after which cells were collected and analysed. Data are presented as the mean±SEM of three independent experiments *$p<0.05$ compared with Topo II poison alone.

5.10 DOES EXPOSURE TO GEFITINIB FOR 48 HOURS INCREASE THE NUMBER OF DNA STRAND BREAKS PRODUCED BY REACTIVE OXYGEN SPECIES?

Topo II poisons, particularly doxorubicin, produce ROS in addition to poisoning Topo II (Pommier *et al.*, 2010). Continuous TKI exposure for 48 hours has no effect on the induction of DNA strand breaks by m-AMSA as measured by the alkaline Comet assay yet significantly fewer DNA DSBs as measured by the neutral Comet assay and γH2AX foci. This indicates that m-AMSA is mainly inducing single strand breaks in cells treated with TKIs for 48 hours. These strand breaks may be produced through the increased production of ROS by m-AMSA, given that the inducer of ROS, menadione significantly increases the production of DNA strand breaks following continuous exposure to gefitinib for 48 hours (Figure 5.2) and exposure to gefitinib for 48 hours is known to stimulate the production of ROS (Sergina *et al.*, 2007).

To investigate the contribution of ROS in the production of DNA strand breaks in cells treated with continuous TKI, strand break production in the presence of the free radical scavenger N-acetylcysteine (NAC) was assessed using the alkaline Comet assay.

NAC (3 mM) was added to cells treated with gefitinib for 48 hours, one hour prior to exposure to the Topo II poisons doxorubicin, etoposide and m-AMSA. NAC had no effect on the induction of DNA strand breaks by m-AMSA though it significantly reduced the induction of strand breaks by etoposide (Figure 5.14). Doxorubicin failed to produce significant numbers of DNA strand breaks regardless of the presence of NAC.

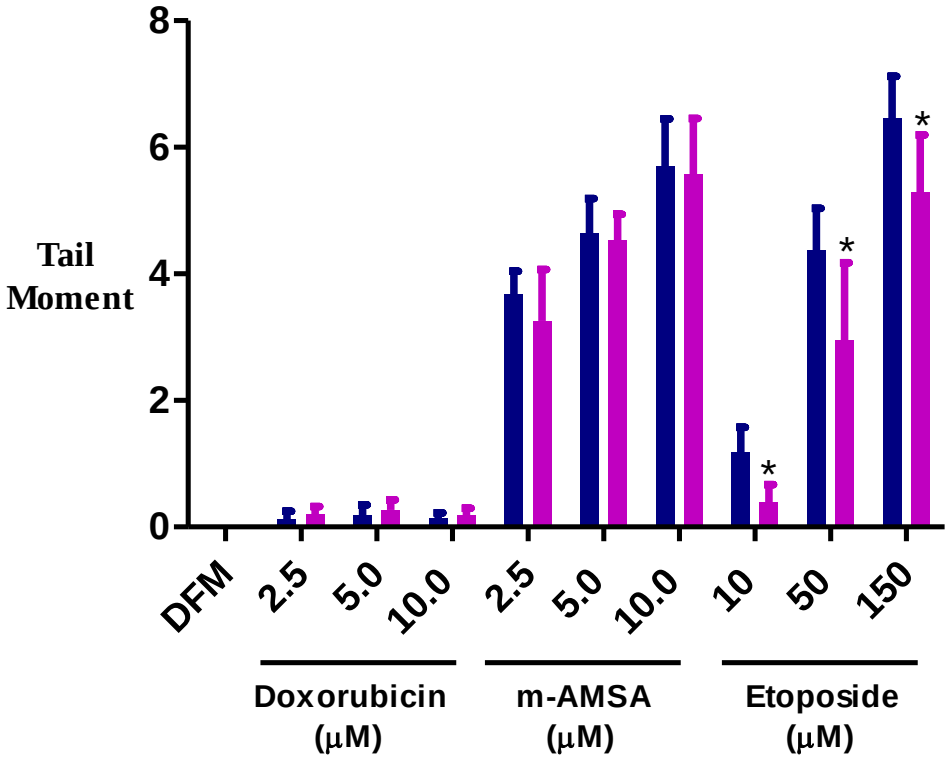

Figure 5.14 Effect of free radical scavenger on DNA strand production
SK-Br-3 cells were treated with gefitinib 5 μM for 48 hours, with drug replacement every 24 hours. At the final addition of gefitinib 3 mM of NAC was added for 1 hours, followed by exposure to doxorubicin, m-AMSA or etoposide. Cells were collected after one or two hours and analysed using the alkaline comet assay. –NAC (■) and +NAC (■). Data are presented as the mean±SEM of three independent experiments. *P<0.05.

5.11 MIGHT TYROSINE KINASE INHIBITORS RENDER CELL RESISTANT TO TOPOISOMERASE II POISONS IN THE CLINIC?

In the experiments described in both this Chapter and Chapter Four lapatinib is used at a concentration of 2 μM, a concentration which is achievable in patients at the licensed dose of lapatinib (Burris *et al.*, 2009). However, gefitinib is used at a concentration of 5 μM to induce a reactivation of HER3 and PI3K signalling as demonstrated by Sergina *et al*. (Sergina *et al.*, 2007). In patients, lower concentrations of gefitinib are achieved at the licensed dose which produces plasma concentrations of around 1-2 μM, though concentrations as high as 20 μM can be detected in tumours (Haura *et al.*, 2010; McKillop *et al.*, 2005). In order to investigate if the reduction in DNA strand breaks following continuous gefitinib exposure for 48 hours is due to the high concentration of gefitinib used in this study, the effect of 2 μM gefitinib on the

induction of strand breaks by Topo II poisons was investigated using the alkaline Comet assay.

5.11.1 Effect of exposure to 2 µM gefitinib on the induction of DNA strand breaks by doxorubicin and etoposide

Cells were pre-treated with 2 µM gefitinib for 48 hours, with drug replacement at 23 and 47 hours. Cells were then treated with varying concentrations of doxorubicin or etoposide for 2 hours, then collected and processed for analysis using the alkaline Comet assay. The results demonstrate that pre-treatment of cells with gefitinib 2 µM for 48 hours produces resistance to the induction of DNA strand breaks by etoposide and doxorubicin (Figure 5.15).

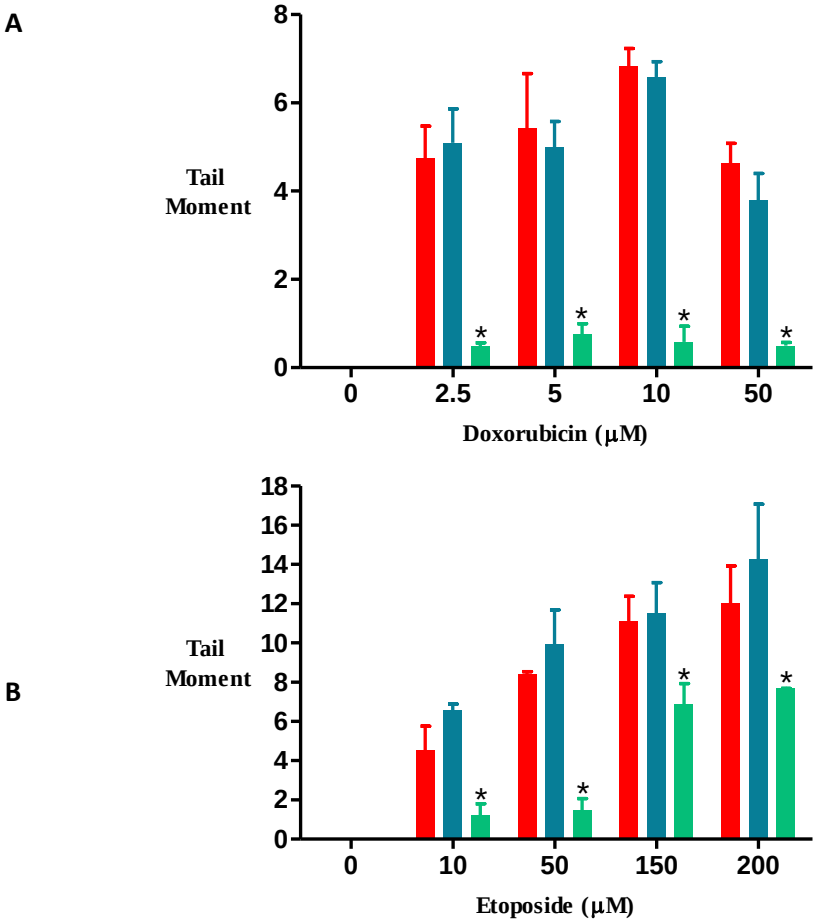

Figure 5.15 Effects of 2 µM gefitinib on the induction of DNA strand breaks
SK-Br-3 cells were treated with drug free media (■), 2 µM gefitinib 1 hour (■), or 2 µM gefitinib 48 hours (■), prior to the addition of doxorubicin (A) or etoposide (B) for two hours. Cells were then collected and DNA strand breaks assessed using the alkaline Comet assay. Data are presented as the mean±SEM of three independent experiments. *P<0.05 compared with Topo II poison alone.

5.11.2 Modulation of topoisomerase gene expression by lapatinib

Whilst the concentration of lapatinib used in this study is clinically relevant, the reduction in the expression of Topo IIα by lapatinib may not translate into the clinical setting. To explore this further we obtained the gene expression data for Topo II from eight patients with breast cancer treated with lapatinib (provided by Dr J Chang, Baylor College of Medicine, USA). These patients received neo-adjuvant treatment, for breast cancer with lapatinib for six weeks. Tumour biopsies were taken before and after treatment and gene expression assessed using gene microarray. Raw expression data were normalised for median gene expression to allow comparison.

The array contained two probe sets for Topo IIα and one for Topo IIβ. Topo IIα gene expression fell in both probe sets by at least 50 % (Figure 5.16), in contrast Topo IIβ levels were unaltered. These data suggest that at the gene level, lapatinib reduces Topo IIα gene expression in patients treated with lapatinib.

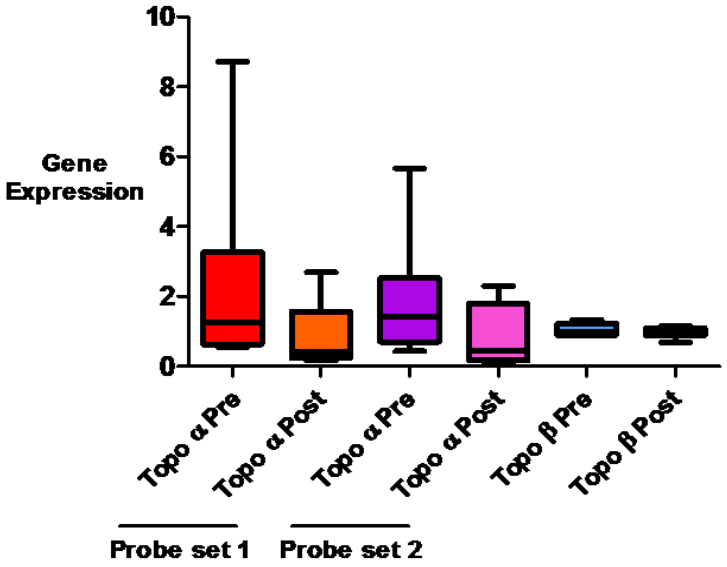

Figure 5.16 Modulation of the gene expression of topoisomerase by lapatinib
The effect of lapatinib on Topo IIα and Topo IIβ gene expression was investigated by probing the microarray data obtained from eight patients treated with neo-adjuvant lapatinib for six weeks. Tumour biopsies were taken before and after treatment and gene expression assessed using gene microarray. Raw expression data were normalised for median gene expression to allow comparison. The array contained two probe sets for Topo IIα and one for Topo IIβ.

5.12 DISCUSSION

Data presented in Chapter Four demonstrated that exposure of SK-Br-3 cells to gefitinib or lapatinib for 48 hours reduces the ability of the Topo II poisons etoposide and doxorubicin to induce DNA stand breaks, as detected by both the alkaline Comet assay and measurement of H2AX foci. This chapter examines the influence of duration of exposure to TKIs on the effects of the Topo II poison m-AMSA, Topo II expression and activity, the cell cycle and production of DNA DSBs by doxorubicin, m-AMSA and etoposide.

5.12.1 Modulation the effects of m-AMSA by gefitinib and lapatinib

In contrast to doxorubicin and etoposide, the production of DNA strand breaks by m-AMSA is not significantly altered by the duration of TKI exposure as assessed using the alkaline Comet assay (Figure 5.1). Both measurement of γH2AX foci and the neutral Comet assay demonstrate that in cells pre-treated with gefitinib for 48 hours, fewer DNA DSBs are produced by m-AMSA (Figures 5.4 and 5.13). This indicates that the strand breaks measured by the alkaline Comet assay following continuous TKI treatment contain a higher proportion of single strand breaks than cells treated with m-AMSA alone. We hypothesised that these single strand breaks were produced by an increase in ROS. This is supported by a significant increase in the induction of strand breaks by the ROS generator menadione in cells treated with gefitinib for 48 hours (Figure 5.2). However, the free radical scavenger NAC does not affect the induction of strand breaks by m-AMSA in cells treated with gefitinib for 48 hours, indicating that these breaks are not produced by free radicals (Figure 5.14).

5.12.2 Modulation of topoisomerase II expression by gefitinib and lapatinib

The Topo II poisons doxorubicin, etoposide and m-AMSA all prevent the religation of DNA DSBs produced as part of the normal function of Topo II (Pommier *et al.*, 2010). The data presented in this chapter demonstrates that Topo II function is reduced, though not abolished by gefitinib or lapatinib treatment for 48 hours and that Topo IIα but not Topo IIβ expression falls.

Topo IIα expression is known to increase during S and G2/M- phases of the cell cycle whereas Topo IIβ levels remains constant (Pommier *et al.*, 2010). A reduction in Topo

IIα expression would be expected with continuous TKI treatment due to the induction of a G0/G1 cell cycle arrest. Gefitinib induces a G0/G1 cell cycle arrest at 24 hours, which is sustained over a 72 hour period (Figure 5.11) and Topo IIα levels fall at 24 hours with little protein detected at 48 hours onwards (Figure 5.11). This raises the question as to whether the fall in Topo IIα level is purely a reflection of G1 cell cycle arrest, or a direct effect of gefitinib. The precise mechanisms through which cell cycle arrest is mediated by TKIs are still under investigation though the dephosphorylation of the forkhead transcription factor FOXO3a, in response to the inhibition of AKT phosphorylation, has been implicated (Krol *et al.*, 2007).

In SK-Br-3 cells, gefitinib treatment induces the transport of unphosphorylated FOXO3a back into the nucleus. This in turn increases the expression of the cell cycle control protein $p27^{kip1}$, producing G1 cell cycle arrest (Krol *et al.*, 2007) and reducing the gene and protein expression of another forkhead transcription factor, FOXM1 (Francis *et al.*, 2009). FOXM1 has been shown to bind to the promoter of the mouse Topo IIα gene and activate its transcription (Wang *et al.*, 2009). This is a possible mechanism through which gefitinib could reduce the expression of Topo IIα (illustrated in Figure 5.17). However, in the study by McGovern *et al.* following 48 hours gefitinib treatment, increases in RNA and protein levels of FOXM1 could be detected (McGovern *et al.*, 2009). It is unclear if this is due to the development of resistant cell clone, as suggested by the investigators, or due to the washout of gefitinib as it is not reported whether gefitinib was replaced every 24 hours in this study (McGovern *et al.*, 2009).

Overexpression of FOXM1 has been linked to the overexpression of HER2 in both breast cancer cell lines and tissue and the knockdown of HER2 expression reduces the expression of FOXM1 (Francis *et al.*, 2009). Lapatinib 1 μM also reduces the expression of FOXM1 within 12 hours, with G1 cell arrest occurring later, indicating that the fall in expression is not due to cell cycle arrest (Francis *et al.*, 2009).

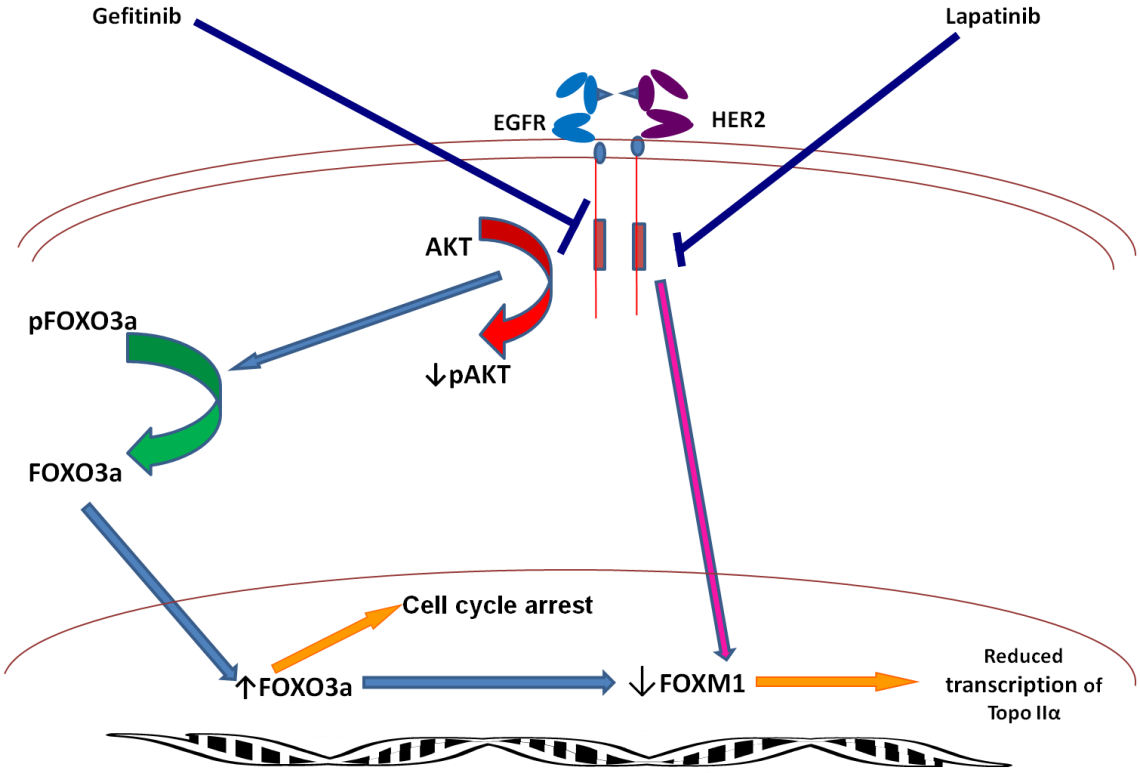

Figure 5.17 Possible mechanism of down-regulation of topoisomerase IIα expression by gefitinib or lapatinib
Both gefitinib and lapatinib have been demonstrated to down-regulate the expression of the transcription factor FOXM1 which may be regulate the transcription of topoisomerase IIα.

We have obtained the Topo II gene expression data for eight patients treated with pre-operative lapatinib. Whilst this small data set indicates that Topo IIα expression is reduced by lapatinib it should be remembered that Topo II gene status and protein expression do not always correlate, with gene amplification or deletion not necessarily resulting in a detectable alteration in Topo IIα expression (Mueller *et al.*, 2004; Usha *et al.*, 2008).

5.12.3 Modulation of topoisomerase II activity by gefitinib and lapatinib

Continuous exposure to gefitinib significantly reduces the induction of γH2AX foci by doxorubicin, etoposide and m-AMSA, indicative of a reduction in the number of DSBs. This is supported by the neutral Comet assay data which confirms a reduced induction of DNA DSBs in cells treated with gefitinib for 48 hours (Figure 5.13). These data also demonstrate a reduction in the number of DSBs induced by 5 µM and 10 µM of m-AMSA in cells pre-treated with gefitinib one hour which is not observed with either

doxorubicin or etoposide (Figure 5.13). A reduction in the number of DSBs breaks in cells treated with TKI for one or 48 hours may explain the observation of faster repair of DNA strand breaks, as assessed by the alkaline Comet assay (Figure 5.3). However, at the concentration of 5 μM m-AMSA used in the alkaline Comet assay, the neutral Comet assay demonstrates only a small and non-significant decrease in DSB induction in cells pre-treated with gefitinib for one hour compared with cells treated with m-AMSA alone (Figure 5.13). Despite this, the repair of DNA lesions as assessed by the alkaline Comet assay following gefitinib for one or 48 hours exactly mirrors each other, suggesting that the faster repair observed in these cells is not due to a reduction in the number of DSBs produced (Figures 5.3). This means that the gefitinib promoted increase in the rate of repair of m-AMSA-induced DNA strand breaks is due to an ability to repair the predominant DNA single strand breaks more quickly.

Topo II-DNA cleavable complexes are reversible and Topo II is able to ligate the DNA DSB that makes up the cleavable complex (Nitiss, 2009b). Doxorubicin, etoposide and m-AMSA prevent the ligation of the DNA DSB contained within the cleavable complex (Pommier *et al.*, 2010). However, the binding of a Topo II poison to Topo II is reversible, and the dissociation of the poison from Topo II allows the enzyme to function normally (Nitiss, 2009b). Therefore the increased rate of repair of m-AMSA induced DNA strand breaks may be explained by a reduced affinity of the poison for Topo II, so that on removal of the drugs the DNA strands can be religated by Topo II, as per its normal function.

As discussed in Chapter One, section 1.7.3.3.2, Topo II activity is controlled by phosphorylation with the phosphorylation at ser1106 within the catalytic domain of Topo IIα important in controlling the sensitivity to etoposide and m-AMSA (Chikamori *et al.*, 2003). Amino acid substitution at this site produces a two-four fold reduction in the formation of etoposide-induced cleavable complexes. This site is phosphorylated by the serine/threonine kinase casein kinase 1δ and 1ε (Grozav *et al.*, 2009). Casein kinase 1δ inhibition has been demonstrated with gefitinib, though at a high concentration (Brehmer *et al.*, 2005). This indicates the possibility that the activity of Topo IIα is inhibited by gefitinib, through the inhibition of casein kinase 1δ.

5.12.4 HER2, topoisomerase IIα and casein kinase 1δ

Clinical studies have confirmed that the HER2 gene amplification is able predict for an improved benefit for treatment with anthracyclines in breast cancer (Pritchard *et al.*, 2008). As both HER2 and Topo IIα are located in close proximity on chromosome 17q investigations have focussed on whether Topo IIα gene amplification in HER2 amplified breast cancer explains the clinical benefit from anthracyclines. Within HER2 over-expressing tumours, co-amplification of Topo II is reported in between 32-54% of tumours and gene deletions in 14-35% (Slamon and Press, 2009), both of which are associated with clinical response to anthracyclines (O'Malley *et al.*, 2009).

Direct action by HER2 on Topo IIα activity is not supported by the literature with the transfection of HER2 into cell lines not increasing sensitivity to doxorubicin (Pegram *et al.*, 1997). As postulated above inhibition of casein kinase Iδ activity by gefitinib may provide a link between TKI and reduced Topo II expression and activity. Interestingly casein kinase Iδ is located on chromosome 17q, like HER2 and Topo IIα and may provide the link between HER2 amplification and sensitivity to anthracyclines in HER2 positive breast cancer.

5.13 CONCLUSIONS AND FUTURE WORK

Continued TKI exposure for 48 hours renders cells resistant to the effects of Topo II poisons through the down regulation of their target, Topo IIα, and possibly through the modulation of Topo IIα activity.

Further work is needed to clarify the effect of TKI exposure on the expression of Topo II in clinical samples. If this is confirmed it would give a clear indication that TKI use concurrently or immediately prior to Topo II poison use may not be clinically beneficial. This is important as clinical trials are currently being conducted examining the combination of liposomal doxorubicin and lapatinib and neo-adjuvant lapatinib in patients with breast cancer (National Cancer Institute, 2011a; National Cancer Institute, 2011c). This could be achieved by the analysis of Topo II expression by IHC in tissue samples from patients before and after treatment with lapatinib or gefitinib. For example in patients with breast cancer prior to surgery, allowing comparison of Topo II

expression in diagnostic and post surgical specimens or in patients with NSCLC with accessible lymph nodes or subcutaneous nodules.

In addition, the effects of TKI exposure on the ability of drugs to poison Topo II warrants further investigation, especially the effect of TKI on the phosphorylation of Topo II. This area of investigation is limited by the lack of useful phosphorylated Topo II site specific antibodies, and requires the use of mass spectrometry requiring specific expertise; this also prevents the analysis of phosphorylation of Topo II in clinical samples.

HER2 mediated cisplatin resistance

6.1 INTRODUCTION

HER2 targeted antibodies increase the cytotoxic effect of cisplatin in breast and ovarian cancer cell lines (Hancock *et al.*, 1991). The role of HER2 in mediating resistance to cisplatin is further supported by the observation that the transfection of HER2 into MCF-7 cells reduces their sensitivity to cisplatin by two-four times (Benz *et al.*, 1992). Sensitisation to cisplatin by HER2 targeted antibodies is through the inhibition of DNA repair, with a reduction in unscheduled DNA synthesis and reduced repair of cisplatin-induced adducts observed (Pietras *et al.*, 1994). These findings translate into the clinic with the combination of the HER2 antibody, trastuzumab with cisplatin, producing higher clinical response rates than historical controls in patients with metastatic breast cancer (Pegram *et al.*, 1998). As discussed in Chapter One section 1.8.5.2, EGFR translocates to the nucleus in response to cisplatin and IR, modulating the repair of DNA damage though its interaction with DNA-PK_{CS} (Dittmann *et al.*, 2005b; Hsu *et al.*, 2009). The precise mechanisms by which HER2 increases resistance to cisplatin have yet to be elucidated.

Cisplatin forms interstrand and intrastrand DNA crosslinks, together with DNA-protein adducts, preventing DNA replication (Wang and Lippard, 2005). The removal of these lesions requires the DNA repair processes of NER, HR and TLS as discussed in Chapter One, section 1.7.5.1. Like EGFR, full length HER2 can be detected in the nuclei of HER2-expressing breast cancer cell lines and in breast cancer tissue (Beguelin *et al.*, 2010; Wang *et al.*, 2004), where it has been shown to bind and transactivate the promoters of genes through binding to a specific sequence of nine nucleotides within the promoter region (Wang *et al.*, 2004) or through the formation of a complex with STAT3 to activate the cyclin D1 promoter (Beguelin *et al.*, 2010).

6.1.1 Nuclear transport of HER2

As discussed in Chapter One section 1.3.3.5, nuclear transport of HER proteins is dependent upon a 13 amino acid sequence, conserved across the four receptors, known as the NLS (Hsu and Hung, 2007). The transport of HER2 into the nucleus is dependent upon its phosphorylation, with transport inhibited by the tyrosine kinase

inhibitor AG825 (Wang *et al.*, 2004). Following phosphorylation, the membrane located receptor is endocytosed, interacts with importin β and the nuclear pore protein Nup358, to enter the nucleus (Giri *et al.*, 2005). Nuclear translocation and the interaction with importin β is dependent upon the NLS with deletion of this sequence reducing translocation of HER2 into the nucleus, through reduced interaction with importin β (Giri *et al.*, 2005).

6.1.1.1 Nuclear HER2 and the repair of cisplatin-induced crosslinks

We transfected the HER2 negative MDA-MB-468 cell line, with the HER2 constructs used by Giri *et al*. to demonstrate the requirement of the NLS to mediate the nuclear transport of HER2. Cells transfected with full length HER2 were more resistant to the inhibition of cell proliferation by cisplatin (Boone *et al.*, 2009). This effect is mediated through an increase in the rate of repair of cisplatin-induced interstrand crosslinks (Boone *et al.*, 2009). Using cells transfected with a HER2 from which the 13 amino acids NLS has been deleted, we demonstrated that reduced HER2 nuclear translocation increases cellular sensitivity to cisplatin, through reduced repair of cisplatin-induced interstrand crosslinks (Boone *et al.*, 2009).

Nuclear HER2 binds directly to a nine nucleotide sequence (called HER2-associated sequences) within promoter regions of targeted genes, stimulating their transcription. Gene promoters containing HER2-asscociated sequences include the COX2, p53 related protein kinase, matrix metalloproteinase-16 and the Fanconi anaemia complementation group C (FANCC) genes (Wang *et al.*, 2004). FANCC is of interest as it is involved in the repair of interstrand crosslinks, assembling with seven other Fanconi anaemia proteins to form a nuclear ubiquitin ligase complex known as the Fanconi anaemia core complex (D'Andrea, 2010). This complex monoubiquitinates the proteins FANCI and FANCD2 which form DNA-repair foci involved in the repair of cisplatin-induced interstrand crosslinks (D'Andrea, 2010). The ability of the nuclear translocation of HER2 to promote the repair of cisplatin-induced interstrand crosslinks together with the discovery that nuclear HER2 can regulate gene transcription, indicates that HER2 may mediate resistance to cisplatin through gene regulation, possibly through up-regulation of FANCC gene expression.

6.1.2 Mechanisms for identifying the targets of nuclear HER2

In order to identify other potential targets of HER2, the techniques of gene expression microarray and ChIP were utilised to generate hypotheses as to the nuclear targets of HER2.

6.1.2.1 Chromatin Immunoprecipitation

ChIP allows the interaction between proteins and DNA to be examined. This technique was used by Wang *et al.* to identify the binding of the COX2 promoter by HER2 (Wang *et al.*, 2004). ChIP involves the reversible crosslinking of DNA using formaldehyde, which fixes DNA-protein interactions. The protein of interest (HER2) is immunoprecipitated using an antibody directed against it, isolating HER2-DNA complexes from which the bound DNA is eluted. Identification of the specific DNA sequences can be achieved with high throughput mass sequencing.

6.1.2.2 Gene expression microarray

Gene expression arrays allow the comparison of gene expression between cells lines under different conditions. Each gene is represented by around 40 probes, with each exon covered by approximately four probes, with a total of 5.5 million probes on each array (Affymetrix, 2005).

6.2 AIMS

This chapter describes experiments conducted to identify the mechanism through which HER2 increases the rate of cisplatin-induced interstrand crosslink repair. Experiments were conducted in MDA-MB-468 breast cancer cells transfected with a vector control (MDA-MB-468-Vector), HER2 (MDA-MB-468-HER2), or a mutated HER2 lacking the NLS sequence (MDA-MB-468-NLS).

1. To **characterise** the transfected MDA-MB-468 cell lines and the activity of HER2.
2. To **investigate** the DNA targets of nuclear HER2 using the technique of chromatin immunoprecipitation.
3. To **identify** the transcription targets of nuclear HER2 using DNA expression array.

6.3 CHARACTERISATION OF MDA-MB-468 HER2 TRANSFECTED CELL LINES

The MDA-MB-468 breast cancer cell line is derived from a pleural effusion of a woman with a metastatic adenocarcinoma of the breast as discussed in Chapter Three. It is recognised to overexpress EGFR, have low expression of HER2 and be PTEN deleted (Lacroix and Leclercq, 2004). This cell line was stably transfected using a vector containing a fluorescence green protein (MDA-MB-468-Vector), full length wild type HER2 (MDA-MB-468-HER2) and a mutant HER2 from which the NLS sequence has been deleted (MDA-MB-468-NLS), all a kind gift from MC Hung (MD Anderson, USA).

6.3.1 HER2 expression in transfected MDA-MB-468 cells

Following the creation of stably transfected cell lines, the expression of HER2 protein was assessed using Western blotting. No HER2 is detected the MDA-MB-468 cells transfected with vector alone, but is present in cells transfected with either full length HER2 or HER2 with a deletion of the 13 nucleotide NLS (Figure 6.1)

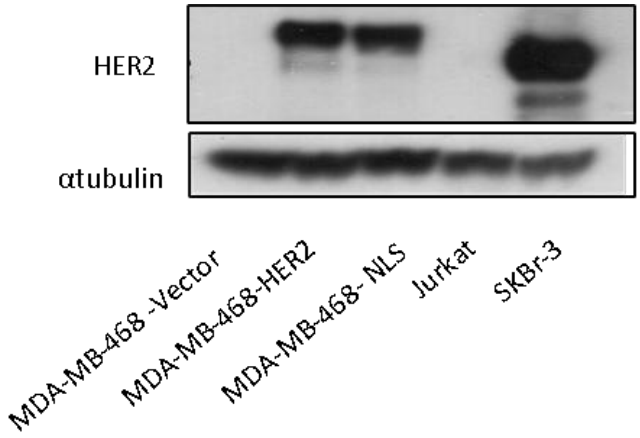

Figure 6.1 HER2 expression in transfected MDA-MB-468 cell lines
MDA-MB-468 cells were stably transfected with vector (MDA-MB-468-Vector), full length HER2 (MDA-MB-468-HER2) or HER2 with a deleted NLS (MDA-MB-468-NLS). HER2 expression was assessed using Western blotting with αtubulin as a loading control. Jurkat cells which do not express HER2 were used as a negative control and SK-Br-3 cells which over express HER2 as a positive control. Image is representative of more than three individual blots.

6.3.2 The effect of HER2 on cell proliferation

HER2 is an oncogene, driving tumour growth (Pegram *et al.*, 1997) and identifies a more aggressive type of breast cancer with a poorer survival (Slamon *et al.*, 1987). In

order to assess if the transfection of HER2 into the MDA-MB-468 cell line increases the rate of cell proliferation, the SRB assay was used to assess cell doubling times. The expression of full length HER2 increases the rate of cell proliferation with the number of cells doubling within 21 hours compared with control cells, which took 55 hours to double (Figure 6.2). In comparison, the transfection of HER2 with a deleted NLS, slowed the rate of cell proliferation in the first 48 hours but there was a rapid growth between 48 and 72 hours.

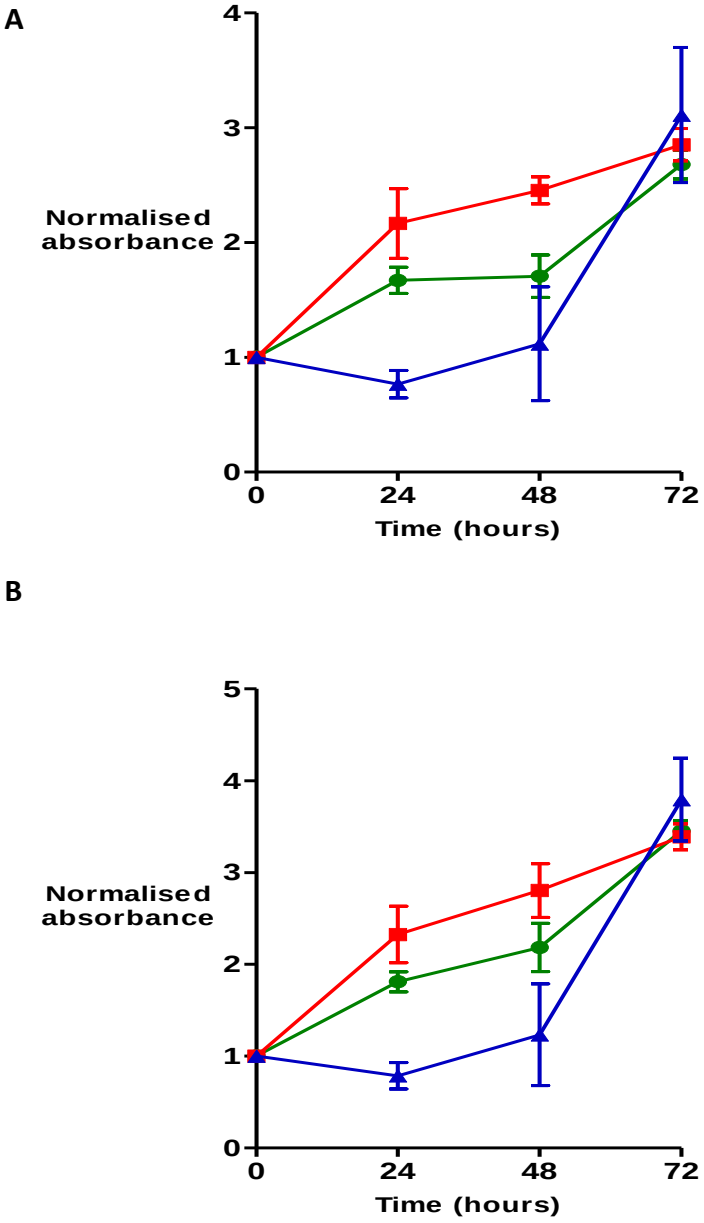

Figure 6.2 HER2-induced modulation of cell proliferation
MDA-MB-468 cells were stably transfected with a vector (●), full length HER2 (■) or HER2-NLS (▲). Cells were plated at a concentration of $4x10^4$ cells/ml (A) or $6x10^4$ cells/ml (B) in 96 well plates and left overnight to adhere. Cells were then grown for 72 hours and plates removed every 24 hours, the absorbance measured and normalised to level at time zero. Data are presented a mean±SEM.

6.3.3 The effect of trastuzumab on HER2 phosphorylation

HER2 has no identified ligand, though the induction of HER2 phosphorylation can be stimulated by ligands targeted against EGFR and HER3 (Kong *et al.*, 2008). HER2 phosphorylation is also induced by the monoclonal antibody trastuzumab in the SK-Br-3 cell line (Scaltriti *et al.*, 2009). Trastuzumab induced HER2 phosphorylation in both the MDA-MB-468-HER2 and MDA-MB-468-NLS cell lines, with the effect more pronounced in the MDA-MB-468-HER2 cell line (Figure 6.3). This indicates that the transfected HER2 and the HER2-NLS are capable of undergoing phosphorylation.

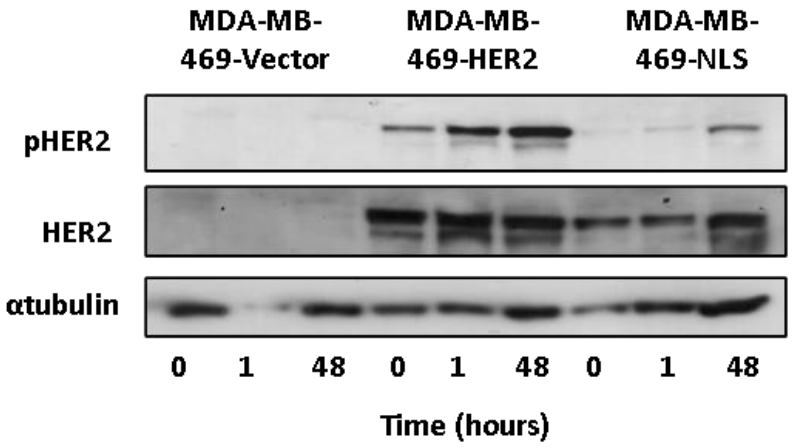

Figure 6.3 Induction of HER2 phosphorylation by trastuzumab
MDA-MB-468 cells stably transfected with a vector, full length HER2 or HER with a deleted NLS were treated with trastuzumab 40 µg/ml. Cells were lysed at the indicated times and phosphorylated HER2 detected using Western blotting.

6.3.4 The induction of nuclear translocation of HER2 by cisplatin

The localisation of HER2 and the induction of nuclear translocation were investigated using confocal microscopy. No HER2 fluorescence can be detected in the MDA-MB-468-Vector cell line under any condition (Figure 6.4). In MDA-MB-468-HER2 cells, the HER2 protein can be visualised mainly located on the cell membrane in untreated cells (Figure 6.4). Treatment with trastuzumab reduces the level of HER2 protein located on the cell membrane but increases the level within the cytoplasm. Cisplatin treatment induces the translocation of HER2 into the nucleus, a process prevented by the addition of trastuzumab (Figure 6.4). The deletion of the NLS sequence from HER2 results in membrane located HER2, with no increase in nuclear HER2 observed following cisplatin treatment (Figure 6.4).

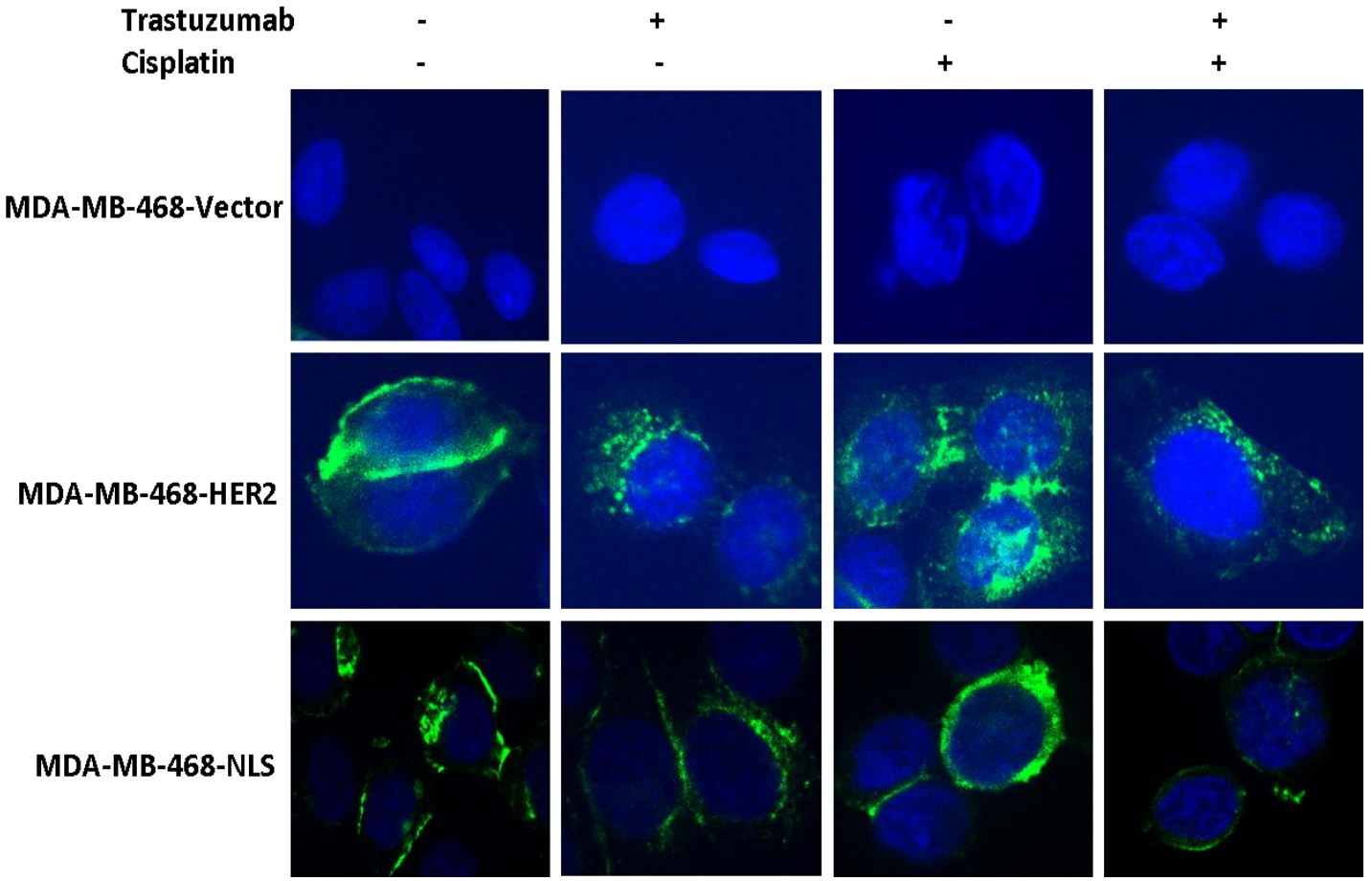

Figure 6.4 Cisplatin-induced HER2 translocation to the nucleus is inhibited by trastuzumab
MDA-MB-468 cells were stably transfected with vector (MDA-MB-468-Vector), full length HER2 (MDA-MB-468-HER2) or HER2 with a deleted NLS (MDA-MB-468-NLS). Cells were treated with 100 µM cisplatin for one hour, trastuzumab 40 µg/ml or both drugs in combination followed by trastuzumab 40 µg/ml continuously. The cellular localisation of HER2 24 hours following exposure to cisplatin was visualised by confocal microscopy. Picture taken from Boone *et al*. 2009.

6.3.5 The dependence of MDA-MB-468-HER2 cells on HER2 expression

We have demonstrated that trastuzumab inhibits the repair of cisplatin-induced interstrand crosslinks in the MDA-MB-468-HER2 cell line (Boone *et al.*, 2009). In order to assess if these cells have become dependent upon HER2 to repair cisplatin-induced interstrand crosslinks, the effect of HER2 knockdown on their repair was investigated using the modified alkaline Comet assay. The expression of HER2 was reduced by the transfection of siRNA against HER2 (Figure 6.5A). Cisplatin produces interstrand crosslinks in both cell lines, but cells with reduced expression of HER2 are unable to repair any of these interstrand crosslinks (Figure 6.5B). These results demonstrate that a reduction in HER2 expression in the MDA-MB-468-HER2 cell line inhibits the repair of cisplatin-induced interstrand crosslinks, indicating that these cells are dependent upon the expression of HER2.

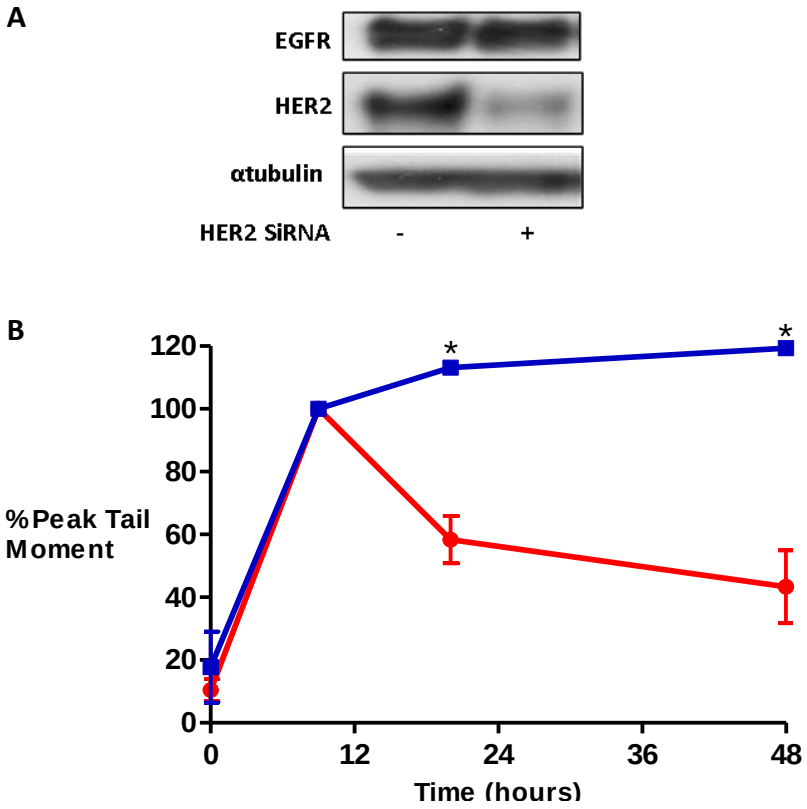

Figure 6.5 Effect of reduced HER2 expression on the repair of cisplatin-induced interstrand crosslinks

HER2 expression in the MDA-MB-468-HER2 cell line was reduced by the transfection of HER targeted siRNA (A). The effect of the knockdown of HER2 expression on the repair of interstrand crosslinks was investigated using the modified Comet assay. MDA-MB-468-HER2 control cells (●) and cells transfected with siRNA against HER2 (■) were treated with cisplatin 100 µM for one hour followed by replacement with DFM. Cells were collected at the time points indicated and analysed using the modified alkaline Comet assay. Data are presented as the mean±SEM of two independent experiments. *p>0.05.

6.4 CHROMATIN IMMUNOPRECIPITATION TO IDENTIFY THE DNA TARGETS OF NUCLEAR HER2

ChiP was carried out in the MDA-MB-468-HER2 cell line as described in Chapter Two section 2.12 and outlined Figure 6.6. Extracted DNA was hybridised to BAC arrays to examine if the process of HER2-ChIP could be used to identify the DNA targets of HER2. Each BAC array contains over 32, 000 clones, covering the entire human genome with the average size of a clone of 170 base pairs.

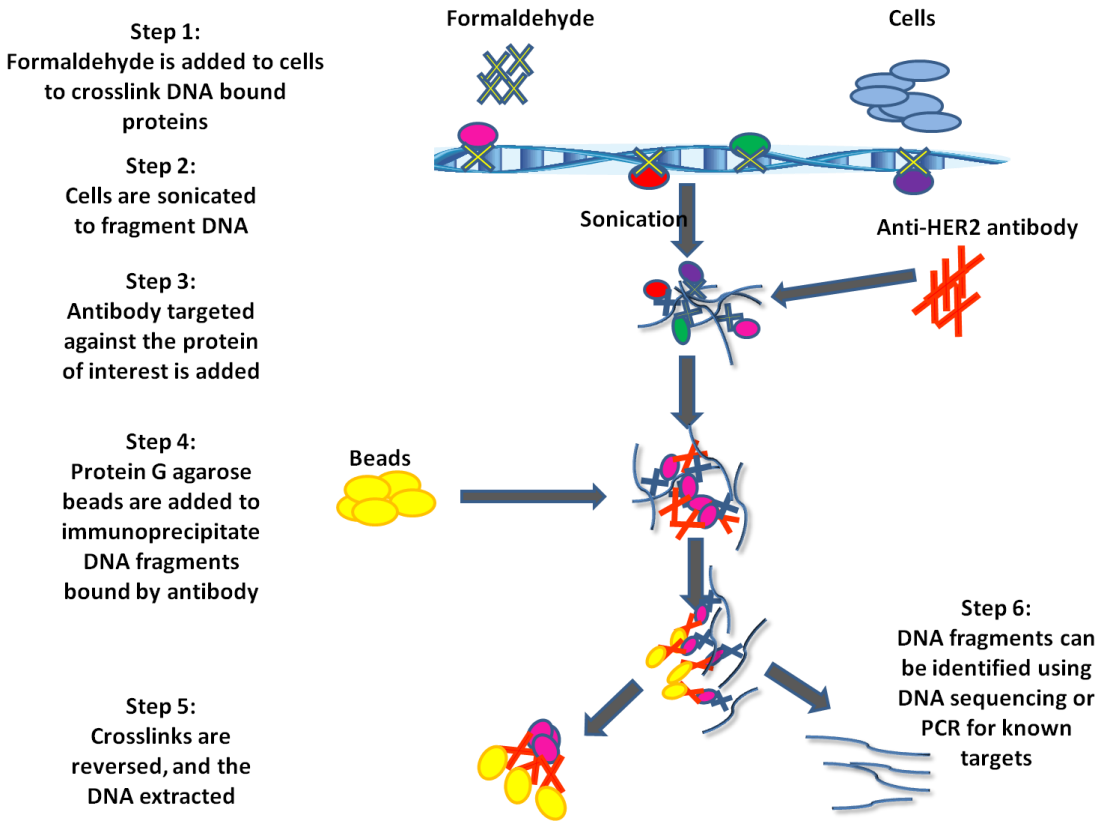

Figure 6.6 Process of chromatin immunoprecipitation
A pictorial representation of the process of chromatin immunoprecipitation.
Following treatment of cells, formaldehyde is added to crosslink DNA bound proteins. Cells are then collected and subjected to sonication to fragment DNA, followed by the addition of an antibody against the protein of interest. DNA fragments bound by the protein of interest are isolated through immuoprecipitation with agarose beads. The DNA fragments are then separated from the protein of interest by reversal of the crosslinks and the DNA isolated.

The initial experiment yielded hybridisation to 150 clones. In order to further validate the use of BAC arrays as a screening tool to investigate DNA-protein interactions the experiment was repeated a further three times. Unfortunately these experiments proved that our initial results were not reproducible, with only two clones in common

across the four experiments (Table 6.1). In view of this ChiP-sequencing was not performed as the process is time consuming, expensive and was unlikely to be reproducible. It is unclear from these experiments whether this approach failed due to technical issues or that under these conditions HER2 is not bound to DNA. Technical problems include the fact that ChIP grade antibodies against HER2 do not exist. We used the same antibody as used by Wang *et al.* who have identified the nucleotide sequence bound by HER2 (Wang *et al.*, 2004) but despite this our results were not reproducible. Another consideration may be that BAC arrays are not sensitive enough to identify potential genes.

	Experiment 1	Experiment 2	Experiment 3
No. of Clones identified	457	115	227

Table 6.1 HER2-Chromatin immunoprecipitation and hybridisation to bacterial artificial chromosome arrays
ChiP was performed using an antibody against HER2 in the MDA-MB-468-HER2 cell line. The isolated DNA was hybridised to BAC arrays to examine if the process of ChiP was successful. Rabbit IgG was used as a control antibody and for normalisation.

6.5 DNA EXPRESSION MICROARRAY TO IDENTIFY THE TRANSCRIPTION TARGETS OF NUCLEAR HER2

The technique of RNA expression arrays were used to assess to identify potential gene targets of HER2. Gene expression was assessed in MDA-MB-468-Vector, MDA-MB-468-HER and MDA-MB-468-NLS cells to ascertain whether the transfection of HER2 up-regulated gene expression. Two separate experiments were conducted; the first in cells treated with and without 100 µM cisplatin for one hour followed by RNA extraction 24 hours later. The second experiment in cells that were grown for 3-5 days and RNA extracted from cells at 80% confluence.

In both experiments the MDA-MB-468-HER2 and MDA-MB-468-NLS cell lines clustered close together and separate from the MDA-MB-468-Vector cell line. Differentially expressed genes were identified using ANOVA and gene lists created based upon a false discovery threshold of 0.05. Analysis of the both sets of arrays using box plot analysis confirmed that the arrays were successful with all array distributions

clustering around the same median. Principle component analysis and hierarchical clustering demonstrated that the MDA-MB-468-Vector cell line separated from both the MDA-MB-468-HER2 and MDA-MB-468-NLS cell lines (Figure 6.7)

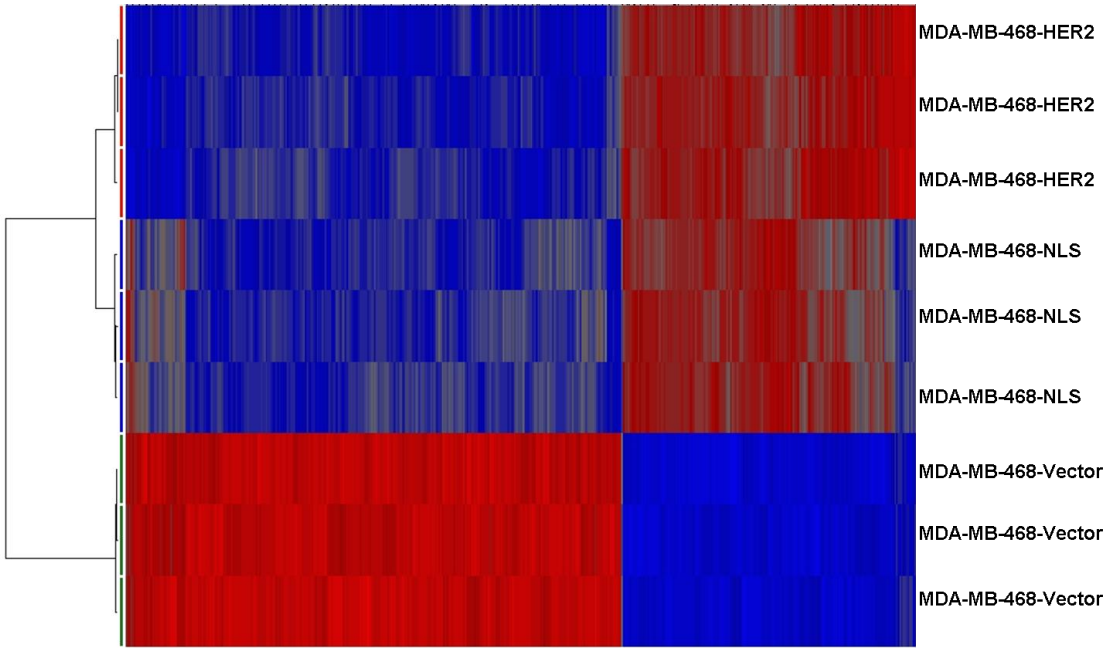

Figure 6.7 An example of the hierarchical clustering of MDA-MB-468 HER transfected cell line gene expression
Gene expression in MDA-MB-468 stably transfected with vector control, full length HER2 or HER2-NLS was studied using gene expression analysis. The example above is from proliferating cells at 80% confluence when RNA was extracted for analysis.

6.5.1 The modulation of gene expression by HER2 and cisplatin

Gene expression data were assessed in three different comparisons. The first compared the expression of untreated cells with the same cell line treated with cisplatin, the second between the three cells lines following cisplatin treatment, and the third between the three different cell lines, in the absence of cisplatin.

No significant differences were detected in gene expression between untreated cells and those treated with cisplatin 100 µM for one hour in either MDA-MB-468-Vector, MDA-MB-468-HER or MDA-MB-468-NLS cells (Table 6.2). Comparisons between the lines treated with cisplatin identified a single gene, lactate dehydrogenase B, is

significantly increased by 2.1 fold in MDA-MB-468-NLS cisplatin treated cells compared with MDA-MB-468- Vector cells treated with cisplatin.

There are no differences in gene expression between MDA-MB-468-Vector and MDA-MB-468-HER2 cells and MDA-MB-468-HER2 and MDA-MB-468-NLS cells following treatment with cisplatin (Table 6.2).

Comparison	No. Genes
MDA-MB-468-Vector vs. MDA –MB-486-Vector+cisplatin	0
MDA-MB-468-HER2 vs. MDA –MB-486-HER2+cisplatin	0
MDA-MB-468-NLS vs. MDA –MB-486-NLS+cisplatin	0
MDA-MB-468-Vector+cisplatin vs. MDA–MB-486-HER2+cisplatin	0
MDA-MB-468-Vector+cisplatin vs. MDA –MB-486-NLS+cisplatin	1
MDA-MB-468-HER2+cisplatin vs. MDA –MB-486-NLS+cisplatin	0
MDA-MB-468-Vector vs. MDA –MB-486-HER2	0
MDA-MB-468-Vector vs. MDA –MB-486-NLS	5
MDA-MB-468-HER2 vs. MDA –MB-486-NLS	0

Table 6.2 Gene expression profiles of MDA-MB-468 HER2 transfected cell lines
MDA-MB-468-Vector, MDA-MB-468-HER2 and MDA-MB-468-NLS cells were treated with or without cisplatin 100 µM for one hour, then left to grow in drug free media for 24 hours before undergoing RNA extraction and gene expression analysis. Each experiment was conducted in triplicate and the number of significantly differentially expressed genes analysed between the cell lines, and cells treated with or without cisplatin.

Comparisons between untreated cells identifies that the expression of five genes differ between MDA-MB-468-Vector and MDA-MB-NLS cells (Table 6.3). There are no significant differences in gene expression between the MDA-MB-468-Vector and MDA-MB-468-HER2 cell lines or between the MDA-MB-468-HER2 and MDA-MB-468-NLS cell line (Table 6.2).

GeneBank ID	Gene Symbol	Regulation	Fold Change	Adjusted P Value	Gene Name
LDHB	NM_002300	Up	2.28	0.006	Lactate dehydrogenase B
IRS-1	NM_005544	Up	2.5	0.006	Insulin receptor substrate 1
SCGB2A2	BC067220	Down	4.4	0.02	Secretoglobin family 2A member 2
BACC1	NM_001080519	Up	2.2	0.03	BAH domain and coiled-coil containing 1
DACHI	NM_080759	Down	1.6	0.03	Dachshund homolog 1 (Drosophila)

Table 6.3 Five genes are differentially expressed between the MDA-MB-468-Vector and MDA-MB-468-NLS cell lines

6.5.2 Modulation of gene expression in proliferating MDA-MB-468 cells by HER2

Further RNA expression arrays were conducted in MDA-MB-468 transfected cells. Unlike the experiment described in section 6.5.1, RNA was extracted from cells when they were 80% confluent. Differences were identified in gene expression between MDA-MB-468-Vector and MDA-MB-468-HER2 cells and MDA-MB-468-Vector and MDA-MB-468-NLS cells lines but not MDA-MB-468-HER2 and MDA-MB-468-NLS cells (Table 6.4).

Comparison	Genes ($p<0.05$)
MDA-MB-468-Vector vs. MDA –MB-486-HER2	962
MDA-MB-468-Vector vs. MDA –MB-486-NLS	1052
MDA-MB-468-HER2 vs. MDA –MB-486-NLS	0

Table 6.4 Gene expression profiles of MDA-MB-468 HER2 transfected proliferating cells
MDA-MB-468-Vector, MDA-MB-468-HER2 and MDA-MB-468-NLS cells were grown until 80% confluent and then subjected to RNA extraction and gene expression analysis. Each experiment was conducted in triplicate and the number of significantly differentially expressed genes analysed between the cell lines.

6.5.2.1 Identification of genes of interest

Due to the larger number of genes identified the data were mined for the presence of known genes involved in DNA repair, nuclear transport and other HER family members (gene lists are described in Appendix One). This work identifies alterations in seven genes between the MDA-MB-468-Vector and MDA-MB-468-HER2 cell lines (Table 6.5). None of the genes identified in Table 6.3 were identified as being differentially

expressed in this gene expression array experiment. Of specific interest in this experiment is the up-regulation of the HER2 gene and the HER2 interactive protein in MDA-MB-468-HER2 and MDA-MB-468-NLS cells.

GeneBank ID	Gene Function	Regulation compared with MDA-MB-468-Vector	Fold Change MDA-MB-468-HER2	Fold Change MDA-MB-468-NLS
EGFR		Down	1.5	ns
HER2		Up	19.6	18.5
HER2IP	HER2 interactive protein. Binds to the unphosphorylated HER2 receptor and regulates localisation and function (Borg *et al.*, 2000).	Up	87.8	76.0
PIKFYVE	Involved in the endosomal transport of membrane receptors, including EGFR (Kim *et al.*, 2007)	Up	1.8	1.6
ADAM10	Disintegrin and metalloproteinase domain-containing protein 10, which may be involved in the shedding of HER2 from the cell membrane (Liu *et al.*, 2006).	Down	1.2	ns
FANCG	The protein Fanconi complementation group G is also known as XRCC9 and is involved in the process of homologous recombination ((Wilson *et al.*, 2001))	Down	2.9	2.7
BRCA2	Breast cancer 2 susceptibility protein, also known as FANCD1, is involved in homologous recombination and interstrand crosslink repair (Cipak *et al.*, 2006).	Down	1.4	ns

Table 6.5 Significantly differentially expressed genes of interest in the MDA-MB-468-HER2 and MDA-MB-468-NLS cell lines compared with the MDA-MB-468-Vector cell line
There are no significant differences in gene expression between the MDA-MB-468-HER2 and MDA-MB-468-NLS cell lines. ns= not significant.

6.5.2.1.1 Gene set enrichment analysis for functional annotation

In order to examine if certain cellular pathways were altered by the transfection of HER2, enrichment by protein function was performed using Partek Genomic suite software. This analysis involves the clustering of genes by their function as described by their gene ontology annotation and the calculation of an enrichment score based

upon minus log value of the mean p-values within in a gene cluster. This essentially identifies statistically over-represented clusters of genes (Huang da *et al.*, 2009). The enrichment score can be used as a guide to indicate if a specific cluster of genes are biologically significantly altered within the expression array analysis (Huang da *et al.*, 2009).

Two comparisons were analysed, MDA-MB-468-Vector against MDA-MB-468-HER2 (Table 6.6) and MDA-MB-468-Vector and MDA-MB-468-NLS (Table 6.7). Five functional groups are highly enriched in both comparisons: localisation, prostanoid metabolic process, prostaglandin metabolic process, regulation of cell proliferation and negative regulation of epithelial cell proliferation.

Gene Ontology ID	Enrichment Score	Function	No. altered genes	Total No. of genes
006	19.3405	Epidermal growth factor receptor activity	2	2
51179	18.9658	Localisation	10	64
6692	18.3621	Prostanoid metabolic process	3	6
6693	18.3621	Prostaglandin metabolic process	3	6
50678	15.7378	Regulation of epithelial cell proliferation	5	21
15183	15.3737	L-aspartate transmembrane transporter activity	2	3
15810	15.3737	Aspartate transport	2	3
50680	14.7657	Negative regulation of epithelial cell proliferation	3	8
10564	14.7657	Regulation of cell cycle process	3	8
8104	13.2254	Protein localisation	5	25

Table 6.6 Gene set enrichment analysis for MDA-MB-468-Vector with MDA-MB-468-HER2
Gene enrichment scores were calculated for set of genes as defined by their function. The ten highest gene sets are presented. Five sets of gene functions (in black) are common between this analysis and gene enrichment analysis between MDA-MB-468-vector and MDA-MB-468-NLS gene expression. Five gene sets (in red) are only enriched in this analysis.

A further five functions are highly enriched in the comparison of MDA-MB-468-Vector with MDA-MB-468-HER2. These are the functions of EGFR activity, L-aspartate transmembrane transporter activity, aspartate transport, regulation of the cell cycle and protein localisation (Table 6.6). In the comparison of MDA-MB-468-Vector with MDA-MB-468-NLS gene expression the additional five enriched functions are

oncostatin-M receptor activity, establishment of chromosome localization, muscle thin filament tropomyosin, sugar:hydrogen symporter activity and bile acid binding (Table 6.7).

Gene Ontology ID	Enrichment Score	Function	No. altered genes	Total no. of genes
6692	16.6413	Prostanoid metabolic process	3	6
6693	16.6413	Prostaglandin metabolic process	3	6
50678	14.0903	Regulation of epithelial cell proliferation	5	21
4924	13.9874	Oncostatin-M receptor activity	2	3
50680	13.3505	Negative regulation of epithelial cell proliferation	3	8
51303	13.3505	Establishment of chromosome localization	3	8
5862	11.552	Muscle thin filament tropomyosin	2	4
5351	11.552	Sugar:hydrogen symporter activity	2	4
32052	11.552	Bile acid binding	2	4
51179	10.2762	Localization	8	64

Table 6.7 Gene set enrichment analysis for MDA-MB-468-Vector with MDA-MB-468-NLS
Gene enrichment scores were calculated for set of genes as defined by their function. The ten highest gene sets are presented. Five sets of gene functions (in black) are common between this analysis and gene enrichment analysis between MDA-MB-468-vector and MDA-MB-468-HER2 gene expression. Five gene sets (in red) are only enriched in this analysis.

6.6 The modulation of insulin receptor substrate-1 by HER2 expression and cisplatin

As demonstrated on section 6.5.1 there is a significant 2.5 fold increase in the gene expression of insulin receptor substrate1 (IRS-1) in MDA-MB-468-NLS cells compared with MDA-MB-468-Vector cells (p 0.006) and a 2.3 fold increase in the expression of IRS-1 gene in MDA-MB-468-HER2 cell line compared with MDA-MB-468-Vector cells (p 0.05) (Table 6.3). As IRS-1 is implicated in the process of HR through an interaction with Rad51 (Jeon *et al.*, 2008; Trojanek *et al.*, 2003), the expression of IRS1 was investigated further using RT-PCR to confirm the RNA expression array results and using Western blotting to examine protein expression.

RT-PCR demonstrates that the gene expression of IRS-1 is increased in both the MDA-MB-468-HER2 and MDA-MB-468-NLS cell lines compared with the MDA-MB-468-Vector cells (Figure 6.8A). However, the expression of IRS-1 is reduced in both the MDA-MB-468-HER2 and MDA-MB-468-NLS compared with the MDA-MB-468-Vector cells (Figure 6.8B).

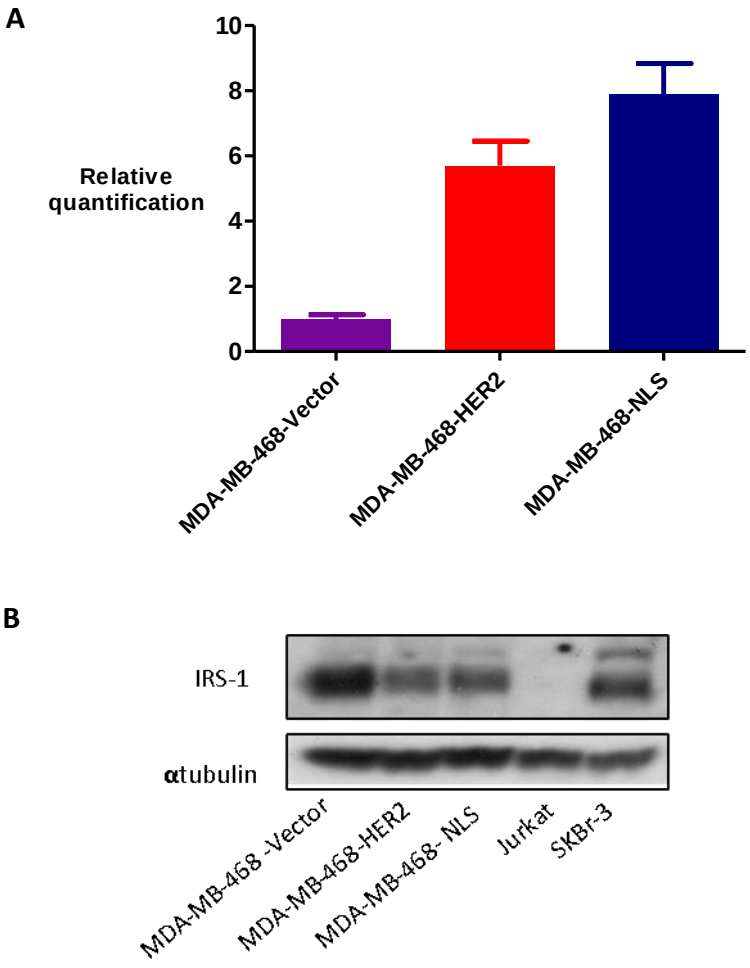

Figure 6.8 Modulation of IRS-1 gene and protein expression by HER2 and cisplatin
(A) RT-PCR was performed on the same RNA samples as used in the gene expression array. Data are presented as the mean±SEM of three triplicate experiments (B) The expression of IRS-1 in MDA-MB-468-Vector, MDA-B-468-HER2 and MDA-MD-468-NLS cells was assessed by Western Blotting. Figure is representative of three independent experiments.

The modulation of IRS-1 by cisplatin in all three cell lines was investigated using Western blotting though this experiment was only conducted once. Treatment of the MDA-MB-468-HER2 cells with cisplatin or trastuzumab increases the phosphorylation of HER2 and the combination of cisplatin and trastuzumab has no effect on the level of

HER2 phosphorylation, over either drug given alone (Figure 6.9). In the MDA-MB-468-NLS cell line the effect of cisplatin or trastuzumab on the phosphorylation of HER2 is less than that observed in the MDA-MB-468-HER2 cell line. The combination of cisplatin and trastuzumab increases the level of phosphorylation of HER2-NLS over that seen with either drug alone. No phosphorylated HER2 is detected in the MDA-MB-468-Vector cell line under the conditions examined.

IRS-1 expression increases in response to cisplatin in all three cell lines but the degree of increase maybe higher in both the MDA-MB-468-Vector and MDA-MB-468-NLS cells lines, compared with the MDA-MB-469-HER2 cell line (Figure 6.9). This experiment would need to be repeated to confirm this result. Trastuzumab in combination with cisplatin has no effect on the expression of IRS-1 in any of the three cell lines.

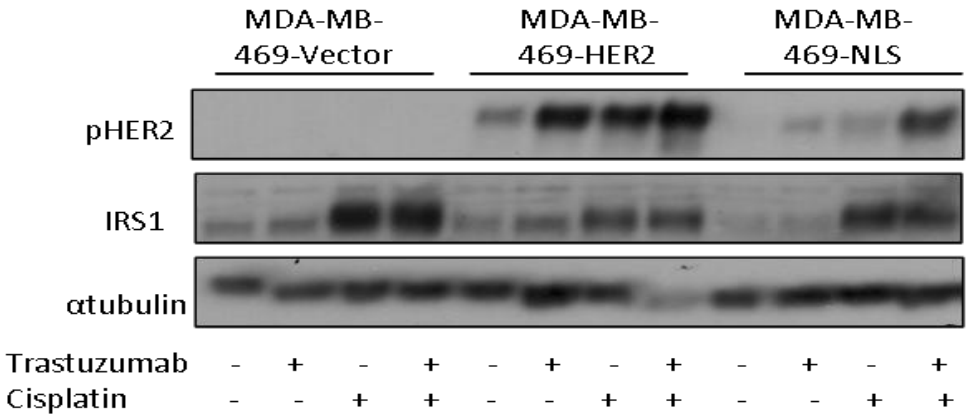

Figure 6.9 Modulation of IRS1 protein expression by cisplatin
The modulation of IRS1 expression by cisplatin and trastuzumab was investigated in the MDA-MB-468-Vector, MDA-B-468-HER2 and MDA-MD-468-NLS cells. Cells were treated with cisplatin (50 μM) for one hour ± trastuzumab for 2 hours, followed by DFM or trastuzumab for 24 hours. Cells were then lysed and immunoblotted for the expression of pHER2 and IRS-1. αtubulin is used as a loading control. This experiment has only been conducted once.

6.7 The modulation of FANCC gene expression by HER2

As discussed in the introduction, FANCC plays a key role in the repair of interstrand crosslinks and its promoter contains the specific sequence which is bound by nuclear HER2. Whilst this gene was not found to be significantly differentially expressed in either of the RNA expression arrays, in view of the fact that its promoter has been identified as a target of HER2 (Wang *et al.*, 2004), we confirmed our results using RT-PCR. These data demonstrate lower expression in the MDA-MB-468-HER2 and MDA-

MB-NLS cell lines (Figure 6.10). If nuclear HER2 promoted the transcription of the FANCC gene, we would to observe a difference in the FANCC RNA levels between the MDA-MB-468-HER and MDA-MB-468-NLS cell lines. RT-PCR demonstrates that there is no difference in the FANCC RNA levels between MDA-MB-468-HER2 and MDA-MB-468-NLS cells indicating that in the MDA-MB-468 cell line, nuclear HER2 does not regulate the transcription of FANCC.

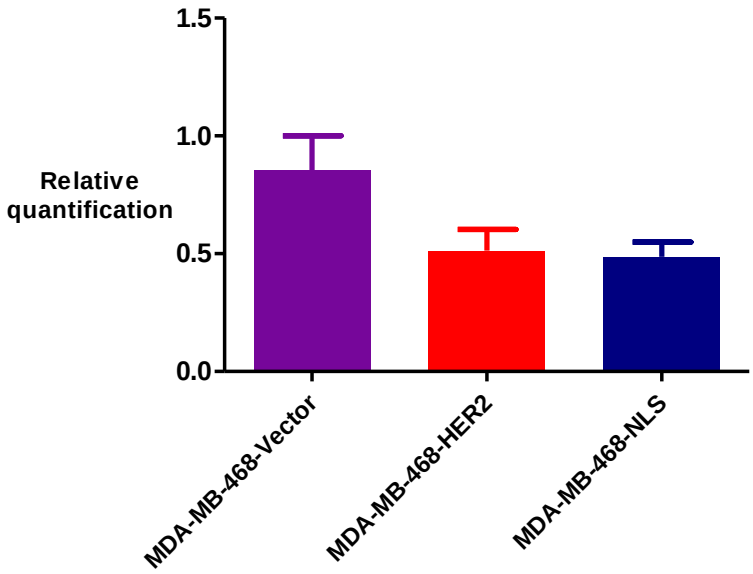

Figure 6.10 Modulation of FANCC gene expression by HER2 transfection
RT-PCR was performed on the same RNA samples as used in the gene expression array. Data are presented as the mean±SEM of three triplicate experiments.

6.8 DISCUSSION

This chapter describes experiments to investigate the mechanism through which HER2 is able to mediate resistance to cisplatin and increase the rate of repair of cisplatin-induced interstrand crosslinks. The main aim of these experiments was to generate hypotheses to form the basis of further investigation.

6.8.1 The modulation of cellular phenotype by HER2 expression

The transfection of either full length HER2 or HER2 with a deleted NLS does not alter cell signalling in the key PI3K/AKT or Ras-Raf-MAPK pathways (Boone *et al.*, 2009). In order to further characterise the activity of HER2 in MDA-MB-468 cells the effect on cell proliferation was further characterised. The transfection of HER2 increased the

rate of cell proliferation compared with cells transfected with the vector alone, whereas cell proliferation was initially slower in cells transfected with HER2 with a deleted NLS, but accelerated between 48 and 72 hours (Figure 6.2).

Both forms of HER2 are phosphorylated in response to the anti-HER2 antibody trastuzumab (Figure 6.3). The dependence of MDA-MB-468 cells stably transfected with full length HER2 is demonstrated by the inhibition of the repair of cisplatin-induced interstrand crosslinks when the expression of the transfected HER2 is reduced using siRNA (Figure 6.5). Taken together these results demonstrate that despite not altering the PI3K/AKT and Ras-Raf-MAPK pathways, transfected HER2 is able to alter the phenotype of transfected cells and is active

6.8.2 Identification of the targets of HER2

Given that HER2 is able to bind to a nine nucleotide sequence within gene promoters, we hypothesised that the explanation for HER2 induced resistance to cisplatin was due to the upregulation of specific genes by HER2. To identify possible genes two techniques were utilised, ChiP and gene expression analysis. HER2 bound DNA was immunoprecipitated from MDA-MB-468 cells transfected with either a vector or full length HER2. Whilst the initial results appeared promising, the experiments were not reproducible, so ChiP-sequencing was not undertaken. The reasons for this failure include the lack of specific ChiP antibodies against HER2 and that we used an antibody designed for used in the immunoprecipitation of proteins, though it has previously been used in ChiP experiments to identify the gene promoter targets of HER2 (Wang *et al.*, 2004).

RNA expression was studied in two separate experiments. The first identified five genes differentially expressed between the MDA-MB-468-Vector and the MDA-MB-468-NLS cell lines, including IRS1. The modulation of IRS1 by cisplatin and trastuzumab was investigated further in view of published data indicating a role for IRS1 in HR (discussed further below).

The second RNA expression study was carried out in cells allowed to grow to 80% confluence. This experiment yielded different results to the first, with a greater

number of genes identified as being differentially expressed between MDA-MB-468-Vector cells and MDA-MB-468-HER2 and MDA-MB-468-NLS cells. Both RNA expression studies did not identify any differences in gene expression between the MDA-MB-468-HER2 and MDA-MB-468-NLS lines.

Analysis for the expression of genes known to be involved in DNA repair and the HER pathway identified the down-regulation of FANCG and BRCA2 in cells transfected with HER2 compared with the vector control; both these proteins are involved in HR (Scott and Pandita, 2006; Wyman *et al.*, 2004). PIKFYVE, which involved in the nuclear transport EGFR (Kim *et al.*, 2007), is upregulated in MDA-MB-468-HER2 cells. The expression of these genes will need to be quantitated using RT-PCR and their protein expression analysed.

6.8.3 The modulation of IRS1 expression by HER2 transfection

RNA expression arrays indicate that the IRS1 gene is significantly upregulated in MDA-MB-468-NLS cells compared with the MDA-MB-468-Vector cell line by 2.5 fold (Table 6.1). In addition there is a 2.3 fold increase in the MDA-MB-468-HER2 cells compared with the MDA-MB-468-Vector cell line, though the p value is 0.05. RT-PCR confirms an increase in IRS1 RNA levels in both MDA-MB-468-NLS and MDA-MB-468-HER cell lines compared with the MDA-MB-468-Vector cell line (Figure 6.7A). However, IRS1 protein expression is lower in cells transfected with either full length HER2 or HER2 with a deleted NLS, compared with cells transfected with the vector only (Figure 6.8B). Whilst at first this observation appears contradictory, this could be explained by an increase in signalling utilising IRS1, resulting in its degradation.

IRS1 transmits signals between the insulin receptor and IGFR to the PI3K/AKT and Ras-Raf-MAPK signalling pathways (Pollak, 2008). Activated IGFR, attracts and phosphorylates the protein IRS-1 which has a number of phosphorylation sites, including sites which bind Grb2, SH and the PI3K regulatory subunit, p85 (Pollak, 2008). IGFR signalling is highly complex and implicated in mediating resistance to chemotherapy (Hopkins *et al.*, 2011). The formation of dimers between IGFR and HER2 is an identified mechanism of resistance to trastuzumab, with insulin growth factor (IGF) stimulation of IGFR resulting in HER2 phosphorylation (Lu *et al.*, 2001; Nahta *et*

al., 2005). Therefore, IRS1 links to IGFR through the same downstream signalling pathways as the HER family. The role of IRS1 in HER2 mediated resistance to cisplatin warrants further investigation as there is evidence of its ability to regulate the process of HR as IRS1 binds RAD51, a key protein involved in the process of step of strand invasion and the search for homology within the sister chromatid both essential for HR (Trojanek *et al.*, 2003). The phosphorylation of IRS1 through the activation of IGFR, releases RAD51 from the cytoplasmic IRS1/RAD51 complex allowing RAD51 to translocate to the nucleus and localise to sites of DNA damage (Trojanek *et al.*, 2003). In contrast, transport of IRS1 into the nucleus in cells transformed by the viral proto-oncogenes human polyomavirus JC (Trojanek *et al.*, 2006a) and SV40 T-antigen (DeAngelis *et al.*, 2006; Prisco *et al.*, 2002), increases sensitivity to both cisplatin and IR through the co-localisation of IRS1 with RAD51 in the nucleus (Trojanek *et al.*, 2006b) which inhibits HR (Urbanska *et al.*, 2009).

IGF1 reduces the apoptotic and DNA damaging effects of cisplatin through the inhibition of the nuclear translocation of IRS1 in response to cisplatin, indicating that phosphorylated IRS1 does not translocate to the nucleus (Jeon *et al.*, 2008). Therefore, a hypothesis would be that the expression of HER2 in MDA-MB-468 cells, increases IGF signalling through dimerisation of HER2 with IGFR, increasing the phosphorylation of IRS1 preventing its translocation to the nucleus and releasing IRS1 from RAD51 promoting the process of DNA repair by HR.

However, this hypothesis is not supported by the data as the MDA-MB-468-NLS cells repair fewer interstrand crosslinks than the MDA-MB-468-HER cells (Boone *et al.*, 2009), despite increased IRS1 gene expression. In addition these cells repair fewer interstrand crosslinks than the MDA-MB-468-Vector cells, indicating that the deletion of the NLS, actually inhibits their repair. This observation could be explained by the initial slower rate of proliferation observed in MDA-MB-468-NLS cells (Figure 6.2) thereby slowing DNA repair or an alteration in the function or location of a critical protein due to the deletion of the NLS. This protein may be involved in cell to cell communication, as MDA-MB-468-NLS cells have a slower proliferation rate for the first 48 hours after plating, which increases exponentially between 48 to 72 hours implying that cell confluence influences cell proliferation (Figure 6.2). This may also explain

differences in the two gene expression array studies undertaken. The first array investigated gene expression in cells allowed to grow for 48 hours, where as the second study investigated cells at 80% confluence which took 96-120 hours.

6.9 CONCLUSIONS AND FUTURE WORK

The transfection of HER2 into the HER2 negative MDA-MB-468 cells increases the rate of cell proliferation and resistance to cisplatin. HER2 transfected cells became dependent upon the HER2 protein, with its inhibition by trastuzumab rendering cells unable to unhook cisplatin-induced interstrand crosslinks.

Examination of gene expression indicates that the IRS1 gene is upregulated in HER2 and HER2-NLS transfected cells, yet the protein expression is reduced. Preliminary data indicates that IRS1 expression is increased in response to cisplatin and that there may be differences on the modulation of IRS1 between the three cell lines investigated. If these results are confirmed, further investigation into the modulation of IRS1 by HER2 in response to cisplatin would be warranted to test the requirement for the phosphorylation of IRS1 to promote the process of HR, as reported in the literature.

RNA expression analysis in cells allowed to reach 80% confluence indicates that a number of functional pathways are modulated by the expression of HER2. Prior to further work into the role of these pathways, confirmation of differences in the ability of these cells to repair cisplatin-induce interstrand crosslinks will need to be obtained.

Conclusions

The main aim of this study was to investigate the modulation of DNA damage induced by anti-cancer agents and its repair, by duration of exposure to TKIs targeted against EGFR and HER2. The second part of this study describes experiments to examine the role of HER2 in mediating resistance to the cytotoxic effects of cisplatin.

Activation of HER family signalling is involved in mediating resistance to anti-cancer agents including IR and cisplatin, with the most widely studied mechanism the modulation of DNA-PK activity and localisation by EGFR, which interferes with the process of NHEJ. As discussed in Chapter One section 1.8, small molecule TKIs targeted against EGFR and HER2 are able to modulate the expression of thymidylate synthase and glutathione, inhibit multi-drug transporters, DNA repair and cell signalling pathways involved in cell proliferation. Despite this, combinations of chemotherapy drugs with TKIs have produced modest results in the case of lapatinib in combination with capecitabine or paclitaxel and studies conducted with gefitinib in lung cancer, failed to demonstrate any benefit from the addition of gefitinib to standard chemotherapy.

Recent studies indicate that initial exposure to TKIs rapidly inhibits EGFR and HER2 signalling within 60 minutes, but that with continued treatment, resistance can be induced through the stimulation of HER3 signalling. This raises the question as to whether this resistance can explain why combinations of TKIs with cytotoxic agents have not produced the results anticipated.

The following objectives were studied:

- The ability of lapatinib to synergise with cisplatin and doxorubicin and the effect of schedule (Chapter Three).
- The modulation of induction of DNA strand breaks by cisplatin, IR, etoposide and doxorubicin by short and long exposure to gefitinib or lapatinib (Chapter Four).
- The modulation of topoisomerase IIα by gefitinib (Chapter Five).
- The role of HER2 in mediating resistance to cisplatin (Chapter Six).

7.1 THE IMPORTANCE OF SCHEDULE IN COMBINING LAPATINIB WITH CISPLATIN OR DOXORUBICIN

Using the techniques of median effect and isobologram analysis, data presented in Chapter Three demonstrates that schedule produces a greater impact on the inhibition of cell proliferation by cisplatin, than doxorubicin. Across the three breast cancer cell lines investigated, the schedule of cisplatin first produces greater synergy than observed with the schedules in which lapatinib is given first, or both drugs continuously. Whilst isobologram analysis demonstrates a lesser influence of schedule on the inhibition of cell proliferation by doxorubicin, median effect analysis indicates that the least efficacious schedule is when lapatinib is scheduled before doxorubicin.

Experiments were conducted with low concentrations of lapatinib which inhibited cell proliferation by around 20%. At these concentrations, lapatinib does not fully inhibit HER2 function and these experiments may have underestimated the full effects of lapatinib in combination with doxorubicin or cisplatin. When using targeted agents, it may be better to utilise a concentration of lapatinib which inhibits HER2 phosphorylation for a shorter period of time. For example 1 μM lapatinib for one hour, prior to, in combination with or following chemotherapy, but then have allowed cells to grow in drug free media for the required duration. Furthermore, these drug combination assays do not identify the possible mechanisms through which lapatinib produces its effects. This could be achieved by using siRNA to knockdown specific genes of interest or entire signalling pathways, such as those involved in DNA repair.

7.2 THE MODULATION OF DNA DAMAGE INDUCTION AND REPAIR BY DURATION OF EXPOSURE TO GEFITINIB OR LAPATINIB

This study demonstrates that the exposure to either gefitinib or lapatinib for 48 hours results in the resumption of PI3K/AKT signalling despite initial inhibition, in agreement with the published data. Whilst duration of exposure to either gefitinib or lapatinib has no effect on the induction of interstrand crosslinks by cisplatin or DNA strand breaks by IR, gefitinib treatment for 48 hours significantly delays its repair. Lapatinib exposure for 48 hours has a lesser impact on the repair of DNA damage induced by either cisplatin or IR. The study of DNA repair using the Comet assay is limited by the fact that

cells are removed for analysis at different time points, rather than a single cell followed over time, as for example in a reporter assay. Additionally, over time cells are lost due to cell death, leaving behind cells which are either resistant to the DNA damaging agent under investigation or daughters of repaired cells. The Comet assay is unable to distinguish between cells which have fully repaired their damaged DNA and those that were undamaged, or are new. Comet tails are also lengthened during apoptosis due to DNA fragmentation and the assay relies on the visual recognition of cells undergoing apoptosis, over those with DNA strand breaks.

The most striking observation in this study is the effect of continued exposure to gefitinib or lapatinib on the induction of DNA lesions by the Topo II poisons doxorubicin, etoposide and m-AMSA, with the production of DNA DSBS, inhibited following TKI exposure for 48 hours. This was demonstrated by both the alkaline and neutral Comet assays and assessment of γH2AX. The concentration of Topo II poison was substantially reduced to allow γH2AX foci to be counted, which may have altered the numbers and ratio of DNA single to double strand breaks induced by the poisons, impacting on the results presented. However, these data demonstrate significant differences in the production and resolution of γH2AX foci in cells treated with Topo II poison alone and those pre-treated with TKI for 48 hours.

The repair of DNA strand breaks produced by Topo II poisons in cells treated with TKI for 48 hours could not be investigated due to the very low numbers detected, either by the Comet assay or measurement of γH2AX foci. Whilst this may have been possible if the dose of TKI had been reduced substantially, this would have altered the amount of reactivated AKT present in cells, as demonstrated Amin *et al*. with higher phosphorylated AKT detected in cells treated with lapatinib 200 nM for 48 hours compared with 1 or 5 μM (Amin *et al.*, 2010), thereby significantly altering experimental conditions.

7.2.1 Differences between topoisomerase II poisons

In Chapters Four and Five clear differences in the DNA damaging effects of the three Topo II poisons investigated are reported. Doxorubicin-induces DNA strand breaks as detected by the alkaline and neutral Comet assays and γH2AX formation in cells

treated with TKIs for one hour, but this is significantly inhibited in cells treated for 48 hours. Doxorubicin produces single and double strand breaks in an equal ratio (Pommier *et al.*, 2010), yet the alkaline Comet assay detects few strand breaks, indicating that ability of doxorubicin to induce single or double strand breaks is significantly affected following exposure to TKI for 48 hours.

Like doxorubicin, etoposide-induces DNA strand breaks in cells treated with either TKI for one hour, and significantly fewer in cells treated with TKI for 48 hours, as indicated by the alkaline Comet assay. Data from the neutral Comet assay and measurement of γH2AX foci indicates that continuous TKI treatment for 48 hours significantly inhibits its ability to induce DNA DSBs. This suggests that the strand breaks detected in the alkaline Comet assay are single stranded DNA breaks and these are rapidly repaired following the removal of etoposide.

M-AMSA induces strand breaks to the same degree regardless of the duration of TKI exposure as measured by the alkaline Comet assay. However, the neutral Comet assay and γH2AX foci formation indicate that fewer DSBs are produced in cells treated with TKI for 48 hours. TKI also promotes the repair of DNA strand breaks, regardless of the duration of TKI exposure, which cannot be explained by a reduction in the number of DSB, as TKI exposure for one hour reduces the production of DSB by a non-significant amount at the concentrations of m-AMSA investigated. These differences cannot be easily explained, though one possibility is that the reduced number of DSBs is enough to increase the rate of repair of DNA damage as detected in the alkaline Comet assay, despite no statistically significant difference in DSBs detected by both the neutral Comet assay and measurement of γH2AX foci. This hypothesis could be explored by increasing the number or repeat experiments performed in neutral Comet assay and measurement of γH2AX foci which would increase the sensitivity of the assay for detection of smaller differences. An alternative possibility is that m-AMSA dissociates more easily from the Topo II enzyme, allowing it to function normally.

It should be noted that the alkaline Comet assay detects both single and double DNA strand breaks, in contrast to the neutral assay and γH2AX foci which are more sensitive to the presence of DNA double stranded breaks.

7.2.2 Binding of topoisomerase II poisons to topoisomerase II

There is little published data on the precise sites at which doxorubicin and m-AMSA bind to Topo II. Both drugs exert base preferences within the Topo II-DNA complex and it is felt they target the Topo II protein when it is bound to DNA (Nitiss, 2009a; Pommier *et al.*, 2010). The binding of etoposide to Topo II is the most widely studied interaction between the Topo II enzyme and its poison. Etoposide binds to Topo II at two sites, one contained in the catalytic core and the other in the ATP-binding N-terminal domain (Vilain *et al.*, 2003). To form a DSB an etoposide molecule is required to bind each of the two Topo II molecules which make up the Topo II homodimer, with single strand breaks formed if only one Topo II molecule is targeted (Bromberg *et al.*, 2003). Etoposide produces 7-20 single strand breaks for every DSB (Pommier *et al.*, 2010).

Hypophosphorylation of Topo IIα enzyme confers resistance to doxorubicin, m-AMSA and etoposide (Chikamori *et al.*, 2003). The precise sites of hypophosphorylation and their relevance to the function of Topo II poisons have not all been investigated, though dephosphorylation at serine 1106 renders cells resistant to the cytotoxic effects of both m-AMSA and etoposide (Chikamori *et al.*, 2003).

Chapter Five demonstrates that continued exposure to either gefitinib or lapatinib for 48 hours induces a cell cycle arrest and reduces the expression of Topo IIα, a mechanism which is known to render cells resistant to the effects of Topo II poisons (Nitiss, 2009b; Pommier *et al.*, 2010). However, etoposide is still able to induce a concentration dependent increase in both single and double DNA strand breaks in cells treated with TKI for 48 hours, as detected in both the alkaline and neutral Comet assays. This indicates that the reduction in strand breaks induction is not just attributable to a reduction in the expression of Topo IIα, but may be due to reduced affinity of etoposide for Topo II, which is overcome by higher concentrations of the drug. This observation is in contrast to both doxorubicin and m-AMSA, as the neutral Comet assay does not demonstrate a concentration dependent increase in the number of DSBs produced by either drug in cells treated with gefitinib for 48 hours. These differences may be explained by the targeting of different sites on Topo IIα. This is

supported by the literature with etoposide inducing cleavable complexes at more than one DNA site, compare with m-AMSA and doxorubicin which act at a single site.

7.3 FUTURE DIRECTIONS

7.3.1 Does the scheduling of TKI following chemotherapy inhibit DNA repair more than concurrent treatment?

Chapter Three examined the influence of schedule on the inhibition of cell proliferation by doxorubicin and cisplatin in combination with lapatinib. We found that schedules in which lapatinib is given following exposure to chemotherapy are the most efficacious. The use of short course intermittent TKI is supported by small phase II clinical trials in which erlotinib was given on days 5-15 (Riely *et al.*, 2009) or days 15-28 (Mok *et al.*, 2009b) following gemcitabine and cisplatin or high dose erlotinib at a dose of 1500 mg given for two days prior to carboplatin and paclitaxel chemotherapy (Zwitter *et al.*, 2011).

Having demonstrated that continuous exposure to TKI leads to resistance to Topo II poisons, including doxorubicin, it would be interesting to examine the effect on DNA repair and apoptosis of treating cells with a DNA damaging agent first, followed by exposure to TKI and how it compares with the results presented here.

7.3.2 Does exposure to gefitinib or lapatinib downregulate the targets of chemotherapy?

Doxorubicin, epirubicin, etoposide and m-AMSA all target Topo IIα in order to produce DNA strand breaks. Topo IIα downregulation was observed in the SK-Br-3 cell line by 48 hours, following treatment with gefitinib or lapatinib, leading to resistance to doxorubicin, etoposide and m-AMSA. If the downregulation of Topo IIα occurs in patients, this could also lead to resistance to drugs which target this enzyme. Therefore it is important to establish whether this finding translates into the clinic given a number of clinical trials currently being undertaken. These include the neo-ALLTO trial investigating the use of neo-adjuvant lapatinib in patients with breast cancer who would be expected to receive adjuvant anthracycline based chemotherapy (National Cancer Institute, 2011c). If lapatinib leads to resistance to anthracyclines through the downregulation of Topo IIα, it could reduce the benefits of adjuvant

anthracycline based chemotherapy. In addition phase III randomised placebo control trials are being conducted to examine lapatinib in combination with liposomal doxorubicin in patients with metastatic breast cancer (National Cancer Institute, 2011a) and in combination with epirubicin, cisplatin and capecitabine in patients with HER2 overexpressing gastric cancer (NCRI ST03 and EORTC 40071 trials).

The expression of Topo IIα, could be investigated in patients with breast cancer who do not require neo-adjuvant chemotherapy. These patients could be treated with gefitinib or lapatinib for two days or more, just prior to surgery, allowing the measurement of Topo II expression by IHC, in their diagnostic biopsy and the surgical specimens. Similar investigations could be undertaken in patients with NSCLC with subcutaneous nodules, cervical lymph nodes or pleural effusions who receive erlotinib in the second line setting, with biopsies taken just prior to commencement of erlotinib and a few days later. As well as assessing Topo IIα expression, other targets of chemotherapy drugs could be examined, including Topo I and thymidylate synthase, a target of 5-FU.

As discussed in Chapter One, section 1.8.4, *in vitro* data demonstrates that TKIs can reduce the expression of thymidylate synthase and increase the expression of thymidine phosphorylase, enhancing sensitivity to 5-FU. This may explain why lapatinib in combination with capecitabine is more efficacious than capecitabine alone in patients with metastatic breast cancer. A clinical trial is currently being undertaken to examine lapatinib in combination with oxaliplatin and capecitabine in patients with HER2 overexpressing gastric or oesophageal cancer (National Cancer Institute, 2011b), to ascertain if this synergy translates into other tumour types. Mesothelioma is another tumour in which combinations of TKI with the thymidylate synthase inhibitor, pemetrexed could be investigated as around 50% of these tumours express EGFR (Destro *et al.*, 2006). Mesothelioma also offers the opportunity to obtain repeat pleural fluid cytology or pleural biopsies to allow the examination of protein expression during treatment.

7.3.3 Is the effect of tyrosine kinase inhibition on topoisomerase II protein expression and activity linked to HER2?

The enzyme casein kinase Iδ is known to regulate the activity and sensitivity of Topo IIα to Topo II poisons and casein kinase Iδ function is inhibited by gefitinib. It is not known if this inhibition is due to a direct, off target effect of gefitinib or due to the inhibition of EGFR and HER2 signalling. The first step in investigating a connection between HER signalling and Topo II, would be to confirm the *in vitro* observation of a reduction in Topo IIα expression in response to TKI exposure, occurs in the clinical setting.

7.3.4 Are differences between the effects of gefitinib and lapatinib on the repair of cisplatin-induced interstrand crosslinks and IR-induced DNA damage explained by DNA-PK?

DNA-PK is involved in the repair of DNA damage induced by both cisplatin and IR (Dittmann *et al.*, 2005b; Friedmann *et al.*, 2006) and the TKI erlotinib, which like gefitinib binds to EGFR when it is in an active conformation inhibits the phosphorylation of DNA-PK_{CS}, but the HER2 targeted TKI AG825 does not (Toulany *et al.*, 2010). Lapatinib, regardless of duration does not inhibit the repair of IR-induced DNA lesions and has a lesser effect on the repair of cisplatin-induced DNA lesions than gefitinib. This could be due to the fact that lapatinib does not inhibit the activity of the DNA-PK_{CS} in contrast to gefitinib, due to differences in the inhibition of EGFR between gefitinib and lapatinib. This could be investigated by examining the effect of lapatinib on the phosphorylation of DNA-PK_{CS} by both cisplatin and IR. In addition further experiments to examine differences between the two TKIs on the localisation of both EGFR and DNA-PK in response to cisplatin and IR could be investigated using confocal microscopy and proximity ligation assays.

7.3.5 Are IRS1 and RAD51 modulated by HER2 leading to resistance to cisplatin in patients with HER2 amplified breast cancer?

Data presented in Chapter Six requires further confirmation by the replication of the experiments as described. If these confirm differences in the expression of IRS1 in the MDA-MB-468-Vector, MDA-MB-468-HER2 and MDA-MB-468-NLS cells, further work on

the localisation of IRS1 and RAD51 in response to cisplatin may explain the observed alteration in the unhooking of cisplatin-induced interstrand crosslinks. This could be achieved through the use of confocal microscopy to examine the localisation of IRS1 and RAD51 in response to cisplatin in the MDA-MB-468-Vector and MDA-MB-468-HER2 cells. If HER2 is involved in the phosphorylation of IRS1, which releases RAD51, we would expect to observe a greater formation of RAD51 foci in response to cisplatin in the MDA-MB-468-HER2 cells than the MDA-MB-468-Vector cells, together with possible differences in the localisation of IRS1 between the two cell lines. If this was confirmed, further studies could be undertaken to assess if the NLS sequence is important in the link between HER2, IRS1 and RAD51, explaining why the MDA-MB-468-NLS cells are less able to repair cisplatin-induced interstrand crosslink than their vector control.

7.4 CONCLUSIONS

We have established that continued exposure to gefitinib or lapatinib does not alter the induction DNA lesions induced by either IR or cisplatin, but differences exist between the two TKIs and DNA repair. In contrast, continued exposure to TKI renders cells resistant cytotoxic effects of the topoisomerase IIα poisons doxorubicin, etoposide and m-AMSA, through the down-regulation of the expression of topoisomerase IIα and the reduction in the induction of DNA double stand breaks as indicated by both the neutral Comet assay and the expression of γH2AX foci.

Further work is needed to ascertain if the *in vitro* findings discussed here are relevant in the clinic. To date a number of randomised phase II and phase III trials examining the used of anti-EGFR therapies, either in the form of monoclonal antibodies or TKI in combination with standard chemotherapy in lung, colorectal and oesophagogasric cancer have not found a benefit from the targeting of EGFR (Gatzemeier *et al.*, 2007; Herbst *et al.*, 2005; Maughan *et al.*, 2011; Rao *et al.*, 2010). If further ongoing combination studies are also negative, we may be in danger of throwing out useful drug combinations because we do not fully understand the role of EGFR and HER2 in modulating DNA repair and promoting resistance. There is evidence that inhibition of EGFR and HER2 phosphorylation alone may not be important, but also their cellular location, binding to DNA-PK or other proteins, the ability of cells to switch to

alternative mechanisms of activating key signalling pathways and the fact that their inhibition may downregulate the target of Topo II poisons, explaining why schedule has an impact on efficacy when combining TKIs with chemotherapy.

8.0 REFERENCES

Adachi S, Natsume H, Yamauchi J, Matsushima-Nishiwaki R, Joe AK, Moriwaki H *et al.* (2009)**:** p38 MAP kinase controls EGF receptor downregulation via phosphorylation at Ser1046/1047. *Cancer Lett* 277**:** 108-113

Adjuvant! Online Adjuvant! Online: Decision making tools for health care professionals. https://www.adjuvantonline.com/index.jsp

Affymetrix (2005):Gene chip exam array design http://www.affymetrix.com/support/technical/technotes/exon_array_design_technote.pdf. Date accessed Jan 2011

Ahsan A, Hiniker SM, Davis MA, Lawrence TS, Nyati MK (2009)**:** Role of cell cycle in epidermal growth factor receptor inhibitor-mediated radiosensitization. *Cancer Res* 69**:** 5108-5114

Ahsan A, Hiniker SM, Ramanand SG, Nyati S, Hegde A, Helman A *et al.* (2010)**:** Role of epidermal growth factor receptor degradation in cisplatin-induced cytotoxicity in head and neck cancer. *Cancer Res* 70**:** 2862-2869

Al-Ejeh F, Kumar R, Wiegmans A, Lakhani SR, Brown MP, Khanna KK (2010)**:** Harnessing the complexity of DNA-damage response pathways to improve cancer treatment outcomes. *Oncogene* 29**:** 6085-6098

Albain KS, Barlow WE, Shak S, Hortobagyi GN, Livingston RB, Yeh IT *et al.* (2010)**:** Prognostic and predictive value of the 21-gene recurrence score assay in postmenopausal women with node-positive, oestrogen-receptor-positive breast cancer on chemotherapy: a retrospective analysis of a randomised trial. *Lancet Oncol* 11**:** 55-65

Albain KS, Nag SM, Calderillo-Ruiz G, Jordaan JP, Llombart AC, Pluzanska A *et al.* (2008)**:** Gemcitabine plus Paclitaxel versus Paclitaxel monotherapy in patients with metastatic breast cancer and prior anthracycline treatment. *J Clin Oncol* 26**:** 3950-3957

Allgayer H, Babic R, Gruetzner KU, Tarabichi A, Schildberg FW, Heiss MM (2000)**:** c-erbB-2 is of independent prognostic relevance in gastric cancer and is associated with the expression of tumor-associated protease systems. *J Clin Oncol* 18**:** 2201-2209

Amado RG, Wolf M, Peeters M, Van Cutsem E, Siena S, Freeman DJ *et al.* (2008)**:** Wild-type KRAS is required for panitumumab efficacy in patients with metastatic colorectal cancer. *J Clin Oncol* 26**:** 1626-1634

Amin DN, Sergina N, Ahuja D, McMahon M, Blair JA, Wang D *et al.* (2010)**:** Resiliency and vulnerability in the HER2-HER3 tumorigenic driver. *Sci Transl Med* 2**:** 16ra7

Anastasi S, Fiorentino L, Fiorini M, Fraioli R, Sala G, Castellani L *et al.* (2003)**:** Feedback inhibition by RALT controls signal output by the ErbB network. *Oncogene* 22**:** 4221-4234

Andl CD, Mizushima T, Oyama K, Bowser M, Nakagawa H, Rustgi AK (2004)**:** EGFR-induced cell migration is mediated predominantly by the JAK-STAT pathway in primary esophageal keratinocytes. *Am J Physiol Gastrointest Liver Physiol* 287**:** G1227-1237

Ang KK, Andratschke NH, Milas L (2004)**:** Epidermal growth factor receptor and response of head-and-neck carcinoma to therapy. *Int J Radiat Oncol Biol Phys* 58**:** 959-965

Annecke K, Schmitt M, Euler U, Zerm M, Paepke D, Paepke S *et al.* (2008)**:** uPA and PAI-1 in breast cancer: review of their clinical utility and current validation in the prospective NNBC-3 trial. *Adv Clin Chem* 45**:** 31-45

Arteaga CL, Ramsey TT, Shawver LK, Guyer CA (1997)**:** Unliganded epidermal growth factor receptor dimerization induced by direct interaction of quinazolines with the ATP binding site. *J Biol Chem* 272**:** 23247-23254

Aubele M, Auer G, Walch AK, Munro A, Atkinson MJ, Braselmann H *et al.* (2007)**:** PTK (protein tyrosine kinase)-6 and HER2 and 4, but not HER1 and 3 predict long-term survival in breast carcinomas. *Br J Cancer* 96**:** 801-807

Balak MN, Gong Y, Riely GJ, Somwar R, Li AR, Zakowski MF *et al.* (2006)**:** Novel D761Y and common secondary T790M mutations in epidermal growth factor receptor-mutant lung adenocarcinomas with acquired resistance to kinase inhibitors. *Clin Cancer Res* 12**:** 6494-6501

Balana ME, Labriola L, Salatino M, Movsichoff F, Peters G, Charreau EH *et al.* (2001)**:** Activation of ErbB-2 via a hierarchical interaction between ErbB-2 and type I insulin-like growth factor receptor in mammary tumor cells. *Oncogene* 20**:** 34-47

Banath JP, Klokov D, MacPhail SH, Banuelos CA, Olive PL (2010)**:** Residual gammaH2AX foci as an indication of lethal DNA lesions. *BMC Cancer* 10**:** 4

Banath JP, Olive PL (2003)**:** Expression of phosphorylated histone H2AX as a surrogate of cell killing by drugs that create DNA double-strand breaks. *Cancer Res* 63**:** 4347-4350

Bang YJ, Van Cutsem E, Feyereislova A, Chung HC, Shen L, Sawaki A *et al.* (2010)**:** Trastuzumab in combination with chemotherapy versus chemotherapy alone for treatment of HER2-positive advanced gastric or gastro-oesophageal junction cancer (ToGA): a phase 3, open-label, randomised controlled trial. *Lancet* 376**:** 687-697

Bartlett JM, Thomas J, Ross DT, Seitz RS, Ring BZ, Beck RA *et al.* (2010)**:** Mammostrat as a tool to stratify breast cancer patients at risk of recurrence during endocrine therapy. *Breast Cancer Res* 12**:** R47

Baselga J, Swain SM (2010)**:** CLEOPATRA: a phase III evaluation of pertuzumab and trastuzumab for HER2-positive metastatic breast cancer. *Clin Breast Cancer* 10**:** 489-491

Bastien RR, Ebbert MT, Boucher KM, Kelly CM, Wang B, Iwamoto T *et al.* (2011)**:** Using the PAM50 breast cancer intrinsic classifier to assess risk in ER+ breast cancers: A direct comparison to Oncotype DX. *J Clin Oncol* 29**:** abstr 503

Bean J, Riely GJ, Balak M, Marks JL, Ladanyi M, Miller VA *et al.* (2008)**:** Acquired resistance to epidermal growth factor receptor kinase inhibitors associated with a novel T854A mutation in a patient with EGFR-mutant lung adenocarcinoma. *Clin Cancer Res* 14**:** 7519-7525

Beatson CT (1896)**:** On treatment of inoperable cases of carcinoma of the mamma: suggestions for a new method of treatment with illustrative cases. *Lancet* 2**:** 162–165

Beguelin W, Diaz Flaque MC, Proietti CJ, Cayrol F, Rivas MA, Tkach M *et al.* (2010)**:** Progesterone receptor induces ErbB-2 nuclear translocation to promote breast cancer growth via a novel transcriptional effect: ErbB-2 function as a coactivator of Stat3. *Mol Cell Biol* 30**:** 5456-5472

Bell DW, Lynch TJ, Haserlat SM, Harris PL, Okimoto RA, Brannigan BW *et al.* (2005)**:** Epidermal growth factor receptor mutations and gene amplification in non-small-cell lung cancer: molecular analysis of the IDEAL/INTACT gefitinib trials. *J Clin Oncol* 23**:** 8081-8092

Benhar M, Engelberg D, Levitzki A (2002)**:** Cisplatin-induced activation of the EGF receptor. *Oncogene* 21**:** 8723-8731

Benz CC, Scott GK, Sarup JC, Johnson RM, Tripathy D, Coronado E *et al.* (1992)**:** Estrogen-dependent, tamoxifen-resistant tumorigenic growth of MCF-7 cells transfected with HER2/neu. *Breast Cancer Res Treat* 24**:** 85-95

Beug H, von Kirchbach A, Doderlein G, Conscience JF, Graf T (1979)**:** Chicken hematopoietic cells transformed by seven strains of defective avian leukemia viruses display three distinct phenotypes of differentiation. *Cell* 18**:** 375-390

Bhargava R, Gerald WL, Li AR, Pan Q, Lal P, Ladanyi M *et al.* (2005)**:** EGFR gene amplification in breast cancer: correlation with epidermal growth factor receptor mRNA and protein expression and HER-2 status and absence of EGFR-activating mutations. *Mod Pathol* 18**:** 1027-1033

Bianco C, Tortora G, Bianco R, Caputo R, Veneziani BM, Caputo R *et al.* (2002)**:** Enhancement of antitumor activity of ionizing radiation by combined treatment with the selective epidermal growth factor receptor-tyrosine kinase inhibitor ZD1839 (Iressa). *Clin Cancer Res* 8**:** 3250-3208

Bianco R, Gelardi T, Damiano V, Ciardiello F, Tortora G (2007)**:** Rational bases for the development of EGFR inhibitors for cancer treatment. *Int J Biochem Cell Biol* 39**:** 1416-1431

Bieche I, Onody P, Tozlu S, Driouch K, Vidaud M, Lidereau R (2003)**:** Prognostic value of ERBB family mRNA expression in breast carcinomas. *Int J Cancer* 106**:** 758-765

Binaschi M, Capranico G, De Isabella P, Mariani M, Supino R, Tinelli S *et al.* (1990)**:** Comparison of DNA cleavage induced by etoposide and doxorubicin in two human small-cell lung cancer lines with different sensitivities to topoisomerase II inhibitors. *Int J Cancer* 45**:** 347-352

Blanchot-Jossic F, Jarry A, Masson D, Bach-Ngohou K, Paineau J, Denis MG *et al.* (2005)**:** Up-regulated expression of ADAM17 in human colon carcinoma: co-expression with EGFR in neoplastic and endothelial cells. *J Pathol* 207**:** 156-163

Bokemeyer C, Bondarenko I, Makhson A, Hartmann JT, Aparicio J, de Braud F *et al.* (2009)**:** Fluorouracil, leucovorin, and oxaliplatin with and without cetuximab in the first-line treatment of metastatic colorectal cancer. *J Clin Oncol* 27**:** 663-671

Bonadonna G, Valagussa P, Moliterni A, Zambetti M, Brambilla C (1995)**:** Adjuvant cyclophosphamide, methotrexate, and fluorouracil in node-positive breast cancer: the results of 20 years of follow-up. *N Engl J Med* 332**:** 901-906

Bonner JA, Harari PM, Giralt J, Cohen RB, Jones CU, Sur RK *et al.* (2010)**:** Radiotherapy plus cetuximab for locoregionally advanced head and neck cancer: 5-year survival data from a phase 3 randomised trial, and relation between cetuximab-induced rash and survival. *Lancet Oncol* 11**:** 21-28

Bonner WM, Redon CE, Dickey JS, Nakamura AJ, Sedelnikova OA, Solier S *et al.* (2008)**:** GammaH2AX and cancer. *Nat Rev Cancer* 8**:** 957-967

Boone JJ, Bhosle J, Tilby MJ, Hartley JA, Hochhauser D (2009)**:** Involvement of the HER2 pathway in repair of DNA damage produced by chemotherapeutic agents. *Mol Cancer Ther* 8**:** 3015-3023

Borg JP, Marchetto S, Le Bivic A, Ollendorff V, Jaulin-Bastard F, Saito H *et al.* (2000)**:** ERBIN: a basolateral PDZ protein that interacts with the mammalian ERBB2/HER2 receptor. *Nat Cell Biol* 2**:** 407-414

Brehmer D, Greff Z, Godl K, Blencke S, Kurtenbach A, Weber M *et al.* (2005)**:** Cellular targets of gefitinib. *Cancer Res* 65**:** 379-382

Bromberg KD, Burgin AB, Osheroff N (2003)**:** A two-drug model for etoposide action against human topoisomerase IIalpha. *J Biol Chem* 278**:** 7406-7412

Buchholz TA, Tu X, Ang KK, Esteva FJ, Kuerer HM, Pusztai L *et al.* (2005)**:** Epidermal growth factor receptor expression correlates with poor survival in patients who have breast carcinoma treated with doxorubicin-based neoadjuvant chemotherapy. *Cancer* 104**:** 676-681

Budman DR, Soong R, Calabro A, Tai J, Diasio R (2006)**:** Identification of potentially useful combinations of epidermal growth factor receptor tyrosine kinase antagonists with conventional cytotoxic agents using median effect analysis. *Anticancer Drugs* 17**:** 921-928

Burgaud JL, Baserga R (1996)**:** Intracellular transactivation of the insulin-like growth factor I receptor by an epidermal growth factor receptor. *Exp Cell Res* 223**:** 412-419

Burgess DJ, Doles J, Zender L, Xue W, Ma B, McCombie WR *et al.* (2008)**:** Topoisomerase levels determine chemotherapy response in vitro and *in vivo*. *Proc Natl Acad Sci U S A* 105**:** 9053-9058

Burke PM, Wiley HS (1999)**:** Human mammary epithelial cells rapidly exchange empty EGFR between surface and intracellular pools. *J Cell Physiol* 180**:** 448-460

Burness ML, Grushko TA, Olopade OI (2010)**:** Epidermal growth factor receptor in triple-negative and basal-like breast cancer: promising clinical target or only a marker? *Cancer J* 16**:** 23-32

Burris HA, 3rd, Taylor CW, Jones SF, Koch KM, Versola MJ, Arya N *et al.* (2009)**:** A phase I and pharmacokinetic study of oral lapatinib administered once or twice daily in patients with solid malignancies. *Clin Cancer Res* 15**:** 6702-6708

Burstein HJ, Prestrud AA, Seidenfeld J, Anderson H, Buchholz TA, Davidson NE *et al.* (2010)**:** American Society of Clinical Oncology clinical practice guideline: update on adjuvant endocrine therapy for women with hormone receptor-positive breast cancer. *J Clin Oncol* 28**:** 3784-3796

Burtness B, Goldwasser MA, Flood W, Mattar B, Forastiere AA (2005)**:** Phase III randomized trial of cisplatin plus placebo compared with cisplatin plus cetuximab in metastatic/recurrent head and neck cancer: an Eastern Cooperative Oncology Group study. *J Clin Oncol* 23**:** 8646-8654

Buyse M, Loi S, van't Veer L, Viale G, Delorenzi M, Glas AM *et al.* (2006)**:** Validation and clinical utility of a 70-gene prognostic signature for women with node-negative breast cancer. *J Natl Cancer Inst* 98**:** 1183-1192

Byrski T, Gronwald J, Huzarski T, Grzybowska E, Budryk M, Stawicka M *et al.* (2010)**:** Pathologic complete response rates in young women with BRCA1-positive breast cancers after neoadjuvant chemotherapy. *J Clin Oncol* 28**:** 375-379

Caldecott K, Jeggo P (1991)**:** Cross-sensitivity of gamma-ray-sensitive hamster mutants to cross-linking agents. *Mutat Res* 255**:** 111-121

Calikusu Z, Yildirim Y, Akcali Z, Sakalli H, Bal N, Unal I *et al.* (2009)**:** The effect of HER2 expression on cisplatin-based chemotherapy in advanced non-small cell lung cancer patients. *J Exp Clin Cancer Res* 28**:** 97

Cameron D, Casey M, Press M, Lindquist D, Pienkowski T, Romieu CG *et al.* (2008)**:** A phase III randomized comparison of lapatinib plus capecitabine versus capecitabine alone in women with advanced breast cancer that has progressed on trastuzumab: updated efficacy and biomarker analyses. *Breast Cancer Res Treat* 112**:** 533-543

Campbell MR, Amin D, Moasser MM (2010)**:** HER3 comes of age: new insights into its functions and role in signaling, tumor biology, and cancer therapy. *Clin Cancer Res* 16**:** 1373-1383

Cantley LC (2002)**:** The phosphoinositide 3-kinase pathway. *Science* 296**:** 1655-1657

Cappuzzo F, Toschi L, Domenichini I, Bartolini S, Ceresoli GL, Rossi E *et al.* (2005)**:** HER3 genomic gain and sensitivity to gefitinib in advanced non-small-cell lung cancer patients. *Br J Cancer* 93**:** 1334-1340

Carey LA, Perou CM, Livasy CA, Dressler LG, Cowan D, Conway K *et al.* (2006)**:** Race, breast cancer subtypes, and survival in the Carolina Breast Cancer Study. *Jama* 295**:** 2492-2502

Carpenter AJ, Porter AC (2004)**:** Construction, characterization, and complementation of a conditional-lethal DNA topoisomerase II alpha mutant human cell line. *Mol Biol Cell* 15**:** 5700-5711

Chandarlapaty S, Sawai A, Scaltriti M, Rodrik-Outmezguine V, Grbovic-Huezo O, Serra V *et al.* (2011)**:** AKT inhibition relieves feedback suppression of receptor tyrosine kinase expression and activity. *Cancer Cell* 19**:** 58-71

Chen C, Kane M, Song J, Campana J, Raben A, Hu K *et al.* (2007)**:** Phase I trial of gefitinib in combination with radiation or chemoradiation for patients with locally advanced squamous cell head and neck cancer. *J Clin Oncol* 25**:** 4880-4886

Chia S, Gradishar W, Mauriac L, Bines J, Amant F, Federico M *et al.* (2008)**:** Double-blind, randomized placebo controlled trial of fulvestrant compared with exemestane after prior nonsteroidal aromatase inhibitor therapy in postmenopausal women with hormone receptor-positive, advanced breast cancer: results from EFECT. *J Clin Oncol* 26**:** 1664-1670

Chikamori K, Grabowski DR, Kinter M, Willard BB, Yadav S, Aebersold RH *et al.* (2003)**:** Phosphorylation of serine 1106 in the catalytic domain of topoisomerase II alpha regulates enzymatic activity and drug sensitivity. *J Biol Chem* 278**:** 12696-12702

Chinnaiyan P, Huang S, Vallabhaneni G, Armstrong E, Varambally S, Tomlins SA *et al.* (2005)**:** Mechanisms of enhanced radiation response following epidermal growth factor receptor signaling inhibition by erlotinib (Tarceva). *Cancer Res* 65**:** 3328-3335

Cho HS, Mason K, Ramyar KX, Stanley AM, Gabelli SB, Denney DW, Jr. *et al.* (2003)**:** Structure of the extracellular region of HER2 alone and in complex with the Herceptin Fab. *Nature* 421**:** 756-760

Chou TC (2006)**:** Theoretical basis, experimental design, and computerized simulation of synergism and antagonism in drug combination studies. *Pharmacol Rev* 58**:** 621-681

Chou TC (2010)**:** Drug combination studies and their synergy quantification using the Chou-Talalay method. *Cancer Res* 70**:** 440-446

Chun PY, Feng FY, Scheurer AM, Davis MA, Lawrence TS, Nyati MK (2006)**:** Synergistic effects of gemcitabine and gefitinib in the treatment of head and neck carcinoma. *Cancer Res* 66**:** 981-988

Chung I, Akita R, Vandlen R, Toomre D, Schlessinger J, Mellman I (2010)**:** Spatial control of EGF receptor activation by reversible dimerization on living cells. *Nature* 464**:** 783-787

Ciardiello F, Caputo R, Bianco R, Damiano V, Pomatico G, De Placido S *et al.* (2000)**:** Antitumor effect and potentiation of cytotoxic drugs activity in human cancer cells by ZD-1839 (Iressa), an epidermal growth factor receptor-selective tyrosine kinase inhibitor. *Clin Cancer Res* 6**:** 2053-2063

Ciardiello F, Kim N, Saeki T, Dono R, Persico MG, Plowman GD *et al.* (1991)**:** Differential expression of epidermal growth factor-related proteins in human colorectal tumors. *Proc Natl Acad Sci U S A* 88**:** 7792-7796

Ciardiello F, Troiani T, Caputo F, De Laurentiis M, Tortora G, Palmieri G *et al.* (2006)**:** Phase II study of gefitinib in combination with docetaxel as first-line therapy in metastatic breast cancer. *Br J Cancer* 94**:** 1604-1609

Clarke R, Leonessa F, Trock B (2005)**:** Multidrug resistance/P-glycoprotein and breast cancer: review and meta-analysis. *Semin Oncol* 32**:** S9-15

Clevenger CV (2004)**:** Roles and regulation of stat family transcription factors in human breast cancer. *Am J Pathol* 165**:** 1449-1460

Clingen PH, Wu JY, Miller J, Mistry N, Chin F, Wynne P *et al.* (2008)**:** Histone H2AX phosphorylation as a molecular pharmacological marker for DNA interstrand crosslink cancer chemotherapy. *Biochem Pharmacol* 76**:** 19-27

Cohen EE, Haraf DJ, Kunnavakkam R, Stenson KM, Blair EA, Brockstein B *et al.* (2010)**:** Epidermal growth factor receptor inhibitor gefitinib added to chemoradiotherapy in locally advanced head and neck cancer. *J Clin Oncol* 28**:** 3336-3343

Cohen S (1964)**:** Isolation and Biological Effects of an Epidermal Growth-Stimulating Protein. *Natl Cancer Inst Monogr* 13**:** 13-37

Coley HM, Shotton CF, Ajose-Adeogun A, Modjtahedi H, Thomas H (2006)**:** Receptor tyrosine kinase (RTK) inhibition is effective in chemosensitising EGFR-expressing drug resistant human ovarian cancer cell lines when used in combination with cytotoxic agents. *Biochem Pharmacol* 72**:** 941-948

Cunningham D, Humblet Y, Siena S, Khayat D, Bleiberg H, Santoro A *et al.* (2004)**:** Cetuximab monotherapy and cetuximab plus irinotecan in irinotecan-refractory metastatic colorectal cancer. *N Engl J Med* 351**:** 337-345

Curigliano G, Bagnardi V, Viale G, Fumagalli L, Rotmensz N, Aurilio G *et al.* (2011)**:** Should liver metastases of breast cancer be biopsied to improve treatment choice? *Ann Oncol* 22: 2227-2233

D'Alessio A, De Luca A, Maiello MR, Lamura L, Rachiglio AM, Napolitano M *et al.* (2009)**:** Effects of the combined blockade of EGFR and ErbB-2 on signal transduction and regulation of cell cycle regulatory proteins in breast cancer cells. *Breast Cancer Res Treat* 123: 387-396

D'Andrea AD (2010)**:** Susceptibility pathways in Fanconi's anemia and breast cancer. *N Engl J Med* 362**:** 1909-1919

D'Arpa P, Beardmore C, Liu LF (1990)**:** Involvement of nucleic acid synthesis in cell killing mechanisms of topoisomerase poisons. *Cancer Res* 50**:** 6919-6924

Dai CL, Tiwari AK, Wu CP, Su XD, Wang SR, Liu DG *et al.* (2008)**:** Lapatinib (Tykerb, GW572016) reverses multidrug resistance in cancer cells by inhibiting the activity of ATP-binding cassette subfamily B member 1 and G member 2. *Cancer Res* 68**:** 7905-7914

Dai Y, Grant S (2010)**:** New insights into checkpoint kinase 1 in the DNA damage response signaling network. *Clin Cancer Res* 16**:** 376-383

Davies SL, Bergh J, Harris AL, Hickson ID (1997)**:** Response to ICRF-159 in cell lines resistant to cleavable complex-forming topoisomerase II inhibitors. *Br J Cancer* 75**:** 816-821

Dawson JP, Bu Z, Lemmon MA (2007)**:** Ligand-induced structural transitions in ErbB receptor extracellular domains. *Structure* 15**:** 942-954

de Campos-Nebel M, Larripa I, Gonzalez-Cid M (2010)**:** Topoisomerase II-mediated DNA damage is differently repaired during the cell cycle by non-homologous end joining and homologous recombination. *PLoS One* 5 e12541

De Roock W, Jonker DJ, Di Nicolantonio F, Sartore-Bianchi A, Tu D, Siena S *et al.* (2010)**:** Association of KRAS p.G13D mutation with outcome in patients with chemotherapy-refractory metastatic colorectal cancer treated with cetuximab. *Jama* 304**:** 1812-1820

DeAngelis T, Chen J, Wu A, Prisco M, Baserga R (2006)**:** Transformation by the simian virus 40 T antigen is regulated by IGF-I receptor and IRS-1 signaling. *Oncogene* 25**:** 32-42

Deng R, Tang J, Ma JG, Chen SP, Xia LP, Zhou WJ *et al.* (2011)**:** PKB/Akt promotes DSB repair in cancer cells through upregulating Mre11 expression following ionizing radiation. *Oncogene* 30**:** 944-955

Dennison SK, Jacobs SA, Wilson JW, Seeger J, Cescon TP, Raymond JM *et al.* (2007)**:** A phase II clinical trial of ZD1839 (Iressa) in combination with docetaxel as first-line treatment in patients with advanced breast cancer. *Invest New Drugs* 25**:** 545-551

Destro A, Ceresoli GL, Falleni M, Zucali PA, Morenghi E, Bianchi P *et al.* (2006)**:** EGFR overexpression in malignant pleural mesothelioma. An immunohistochemical and molecular study with clinico-pathological correlations. *Lung Cancer* 51**:** 207-215

Di Fiore PP, Pierce JH, Kraus MH, Segatto O, King CR, Aaronson SA (1987)**:** erbB-2 is a potent oncogene when overexpressed in NIH/3T3 cells. *Science* 237**:** 178-182

Di Leo A, Biganzoli L, Claudino W, Licitra S, Pestrin M, Larsimont D (2008a)**:** Topoisomerase II alpha as a marker predicting anthracyclines' activity in early breast cancer patients: ready for the primetime? *Eur J Cancer* 44**:** 2791-2798

Di Leo A, Gomez HL, Aziz Z, Zvirbule Z, Bines J, Arbushites MC *et al.* (2008b)**:** Phase III, Double-Blind, Randomized Study Comparing Lapatinib Plus Paclitaxel With Placebo Plus Paclitaxel As First-Line Treatment for Metastatic Breast Cancer. *J Clin Oncol* 26**:** 5544-5552

Dickstein BM, Wosikowski K, Bates SE (1995)**:** Increased resistance to cytotoxic agents in ZR75B human breast cancer cells transfected with epidermal growth factor receptor. *Mol Cell Endocrinol* 110**:** 205-211

Diermeier S, Horvath G, Knuechel-Clarke R, Hofstaedter F, Szollosi J, Brockhoff G (2005)**:** Epidermal growth factor receptor coexpression modulates susceptibility to Herceptin in HER2/neu overexpressing breast cancer cells via specific erbB-receptor interaction and activation. *Exp Cell Res* 304**:** 604-619

Dittmann K, Mayer C, Fehrenbacher B, Schaller M, Raju U, Milas L *et al.* (2005a)**:** Radiation-induced epidermal growth factor receptor nuclear import is linked to activation of DNA-dependent protein kinase. *J Biol Chem* 280**:** 31182-31189

Dittmann K, Mayer C, Kehlbach R, Rodemann HP (2008)**:** Radiation-induced caveolin-1 associated EGFR internalization is linked with nuclear EGFR transport and activation of DNA-PK. *Mol Cancer* 7**:** 69

Dittmann K, Mayer C, Kehlbach R, Rothmund MC, Peter Rodemann H (2009)**:** Radiation-induced lipid peroxidation activates src kinase and triggers nuclear EGFR transport. *Radiother Oncol* 92**:** 379-82

Dittmann K, Mayer C, Rodemann HP (2005b)**:** Inhibition of radiation-induced EGFR nuclear import by C225 (Cetuximab) suppresses DNA-PK activity. *Radiother Oncol* 76**:** 157-161

Douillard JY, Siena S, Cassidy J, Tabernero J, Burkes R, Barugel M *et al.* (2010)**:** Randomized, phase III trial of panitumumab with infusional fluorouracil, leucovorin, and oxaliplatin (FOLFOX4) versus FOLFOX4 alone as first-line treatment in patients with previously untreated metastatic colorectal cancer: the PRIME study. *J Clin Oncol* 28**:** 4697-4705

Downward J, Yarden Y, Mayes E, Scrace G, Totty N, Stockwell P *et al.* (1984)**:** Close similarity of epidermal growth factor receptor and v-erb-B oncogene protein sequences. *Nature* 307**:** 521-527

Dronkert ML, Kanaar R (2001)**:** Repair of DNA interstrand cross-links. *Mutat Res* 486**:** 217-247

Dubska L, Andera L, Sheard MA (2005)**:** HER2 signaling downregulation by trastuzumab and suppression of the PI3K/Akt pathway: an unexpected effect on TRAIL-induced apoptosis. *FEBS Lett* 579**:** 4149-4158

EBCTCG (2005)**:** Effects of chemotherapy and hormonal therapy for early breast cancer on recurrence and 15-year survival: an overview of the randomised trials. *Lancet* 365**:** 1687-1717

Edge SB, Byrd DR, CC C (2010): *AJCC Cancer Staging Manual*, 7th edn. Springer: N.Y.

Elkhuizen PH, van Slooten HJ, Clahsen PC, Hermans J, van de Velde CJ, van den Broek LC *et al.* (2000)**:** High local recurrence risk after breast-conserving therapy in node-negative premenopausal breast cancer patients is greatly reduced by one course of perioperative chemotherapy: A European Organization for Research and Treatment of Cancer Breast Cancer Cooperative Group Study. *J Clin Oncol* 18**:** 1075-1083

Ellis P, Barrett-Lee P, Johnson L, Cameron D, Wardley A, O'Reilly S *et al.* (2009)**:** Sequential docetaxel as adjuvant chemotherapy for early breast cancer (TACT): an open-label, phase III, randomised controlled trial. *Lancet* 373**:** 1681-1692

Endoh H, Yatabe Y, Kosaka T, Kuwano H, Mitsudomi T (2006)**:** PTEN and PIK3CA expression is associated with prolonged survival after gefitinib treatment in EGFR-mutated lung cancer patients. *J Thorac Oncol* 1**:** 629-634

Engel R, Valkov NI, Gump JL, Hazlehurst L, Dalton WS, Sullivan DM (2004)**:** The cytoplasmic trafficking of DNA topoisomerase II alpha correlates with etoposide resistance in human myeloma cells. *Exp Cell Res* 295**:** 421-431

Engelman JA, Zejnullahu K, Mitsudomi T, Song Y, Hyland C, Park JO *et al.* (2007)**:** MET amplification leads to gefitinib resistance in lung cancer by activating ERBB3 signaling. *Science* 316**:** 1039-1043

Errington F, Willmore E, Leontiou C, Tilby MJ, Austin CA (2004)**:** Differences in the longevity of topo IIalpha and topo IIbeta drug-stabilized cleavable complexes and the relationship to drug sensitivity. *Cancer Chemother Pharmacol* 53**:** 155-162

Ewald JA, Wilkinson JC, Guyer CA, Staros JV (2003)**:** Ligand- and kinase activity-independent cell survival mediated by the epidermal growth factor receptor expressed in 32D cells. *Exp Cell Res* 282**:** 121-131

Fan JR, Peng AL, Chen HC, Lo SC, Huang TH, Li TK (2008)**:** Cellular processing pathways contribute to the activation of etoposide-induced DNA damage responses. *DNA Repair (Amst)* 7**:** 452-463

Feng FY, Varambally S, Tomlins SA, Chun PY, Lopez CA, Li X *et al.* (2007)**:** Role of epidermal growth factor receptor degradation in gemcitabine-mediated cytotoxicity. *Oncogene* 26**:** 3431-3439

Fiorentino L, Pertica C, Fiorini M, Talora C, Crescenzi M, Castellani L *et al.* (2000)**:** Inhibition of ErbB-2 mitogenic and transforming activity by RALT, a mitogen-induced signal transducer which binds to the ErbB-2 kinase domain. *Mol Cell Biol* 20**:** 7735-7750

Fisher B, Anderson S, Bryant J, Margolese RG, Deutsch M, Fisher ER *et al.* (2002)**:** Twenty-year follow-up of a randomized trial comparing total mastectomy, lumpectomy, and lumpectomy plus irradiation for the treatment of invasive breast cancer. *N Engl J Med* 347**:** 1233-1241

Fisher B, Brown A, Mamounas E, Wieand S, Robidoux A, Margolese RG *et al.* (1997)**:** Effect of preoperative chemotherapy on local-regional disease in women with operable breast cancer: findings from National Surgical Adjuvant Breast and Bowel Project B-18. *J Clin Oncol* 15**:** 2483-2493

Fisher GA, Kuo T, Ramsey M, Schwartz E, Rouse RV, Cho CD *et al.* (2008)**:** A phase II study of gefitinib, 5-fluorouracil, leucovorin, and oxaliplatin in previously untreated patients with metastatic colorectal cancer. *Clin Cancer Res* 14**:** 7074-7079

Fountzilas G, Pectasides D, Kalogera-Fountzila A, Skarlos D, Kalofonos HP, Papadimitriou C *et al.* (2005)**:** Paclitaxel and carboplatin as first-line chemotherapy combined with gefitinib (IRESSA) in patients with advanced breast cancer: a phase I/II study conducted by the Hellenic Cooperative Oncology Group. *Breast Cancer Res Treat* 92**:** 1-9

Fox EM, Bernaciak TM, Wen J, Weaver AM, Shupnik MA, Silva CM (2008)**:** Signal transducer and activator of transcription 5b, c-Src, and epidermal growth factor receptor signaling play integral roles in estrogen-stimulated proliferation of estrogen receptor-positive breast cancer cells. *Mol Endocrinol* 22**:** 1781-1796

Francis RE, Myatt SS, Krol J, Hartman J, Peck B, McGovern UB *et al.* (2009)**:** FoxM1 is a downstream target and marker of HER2 overexpression in breast cancer. *Int J Oncol* 35**:** 57-68

Friedmann B, Caplin M, Hartley JA, Hochhauser D (2004)**:** Modulation of DNA repair in vitro after treatment with chemotherapeutic agents by the epidermal growth factor receptor inhibitor gefitinib (ZD1839). *Clin Cancer Res* 10**:** 6476-6486

Friedmann BJ, Caplin M, Savic B, Shah T, Lord CJ, Ashworth A *et al.* (2006)**:** Interaction of the epidermal growth factor receptor and the DNA-dependent protein kinase pathway following gefitinib treatment. *Mol Cancer Ther* 5**:** 209-218

Frosi Y, Anastasi S, Ballaro C, Varsano G, Castellani L, Maspero E *et al.* (2010)**:** A two-tiered mechanism of EGFR inhibition by RALT/MIG6 via kinase suppression and receptor degradation. *J Cell Biol* 189**:** 557-571

Fry AM, Chresta CM, Davies SM, Walker MC, Harris AL, Hartley JA *et al.* (1991)**:** Relationship between topoisomerase II level and chemosensitivity in human tumor cell lines. *Cancer Res* 51**:** 6592-6595

Gan HK, Kaye AH, Luwor RB (2009)**:** The EGFRvIII variant in glioblastoma multiforme. *J Clin Neurosci* 16**:** 748-754

Gasparini G, Sarmiento R, Amici S, Longo R, Gattuso D, Zancan M *et al.* (2005)**:** Gefitinib (ZD1839) combined with weekly epirubicin in patients with metastatic breast cancer: a phase I study with biological correlate. *Ann Oncol* 16**:** 1867-1873

Gatzemeier U, Pluzanska A, Szczesna A, Kaukel E, Roubec J, De Rosa F *et al.* (2007)**:** Phase III study of erlotinib in combination with cisplatin and gemcitabine in advanced non-small-cell lung cancer: the Tarceva Lung Cancer Investigation Trial. *J Clin Oncol* 25**:** 1545-1552

Gewirtz DA (1999)**:** A critical evaluation of the mechanisms of action proposed for the antitumor effects of the anthracycline antibiotics adriamycin and daunorubicin. *Biochem Pharmacol* 57**:** 727-741

Geyer CE, Forster J, Lindquist D, Chan S, Romieu CG, Pienkowski T *et al.* (2006)**:** Lapatinib plus capecitabine for HER2-positive advanced breast cancer. *N Engl J Med* 355**:** 2733-2743

Giaccone G, Herbst RS, Manegold C, Scagliotti G, Rosell R, Miller V *et al.* (2004)**:** Gefitinib in combination with gemcitabine and cisplatin in advanced non-small-cell lung cancer: a phase III trial--INTACT 1. *J Clin Oncol* 22**:** 777-784

Gianni L, Dafni U, Gelber RD, Azambuja E, Muehlbauer S, Goldhirsch A *et al.* (2011)**:** Treatment with trastuzumab for 1 year after adjuvant chemotherapy in patients with HER2-positive early breast cancer: a 4-year follow-up of a randomised controlled trial. *Lancet Oncol* 12**:** 236-244

Giovannetti E, Lemos C, Tekle C, Smid K, Nannizzi S, Rodriguez JA *et al.* (2008)**:** Molecular mechanisms underlying the synergistic interaction of erlotinib, an epidermal growth factor receptor tyrosine kinase inhibitor, with the multitargeted antifolate pemetrexed in non-small-cell lung cancer cells. *Mol Pharmacol* 73**:** 1290-1300

Giralt J, de las Heras M, Cerezo L, Eraso A, Hermosilla E, Velez D *et al.* (2005)**:** The expression of epidermal growth factor receptor results in a worse prognosis for patients with rectal cancer treated with preoperative radiotherapy: a multicenter, retrospective analysis. *Radiother Oncol* 74**:** 101-108

Giri DK, Ali-Seyed M, Li LY, Lee DF, Ling P, Bartholomeusz G *et al.* (2005)**:** Endosomal transport of ErbB-2: mechanism for nuclear entry of the cell surface receptor. *Mol Cell Biol* 25**:** 11005-11018

Go RS, Adjei AA (1999)**:** Review of the comparative pharmacology and clinical activity of cisplatin and carboplatin. *J Clin Oncol* 17**:** 409-422

Gold PJ, Goldman B, Iqbal S, Leichman LP, Zhang W, Lenz HJ *et al.* (2010)**:** Cetuximab as Second-Line Therapy in Patients with Metastatic Esophageal Adenocarcinoma: A Phase II Southwest Oncology Group Study (S0415). *J Thorac Oncol*

Golding SE, Morgan RN, Adams BR, Hawkins AJ, Povirk LF, Valerie K (2009)**:** Pro-survival AKT and ERK signaling from EGFR and mutant EGFRvIII enhances DNA double-strand break repair in human glioma cells. *Cancer Biol Ther* 8**:** 730-738

Goldstein NI, Prewett M, Zuklys K, Rockwell P, Mendelsohn J (1995)**:** Biological efficacy of a chimeric antibody to the epidermal growth factor receptor in a human tumor xenograft model. *Clin Cancer Res* 1**:** 1311-1318

Goodman LS, Wintrobe MM, Dameshek W, Goodman MJ, Gilman A, McLennan MT (1984)**:** Landmark article Sept. 21, 1946: Nitrogen mustard therapy. Use of methyl-bis(beta-chloroethyl)amine hydrochloride and tris(beta-chloroethyl)amine hydrochloride for Hodgkin's disease, lymphosarcoma, leukemia and certain allied and miscellaneous disorders. By Louis S. Goodman, Maxwell M. Wintrobe, William Dameshek, Morton J. Goodman, Alfred Gilman and Margaret T. McLennan. *Jama* 251**:** 2255-2261

Gottesman MM, Fojo T, Bates SE (2002)**:** Multidrug resistance in cancer: role of ATP-dependent transporters. *Nat Rev Cancer* 2**:** 48-58

Graham DL, Hillman DW, Hobday TJ, SR R, Nair SG, Soori GS *et al.* (2005)**:** N0234: Phase II study of erlotinib (OSI-774) plus gemcitabine as first-or second-line therapy for metastatic breast cancer (MBC) *2005 ASCO Annual Meeting Proceedings.* 23**:** 644

Graus-Porta D, Beerli RR, Daly JM, Hynes NE (1997)**:** ErbB-2, the preferred heterodimerization partner of all ErbB receptors, is a mediator of lateral signaling. *Embo J* 16**:** 1647-1655

Gray R, Bhattacharya S, Bowden C, Miller K, Comis RL (2009)**:** Independent review of E2100: a phase III trial of bevacizumab plus paclitaxel versus paclitaxel in women with metastatic breast cancer. *J Clin Oncol* 27**:** 4966-4972

Greulich H, Chen TH, Feng W, Janne PA, Alvarez JV, Zappaterra M *et al.* (2005)**:** Oncogenic transformation by inhibitor-sensitive and -resistant EGFR mutants. *PLoS Med* 2**:** e313

Grozav AG, Chikamori K, Kozuki T, Grabowski DR, Bukowski RM, Willard B *et al.* (2009)**:** Casein kinase I delta/epsilon phosphorylates topoisomerase IIalpha at serine-1106 and modulates DNA cleavage activity. *Nucleic Acids Res* 37**:** 382-392

Grozav AG, Willard BB, Kozuki T, Chikamori K, Micluta MA, Petrescu AJ *et al.* (2011)**:** Tyrosine 656 in topoisomerase IIbeta is important for the catalytic activity of the enzyme: Identification based on artifactual +80-Da modification at this site. *Proteomics* 11: 829-842

Gumuskaya B, Alper M, Hucumenoglu S, Altundag K, Uner A, Guler G (2010)**:** EGFR expression and gene copy number in triple-negative breast carcinoma. *Cancer Genet Cytogenet* 203**:** 222-229

Guy PM, Platko JV, Cantley LC, Cerione RA, Carraway KL, 3rd (1994)**:** Insect cell-expressed p180erbB3 possesses an impaired tyrosine kinase activity. *Proc Natl Acad Sci U S A* 91**:** 8132-8136

Habib AA, Hognason T, Ren J, Stefansson K, Ratan RR (1998)**:** The epidermal growth factor receptor associates with and recruits phosphatidylinositol 3-kinase to the platelet-derived growth factor beta receptor. *J Biol Chem* 273**:** 6885-6891

Hanada N, Lo HW, Day CP, Pan Y, Nakajima Y, Hung MC (2006)**:** Co-regulation of B-Myb expression by E2F1 and EGF receptor. *Mol Carcinog* 45**:** 10-17

Hanahan D, Weinberg RA (2000)**:** The hallmarks of cancer. *Cell* 100**:** 57-70

Hanahan D, Weinberg RA (2011)**:** Hallmarks of cancer: the next generation. *Cell* 144**:** 646-674

Hanauske AR, Cassidy J, Sastre J, Bolling C, Jones RJ, Rakhit A *et al.* (2007)**:** Phase 1b dose escalation study of erlotinib in combination with infusional 5-Fluorouracil, leucovorin, and oxaliplatin in patients with advanced solid tumors. *Clin Cancer Res* 13**:** 523-531

Hancock MC, Langton BC, Chan T, Toy P, Monahan JJ, Mischak RP *et al.* (1991)**:** A monoclonal antibody against the c-erbB-2 protein enhances the cytotoxicity of cis-diamminedichloroplatinum against human breast and ovarian tumor cell lines. *Cancer Res* 51**:** 4575-4580

Harrington KJ, El-Hariry IA, Holford CS, Lusinchi A, Nutting CM, Rosine D *et al.* (2009)**:** Phase I study of lapatinib in combination with chemoradiation in patients with locally advanced squamous cell carcinoma of the head and neck. *J Clin Oncol* 27**:** 1100-1107

Hartley JM, Spanswick VJ, Gander M, Giacomini G, Whelan J, Souhami RL *et al.* (1999)**:** Measurement of DNA cross-linking in patients on ifosfamide therapy using the single cell gel electrophoresis (comet) assay. *Clin Cancer Res* 5**:** 507-512

Haura EB, Sommers E, Song L, Chiappori A, Becker A (2010)**:** A pilot study of preoperative gefitinib for early-stage lung cancer to assess intratumor drug concentration and pathways mediating primary resistance.*J Thorac Oncol* 5**:** 1806-1814

Hayashi M, Inokuchi M, Takagi Y, Yamada H, Kojima K, Kumagai J *et al.* (2008)**:** High expression of HER3 is associated with a decreased survival in gastric cancer. *Clin Cancer Res* 14**:** 7843-7849

Heck MM, Hittelman WN, Earnshaw WC (1989)**:** *In vivo* phosphorylation of the 170-kDa form of eukaryotic DNA topoisomerase II. Cell cycle analysis. *J Biol Chem* 264**:** 15161-15164

Helleday T (2010)**:** Homologous recombination in cancer development, treatment and development of drug resistance. *Carcinogenesis* 31**:** 955-960

Hellyer NJ, Cheng K, Koland JG (1998)**:** ErbB3 (HER3) interaction with the p85 regulatory subunit of phosphoinositide 3-kinase. *Biochem J* 333 (Pt 3)**:** 757-763

Hennequin C, Giocanti N, Favaudon V (1995)**:** S-phase specificity of cell killing by docetaxel (Taxotere) in synchronised HeLa cells. *Br J Cancer* 71**:** 1194-1198

Herbst RS, Giaccone G, Schiller JH, Natale RB, Miller V, Manegold C *et al.* (2004)**:** Gefitinib in combination with paclitaxel and carboplatin in advanced non-small-cell lung cancer: a phase III trial--INTACT 2. *J Clin Oncol* 22**:** 785-794

Herbst RS, Prager D, Hermann R, Fehrenbacher L, Johnson BE, Sandler A *et al.* (2005)**:** TRIBUTE: a phase III trial of erlotinib hydrochloride (OSI-774) combined with carboplatin and paclitaxel chemotherapy in advanced non-small-cell lung cancer. *J Clin Oncol* 23**:** 5892-5899

Higashiyama S, Iwabuki H, Morimoto C, Hieda M, Inoue H, Matsushita N (2008)**:** Membrane-anchored growth factors, the epidermal growth factor family: beyond receptor ligands. *Cancer Sci* 99**:** 214-220

Hirata A, Hosoi F, Miyagawa M, Ueda S, Naito S, Fujii T *et al.* (2005)**:** HER2 overexpression increases sensitivity to gefitinib, an epidermal growth factor receptor tyrosine kinase inhibitor, through inhibition of HER2/HER3 heterodimer formation in lung cancer cells. *Cancer Res* 65**:** 4253-4260

Hoeijmakers JH (2009)**:** DNA damage, aging, and cancer. *N Engl J Med* 361**:** 1475-1485

Holm C, Covey JM, Kerrigan D, Pommier Y (1989a)**:** Differential requirement of DNA replication for the cytotoxicity of DNA topoisomerase I and II inhibitors in Chinese hamster DC3F cells. *Cancer Res* 49**:** 6365-6368

Holm C, Stearns T, Botstein D (1989b)**:** DNA topoisomerase II must act at mitosis to prevent nondisjunction and chromosome breakage. *Mol Cell Biol* 9**:** 159-168

Hopkins A, Crowe PJ, Yang JL (2011)**:** Effect of type 1 insulin-like growth factor receptor targeted therapy on chemotherapy in human cancer and the mechanisms involved. *J Cancer Res Clin Oncol* 136**:** 639-650

Hsu SC, Hung MC (2007)**:** Characterization of a novel tripartite nuclear localization sequence in the EGFR family. *J Biol Chem* 282**:** 10432-10440

Hsu SC, Miller SA, Wang Y, Hung MC (2009)**:** Nuclear EGFR is required for cisplatin resistance and DNA repair. *Am J Transl Res* 1**:** 249-258

Huang da W, Sherman BT, Lempicki RA (2009)**:** Systematic and integrative analysis of large gene lists using DAVID bioinformatics resources. *Nat Protoc* 4**:** 44-57

Huang F, Sorkin A (2005)**:** Growth factor receptor binding protein 2-mediated recruitment of the RING domain of Cbl to the epidermal growth factor receptor is essential and sufficient to support receptor endocytosis. *Mol Biol Cell* 16**:** 1268-1281

Huang G, Mills L, Worth LL (2007)**:** Expression of human glutathione S-transferase P1 mediates the chemosensitivity of osteosarcoma cells. *Mol Cancer Ther* 6**:** 1610-1619

Huang S, Armstrong EA, Benavente S, Chinnaiyan P, Harari PM (2004)**:** Dual-agent molecular targeting of the epidermal growth factor receptor (EGFR): combining anti-EGFR antibody with tyrosine kinase inhibitor. *Cancer Res* 64**:** 5355-5362

Hudziak RM, Schlessinger J, Ullrich A (1987)**:** Increased expression of the putative growth factor receptor p185HER2 causes transformation and tumorigenesis of NIH 3T3 cells. *Proc Natl Acad Sci U S A* 84**:** 7159-7163

Huerta S, Goulet EJ, Huerta-Yepez S, Livingston EH (2007)**:** Screening and detection of apoptosis. *J Surg Res* 139**:** 143-156

Hung LY, Tseng JT, Lee YC, Xia W, Wang YN, Wu ML *et al.* (2008)**:** Nuclear epidermal growth factor receptor (EGFR) interacts with signal transducer and activator of transcription 5 (STAT5) in activating Aurora-A gene expression. *Nucleic Acids Res* 36**:** 4337-4351

Imai K, Takaoka A (2006)**:** Comparing antibody and small-molecule therapies for cancer. *Nat Rev Cancer* 6**:** 714-727

Irvin WJ, Jr., Carey LA (2008)**:** What is triple-negative breast cancer? *Eur J Cancer* 44**:** 2799-2805

Ishida R, Iwai M, Marsh KL, Austin CA, Yano T, Shibata M *et al.* (1996)**:** Threonine 1342 in human topoisomerase IIalpha is phosphorylated throughout the cell cycle. *J Biol Chem* 271**:** 30077-30082

Jancik S, Drabek J, Radzioch D, Hajduch M (2010)**:** Clinical relevance of KRAS in human cancers. *J Biomed Biotechnol* 2010**:** 150960

Jenkins JR, Ayton P, Jones T, Davies SL, Simmons DL, Harris AL *et al.* (1992)**:** Isolation of cDNA clones encoding the beta isozyme of human DNA topoisomerase II and localisation of the gene to chromosome 3p24. *Nucleic Acids Res* 20**:** 5587-5592

Jensen PB, Jensen PS, Demant EJ, Friche E, Sorensen BS, Sehested M *et al.* (1991)**:** Antagonistic effect of aclarubicin on daunorubicin-induced cytotoxicity in human small cell lung cancer cells: relationship to DNA integrity and topoisomerase II. *Cancer Res* 51**:** 5093-5099

Jeon JH, Kim SK, Kim HJ, Chang J, Ahn CM, Chang YS (2008)**:** Insulin-like growth factor-1 attenuates cisplatin-induced gammaH2AX formation and DNA double-strand breaks repair pathway in non-small cell lung cancer. *Cancer Lett* 272**:** 232-241

Ji H, Zhao X, Yuza Y, Shimamura T, Li D, Protopopov A *et al.* (2006)**:** Epidermal growth factor receptor variant III mutations in lung tumorigenesis and sensitivity to tyrosine kinase inhibitors. *Proc Natl Acad Sci U S A* 103**:** 7817-7822

Jiang X, Huang F, Marusyk A, Sorkin A (2003)**:** Grb2 regulates internalization of EGF receptors through clathrin-coated pits. *Mol Biol Cell* 14**:** 858-870

Joensuu H, Bono P, Kataja V, Alanko T, Kokko R, Asola R *et al.* (2009)**:** Fluorouracil, epirubicin, and cyclophosphamide with either docetaxel or vinorelbine, with or without trastuzumab, as adjuvant treatments of breast cancer: final results of the FinHer Trial. *J Clin Oncol* 27**:** 5685-5692

Johannessen LE, Pedersen NM, Pedersen KW, Madshus IH, Stang E (2006)**:** Activation of the epidermal growth factor (EGF) receptor induces formation of EGF receptor- and Grb2-containing clathrin-coated pits. *Mol Cell Biol* 26**:** 389-401

Johnson LN (2009)**:** Protein kinase inhibitors: contributions from structure to clinical compounds. *Q Rev Biophys* 42**:** 1-40

Jones SE, Erban J, Overmoyer B, Budd GT, Hutchins L, Lower E *et al.* (2005)**:** Randomized phase III study of docetaxel compared with paclitaxel in metastatic breast cancer. *J Clin Oncol* 23**:** 5542-5551

Junttila TT, Akita RW, Parsons K, Fields C, Lewis Phillips GD, Friedman LS *et al.* (2009)**:** Ligand-independent HER2/HER3/PI3K complex is disrupted by trastuzumab and is effectively inhibited by the PI3K inhibitor GDC-0941. *Cancer Cell* 15**:** 429-440

Jura N, Shan Y, Cao X, Shaw DE, Kuriyan J (2009)**:** Structural analysis of the catalytically inactive kinase domain of the human EGF receptor 3. *Proc Natl Acad Sci U S A* 106**:** 21608-21613

Karapetis CS, Khambata-Ford S, Jonker DJ, O'Callaghan CJ, Tu D, Tebbutt NC *et al.* (2008)**:** K-ras mutations and benefit from cetuximab in advanced colorectal cancer. *N Engl J Med* 359**:** 1757-1765

Kartalou M, Essigmann JM (2001)**:** Recognition of cisplatin adducts by cellular proteins. *Mutat Res* 478**:** 1-21

Karunagaran D, Tzahar E, Beerli RR, Chen X, Graus-Porta D, Ratzkin BJ *et al.* (1996)**:** ErbB-2 is a common auxiliary subunit of NDF and EGF receptors: implications for breast cancer. *Embo J* 15**:** 254-264

Kasahara K, Fujiwara Y, Sugimoto Y, Nishio K, Tamura T, Matsuda T *et al.* (1992)**:** Determinants of response to the DNA topoisomerase II inhibitors doxorubicin and etoposide in human lung cancer cell lines. *J Natl Cancer Inst* 84**:** 113-118

Kenny PA, Lee GY, Myers CA, Neve RM, Semeiks JR, Spellman PT *et al.* (2007)**:** The morphologies of breast cancer cell lines in three-dimensional assays correlate with their profiles of gene expression. *Mol Oncol* 1**:** 84-96

Khambata-Ford S, Harbison CT, Hart LL, Awad M, Xu LA, Horak CE *et al.* (2010)**:** Analysis of potential predictive markers of cetuximab benefit in BMS099, a phase III study of cetuximab and first-line taxane/carboplatin in advanced non-small-cell lung cancer. *J Clin Oncol* 28**:** 918-927

Khan EM, Heidinger JM, Levy M, Lisanti MP, Ravid T, Goldkorn T (2006)**:** Epidermal growth factor receptor exposed to oxidative stress undergoes Src- and caveolin-1-dependent perinuclear trafficking. *J Biol Chem* 281**:** 14486-14493

Kim ES, Hirsh V, Mok T, Socinski MA, Gervais R, Wu YL *et al.* (2008a)**:** Gefitinib versus docetaxel in previously treated non-small-cell lung cancer (INTEREST): a randomised phase III trial. *Lancet* 372**:** 1809-1818

Kim HP, Yoon YK, Kim JW, Han SW, Hur HS, Park J *et al.* (2009)**:** Lapatinib, a dual EGFR and HER2 tyrosine kinase inhibitor, downregulates thymidylate synthase by inhibiting the nuclear translocation of EGFR and HER2. *PLoS One* 4**:** e5933

Kim J, Adam RM, Freeman MR (2005)**:** Trafficking of nuclear heparin-binding epidermal growth factor-like growth factor into an epidermal growth factor receptor-dependent autocrine loop in response to oxidative stress. *Cancer Res* 65**:** 8242-8249

Kim J, Jahng WJ, Di Vizio D, Lee JS, Jhaveri R, Rubin MA *et al.* (2007)**:** The phosphoinositide kinase PIKfyve mediates epidermal growth factor receptor trafficking to the nucleus. *Cancer Res* 67**:** 9229-9237

Kim JW, Kim HP, Im SA, Kang S, Hur HS, Yoon YK *et al.* (2008b)**:** The growth inhibitory effect of lapatinib, a dual inhibitor of EGFR and HER2 tyrosine kinase, in gastric cancer cell lines. *Cancer Lett* 272**:** 296-306

Kim MA, Lee HS, Lee HE, Jeon YK, Yang HK, Kim WH (2008c)**:** EGFR in gastric carcinomas: prognostic significance of protein overexpression and high gene copy number. *Histopathology* 52**:** 738-746

Kimple RJ, Vaseva AV, Cox AD, Baerman KM, Calvo BF, Tepper JE *et al.* (2010)**:** Radiosensitization of epidermal growth factor receptor/HER2-positive pancreatic cancer is mediated by inhibition of Akt independent of ras mutational status. *Clin Cancer Res* 16**:** 912-923

Kishida O, Miyazaki Y, Murayama Y, Ogasa M, Miyazaki T, Yamamoto T *et al.* (2005)**:** Gefitinib (Iressa, ZD1839) inhibits SN38-triggered EGF signals and IL-8 production in gastric cancer cells. *Cancer Chemother Pharmacol* 55**:** 584-594

Kitazaki T, Oka M, Nakamura Y, Tsurutani J, Doi S, Yasunaga M *et al.* (2005)**:** Gefitinib, an EGFR tyrosine kinase inhibitor, directly inhibits the function of P-glycoprotein in multidrug resistant cancer cells. *Lung Cancer* 49**:** 337-343

Knipscheer P, Raschle M, Smogorzewska A, Enoiu M, Ho TV, Scharer OD *et al.* (2009)**:** The Fanconi anemia pathway promotes replication-dependent DNA interstrand cross-link repair. *Science* 326**:** 1698-1701

Ko JC, Ciou SC, Jhan JY, Cheng CM, Su YJ, Chuang SM *et al.* (2009)**:** Roles of MKK1/2-ERK1/2 and phosphoinositide 3-kinase-AKT signaling pathways in erlotinib-induced Rad51 suppression and cytotoxicity in human non-small cell lung cancer cells. *Mol Cancer Res* 7**:** 1378-1389

Kobayashi S, Boggon TJ, Dayaram T, Janne PA, Kocher O, Meyerson M *et al.* (2005)**:** EGFR mutation and resistance of non-small-cell lung cancer to gefitinib. *N Engl J Med* 352**:** 786-792

Komoto M, Nakata B, Amano R, Yamada N, Yashiro M, Ohira M *et al.* (2009a)**:** HER2 overexpression correlates with survival after curative resection of pancreatic cancer. *Cancer Sci* 100**:** 1243-1247

Komoto M, Nakata B, Nishii T, Kawajiri H, Shinto O, Amano R *et al.* (2009b)**:** *In vitro* and *in vivo* evidence that a combination of lapatinib plus S-1 is a promising treatment for pancreatic cancer. *Cancer Sci* 101: 468-473

Konecny GE, Pegram MD, Venkatesan N, Finn R, Yang G, Rahmeh M *et al.* (2006)**:** Activity of the dual kinase inhibitor lapatinib (GW572016) against HER-2-overexpressing and trastuzumab-treated breast cancer cells. *Cancer Res* 66**:** 1630-1639

Konecny GE, Venkatesan N, Yang G, Dering J, Ginther C, Finn R *et al.* (2008)**:** Activity of lapatinib a novel HER2 and EGFR dual kinase inhibitor in human endometrial cancer cells. *Br J Cancer* 98**:** 1076-1084

Kong A, Calleja V, Leboucher P, Harris A, Parker PJ, Larijani B (2008)**:** HER2 oncogenic function escapes EGFR tyrosine kinase inhibitors via activation of alternative HER receptors in breast cancer cells. *PLoS One* 3**:** e2881

Kountourakis P, Pavlakis K, Psyrri A, Rontogianni D, Xiros N, Patsouris E *et al.* (2006)**:** Prognostic significance of HER3 and HER4 protein expression in colorectal adenocarcinomas. *BMC Cancer* 6**:** 46

Krag DN, Anderson SJ, Julian TB, Brown AM, Harlow SP, Costantino JP *et al.* (2010)**:** Sentinel-lymph-node resection compared with conventional axillary-lymph-node dissection in clinically node-negative patients with breast cancer: overall survival findings from the NSABP B-32 randomised phase 3 trial. *Lancet Oncol* 11**:** 927-933

Krol J, Francis RE, Albergaria A, Sunters A, Polychronis A, Coombes RC *et al.* (2007)**:** The transcription factor FOXO3a is a crucial cellular target of gefitinib (Iressa) in breast cancer cells. *Mol Cancer Ther* 6**:** 3169-3179

Kuang YH, Shen T, Chen X, Sodani K, Hopper-Borge E, Tiwari AK *et al.* (2010)**:** Lapatinib and erlotinib are potent reversal agents for MRP7 (ABCC10)-mediated multidrug resistance. *Biochem Pharmacol* 79**:** 154-161

Kumar B, Cordell KG, Lee JS, Worden FP, Prince ME, Tran HH *et al.* (2008)**:** EGFR, p16, HPV Titer, Bcl-xL and p53, sex, and smoking as indicators of response to therapy and survival in oropharyngeal cancer. *J Clin Oncol* 26**:** 3128-3137

Kyula JN, Van Schaeybroeck S, Doherty J, Fenning CS, Longley DB, Johnston PG (2010)**:** Chemotherapy-induced activation of ADAM-17: a novel mechanism of drug resistance in colorectal cancer. *Clin Cancer Res* 16**:** 3378-3389

LaBonte MJ, Manegold PC, Wilson PM, Fazzone W, Louie SG, Lenz HJ *et al.* (2009)**:** The dual EGFR/HER-2 tyrosine kinase inhibitor lapatinib sensitizes colon and gastric cancer cells to the irinotecan active metabolite SN-38. *Int J Cancer* 125**:** 2957-2969

Lacroix M, Leclercq G (2004)**:** Relevance of breast cancer cell lines as models for breast tumours: an update. *Breast Cancer Res Treat* 83**:** 249-289

Lee AH, Ellis IO (2008)**:** The Nottingham prognostic index for invasive carcinoma of the breast. *Pathol Oncol Res* 14**:** 113-115

Lee AH, Pinder SE, Macmillan RD, Mitchell M, Ellis IO, Elston CW *et al.* (2006a)**:** Prognostic value of lymphovascular invasion in women with lymph node negative invasive breast carcinoma. *Eur J Cancer* 42**:** 357-362

Lee JC, Vivanco I, Beroukhim R, Huang JH, Feng WL, DeBiasi RM *et al.* (2006b)**:** Epidermal growth factor receptor activation in glioblastoma through novel missense mutations in the extracellular domain. *PLoS Med* 3**:** e485

Lee MT, Bachant J (2009)**:** SUMO modification of DNA topoisomerase II: trying to get a CENse of it all. *DNA Repair (Amst)* 8**:** 557-568

Leggas M, Panetta JC, Zhuang Y, Schuetz JD, Johnston B, Bai F *et al.* (2006)**:** Gefitinib modulates the function of multiple ATP-binding cassette transporters *in vivo*. *Cancer Res* 66**:** 4802-4807

Lenferink AE, Pinkas-Kramarski R, van de Poll ML, van Vugt MJ, Klapper LN, Tzahar E *et al.* (1998)**:** Differential endocytic routing of homo- and hetero-dimeric ErbB tyrosine kinases confers signaling superiority to receptor heterodimers. *Embo J* 17**:** 3385-3397

Leroy D, Kajava AV, Frei C, Gasser SM (2001)**:** Analysis of etoposide binding to subdomains of human DNA topoisomerase II alpha in the absence of DNA. *Biochemistry* 40**:** 1624-1634

Levkowitz G, Waterman H, Ettenberg SA, Katz M, Tsygankov AY, Alroy I *et al.* (1999)**:** Ubiquitin ligase activity and tyrosine phosphorylation underlie suppression of growth factor signaling by c-Cbl/Sli-1. *Mol Cell* 4**:** 1029-1040

Li L, Wang H, Yang ES, Arteaga CL, Xia F (2008)**:** Erlotinib attenuates homologous recombinational repair of chromosomal breaks in human breast cancer cells. *Cancer Res* 68**:** 9141-9146

Li T, Ling YH, Goldman ID, Perez-Soler R (2007)**:** Schedule-dependent cytotoxic synergism of pemetrexed and erlotinib in human non-small cell lung cancer cells. *Clin Cancer Res* 13**:** 3413-3422

Liao HJ, Carpenter G (2009)**:** Cetuximab/C225-induced intracellular trafficking of epidermal growth factor receptor. *Cancer Res* 69**:** 6179-6183

Liccardi G, Hartley JA, Hochhauser D (2011)**:** EGFR nuclear translocation modulates DNA repair following cisplatin and ionizing radiation treatment. *Cancer Res* 71**:** 1103-1114

Lichtner RB, Menrad A, Sommer A, Klar U, Schneider MR (2001)**:** Signaling-inactive epidermal growth factor receptor/ligand complexes in intact carcinoma cells by quinazoline tyrosine kinase inhibitors. *Cancer Res* 61**:** 5790-5795

Lin SY, Makino K, Xia W, Matin A, Wen Y, Kwong KY *et al.* (2001)**:** Nuclear localization of EGF receptor and its potential new role as a transcription factor. *Nat Cell Biol* 3**:** 802-808

Liu PC, Liu X, Li Y, Covington M, Wynn R, Huber R *et al.* (2006)**:** Identification of ADAM10 as a major source of HER2 ectodomain sheddase activity in HER2 overexpressing breast cancer cells. *Cancer Biol Ther* 5**:** 657-664

Lo HW, Hsu SC, Hung MC (2006)**:** EGFR signaling pathway in breast cancers: from traditional signal transduction to direct nuclear translocalization. *Breast Cancer Res Treat* 95**:** 211-218

Lo HW, Hung MC (2007)**:** Nuclear EGFR signalling network in cancers: linking EGFR pathway to cell cycle progression, nitric oxide pathway and patient survival. *Br J Cancer* 96 Suppl**:** R16-20

Longley DB, Ferguson PR, Boyer J, Latif T, Lynch M, Maxwell P *et al.* (2001)**:** Characterization of a thymidylate synthase (TS)-inducible cell line: a model system for studying sensitivity to TS- and non-TS-targeted chemotherapies. *Clin Cancer Res* 7**:** 3533-3539

Longley DB, Harkin DP, Johnston PG (2003)**:** 5-fluorouracil: mechanisms of action and clinical strategies. *Nat Rev Cancer* 3**:** 330-338

Lopez JP, Wang-Rodriguez J, Chang C, Chen JS, Pardo FS, Aguilera J *et al.* (2007)**:** Gefitinib inhibition of drug resistance to doxorubicin by inactivating ABCG2 in thyroid cancer cell lines. *Arch Otolaryngol Head Neck Surg* 133**:** 1022-1027

Lu Y, Zi X, Zhao Y, Mascarenhas D, Pollak M (2001)**:** Insulin-like growth factor-I receptor signaling and resistance to trastuzumab (Herceptin). *J Natl Cancer Inst* 93**:** 1852-1857

Ly BH, Nguyen NP, Vinh-Hung V, Rapiti E, Vlastos G (2010)**:** Loco-regional treatment in metastatic breast cancer patients: is there a survival benefit? *Breast Cancer Res Treat* 119**:** 537-545

Lynch TJ, Bell DW, Sordella R, Gurubhagavatula S, Okimoto RA, Brannigan BW *et al.* (2004)**:** Activating mutations in the epidermal growth factor receptor underlying responsiveness of non-small-cell lung cancer to gefitinib. *N Engl J Med* 350**:** 2129-2139

Madshus IH, Stang E (2009)**:** Internalization and intracellular sorting of the EGF receptor: a model for understanding the mechanisms of receptor trafficking. *J Cell Sci* 122**:** 3433-3439

Magne N, Fischel JL, Tiffon C, Formento P, Dubreuil A, Renee N *et al.* (2003)**:** Molecular mechanisms underlying the interaction between ZD1839 ('Iressa') and cisplatin/5-fluorouracil. *Br J Cancer* 89**:** 585-592

Mahaney BL, Meek K, Lees-Miller SP (2009)**:** Repair of ionizing radiation-induced DNA double-strand breaks by non-homologous end-joining. *Biochem J* 417**:** 639-650

Malumbres M, Barbacid M (2009)**:** Cell cycle, CDKs and cancer: a changing paradigm. *Nat Rev Cancer* 9**:** 153-166

Mansel RE, Fallowfield L, Kissin M, Goyal A, Newcombe RG, Dixon JM *et al.* (2006)**:** Randomized multicenter trial of sentinel node biopsy versus standard axillary treatment in operable breast cancer: the ALMANAC Trial. *J Natl Cancer Inst* 98**:** 599-609

Mao C, Qiu LX, Liao RY, Du FB, Ding H, Yang WC *et al.* (2010)**:** KRAS mutations and resistance to EGFR-TKIs treatment in patients with non-small cell lung cancer: a meta-analysis of 22 studies. *Lung Cancer* 69**:** 272-278

Marchionatti AM, Picotto G, Narvaez CJ, Welsh J, Tolosa de Talamoni NG (2009)**:** Antiproliferative action of menadione and 1,25(OH)2D3 on breast cancer cells. *J Steroid Biochem Mol Biol* 113**:** 227-232

Marie Y, Carpentier AF, Omuro AM, Sanson M, Thillet J, Hoang-Xuan K *et al.* (2005)**:** EGFR tyrosine kinase domain mutations in human gliomas. *Neurology* 64**:** 1444-14445

Marone R, Cmiljanovic V, Giese B, Wymann MP (2008)**:** Targeting phosphoinositide 3-kinase: moving towards therapy. *Biochim Biophys Acta* 1784**:** 159-185

Martin M, Pienkowski T, Mackey J, Pawlicki M, Guastalla JP, Weaver C *et al.* (2005)**:** Adjuvant docetaxel for node-positive breast cancer. *N Engl J Med* 352**:** 2302-2313

Matar P, Rojo F, Cassia R, Moreno-Bueno G, Di Cosimo S, Tabernero J *et al.* (2004)**:** Combined epidermal growth factor receptor targeting with the tyrosine kinase inhibitor gefitinib (ZD1839) and the monoclonal antibody cetuximab (IMC-C225): superiority over single-agent receptor targeting. *Clin Cancer Res* 10**:** 6487-6501

Maughan TS, Adams RA, Smith CG, Meade AM, Seymour MT, Wilson RH *et al.* (2011)**:** Addition of cetuximab to oxaliplatin-based first-line combination chemotherapy for treatment of advanced colorectal cancer: results of the randomised phase 3 MRC COIN trial. *Lancet* 377**:** 2103-2114

McGovern UB, Francis RE, Peck B, Guest SK, Wang J, Myatt SS *et al.* (2009)**:** Gefitinib (Iressa) represses FOXM1 expression via FOXO3a in breast cancer. *Mol Cancer Ther* 8**:** 582-591

McHugh LA, Kriajevska M, Mellon JK, Griffiths TR (2007)**:** Combined treatment of bladder cancer cell lines with lapatinib and varying chemotherapy regimens--evidence of schedule-dependent synergy. *Urology* 69**:** 390-394

McKillop D, Partridge EA, Kemp JV, Spence MP, Kendrew J, Barnett S *et al.* (2005)**:** Tumor penetration of gefitinib (Iressa), an epidermal growth factor receptor tyrosine kinase inhibitor. *Mol Cancer Ther* 4**:** 641-649

Mellinghoff IK, Wang MY, Vivanco I, Haas-Kogan DA, Zhu S, Dia EQ *et al.* (2005)**:** Molecular determinants of the response of glioblastomas to EGFR kinase inhibitors. *N Engl J Med* 353**:** 2012-2024

Messersmith WA, Laheru DA, Senzer NN, Donehower RC, Grouleff P, Rogers T *et al.* (2004)**:** Phase I trial of irinotecan, infusional 5-fluorouracil, and leucovorin (FOLFIRI) with erlotinib (OSI-774): early termination due to increased toxicities. *Clin Cancer Res* 10**:** 6522-6527

Meyerhardt JA, Zhu AX, Enzinger PC, Ryan DP, Clark JW, Kulke MH *et al.* (2006)**:** Phase II study of capecitabine, oxaliplatin, and erlotinib in previously treated patients with metastastic colorectal cancer. *J Clin Oncol* 24**:** 1892-1897

Milano G, Spano JP, Leyland-Jones B (2008)**:** EGFR-targeting drugs in combination with cytotoxic agents: from bench to bedside, a contrasted reality. *Br J Cancer* 99**:** 1-5

Miles DW, Chan A, Dirix LY, Cortes J, Pivot X, Tomczak P *et al.* (2010)**:** Phase III study of bevacizumab plus docetaxel compared with placebo plus docetaxel for the first-line treatment of human epidermal growth factor receptor 2-negative metastatic breast cancer. *J Clin Oncol* 28**:** 3239-3247

Miller WR, Bartlett J, Brodie AM, Brueggemeier RW, di Salle E, Lonning PE *et al.* (2008)**:** Aromatase inhibitors: are there differences between steroidal and nonsteroidal aromatase inhibitors and do they matter? *Oncologist* 13**:** 829-937

Mok TS, Wu YL, Thongprasert S, Yang CH, Chu DT, Saijo N *et al.* (2009a)**:** Gefitinib or carboplatin-paclitaxel in pulmonary adenocarcinoma. *N Engl J Med* 361**:** 947-957

Mok TS, Wu YL, Yu CJ, Zhou C, Chen YM, Zhang L *et al.* (2009b)**:** Randomized, placebo-controlled, phase II study of sequential erlotinib and chemotherapy as first-line treatment for advanced non-small-cell lung cancer. *J Clin Oncol* 27**:** 5080-5087

Moore MJ, Goldstein D, Hamm J, Figer A, Hecht JR, Gallinger S *et al.* (2007)**:** Erlotinib plus gemcitabine compared with gemcitabine alone in patients with advanced pancreatic cancer: a phase III trial of the National Cancer Institute of Canada Clinical Trials Group. *J Clin Oncol* 25**:** 1960-1966

Morelli MP, Cascone T, Troiani T, De Vita F, Orditura M, Laus G *et al.* (2005)**:** Sequence-dependent antiproliferative effects of cytotoxic drugs and epidermal growth factor receptor inhibitors. *Ann Oncol* 16 Suppl 4**:** iv61-68

Morgan MA, Parsels LA, Kollar LE, Normolle DP, Maybaum J, Lawrence TS (2008)**:** The combination of epidermal growth factor receptor inhibitors with gemcitabine and radiation in pancreatic cancer. *Clin Cancer Res* 14**:** 5142-149

Moriki T, Maruyama H, Maruyama IN (2001)**:** Activation of preformed EGF receptor dimers by ligand-induced rotation of the transmembrane domain. *J Mol Biol* 311**:** 1011-1026

Moro S, Beretta GL, Dal Ben D, Nitiss J, Palumbo M, Capranico G (2004)**:** Interaction model for anthracycline activity against DNA topoisomerase II. *Biochemistry* 43**:** 7503-7513

Mouridsen H, Gershanovich M, Sun Y, Perez-Carrion R, Boni C, Monnier A *et al.* (2001)**:** Superior efficacy of letrozole versus tamoxifen as first-line therapy for postmenopausal women with advanced breast cancer: results of a phase III study of the International Letrozole Breast Cancer Group. *J Clin Oncol* 19**:** 2596-2606

Mueller RE, Parkes RK, Andrulis I, O'Malley FP (2004)**:** Amplification of the TOP2A gene does not predict high levels of topoisomerase II alpha protein in human breast tumor samples. *Genes Chromosomes Cancer* 39**:** 288-297

Muniandy PA, Liu J, Majumdar A, Liu ST, Seidman MM (2010)**:** DNA interstrand crosslink repair in mammalian cells: step by step. *Crit Rev Biochem Mol Biol* 45**:** 23-49

Munk M, Memon AA, Nexo E, Sorensen BS (2007)**:** Inhibition of the epidermal growth factor receptor in bladder cancer cells treated with the DNA-damaging drug etoposide markedly increases apoptosis. *BJU Int* 99**:** 196-201

Muslimovic A, Nystrom S, Gao Y, Hammarsten O (2009)**:** Numerical analysis of etoposide induced DNA breaks. *PLoS One* 4**:** e5859

Nahta R, Yuan LX, Zhang B, Kobayashi R, Esteva FJ (2005)**:** Insulin-like growth factor-I receptor/human epidermal growth factor receptor 2 heterodimerization contributes to trastuzumab resistance of breast cancer cells. *Cancer Res* 65**:** 11118-111128

Nakamura Y, Oka M, Soda H, Shiozawa K, Yoshikawa M, Itoh A *et al.* (2005)**:** Gefitinib ("Iressa", ZD1839), an epidermal growth factor receptor tyrosine kinase inhibitor, reverses breast cancer resistance protein/ABCG2-mediated drug resistance. *Cancer Res* 65**:** 1541-1546

National Cancer Institute (2011a):Lapatinib Plus Caelyx in Patients With Advanced Metastatic Breast Cancer Following Failure of Trastuzumab Therapy http://clinicaltrials.gov/ct2/show/results/NCT00903656

National Cancer Institute (2011b):LOGiC - Lapatinib Optimization Study in ErbB2 (HER2) Positive Gastric Cancer: A Phase III Global, Blinded Study Designed to Evaluate Clinical Endpoints and Safety of Chemotherapy Plus Lapatinib http://clinicaltrials.gov/ct2/show/NCT00680901

National Cancer Institute (2011c):Neo ALTTO (Neoadjuvant Lapatinib and/or Trastuzumab Treatment Optimisation) Study
http://clinicaltrials.gov/ct2/show/NCT00553358

National Cancer Institute (2011d):The TAILORx Breast Cancer Trial http://www.cancer.gov/clinicaltrials/noteworthy-trials/tailorx

National Institute for Health and Clinical Excellence (2009a):Advanced breast cancer: diagnosis and treatment. CG81.
http://www.nice.org.uk/nicemedia/live/12132/43312/43312.pdf Accessed Jan 2011

National Institute for Health and Clinical Excellence (2009b): Breast cancer (early & locally advanced): diagnosis and treatment CG80
http://www.nice.org.uk/nicemedia/live/12132/43312/43312.pdf Accessed Jan 2011

Ni CY, Murphy MP, Golde TE, Carpenter G (2001)**:** gamma -Secretase cleavage and nuclear localization of ErbB-4 receptor tyrosine kinase. *Science* 294**:** 2179-2181

Nielsen TO, Hsu FD, Jensen K, Cheang M, Karaca G, Hu Z *et al.* (2004)**:** Immunohistochemical and clinical characterization of the basal-like subtype of invasive breast carcinoma. *Clin Cancer Res* 10**:** 5367-5374

Nielsen TO, Parker JS, Leung S, Voduc D, Ebbert M, Vickery T *et al.* (2010)**:** A comparison of PAM50 intrinsic subtyping with immunohistochemistry and clinical prognostic factors in tamoxifen-treated estrogen receptor-positive breast cancer. *Clin Cancer Res* 16**:** 5222-5232

Nieto Y, Nawaz F, Jones RB, Shpall EJ, Nawaz S (2007)**:** Prognostic significance of overexpression and phosphorylation of epidermal growth factor receptor (EGFR) and the presence of truncated EGFRvIII in locoregionally advanced breast cancer. *J Clin Oncol* 25**:** 4405-4413

Nishikawa R, Ji XD, Harmon RC, Lazar CS, Gill GN, Cavenee WK *et al.* (1994)**:** A mutant epidermal growth factor receptor common in human glioma confers enhanced tumorigenicity. *Proc Natl Acad Sci U S A* 91**:** 7727-7731

Nitiss JL (2009a)**:** DNA topoisomerase II and its growing repertoire of biological functions. *Nat Rev Cancer* 9**:** 327-337

Nitiss JL (2009b)**:** Targeting DNA topoisomerase II in cancer chemotherapy. *Nat Rev Cancer* 9**:** 338-350

Noordhuis MG, Eijsink JJ, Ten Hoor KA, Roossink F, Hollema H, Arts HJ *et al.* (2009)**:** Expression of epidermal growth factor receptor (EGFR) and activated EGFR predict poor response to (chemo)radiation and survival in cervical cancer. *Clin Cancer Res* 15**:** 7389-7397

O'Malley FP, Chia S, Tu D, Shepherd LE, Levine MN, Bramwell VH *et al.* (2009)**:** Topoisomerase II alpha and responsiveness of breast cancer to adjuvant chemotherapy. *J Natl Cancer Inst* 101**:** 644-650

O'Shaughnessy J, Miles D, Vukelja S, Moiseyenko V, Ayoub JP, Cervantes G *et al.* (2002)**:** Superior survival with capecitabine plus docetaxel combination therapy in anthracycline-pretreated patients with advanced breast cancer: phase III trial results. *J Clin Oncol* 20**:** 2812-2823

Oestergaard VH, Bjergbaek L, Skouboe C, Giangiacomo L, Knudsen BR, Andersen AH (2004)**:** The transducer domain is important for clamp operation in human DNA topoisomerase IIalpha. *J Biol Chem* 279**:** 1684-1691

Office for National Statistics (October 2010):Cancer Registrations in England,2008 http://www.statistics.gov.uk/downloads/theme_health/MB138/MB1_No38_2007.pdf Accessed Jan 2011

Offterdinger M, Schofer C, Weipoltshammer K, Grunt TW (2002)**:** c-erbB-3: a nuclear protein in mammary epithelial cells. *J Cell Biol* 157**:** 929-939

Okamura T, Singh S, Buolamwini J, Haystead T, Friedman H, Bigner D *et al.* (2009)**:** Tyrosine phosphorylation of the human glutathione S-transferase P1 by epidermal growth factor receptor. *J Biol Chem* 284**:** 16979-16989

Olive PL (1998)**:** The role of DNA single- and double-strand breaks in cell killing by ionizing radiation. *Radiat Res* 150**:** S42-51

Olive PL (2002)**:** The comet assay. An overview of techniques. *Methods Mol Biol* 203**:** 179-194

Olive PL, Banath JP (2006)**:** The comet assay: a method to measure DNA damage in individual cells. *Nat Protoc* 1**:** 23-29

Opresko LK, Chang CP, Will BH, Burke PM, Gill GN, Wiley HS (1995)**:** Endocytosis and lysosomal targeting of epidermal growth factor receptors are mediated by distinct sequences independent of the tyrosine kinase domain. *J Biol Chem* 270**:** 4325-4333

Osheroff N (1989)**:** Effect of antineoplastic agents on the DNA cleavage/religation reaction of eukaryotic topoisomerase II: inhibition of DNA religation by etoposide. *Biochemistry* 28**:** 6157-6160

Ouchi KF, Yanagisawa M, Sekiguchi F, Tanaka Y (2006)**:** Antitumor activity of erlotinib in combination with capecitabine in human tumor xenograft models. *Cancer Chemother Pharmacol* 57**:** 693-702

Oxnard GR, Arcila ME, Sima CS, Riely GJ, Chmielecki J, Kris MG *et al.* (2011)**:** Acquired Resistance to EGFR Tyrosine Kinase Inhibitors in EGFR-Mutant Lung Cancer: Distinct Natural History of Patients with Tumors Harboring the T790M Mutation. *Clin Cancer Res* 17**:** 1616-1622

Paez JG, Janne PA, Lee JC, Tracy S, Greulich H, Gabriel S *et al.* (2004)**:** EGFR mutations in lung cancer: correlation with clinical response to gefitinib therapy. *Science* 304**:** 1497-1500

Paik S, Shak S, Tang G, Kim C, Baker J, Cronin M *et al.* (2004)**:** A multigene assay to predict recurrence of tamoxifen-treated, node-negative breast cancer. *N Engl J Med* 351**:** 2817-2826

Paik S, Tang G, Shak S, Kim C, Baker J, Kim W *et al.* (2006)**:** Gene expression and benefit of chemotherapy in women with node-negative, estrogen receptor-positive breast cancer. *J Clin Oncol* 24**:** 3726-3734

Panico L, D'Antonio A, Salvatore G, Mezza E, Tortora G, De Laurentiis M *et al.* (1996)**:** Differential immunohistochemical detection of transforming growth factor alpha, amphiregulin and CRIPTO in human normal and malignant breast tissues. *Int J Cancer* 65**:** 51-6

Pantel K, Alix-Panabieres C, Riethdorf S (2009)**:** Cancer micrometastases. *Nat Rev Clin Oncol* 6**:** 339-351

Pao W, Miller V, Zakowski M, Doherty J, Politi K, Sarkaria I *et al.* (2004)**:** EGF receptor gene mutations are common in lung cancers from "never smokers" and are associated with sensitivity of tumors to gefitinib and erlotinib. *Proc Natl Acad Sci U S A* 101**:** 13306-13311

Pao W, Miller VA, Politi KA, Riely GJ, Somwar R, Zakowski MF *et al.* (2005)**:** Acquired resistance of lung adenocarcinomas to gefitinib or erlotinib is associated with a second mutation in the EGFR kinase domain. *PLoS Med* 2**:** e73

Park SR, Kook MC, Choi IJ, Kim CG, Lee JY, Cho SJ *et al.* (2010)**:** Predictive factors for the efficacy of cetuximab plus chemotherapy as salvage therapy in metastatic gastric cancer patients. *Cancer Chemother Pharmacol* 65**:** 579-587

Patel D, Bassi R, Hooper A, Prewett M, Hicklin DJ, Kang X (2009)**:** Anti-epidermal growth factor receptor monoclonal antibody cetuximab inhibits EGFR/HER-2 heterodimerization and activation. *Int J Oncol* 34**:** 25-32

Pathology Reporting of Breast Disease (2005):NHS Cancer Screening Programmes/Royal College of Pathologists. NHS BSP Publication No 58. http://www.cancerscreening.nhs.uk/breastscreen/publications/nhsbsp58.html. Accessed Mar 2011

Pawlowski V, Revillion F, Hebbar M, Hornez L, Peyrat JP (2000)**:** Prognostic value of the type I growth factor receptors in a large series of human primary breast cancers quantified with a real-time reverse transcription-polymerase chain reaction assay. *Clin Cancer Res* 6**:** 4217-4225

Peeters M, Price TJ, Cervantes A, Sobrero AF, Ducreux M, Hotko Y *et al.* (2010)**:** Randomized phase III study of panitumumab with fluorouracil, leucovorin, and irinotecan (FOLFIRI) compared with FOLFIRI alone as second-line treatment in patients with metastatic colorectal cancer. *J Clin Oncol* 28**:** 4706-4713

Pegram MD, Finn RS, Arzoo K, Beryt M, Pietras RJ, Slamon DJ (1997)**:** The effect of HER-2/neu overexpression on chemotherapeutic drug sensitivity in human breast and ovarian cancer cells. *Oncogene* 15**:** 537-547

Pegram MD, Lipton A, Hayes DF, Weber BL, Baselga JM, Tripathy D *et al.* (1998)**:** Phase II study of receptor-enhanced chemosensitivity using recombinant humanized anti-p185HER2/neu monoclonal antibody plus cisplatin in patients with HER2/neu-overexpressing metastatic breast cancer refractory to chemotherapy treatment. *J Clin Oncol* 16**:** 2659-2671

Peklak-Scott C, Smitherman PK, Townsend AJ, Morrow CS (2008)**:** Role of glutathione S-transferase P1-1 in the cellular detoxification of cisplatin. *Mol Cancer Ther* 7**:** 3247-3255

Perrin D, van Hille B, Hill BT (1998)**:** Differential sensitivities of recombinant human topoisomerase IIalpha and beta to various classes of topoisomerase II-interacting agents. *Biochem Pharmacol* 56**:** 503-507

Perry J, Ghazaly E, Kitromilidou C, McGrowder EH, Joel S, Powles T (2010)**:** A synergistic interaction between lapatinib and chemotherapy agents in a panel of cell lines is due to the inhibition of the efflux pump BCRP. *Mol Cancer Ther* 9**:** 3322-3329

Piccart-Gebhart MJ, Procter M, Leyland-Jones B, Goldhirsch A, Untch M, Smith I *et al.* (2005)**:** Trastuzumab after adjuvant chemotherapy in HER2-positive breast cancer. *N Engl J Med* 353**:** 1659-1672

Pietras RJ, Fendly BM, Chazin VR, Pegram MD, Howell SB, Slamon DJ (1994)**:** Antibody to HER-2/neu receptor blocks DNA repair after cisplatin in human breast and ovarian cancer cells. *Oncogene* 9**:** 1829-1838

Pinkas-Kramarski R, Lenferink AE, Bacus SS, Lyass L, van de Poll ML, Klapper LN *et al.* (1998)**:** The oncogenic ErbB-2/ErbB-3 heterodimer is a surrogate receptor of the epidermal growth factor and betacellulin. *Oncogene* 16**:** 1249-1258

Pinkas-Kramarski R, Soussan L, Waterman H, Levkowitz G, Alroy I, Klapper L *et al.* (1996)**:** Diversification of Neu differentiation factor and epidermal growth factor signaling by combinatorial receptor interactions. *Embo J* 15**:** 2452-2467

Pirker R, Pereira JR, Szczesna A, von Pawel J, Krzakowski M, Ramlau R *et al.* (2009)**:** Cetuximab plus chemotherapy in patients with advanced non-small-cell lung cancer (FLEX): an open-label randomised phase III trial. *Lancet* 373**:** 1525-1531

Poghosyan Z, Robbins SM, Houslay MD, Webster A, Murphy G, Edwards DR (2002)**:** Phosphorylation-dependent interactions between ADAM15 cytoplasmic domain and Src family protein-tyrosine kinases. *J Biol Chem* 277**:** 4999-5007

Pollak M (2008)**:** Insulin and insulin-like growth factor signalling in neoplasia. *Nat Rev Cancer* 8**:** 915-928

Pommier Y, Leo E, Zhang H, Marchand C (2010)**:** DNA topoisomerases and their poisoning by anticancer and antibacterial drugs. *Chem Biol* 17**:** 421-433

Potter AJ, Gollahon KA, Palanca BJ, Harbert MJ, Choi YM, Moskovitz AH *et al.* (2002)**:** Flow cytometric analysis of the cell cycle phase specificity of DNA damage induced by radiation, hydrogen peroxide and doxorubicin. *Carcinogenesis* 23**:** 389-401

Potter AJ, Rabinovitch PS (2005)**:** The cell cycle phases of DNA damage and repair initiated by topoisomerase II-targeting chemotherapeutic drugs. *Mutat Res* 572**:** 27-44

Prisco M, Santini F, Baffa R, Liu M, Drakas R, Wu A *et al.* (2002)**:** Nuclear translocation of insulin receptor substrate-1 by the simian virus 40 T antigen and the activated type 1 insulin-like growth factor receptor. *J Biol Chem* 277**:** 32078-32085

Pritchard KI, Messersmith H, Elavathil L, Trudeau M, O'Malley F, Dhesy-Thind B (2008)**:** HER-2 and topoisomerase II as predictors of response to chemotherapy. *J Clin Oncol* 26**:** 736-744

Quinn MJ, Cooper N, Rachet B, Mitry E, Coleman MP (2008)**:** Survival from cancer of the breast in women in England and Wales up to 2001. *Br J Cancer* 99 Suppl 1**:** S53-55

Rakha EA, Elsheikh SE, Aleskandarany MA, Habashi HO, Green AR, Powe DG *et al.* (2009)**:** Triple-negative breast cancer: distinguishing between basal and nonbasal subtypes. *Clin Cancer Res* 15**:** 2302-2010

Rao S, Starling N, Cunningham D, Sumpter K, Gilligan D, Ruhstaller T *et al.* (2010)**:** Matuzumab plus epirubicin, cisplatin and capecitabine (ECX) compared with epirubicin, cisplatin and capecitabine alone as first-line treatment in patients with advanced oesophago-gastric cancer: a randomised, multicentre open-label phase II study. *Ann Oncol* 21**:** 2213-2219

Ready N, Janne PA, Bogart J, Dipetrillo T, Garst J, Graziano S *et al.* (2010)**:** Chemoradiotherapy and gefitinib in stage III non-small cell lung cancer with epidermal growth factor receptor and KRAS mutation analysis: cancer and leukemia group B (CALEB) 30106, a CALGB-stratified phase II trial. *J Thorac Oncol* 5**:** 1382-1390

Ren W, Korchin B, Zhu QS, Wei C, Dicker A, Heymach J *et al.* (2008)**:** Epidermal growth factor receptor blockade in combination with conventional chemotherapy inhibits soft tissue sarcoma cell growth *in vitro* and *in vivo. Clin Cancer Res* 14**:** 2785-2795

Riely GJ, Pao W, Pham D, Li AR, Rizvi N, Venkatraman ES *et al.* (2006)**:** Clinical course of patients with non-small cell lung cancer and epidermal growth factor receptor exon 19 and exon 21 mutations treated with gefitinib or erlotinib. *Clin Cancer Res* 12**:** 839-844

Riely GJ, Rizvi NA, Kris MG, Milton DT, Solit DB, Rosen N *et al.* (2009)**:** Randomized phase II study of pulse erlotinib before or after carboplatin and paclitaxel in current or former smokers with advanced non-small-cell lung cancer. *J Clin Oncol* 27**:** 264-270

Rixe O, Franco SX, Yardley DA, Johnston SR, Martin M, Arun BK *et al.* (2009)**:** A randomized, phase II, dose-finding study of the pan-ErbB receptor tyrosine-kinase inhibitor CI-1033 in patients with pretreated metastatic breast cancer. *Cancer Chemother Pharmacol* 64**:** 1139-1148

Roche H, Fumoleau P, Spielmann M, Canon JL, Delozier T, Serin D *et al.* (2006)**:** Sequential adjuvant epirubicin-based and docetaxel chemotherapy for node-positive breast cancer patients: the FNCLCC PACS 01 Trial. *J Clin Oncol* 24**:** 5664-5671

Rodemann HP, Dittmann K, Toulany M (2007)**:** Radiation-induced EGFR-signaling and control of DNA-damage repair. *Int J Radiat Biol* 83**:** 781-791

Rodrigues GA, Falasca M, Zhang Z, Ong SH, Schlessinger J (2000)**:** A novel positive feedback loop mediated by the docking protein Gab1 and phosphatidylinositol 3-kinase in epidermal growth factor receptor signaling. *Mol Cell Biol* 20**:** 1448-1459

Rosell R, Moran T, Queralt C, Porta R, Cardenal F, Camps C *et al.* (2009)**:** Screening for epidermal growth factor receptor mutations in lung cancer. *N Engl J Med* 361**:** 958-967

Rosen LS, Gordon DH, Dugan W, Jr., Major P, Eisenberg PD, Provencher L *et al.* (2004)**:** Zoledronic acid is superior to pamidronate for the treatment of bone metastases in breast carcinoma patients with at least one osteolytic lesion. *Cancer* 100**:** 36-43

Ross DT, Kim CY, Tang G, Bohn OL, Beck RA, Ring BZ *et al.* (2008)**:** Chemosensitivity and stratification by a five monoclonal antibody immunohistochemistry test in the NSABP B14 and B20 trials. *Clin Cancer Res* 14**:** 6602-6609

Ross W, Rowe T, Glisson B, Yalowich J, Liu L (1984)**:** Role of topoisomerase II in mediating epipodophyllotoxin-induced DNA cleavage. *Cancer Res* 44**:** 5857-5860

Rous P (1911)**:** A Sarcoma of the fowl transmissible by an agent separable from the tumour cells. *J Exp Med* 13**:** 397-399

Roussel M, Saule S, Lagrou C, Rommens C, Beug H, Graf T *et al.* (1979)**:** Three new types of viral oncogene of cellular origin specific for haematopoietic cell transformation. *Nature* 281**:** 452-455

Rutqvist LE, Cedermark B, Fornander T, Glas U, Johansson H, Nordenskjold B *et al.* (1989)**:** The relationship between hormone receptor content and the effect of adjuvant tamoxifen in operable breast cancer. *J Clin Oncol* 7**:** 1474-1484

Sansal I, Sellers WR (2004)**:** The biology and clinical relevance of the PTEN tumor suppressor pathway. *J Clin Oncol* 22**:** 2954-2963

Santoro A, Comandone A, Rimassa L, Granetti C, Lorusso V, Oliva C *et al.* (2008)**:** A phase II randomized multicenter trial of gefitinib plus FOLFIRI and FOLFIRI alone in patients with metastatic colorectal cancer. *Ann Oncol* 19**:** 1888-1893

Sasaki H, Endo K, Takada M, Kawahara M, Kitahara N, Tanaka H *et al.* (2007)**:** EGFR exon 20 insertion mutation in Japanese lung cancer. *Lung Cancer* 58**:** 324-328

Sassen A, Rochon J, Wild P, Hartmann A, Hofstaedter F, Schwarz S *et al.* (2008)**:** Cytogenetic analysis of HER1/EGFR, HER2, HER3 and HER4 in 278 breast cancer patients. *Breast Cancer Res* 10**:** R2

Scaltriti M, Verma C, Guzman M, Jimenez J, Parra JL, Pedersen K *et al.* (2009)**:** Lapatinib, a HER2 tyrosine kinase inhibitor, induces stabilization and accumulation of HER2 and potentiates trastuzumab-dependent cell cytotoxicity. *Oncogene* 28**:** 803-814

Scambia G, Benedetti-Panici P, Ferrandina G, Distefano M, Salerno G, Romanini ME *et al.* (1995)**:** Epidermal growth factor, oestrogen and progesterone receptor expression in primary ovarian cancer: correlation with clinical outcome and response to chemotherapy. *Br J Cancer* 72**:** 361-366

Schaefer G, Shao L, Totpal K, Akita RW (2007)**:** Erlotinib directly inhibits HER2 kinase activation and downstream signaling events in intact cells lacking epidermal growth factor receptor expression. *Cancer Res* 67**:** 1228-1238

Schechter AL, Hung MC, Vaidyanathan L, Weinberg RA, Yang-Feng TL, Francke U *et al.* (1985)**:** The neu gene: an erbB-homologous gene distinct from and unlinked to the gene encoding the EGF receptor. *Science* 229**:** 976-978

Schlessinger J (2002)**:** Ligand-induced, receptor-mediated dimerization and activation of EGF receptor. *Cell* 110**:** 669-672

Schmidt-Ullrich RK, Mikkelsen RB, Dent P, Todd DG, Valerie K, Kavanagh BD *et al.* (1997)**:** Radiation-induced proliferation of the human A431 squamous carcinoma cells is dependent on EGFR tyrosine phosphorylation. *Oncogene* 15**:** 1191-1197

Scott SP, Pandita TK (2006)**:** The cellular control of DNA double-strand breaks. *J Cell Biochem* 99**:** 1463-1475

Semba K, Kamata N, Toyoshima K, Yamamoto T (1985)**:** A v-erbB-related protooncogene, c-erbB-2, is distinct from the c-erbB-1/epidermal growth factor-receptor gene and is amplified in a human salivary gland adenocarcinoma. *Proc Natl Acad Sci U S A* 82**:** 6497-6501

Sequist LV, Besse B, Lynch TJ, Miller VA, Wong KK, Gitlitz B *et al.* (2010)**:** Neratinib, an irreversible pan-ErbB receptor tyrosine kinase inhibitor: results of a phase II trial in patients with advanced non-small-cell lung cancer. *J Clin Oncol* 28**:** 3076-3083

Sequist LV, Martins RG, Spigel D, Grunberg SM, Spira A, Janne PA *et al.* (2008)**:** First-line gefitinib in patients with advanced non-small-cell lung cancer harboring somatic EGFR mutations. *J Clin Oncol* 26**:** 2442-2449

Sergina NV, Rausch M, Wang D, Blair J, Hann B, Shokat KM *et al.* (2007)**:** Escape from HER-family tyrosine kinase inhibitor therapy by the kinase-inactive HER3. *Nature* 445**:** 437-441

Shah MA, Schwartz GK (2001)**:** Cell cycle-mediated drug resistance: an emerging concept in cancer therapy. *Clin Cancer Res* 7**:** 2168-2181

Shao CJ, Fu J, Shi HL, Mu YG, Chen ZP (2008)**:** Activities of DNA-PK and Ku86, but not Ku70, may predict sensitivity to cisplatin in human gliomas. *J Neurooncol* 89**:** 27-35

She QB, Solit D, Basso A, Moasser MM (2003)**:** Resistance to gefitinib in PTEN-null HER-overexpressing tumor cells can be overcome through restoration of PTEN function or pharmacologic modulation of constitutive phosphatidylinositol 3'-kinase/Akt pathway signaling. *Clin Cancer Res* 9**:** 4340-4306

Shepherd FA, Rodrigues Pereira J, Ciuleanu T, Tan EH, Hirsh V, Thongprasert S *et al.* (2005)**:** Erlotinib in previously treated non-small-cell lung cancer. *N Engl J Med* 353**:** 123-132

Shi F, Telesco SE, Liu Y, Radhakrishnan R, Lemmon MA (2010)**:** ErbB3/HER3 intracellular domain is competent to bind ATP and catalyze autophosphorylation. *Proc Natl Acad Sci U S A* 107**:** 7692-7697

Shi Z, Peng XX, Kim IW, Shukla S, Si QS, Robey RW *et al.* (2007)**:** Erlotinib (Tarceva, OSI-774) antagonizes ATP-binding cassette subfamily B member 1 and ATP-binding cassette subfamily G member 2-mediated drug resistance. *Cancer Res* 67**:** 11012-11020

Shigematsu H, Lin L, Takahashi T, Nomura M, Suzuki M, Wistuba, II *et al.* (2005)**:** Clinical and biological features associated with epidermal growth factor receptor gene mutations in lung cancers. *J Natl Cancer Inst* 97**:** 339-346

Shih JY, Gow CH, Yang PC (2005)**:** EGFR mutation conferring primary resistance to gefitinib in non-small-cell lung cancer. *N Engl J Med* 353**:** 207-208

Shin DM, Ro JY, Hong WK, Hittelman WN (1994)**:** Dysregulation of epidermal growth factor receptor expression in premalignant lesions during head and neck tumorigenesis. *Cancer Res* 54**:** 3153-3159

Shinagawa H, Miki Y, Yoshida K (2008)**:** BRCA1-mediated ubiquitination inhibits topoisomerase II alpha activity in response to oxidative stress. *Antioxid Redox Signal* 10**:** 939-949

Sierke SL, Cheng K, Kim HH, Koland JG (1997)**:** Biochemical characterization of the protein tyrosine kinase homology domain of the ErbB3 (HER3) receptor protein. *Biochem J* 322 (Pt 3)**:** 757-763

Silva CM, Shupnik MA (2007)**:** Integration of steroid and growth factor pathways in breast cancer: focus on signal transducers and activators of transcription and their potential role in resistance. *Mol Endocrinol* 21**:** 1499-1512

Silver DP, Richardson AL, Eklund AC, Wang ZC, Szallasi Z, Li Q *et al.* (2010)**:** Efficacy of neoadjuvant Cisplatin in triple-negative breast cancer. *J Clin Oncol* 28**:** 1145-1153

Simmons C, Miller N, Geddie W, Gianfelice D, Oldfield M, Dranitsaris G *et al.* (2009)**:** Does confirmatory tumor biopsy alter the management of breast cancer patients with distant metastases? *Ann Oncol* 20**:** 1499-1504

Singh B, Schneider M, Knyazev P, Ullrich A (2009)**:** UV-induced EGFR signal transactivation is dependent on proligand shedding by activated metalloproteases in skin cancer cell lines. *Int J Cancer* 124**:** 531-539

Sirotnak FM, Zakowski MF, Miller VA, Scher HI, Kris MG (2000)**:** Efficacy of cytotoxic agents against human tumor xenografts is markedly enhanced by coadministration of ZD1839 (Iressa), an inhibitor of EGFR tyrosine kinase. *Clin Cancer Res* 6**:** 4885-4892

Siu LL, Soulieres D, Chen EX, Pond GR, Chin SF, Francis P *et al.* (2007)**:** Phase I/II trial of erlotinib and cisplatin in patients with recurrent or metastatic squamous cell carcinoma of the head and neck: a Princess Margaret Hospital phase II consortium and National Cancer Institute of Canada Clinical Trials Group Study. *J Clin Oncol* 25**:** 2178-2183

Slamon DJ, Clark GM, Wong SG, Levin WJ, Ullrich A, McGuire WL (1987)**:** Human breast cancer: correlation of relapse and survival with amplification of the HER-2/neu oncogene. *Science* 235**:** 177-182

Slamon DJ, Leyland-Jones B, Shak S, Fuchs H, Paton V, Bajamonde A *et al.* (2001)**:** Use of chemotherapy plus a monoclonal antibody against HER2 for metastatic breast cancer that overexpresses HER2. *N Engl J Med* 344**:** 783-792

Slamon DJ, Press MF (2009)**:** Alterations in the TOP2A and HER2 genes: association with adjuvant anthracycline sensitivity in human breast cancers. *J Natl Cancer Inst* 101**:** 615-618

Sliwkowski MX, Schaefer G, Akita RW, Lofgren JA, Fitzpatrick VD, Nuijens A *et al.* (1994)**:** Coexpression of erbB2 and erbB3 proteins reconstitutes a high affinity receptor for heregulin. *J Biol Chem* 269**:** 14661-14665

Smart DJ, Halicka HD, Schmuck G, Traganos F, Darzynkiewicz Z, Williams GM (2008)**:** Assessment of DNA double-strand breaks and gammaH2AX induced by the topoisomerase II poisons etoposide and mitoxantrone. *Mutat Res* 641**:** 43-47

Smith I, Procter M, Gelber RD, Guillaume S, Feyereislova A, Dowsett M *et al.* (2007)**:** 2-year follow-up of trastuzumab after adjuvant chemotherapy in HER2-positive breast cancer: a randomised controlled trial. *Lancet* 369**:** 29-36

Sok JC, Coppelli FM, Thomas SM, Lango MN, Xi S, Hunt JL *et al.* (2006)**:** Mutant epidermal growth factor receptor (EGFRvIII) contributes to head and neck cancer growth and resistance to EGFR targeting. *Clin Cancer Res* 12**:** 5064-5073

Solit DB, She Y, Lobo J, Kris MG, Scher HI, Rosen N *et al.* (2005)**:** Pulsatile administration of the epidermal growth factor receptor inhibitor gefitinib is significantly more effective than continuous dosing for sensitizing tumors to paclitaxel. *Clin Cancer Res* 11**:** 1983-1989

Sorensen M, Sehested M, Jensen PB (1999)**:** Effect of cellular ATP depletion on topoisomerase II poisons. Abrogation Of cleavable-complex formation by etoposide but not by amsacrine. *Mol Pharmacol* 55**:** 424-431

Sparano JA, Makhson AN, Semiglazov VF, Tjulandin SA, Balashova OI, Bondarenko IN *et al.* (2009)**:** Pegylated liposomal doxorubicin plus docetaxel significantly improves time to progression without additive cardiotoxicity compared with docetaxel monotherapy in patients with advanced breast cancer previously treated with neoadjuvant-adjuvant anthracycline therapy: results from a randomized phase III study. *J Clin Oncol* 27**:** 4522-4529

Srinivasan R, Poulsom R, Hurst HC, Gullick WJ (1998)**:** Expression of the c-erbB-4/HER4 protein and mRNA in normal human fetal and adult tissues and in a survey of nine solid tumour types. *J Pathol* 185**:** 236-245

Statistics and Outlook for Breast Cancer. (2009). *Vol. Date accessed Nov 2010*. Cancer Research UK.

Steffensen KD, Waldstrom M, Andersen RF, Olsen DA, Jeppesen U, Knudsen HJ *et al.* (2008)**:** Protein levels and gene expressions of the epidermal growth factor receptors, HER1, HER2, HER3 and HER4 in benign and malignant ovarian tumors. *Int J Oncol* 33**:** 195-204

Stehelin D, Varmus HE, Bishop JM, Vogt PK (1976)**:** DNA related to the transforming gene(s) of avian sarcoma viruses is present in normal avian DNA. *Nature* 260**:** 170-173

Stoecklein NH, Luebke AM, Erbersdobler A, Knoefel WT, Schraut W, Verde PE *et al.* (2004)**:** Copy number of chromosome 17 but not HER2 amplification predicts clinical outcome of patients with pancreatic ductal adenocarcinoma. *J Clin Oncol* 22**:** 4737-4745

Szumiel I (2006)**:** Epidermal growth factor receptor and DNA double strand break repair: the cell's self-defence. *Cell Signal* 18**:** 1537-1548

Takimoto CH, Calvo E. (2008). *Cancer Management: A Multidisciplinary Approach*. Pazdur R, Wagman LD, Camphausen KA and WJ H (eds)

Tanaka T, Munshi A, Brooks C, Liu J, Hobbs ML, Meyn RE (2008)**:** Gefitinib radiosensitizes non-small cell lung cancer cells by suppressing cellular DNA repair capacity. *Clin Cancer Res* 14**:** 1266-1273

Tao RH, Maruyama IN (2008)**:** All EGF(ErbB) receptors have preformed homo- and heterodimeric structures in living cells. *J Cell Sci* 121**:** 3207-3217

Taylor JM, Mitchell WM, Cohen S (1974)**:** Characterization of the binding protein for epidermal growth factor. *J Biol Chem* 249**:** 2188-2194

Tobias J, Hochhauser D (2010): *Cancer and its management*, 6th Edition edn. Wiley and Blackwell.

Toikkanen S, Helin H, Isola J, Joensuu H (1992)**:** Prognostic significance of HER-2 oncoprotein expression in breast cancer: a 30-year follow-up. *J Clin Oncol* 10**:** 1044-1048

Toulany M, Minjgee M, Kehlbach R, Chen J, Baumann M, Rodemann HP (2010)**:** ErbB2 expression through heterodimerization with erbB1 is necessary for ionizing radiation-but not EGF-induced activation of Akt survival pathway. *Radiother Oncol* 97: 1506-1514

Toyoda E, Kagaya S, Cowell IG, Kurosawa A, Kamoshita K, Nishikawa K *et al.* (2008)**:** NK314, a topoisomerase II inhibitor that specifically targets the alpha isoform. *J Biol Chem* 283**:** 23711-23720

Treszezamsky AD, Kachnic LA, Feng Z, Zhang J, Tokadjian C, Powell SN (2007)**:** BRCA1-and BRCA2-deficient cells are sensitive to etoposide-induced DNA double-strand breaks via topoisomerase II. *Cancer Res* 67**:** 7078-7081

Trojanek J, Croul S, Ho T, Wang JY, Darbinyan A, Nowicki M *et al.* (2006a)**:** T-antigen of the human polyomavirus JC attenuates faithful DNA repair by forcing nuclear interaction between IRS-1 and Rad51. *J Cell Physiol* 206**:** 35-46

Trojanek J, Ho T, Croul S, Wang JY, Chintapalli J, Koptyra M *et al.* (2006b)**:** IRS-1-Rad51 nuclear interaction sensitizes JCV T-antigen positive medulloblastoma cells to genotoxic treatment. *Int J Cancer* 119**:** 539-548

Trojanek J, Ho T, Del Valle L, Nowicki M, Wang JY, Lassak A *et al.* (2003)**:** Role of the insulin-like growth factor I/insulin receptor substrate 1 axis in Rad51 trafficking and DNA repair by homologous recombination. *Mol Cell Biol* 23**:** 7510-7524

Tsugawa K, Fushida S, Yonemura Y (1993)**:** Amplification of the c-erbB-2 gene in gastric carcinoma: correlation with survival. *Oncology* 50**:** 418-425

Turner JG, Marchion DC, Dawson JL, Emmons MF, Hazlehurst LA, Washausen P *et al.* (2009)**:** Human multiple myeloma cells are sensitized to topoisomerase II inhibitors by CRM1 inhibition. *Cancer Res* 69**:** 6899-6905

Tzahar E, Waterman H, Chen X, Levkowitz G, Karunagaran D, Lavi S *et al.* (1996)**:** A hierarchical network of interreceptor interactions determines signal transduction by Neu differentiation factor/neuregulin and epidermal growth factor. *Mol Cell Biol* 16**:** 5276-5287

Ueda K, Cardarelli C, Gottesman MM, Pastan I (1987)**:** Expression of a full-length cDNA for the human "MDR1" gene confers resistance to colchicine, doxorubicin, and vinblastine. *Proc Natl Acad Sci U S A* 84**:** 3004-3008

Urbanska K, Pannizzo P, Lassak A, Gualco E, Surmacz E, Croul S *et al.* (2009)**:** Estrogen receptor beta-mediated nuclear interaction between IRS-1 and Rad51 inhibits homologous recombination directed DNA repair in medulloblastoma. *J Cell Physiol* 219**:** 392-401

Usha L, Tabesh B, Morrison LE, Rao RD, Jacobson K, Zhu A *et al.* (2008)**:** Topoisomerase II alpha gene copy loss has adverse prognostic significance in ERBB2-amplified breast cancer: a retrospective study of paraffin-embedded tumor specimens and medical charts. *J Hematol Oncol* 1**:** 12

Valerie K, Povirk LF (2003)**:** Regulation and mechanisms of mammalian double-strand break repair. *Oncogene* 22**:** 5792-5812

Van Cutsem E, Kohne CH, Hitre E, Zaluski J, Chang Chien CR, Makhson A *et al.* (2009)**:** Cetuximab and chemotherapy as initial treatment for metastatic colorectal cancer. *N Engl J Med* 360**:** 1408-1417

Van Cutsem E, Peeters M, Siena S, Humblet Y, Hendlisz A, Neyns B *et al.* (2007)**:** Open-label phase III trial of panitumumab plus best supportive care compared with best supportive care alone in patients with chemotherapy-refractory metastatic colorectal cancer. *J Clin Oncol* 25**:** 1658-1664

Van Cutsem E, Verslype C, Beale P, Clarke S, Bugat R, Rakhit A *et al.* (2008)**:** A phase Ib dose-escalation study of erlotinib, capecitabine and oxaliplatin in metastatic colorectal cancer patients. *Ann Oncol* 19**:** 332-339

van de Vijver MJ, He YD, van't Veer LJ, Dai H, Hart AA, Voskuil DW *et al.* (2002)**:** A gene-expression signature as a predictor of survival in breast cancer. *N Engl J Med* 347**:** 1999-2009

van der Hage JA, van de Velde CJ, Julien JP, Tubiana-Hulin M, Vandervelden C, Duchateau L (2001)**:** Preoperative chemotherapy in primary operable breast cancer: results from the European Organization for Research and Treatment of Cancer trial 10902. *J Clin Oncol* 19**:** 4224-4237

Van Schaeybroeck S, Kyula J, Kelly DM, Karaiskou-McCaul A, Stokesberry SA, Van Cutsem E *et al.* (2006)**:** Chemotherapy-induced epidermal growth factor receptor activation determines response to combined gefitinib/chemotherapy treatment in non-small cell lung cancer cells. *Mol Cancer Ther* 5**:** 1154-1165

Van Waes C, Allen CT, Citrin D, Gius D, Colevas AD, Harold NA *et al.* (2010)**:** Molecular and clinical responses in a pilot study of gefitinib with paclitaxel and radiation in locally advanced head-and-neck cancer. *Int J Radiat Oncol Biol Phys* 77**:** 447-454

Velu TJ, Beguinot L, Vass WC, Willingham MC, Merlino GT, Pastan I *et al.* (1987)**:** Epidermal-growth-factor-dependent transformation by a human EGF receptor proto-oncogene. *Science* 238**:** 1408-1410

Vennstrom B, Bishop JM (1982)**:** Isolation and characterization of chicken DNA homologous to the two putative oncogenes of avian erythroblastosis virus. *Cell* 28**:** 135-143

Vermorken JB, Mesia R, Rivera F, Remenar E, Kawecki A, Rottey S *et al.* (2008)**:** Platinum-based chemotherapy plus cetuximab in head and neck cancer. *N Engl J Med* 359**:** 1116-1127

Veronese ML, Sun W, Giantonio B, Berlin J, Shults J, Davis L *et al.* (2005)**:** A phase II trial of gefitinib with 5-fluorouracil, leucovorin, and irinotecan in patients with colorectal cancer. *Br J Cancer* 92**:** 1846-1849

Vichai V, Kirtikara K (2006)**:** Sulforhodamine B colorimetric assay for cytotoxicity screening. *Nature Protocols* 2006**:** 1112-1116

Vilain N, Tsai-Pflugfelder M, Benoit A, Gasser SM, Leroy D (2003)**:** Modulation of drug sensitivity in yeast cells by the ATP-binding domain of human DNA topoisomerase II alpha. *Nucleic Acids Res* 31**:** 5714-5722

Wainberg ZA, Anghel A, Desai AJ, Ayala R, Luo T, Safran B *et al.* (2010)**:** Lapatinib, a dual EGFR and HER2 kinase inhibitor, selectively inhibits HER2-amplified human gastric cancer cells and is synergistic with trastuzumab *in vitro* and *in vivo*. *Clin Cancer Res* 16**:** 1509-1519

Wallace SS (1998)**:** Enzymatic processing of radiation-induced free radical damage in DNA. *Radiat Res* 150**:** S60-79

Wang D, Lippard SJ (2005)**:** Cellular processing of platinum anticancer drugs. *Nat Rev Drug Discov* 4**:** 307-320

Wang H, Mao Y, Zhou N, Hu T, Hsieh TS, Liu LF (2001)**:** ATP-bound topoisomerase ii as a target for antitumor drugs. *J Biol Chem* 276**:** 15990-15995

Wang IC, Meliton L, Ren X, Zhang Y, Balli D, Snyder J *et al.* (2009)**:** Deletion of Forkhead Box M1 transcription factor from respiratory epithelial cells inhibits pulmonary tumorigenesis. *PLoS One* 4**:** e6609

Wang SC, Lien HC, Xia W, Chen IF, Lo HW, Wang Z *et al.* (2004)**:** Binding at and transactivation of the COX-2 promoter by nuclear tyrosine kinase receptor ErbB-2. *Cancer Cell* 6**:** 251-261

Wang YN, Yamaguchi H, Hsu JM, Hung MC (2010)**:** Nuclear trafficking of the epidermal growth factor receptor family membrane proteins. *Oncogene* 29**:** 3997-4006

Weihua Z, Tsan R, Huang WC, Wu Q, Chiu CH, Fidler IJ *et al.* (2008)**:** Survival of cancer cells is maintained by EGFR independent of its kinase activity. *Cancer Cell* 13**:** 385-393

Wells NJ, Addison CM, Fry AM, Ganapathi R, Hickson ID (1994)**:** Serine 1524 is a major site of phosphorylation on human topoisomerase II alpha protein *in vivo* and is a substrate for casein kinase II *in vitro*. *J Biol Chem* 269**:** 29746-29751

Wells NJ, Hickson ID (1995)**:** Human topoisomerase II alpha is phosphorylated in a cell-cycle phase-dependent manner by a proline-directed kinase. *Eur J Biochem* 231**:** 491-497

West Midlands Cancer Intelligence Unit NCINaNCSP (2009):All Breast Cancer Report: A UK analysis of all symptomatic and screen-detected breast cancers diagnosed in 2006. http://www.cancerscreening.nhs.uk/breastscreen/all-breast-cancer-report.pdf.

Willmore C, Holden JA, Layfield LJ (2005)**:** Correlation of HER2 gene amplification with immunohistochemistry in breast cancer as determined by a novel monoplex polymerase chain reaction assay. *Appl Immunohistochem Mol Morphol* 13**:** 333-341

Willmore E, Errington F, Tilby MJ, Austin CA (2002)**:** Formation and longevity of idarubicin-induced DNA topoisomerase II cleavable complexes in K562 human leukaemia cells. *Biochem Pharmacol* 63**:** 1807-1815

Willmore E, Frank AJ, Padget K, Tilby MJ, Austin CA (1998)**:** Etoposide targets topoisomerase IIalpha and IIbeta in leukemic cells: isoform-specific cleavable complexes visualized and quantified in situ by a novel immunofluorescence technique. *Mol Pharmacol* 54**:** 78-85

Wilson JB, Johnson MA, Stuckert AP, Trueman KL, May S, Bryant PE *et al.* (2001)**:** The Chinese hamster FANCG/XRCC9 mutant NM3 fails to express the monoubiquitinated form of the FANCD2 protein, is hypersensitive to a range of DNA damaging agents and exhibits a normal level of spontaneous sister chromatid exchange. *Carcinogenesis* 22**:** 1939-`1946

Winograd-Katz SE, Levitzki A (2006)**:** Cisplatin induces PKB/Akt activation and p38(MAPK) phosphorylation of the EGF receptor. *Oncogene* 25**:** 7381-7390

Woessner RD, Mattern MR, Mirabelli CK, Johnson RK, Drake FH (1991)**:** Proliferation- and cell cycle-dependent differences in expression of the 170 kilodalton and 180 kilodalton forms of topoisomerase II in NIH-3T3 cells. *Cell Growth Differ* 2**:** 209-214

Wojewodzka M, Buraczewska I, Kruszewski M (2002)**:** A modified neutral comet assay: elimination of lysis at high temperature and validation of the assay with anti-single-stranded DNA antibody. *Mutat Res* 518**:** 9-20

Wolff AC, Hammond ME, Schwartz JN, Hagerty KL, Allred DC, Cote RJ *et al.* (2007)**:** American Society of Clinical Oncology/College of American Pathologists guideline recommendations for human epidermal growth factor receptor 2 testing in breast cancer. *J Clin Oncol* 25**:** 118-145

Wollman R, Yahalom J, Maxy R, Pinto J, Fuks Z (1994)**:** Effect of epidermal growth factor on the growth and radiation sensitivity of human breast cancer cells *in vitro*. *Int J Radiat Oncol Biol Phys* 30**:** 91-98

Wong AJ, Ruppert JM, Bigner SH, Grzeschik CH, Humphrey PA, Bigner DS *et al.* (1992)**:** Structural alterations of the epidermal growth factor receptor gene in human gliomas. *Proc Natl Acad Sci U S A* 89**:** 2965-2969

Wong NA, Brett L, Stewart M, Leitch A, Longley DB, Dunlop MG *et al.* (2001)**:** Nuclear thymidylate synthase expression, p53 expression and 5FU response in colorectal carcinoma. *Br J Cancer* 85**:** 1937-1943

Wyman C, Ristic D, Kanaar R (2004)**:** Homologous recombination-mediated double-strand break repair. *DNA Repair (Amst)* 3**:** 827-833

Xia L, Wang L, Chung AS, Ivanov SS, Ling MY, Dragoi AM *et al.* (2002a)**:** Identification of both positive and negative domains within the epidermal growth factor receptor COOH-terminal region for signal transducer and activator of transcription (STAT) activation. *J Biol Chem* 277**:** 30716-30723

Xia W, Gerard CM, Liu L, Baudson NM, Ory TL, Spector NL (2005)**:** Combining lapatinib (GW572016), a small molecule inhibitor of ErbB1 and ErbB2 tyrosine kinases, with therapeutic anti-ErbB2 antibodies enhances apoptosis of ErbB2-overexpressing breast cancer cells. *Oncogene* 24**:** 6213-6221

Xia W, Husain I, Liu L, Bacus S, Saini S, Spohn J *et al.* (2007)**:** Lapatinib antitumor activity is not dependent upon phosphatase and tensin homologue deleted on chromosome 10 in ErbB2-overexpressing breast cancers. *Cancer Res* 67**:** 1170-1175

Xia W, Mullin RJ, Keith BR, Liu LH, Ma H, Rusnak DW *et al.* (2002b)**:** Anti-tumor activity of GW572016: a dual tyrosine kinase inhibitor blocks EGF activation of EGFR/erbB2 and downstream Erk1/2 and AKT pathways. *Oncogene* 21**:** 6255-6263

Xu D, Makkinje A, Kyriakis JM (2005)**:** Gene 33 is an endogenous inhibitor of epidermal growth factor (EGF) receptor signaling and mediates dexamethasone-induced suppression of EGF function. *J Biol Chem* 280**:** 2924-2933

Xu JM, Azzariti A, Colucci G, Paradiso A (2003)**:** The effect of gefitinib (Iressa, ZD1839) in combination with oxaliplatin is schedule-dependent in colon cancer cell lines. *Cancer Chemother Pharmacol* 52**:** 442-448

Xu P, Derynck R (2010)**:** Direct activation of TACE-mediated ectodomain shedding by p38 MAP kinase regulates EGF receptor-dependent cell proliferation. *Mol Cell* 37**:** 551-566

Yamauchi H, Stearns V, Hayes DF (2001)**:** When is a tumor marker ready for prime time? A case study of c-erbB-2 as a predictive factor in breast cancer. *J Clin Oncol* 19**:** 2334-2356

Yan B, Yau EX, Bte Omar SS, Ong CW, Pang B, Yeoh KG *et al.* (2010)**:** A study of HER2 gene amplification and protein expression in gastric cancer. *J Clin Pathol* 63: 839-842

Yan T, Deng S, Metzger A, Godtel-Armbrust U, Porter AC, Wojnowski L (2009)**:** Topoisomerase II{alpha}-dependent and -independent apoptotic effects of dexrazoxane and doxorubicin. *Mol Cancer Ther* 8: 1075-1085

Yanase K, Tsukahara S, Asada S, Ishikawa E, Imai Y, Sugimoto Y (2004)**:** Gefitinib reverses breast cancer resistance protein-mediated drug resistance. *Mol Cancer Ther* 3**:** 1119-1125

Yang CH, Huang CJ, Yang CS, Chu YC, Cheng AL, Whang-Peng J *et al.* (2005)**:** Gefitinib reverses chemotherapy resistance in gefitinib-insensitive multidrug resistant cancer cells expressing ATP-binding cassette family protein. *Cancer Res* 65**:** 6943-6949

Yang J, Stark GR (2008)**:** Roles of unphosphorylated STATs in signaling. *Cell Res* 18**:** 443-451

Yap TA, Vidal L, Adam J, Stephens P, Spicer J, Shaw H *et al.* (2010)**:** Phase I trial of the irreversible EGFR and HER2 kinase inhibitor BIBW 2992 in patients with advanced solid tumors. *J Clin Oncol* 28**:** 3965-3972

Yarden Y, Sliwkowski MX (2001)**:** Untangling the ErbB signalling network. *Nat Rev Mol Cell Biol* 2**:** 127-137

Ying H, Zheng H, Scott K, Wiedemeyer R, Yan H, Lim C *et al.* (2010)**:** Mig-6 controls EGFR trafficking and suppresses gliomagenesis. *Proc Natl Acad Sci U S A* 107**:** 6912-6917

Yoshida T, Okamoto I, Iwasa T, Fukuoka M, Nakagawa K (2008a)**:** The anti-EGFR monoclonal antibody blocks cisplatin-induced activation of EGFR signaling mediated by HB-EGF. *FEBS Lett* 582**:** 4125-4130

Yoshida T, Okamoto I, Okabe T, Iwasa T, Satoh T, Nishio K *et al.* (2008b)**:** Matuzumab and cetuximab activate the epidermal growth factor receptor but fail to trigger downstream signaling by Akt or Erk. *Int J Cancer* 122**:** 1530-1538

Yun CH, Mengwasser KE, Toms AV, Woo MS, Greulich H, Wong KK *et al.* (2008)**:** The T790M mutation in EGFR kinase causes drug resistance by increasing the affinity for ATP. *Proc Natl Acad Sci U S A* 105**:** 2070-2075

Zhang A, Lyu YL, Lin CP, Zhou N, Azarova AM, Wood LM *et al.* (2006)**:** A protease pathway for the repair of topoisomerase II-DNA covalent complexes. *J Biol Chem* 281**:** 35997-36003

Zhang D, Pal A, Bornmann WG, Yamasaki F, Esteva FJ, Hortobagyi GN *et al.* (2008)**:** Activity of lapatinib is independent of EGFR expression level in HER2-overexpressing breast cancer cells. *Mol Cancer Ther* 7**:** 1846-1850

Zheng X, Jiang F, Katakowski M, Zhang ZG, Lu QE, Chopp M (2009)**:** ADAM17 promotes breast cancer cell malignant phenotype through EGFR-PI3K-AKT activation. *Cancer Biol Ther* 8**:** 1045-1054

Zhou H, Kim YS, Peletier A, McCall W, Earp HS, Sartor CI (2004)**:** Effects of the EGFR/HER2 kinase inhibitor GW572016 on EGFR- and HER2-overexpressing breast cancer cell line proliferation, radiosensitization, and resistance. *Int J Radiat Oncol Biol Phys* 58**:** 344-352

Zwang Y, Yarden Y (2006)**:** p38 MAP kinase mediates stress-induced internalization of EGFR: implications for cancer chemotherapy. *Embo J* 25**:** 4195-4206

Zwitter M, Rajer M, Kovac V, Kern I, Vrankar M, Smrdel U (2011)**:** Intermittent chemotherapy and erlotinib for nonsmokers or light smokers with advanced adenocarcinoma of the lung: a phase II clinical trial. *J Biomed Biotechnol* 2011**:** 185646

Appendix

DNA Repair Genes

ABL1	ERCC5	MLH1	POLE3	RFC5	UBE2B
ADPRT	ERCC6	MLH3	POLE4	RIF1	UBE2D2
ADPRTL1	EXO1	MMS19L	POLG1	RPA1	UBE2D3
ADPRTL2	FANCA	MNAT1	POLG2	RPA2	UBE2I
ADPRTL3	FANCB	MPG	POLH	RPA3	UBE2L3
ALKBH	FANCC	MRE11A	POLI	RPA4	UBE2N
APEX1	FANCD2	MRE11B	POLK	RRM1	UBE2V2
APEX2	FANCE	MSH2	POLL	RRM2	UNG
APTX	FANCF	MSH3	POLM	RRM2B	WDR33
ATM	FANCG	MSH4	POLN	RUVBL2	WRN
ATR	BRIP1	MSH5	POLQ	SHFM1	WRNIP1
ATRX	FANCL	MSH6	POLS	SMC1L1	XAB2
BLM	FANCM	MUS81	PRKDC	SMC2L1	XPA
BRCA1	FEN1	MUTYH	PTTG1	SMC3L1	XPC
BRCA2	FLJ35220	N4BP2	RAD1	SMC4L1	XRCC1
CCNH	FRAP1	NBS1	RAD9A	SMC1L2	XRCC2
CDKN1A	GADD45A	NEIL1	RAD17	SMUG1	XRCC3
CDK7	GADD45G	NEIL2	RAD18	SPO11	XRCC4
CETN2	G22P1	NEIL3	RAD21	SSRP1	XRCC5
CETN3	GTF2H1	NTHL1	RAD23A	SUMO1	
CHAF1A	GTF2H2	NUDT1	RAD23B	SUPT16H	
CHAF1B	GTF2H3	NUDT3	RAD50	TDG	
CHEK1	GTF2H4	OGG1	RAD51	TDP1	
CHEK2	GTF2H5	PCNA	RAD51C	TEP1	
CIB1	H2AFX	RAD51AP1	RAD51L1	TERF1	
CKN1	HEL308	PMS1	RAD51L3	TERF2	
CRY1	HMGB1	PMS2	RAD52	TERT	
CRY2	HMGB2	PMS2L1	RAD52B	TINF2	
CSNK1D	HUS1	PMS2L2	RAD54B	TOP1	
CSNK1E	KUB3	PMS2L4	RAD54L	TOP2A	
DCLRE1A	LIG1	PMS2L5	RAD9A	TOP2B	
DCLRE1B	LIG3	PMS2L8	RAD9B	TOPBP1	
DCLRE1C	LIG4	PMS2L3	RBBP4	TOP3A	
DDB1	MAD1L1	PNKP	RBBP8	TOP3B	
DDB2	MAD2L1	POLA	RECQL1	TP53	
DEPC-1	MAD2L2	POLA2	RECQL4	TP53BP1	
DMC1	MBD1	POLB	RECQL5	TP53I3	
DUT	MBD2	POLD1	REV1L	TP73	
EME1	MBD3	POLD2	REV3L	TP73L	
ERCC1	MBD4	POLD3	RFC1	TREX1	
ERCC2	MBD5	POLD4	RFC2	TREX2	
ERCC3	MGC90512	POLE	RFC3	UBE1	
ERCC4	MGMT	POLE2	RFC4	UBE2A	